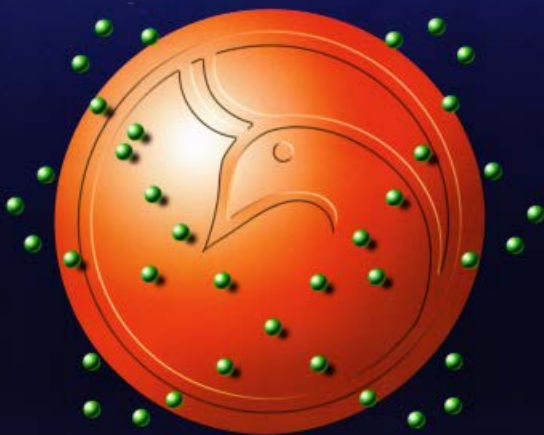




Al-Mustansiriyah  
ISSN 1814 - 635X

Journal of Science

Vol. 26, No. 1, 2015



Issued by College of Science - Mustansiriya University

Vol. 26  
No. 1  
2015

# **Al-Mustansiriyah Journal of Science**

Issued by College of Science, Al-Mustansiriya  
University, Baghdad, Iraq

## **Editor in chief**

Prof. Dr. Saheb K. Al-Saidy

## **Managing Editor**

Assist. Prof. Dr. Salah Mahdi Al-Shukri

## **Technical Personnel**

Hamsa Ali Ahmed  
Maysaa' Nazar Mustafa  
Shatha J. Mohammed

[www.mjs-mu.com](http://www.mjs-mu.com)

e-mail: [mustjsci@yahoo.com](mailto:mustjsci@yahoo.com)

Mobile: 07711184399

Number of Deposit at Iraqi National Library and Archives, 278,  
1977

---

# Al-Mustansiriyah Journal of Science

## Editor in chief

Prof. Dr. Saheb K. Al-Saiddy  
Department of Mathematics, College of Science,  
Mustansiriyh University  
E-mail : dr.saheb@yahoo.com

---

## Editor Managing

Assist. Prof. Dr. Salah Mahdi Al-Shukri  
Department of Chemistry, College of Science, Mustansiriyh University  
salah\_6@yahoo.com: E-mail

## Editorial Board

Prof. Dr. Ibrahim R. Agool  
Department of Physics, College of Science, Mustansiriyh  
University.  
E-mail : ibrahim\_agool@yahoo.com

Prof. Dr. Abd Aljabbar khalaf Atiyah  
Department of chemistry, College of Science,  
Mustansiriyh University  
E-mail : abdel@yahoo.com

Prof. Dr. Hallah Mohamed Ragab  
Engineering and Biotechnology Research  
Division, National Research Center ,Cairo University,  
Egypt  
E-mail : hmragab@yahoo.com

Assist. Prof. Dr. Haider J. Ali  
Department of Mathematics, College of Science,  
Mustansiriyh University  
E-mail : drhaid\_20@yahoo.com

Assist. Prof. Dr. Jameela Harbi  
Department of Computer Science, College of Science, Mustansiriyh University  
E-mail : jameelahharbi@yahoo.com

Prof. Dr. Mahmoud Khalid Jassim  
Department of Mathematics, College of Arts and  
Sciences, Nizwa University, Oman  
E-mail : mkj602007@yahoo.com

Prof. Dr. Wael Mohamed El-Sayed  
Department of parasitology, Medical Research Institute,  
Egypt  
E-mail : waelotfy@yahoo.com

Prof. Nadia Kandile  
Department of Chemistry, University of Ain Shams, Egypt  
E-mail : nadiaghk@yahoo.com

Assist. Prof. Dr. Hadi Muhammad Ali  
Department of Chemistry, Chairman of the  
Committee Dean of the College of Science, Nahrain  
University

Assist. Prof. Dr. Fadel Abid Rissan  
Dean of the College of Science, Baghdad University

Prof. Dr. Dhair AL-Tarky  
Department of Mathematics, University of Liverpool ,Uk  
E-mail : Aljumeily@yahoo.com

Prof. Dr. Abdelfattah Bader  
Department of Biosystematic Botany and Microbiology, College of  
Sciences , Helwan University, Egypt  
E-mail : abadr\_tanta@yahoo.com

Assist. Prof. Dr. Bidoor Yassin  
Department of atmosphere, Mustansiriyh College of Science,  
Mustansiriyh University  
E-mail : bdor\_humood@yahoo.com

Assist. Prof. Dr. Ali Huyssien Alwan  
Department of Biology, College of Science, Mustansiriyh  
University  
E-mail : dr.alialameri72@yahoo.com

## Consultant Committee

Prof. Dr. Tawfiq Abdel Khaliq Abbas  
Department of Computer Science, Dean of the College of  
Information Technology, University of Babylon

Prof. Dr. Baher Abdul Khaliq Mahmoud  
Department of Dairy Science and Technology, National Research  
Center, Egypt  
E-mail : baher\_effat@yahoo.com

Prof. Hanaa A. Hassan  
Department of Chemistry, University of Ain Shams, Egypt  
E-mail : drhanaahassan@yahoo.com

Assist. Prof. Dr. Mohammed Ali Nasser  
Department of Mathematics, College of Education, University of  
Sanaa, Yemen

Assist. Prof. Dr. Abdulsada Abdul Abbas Rahe  
Department of Biology, College of Science, University of Wasit

## **Instructions for Authors**

### *Al-Mustansiriyah Journal of Science (MJS)*

Manuscript text (first submission) should be double spaced on one side of high quality white A4 sheets (21.6×27.9 cm) with margins of one inch all around the page using Microsoft Word 2007 or 2010 using (doc.) type. The typing in Arabic or English must use (Times New Roman, font size of 14 pt). The sections should be arranged in the following order: Title Page, Abstract in English, Abstract in Arabic, Introduction, Materials and Methods (Experimental), Results and Discussion, Conclusion, Acknowledgment (if any), Abbreviations (if any) and list of References. The head of the sections should be capitalized, bolded and centered and font size of 16pt. (e.g. **ABSTRACT, INTRODUCTION, MATERIALS and METHODS (EXPERIMENTAL), RESULTS and DISCUSSION, CONCLUSION, ACKNOWLEDGMENTS, REFERENCES**), and the others (sub-sections) should be in sentence case and bolded as well.

**Title Page:** Includes the title of the article, author's names with full names and affiliations. The affiliation should comprise the department, college, institution (University or Company), and should be typed as a footnote to the author's name. The e-mail address of the author responsible for correspondence (who is designated with an asterisk \*) must be given at the first page under the name and affiliation of authors.

**References:** All references should be cited in using the appropriate Arabic numerals, which are enclosed in parenthesis (e.g. Polyurethane rigid foams are largely used as insulating materials for their combination of low density, low thermal conductivity and good mechanical properties [1-3].)

A list of references should be given in the end of the manuscript. References should be typed single-spaced and numbered sequentially in the order in which they are cited in the text. The number of the reference should be given between two brackets [ ].

#### ❖ **Journal's paper**

[1]. Metallo S. J., Kane R. S., Holmlin R. E., Whitesides G. M., *Journal of American chemical Society*. 125, 5, 4534-4540, 2003.

#### ❖ **Books:**

[2]. Edward M. *Handbook of Adhesives and Sealants*; McGraw-Hill: New York, 2000.

**Tables:** Tables should be created using the Table tool in MS Word using font size 9 point. Tables should be numbered with Arabic numerals and referred to by number in the Text (e.g., Table 1,2,3... etc.). Each Table should be typed with the legend above the Table.

**Figures, Schemes and Diagrams** should be numbered in a consecutive series of Arabic numerals in the order in which they are cited in the text (e.g., Figure 1 or Scheme 1).

---

<b>CONTENTS</b>	<b>Page No.</b>
<b>Detection of bacterial contamination through computer input component</b> Khadija S. Al-Mizury	1-3
<b>Cervical Cancer Cells Classification Using Cytological Optical Images Features</b> Salim J. Attia	4-7
<b>Relationship between Some Bacterial Adhesion Ability to Females' Epithelial Cells and Diabetes</b> Siham Sh. AL-Salihi	8-14
<b>Evaluation of Vitamin D Status in Patients with Type 1 Diabetes Mellitus</b> Abdilkarim Yehia J. AL-Sammraie	15-19
<b>Antibacterial Activity of the Extracts of Chicken Gizzard Membrane Against Some Pathogenic Bacteria Isolated from Urinary Tract Infections</b> Hannaa Farhan Abbas	21-23
<b>Correlation of Gonadal Hormones and Insulin Resistance with Seminal Fluid in Infertile Males Afflicted with Diabetes Mellitus</b> Nawal M. J. AL-Shammaa, Amer Hasan Abdullah, and Aufaira Shaker nsaif	24-31
<b>Synthesis of New 1,3-Oxazole Derivatives</b> Abdul Jabar Kh. Atia and Ali Abdul waheed	32-38
<b>Flow Injection- Spectrophotometric Determination of Clonazepam Based On Its Oxidative Condensation with Promethazine Hydrochloride</b> Mouayed Q. Al-Abachi, and Hind Hadi	39-42
<b>Synthesis and Characterization of 2-Hydrazinyl 3H-imidazol[4,5b]Pyridine Derivatives</b> Nisreen Kais Abood	43-50
<b>A Study of Cloud Shortwave Radiative Properties</b> Abdulwahab Husain Alobaidi	51-53
<b>Bases in the Space of Vector Valued Analytic Multiple Dirichlet Series</b> Mushtaq Shakir A. Hussein and Nagem R. Nagem	54-58
<b>Direct and Inverse Theorems for the Bezier Variant of Operators <math>M_n</math> in <math>L_{\delta,p}</math>-Spaces</b> Lekaa Abdulkareem Hussein	59-63
<b>Some Bayes Estimators for Maxwell Distribution with Conjugate Informative Priors</b> Tasnim H.K. Al-Baldawi	64-69
<b>A New Method for Optimizing Security Site Using Dual Homed Host</b> Raghad Mohammed Hadi	70-76
<b>Modifying Steganography in Android Mobile Image Based on ECC Algorithm</b> Zainab Khyioon Abdalrdha and Mushtaq Talib Ajjah	77-83
<b>Detecting Cancer Cells of Mammographic Images Based on Top-Hat Transformation</b> Layla Hussein	84-91
<b>New Watermark Technique Based on <math>B^+</math> Tree and Mathematical Morphology</b> Hala Bahjet Abdul Wahab	92-104
<b>Net Correlation between Surface Temperature and Pressure Anomaly at Sea Level and North Atlantic Oscillation (NAO) of Baghdad City</b> Ahmed S. Hassan and Iqbal Kh. Khams	105-109
<b>Seasonal Variations of Atmospheric Radio Noise Field Strength of Sunrise and Sunset during Minimum Solar Cycle Over Baghdad</b> Fahmi. A. Mohammed	110-112
<b>The Index of Ground Water Quality For Selective Area Of Dibdibba Aquifer Southern Iraq Using Gis</b> Laith Khalil Ibrahiem	113-116



## Detection of Bacterial Contamination through Computer Input Component

Khadija S. Al-Mizury  
Health and Medical Technical College

### Article info

Received 10/11/2013

Accepted 22/6/2014

### ABSTRACT

This study aims at detecting the probability of bacterial prevalence through the daily computer components usage such as keyboard and mouse. The study included 120 swab samples; 60 were taken from keyboard and 60 from mice. The samples were collected from personal computers, internet cafés and hospitals located in different areas of Baghdad city. The collected samples were inoculated on selective culture media using standard methods. The isolates were identified depending on morphological features of colonies using gram stain and by studying the biochemical characteristics. It was found that 97.5% of the samples were contaminated with different mixed bacterial growth such as *Staphylococcus aureus*, *Staphylococcus epidermidis*, *Escherichia coli*, *Pseudomonas spp.* and *Streptococcus spp.* The results indicated that keyboards and mice at internet cafes showed 100% contamination when compared with other locations. The presence of pathogenic and commensal germs on computer components indicates that they might be an environmental media transmitting pathogenic bacteria.

### الخلاصة

تهدف الدراسة الى التحري عن احتمالية انتقال الجراثيم خلال اجهزة الادخال في جهاز الحاسوب المستعملة يوميا مثال لوحة المفاتيح والفأرة. شملت الدراسة 120 مسحة أخذت 60 منها من لوحة المفاتيح و60 مسحة من الفأرة، جمعت المسحات من مناطق مختلفة في مدينة بغداد من الحواسيب الشخصية ومقاهي الانترنت والمستشفيات. زرعت العينات التي جمعت على أوساط زرعية انتقائية بأبواب قياسي شخضت العزلات اعتماداً على الصفات الشكلية للمتعمرات، باستعمال ملون غرام واختبار الخصائص الكيميائية الحيوية. وجد أن 97,5% من العينات كانت ملوثة بأنواع مختلفة من الجراثيم المختلطة مثل *Staphylococcus aureus*, *Staphylococcus epidermidis*, *Streptococcus spp*, *Escherichia coli*, *Pseudomonas spp* أشارت النتائج الى أن لوحات المفاتيح واجهزة الفأرة في مقاهي الانترنت أظهرت تلوث 100% بالمقارنة مع الأماكن الأخرى. أن وجود الجراثيم المرضية والمتعايشة على مكونات الحاسوب يدل على أنها تمثل وسائط بينية لنقل الجراثيم المرضية.

### INTRODUCTION

Health care-associated infections are important cause of morbidity and mortality in hospitals. Each year more than 2 million patients acquire health care-associated infections, resulting in 90,000 deaths, and healthcare costs are estimated to exceed \$5 billion [1].

Some investigators have suggested that computer keyboards may contribute to cross-transmission because of acquisition of transient hand carriage by healthcare personnel during contact with the contaminated computer keyboard, or mouse [2].

Keyboard and mouse have become reservoirs for pathogens because of increased use of computers in patient areas. [3]

The ability of computer to act as fomites has been previously documented in health care [4] and hospital environment [5]. In work place, contamination of the office environment including computer keyboard and mouse with bacteria is also recognized [6]. The computer in the environments mentioned above are likely to be operated by a few regular users. However, there are increased availability of multiple-users computer which is handled by numerous users on a daily basis. Given that computers are not routinely disinfected, the opportunity of the transmitting contamination microorganisms is potentially great. [7]

In fact 80% of infection spreads through hand contact with infected hands or objects [8]

The aim of this study, is to investigate the presence of bacteria on computer keyboard, and mouse in 3 locations (personal computer, hospital and internet cafes) that are frequently used by people in Baghdad city.

### MATERIALS AND METHODS

A total of 120 swabs; 60 from computer keyboards and 60 from computer mice were collected from different places hospitals (administrative parts, laboratory and pharmacy), internet cafes and personal computers in Baghdad city.

The swabs were placed in sterilized cases to avoid contamination; and then all the samples were taken to the laboratory within an hour for culturing according to standard method [9].

The swabs were inoculated on blood and maconkey agar for presumptive identification of bacterial colonies. Gram positive and negative bacteria were identified as by standard microbiological procedures. Bacterial colonies were differentiated according to colony morphology and colour, gram staining, haemolysis patterns, catalase and coagulates test (for *staphylococci*), and catalase and oxidase tests (for gram negative bacteria) [10].

Suitable biochemical tests were done for further identification of the bacterial isolates.

### RESULTS AND DISCUSSION

Table (1) demonstrates that 100% of internet café computers were contaminated with bacteria in comparison with results of the percentage of contamination in personal (76%) and (89%) hospital computers.

Table (2) shows that *S.aureus* was isolated from all computer keyboards and mice. Isolates of *S.aureus* one of the medical important causative agent for various pus-forming infection in human such

as boils, carbuncles, folliculitis, impetigo, osteomyelitis, toxic-shock syndrome [16].

Table 1: Sites Sample Presence of Bacteria and the Percentage of Contamination

Site	No. of Samples	Contamination percentage	Total
Computer Keyboards	60		
Personal	15	73	90%
Hospital	15	86	
Internet Cafe	30	100	
Computer Mice	60		
Personal	15	80	93%
Hospital	15	93	
Internet Cafe	30	100	

Table(2) also shows that *S. epidermidis* was isolated from most of the samples. This bacteria is a normal habitat of the skin but can

occasionally assume an opportunistic pathogenic role in causing human infection, such as endocarditis [17]. It is of particular interest in our study to isolate bacteria that belong to the family *Enterobacteriaceae* including *E. coli*, which indicates feral contamination [18]. It is well-known that *E. coli* cause urinary tract infection and diarrhea [19].

Table :2 Percentage of Bacterial Isolated on each Object

Isolated bacteria	CK%	CM%
<i>Staphylococcus aureus</i>	%98	%97
<i>E.coli</i>	%53	%57
<i>Pseudomonas spp</i>	%42	%51
<i>Staphylococcus epidermidis</i>	%80	%82
<i>Streptococcus spp</i>	%22	%19

Results shown in table (3) indicate that keyboard, and mouse of internet cafes exhibited the highest percentage of pathogenic bacteria.

Table 3: Bacterial Species that Isolated from Computer Keyboard and Mouse

Location of keyboard	Percentage of Bacterial isolate				
	<i>Pseudomonas spp</i> %	<i>Staph.aureus</i> %	<i>E.coli</i> %	<i>Staph. Epidermidis</i> %	<i>Streptococcus spp</i> %
Personal Hospital	6	93	13	40	0
Internet cafe	66	97	53	53	2
	46	100	73	86	30

Location of mice	Percentage of Bacterial isolate				
	<i>Pseudomonas spp</i> %	<i>Staph.aureus</i> %	<i>E.coli</i> %	<i>Staph. Epidermidis</i> %	<i>Streptococcus spp</i> %
Personal Hospital	2	93	13	60	6
Internet cafe	80	94	63	80	13
	50	100	46	93	26

Previous studies have reported that computer keyboard and mouse could be contaminated with pathogenic bacteria [11]. The present study also shows that bacterial contamination occur on computer surfaces located in three regions (internet café, personal, and hospitals), and this may reflect that multiple-user environment can be the cause of contamination by individuals who carry bacteria such as *Staphylococcus aureus*. The isolation of viable microorganisms suggest that the presented species are able to persist for a period of time on these surfaces [12].

Computer keyboard is one of the most commonly touched and shared surfaces today. By inference any time a keyboard is shared by two or more users it becomes a risk for the spread of infection [20].

Thus keyboards have become reservoirs for pathogens especially in hospital and school [21]. It is worth to mention here that the reason of increasing percentage of contamination by computers is the difficulty of cleaning and disinfection [20].

Depending on the above we think that the low percentage of keyboard and mouse contamination in personal and hospital computers is due to the limited number of users and assumed continuous cleaning percentage of hospital computer keyboards and mice came in between; this could be attributed to the higher number of heterogeneous user periodic cleaning and dusting of the hospital furniture and computers.

Similar to hospital setting, computer keyboards and mice could be mechanism for the transmission of pathogenic bacteria [13]. Previous studies done by (Schult JM) have demonstrated that other shared communication equipment

such as telephones can also be contaminated with potentially pathogenic microorganisms [14].

Other studies found that two deadly drug-resistant types of bacteria (vancomycin-resistant) *Enterococcus faecium* and methicillin-resistant *Staphylococcus aureus* could survive for up to (24) hours on a keyboard while another common bacteria (*Pseudomonas aeruginosa*) could survive for an hour[15]. Research by the Swinburne University Technology in Australia studied the amount and type of bacteria on personal faculty keyboard and shared keyboards and other surfaces around the University. They found that keyboards can have high levels of bacteria and shared keyboards tend to have more bacteria than those used by only one person [11].

### CONCLUSIONS

The increased availability of multiple-user computers in the internet café setting means that these items are handled by numerous users on daily basis. Given that computers are not routinely disinfected, so the opportunity of the transmitting contamination microorganisms is potentially great.

It was recommended that hand-washing hygiene should be adopted before and after using the computers to reduce microbial transmission, and also computer keyboards and mice should be cleaned with alcohol or other disinfectants on a regular basis. Eating should be avoided while using computers and hand washing hygiene practices should be encouraged, and maintained, and keyboard and mice should be cleaned with disinfectant at least weekly, or

frequently and be covered where necessary, which would reduce microbial load on the solid surfaces.

**REFERENCES**

- [1] Burke J.P., "Infection control a problem for patient safety", *N Eng. L J. Med*, 34:651-656, 2003.
- [2] Burse S., Fishbain JT., Uychara CF., Parker JM., and Berg BW., "Computer Keyboard Faucet hurdles as reservoirs of nosocomial pathogens in the intensive care unit", *Am. J. infection control*, 28 :465-471, 2000.
- [3] Hartmann B., Benson M., "computer keyboard and mouse as reservoir of pathogens in an intensive care unit", *J.clin. Monet computer*, 18 : 7-12, 2004.
- [4] Hubar JS., Pelon W., "Low cost screening far microbial contamination in aerosols generated in a dental office *General Dentistry*", 53 :270, 2005.
- [5] Buers S., Fishbain J., Uyehara C., Parker J., and Berg M., "Computer Keyboard and faucet handles as reservoirs of nosocomial pathogen in the intensive care unit", *Am J. infect control*, 28 :465-470, 2000.
- [6] Hirsch S., "Germ are working overtime at the office", <http://www.latimes.com>, 2005.
- [7] Anderson B., Enzo A., "Microbial contamination of computer Keyboard in University setting", *Am J. infect control*, 37 : 507, 2009.
- [8] Reynolds KS., watt PS., Boone SA., and Gerba CP., "Occurrence of bacteria and bio chemical markers on Public surface Int", *J. Environ. Health Res.*, 15 :225-234, 2005.
- [9] Sherman cappuccino, "Biochemical activities of Microorganisms", *Microbiology a Laboratory manual* 7th Ed, 143-203, 2009.
- [10] Green wood D., slack R., peuth every G., and Barer mike, "Medical microbiology", 17<sup>th</sup> ed Edinburgh London new York oxford Philadelphia stlouis Sydney Toronto, 175-293, 2007.
- [11] Anderson H., and palombo, "Microbial contamination of computer Keyboard in a university setting" *Am J. infect control*, 37 :507-509, 2009.
- [12] Rutrola WA., White MS., Gergen MF., And Weber DJ., "Bacterial contamination of disinfectants", *Infect contra and Hosp Epidemiol*, 27 :372, 2006.
- [13] Ferdinandus J., Hensckhe K., and palombo EA., "Isolation of pathogenic bacteria and opportunistic pathogens from public telephones", *Environ Health*, 1 :740, 2001.
- [14] Schult JM., Gill J., "Bacterial contamination of Keyboard in a Teaching Hospital", *Infect Hosp Epidermal*, 24 :302-303, 2003.
- [15] Lankford MG., Collins S., Youngberg L., Rooney D., warren JR., and Noskin GA., "Assessment of materials commonly used in health care: Implication for bacterial survival and transmission", *American journal of Infection control*, 34(5) :258-263, 2006.
- [16] Askok K., and MEENA S., "Computer components in college and its surroundings Encompass the pathogenic bacterial", *Joof Applied sciences in Environmental Sanitation*, 71 :43-47, 2012.
- [17] Anastasia des P., Pratt TL., Rousseau LH., Steinberg WH., And Joubert G., "Staphylococcus aureus on computer mice and Keyboard in intensive care units of the Universities academic hospital, Bloemfontein and ICU staffs Knowledge of its hazard and cleaning practices", *SAFRI J. Epidemiol Infect*, 24 (20) :22-26, 2006.
- [18] Deber E., and Heuvelink AE., "Methods for the detection and isolation of shiga toxin-producing *Escherichia coli*", *Sympersoc Apple Microbial*, (29) :133-143, 2000.
- [19] Fine MS., Smith MA., And Carson CA., "Prognosis and outcomes of patients with community-acquired", *Ameta-analysis JAMA*, 275(2) :134-141, 1996.
- [20] Marsden RA., "Solid-surfaced Infection control computer Key board", [www.cleanKeys.nl/white.pdf](http://www.cleanKeys.nl/white.pdf), pp.155, 2009.
- [21] Diggs R., Diallo A., Kan H., Glymph C., Furness BW., and chai SJ., "Nor virus outbreak in an elementary School-District of Columbia, February 2007. Centers for Disease control and prevention", *Morb, Mortal wkly, Rep*, 51 :1340-1343, 2008.





## Cervical Cancer Cells Classification Using Cytological Optical Images Features

Salim J. Attia

College of Dentistry, Baghdad University

Email: j.salim08@yahoo.com

### Article info

Received 7/9/2014

Accepted 30/11/2014

### ABSTRACT

The discussed approach in this paper is extracting the statistical features of digital optical images. The features include mean, coefficient of variance, contrast, maximum probability density and standard deviation. The decision making step in this research used minimum distance MD approach, which presented as a chosen technique to classify images.

In this paper we focus on human cervical cancer screening system that can be used by cytologists to differentiate benign from malignant in suspicious cases that cytologists face.

**Keywords:** Cervical Cancer, Classification, Benign, Malignant, Optical Images.

### الخلاصة

ان الطريقة المستعملة في هذا البحث هي استخراج الخصائص الاحصائية للصورة الرقمية البصرية. وتشمل هذه الخصائص المعدل ومعامل التباين والقيمة الاعلى لكثافة الاحتمالية والانحراف المعياري. ان مرحلة اتخاذ القرار تستند الى طريقة المسافة الصغرى (MD) بوصفها آلية اختيرت لتصنيف الصور. ركزنا في هذا البحث على نظام كشف سرطان عنق الرحم البشري والذي يستعمله المختصون بعلم الخلية للتفريق بين الانواع الحميدة و الخبيثة للحالات المشبهة بها التي يواجهونها.

### INTRODUCTION

In 2012, more than 12,000 women in the United States were diagnosed with invasive cervical cancer. Most of them are younger than 55. The cervix is part of a woman's reproductive system, it is in the pelvis. The cervix is the lower, narrow part of the uterus (womb). The cervix connects the uterus to the vagina. During a menstrual period, blood flows from the uterus through the cervix into the vagina. The vagina leads to the outside of the body. The cervix makes mucus. During coitus, mucus helps sperm move from the vagina through the cervix into the uterus.

During pregnancy, the cervix is tightly closed to help keep the baby inside the uterus. During childbirth, the cervix opens to allow the fetus to pass through the vagina. Cancer begins in cells and building blocks that make up tissues. Tissues make up the cervix and other organs of the body [1].

Normal cervical cells grow and divide to form new cells as the body needs them. When normal cells grow old or get damaged, they die, and new cells take their place. Sometimes, this process goes wrong. New cells form when the body does not need them, and old or damaged cells do not die as they should. The buildup of extra cells often forms a mass of tissue called a growth or tumor. Growths on the cervix can be benign (not cancer) or malignant (cancer). Benign growths (polyps, cysts, or genital warts) are not harmful don't invade the tissues around them. Malignant growths (cervical cancer) may sometimes be a threat to life as it can invade nearby tissues and organs, and can spread to other parts of the body. Cervical cancer begins in cells on the surface of the cervix but over time, the cervical cancer can invade more deeply into the cervix and nearby tissues [2].

Cervical cancer cells can spread by breaking away from the cervical tumor. They can travel through lymph vessels to nearby lymph nodes. Also, cancer cells can spread through the blood vessels to the lungs, liver, or bones. After spreading, cancer cells may attach other tissues and grow to form new tumors that may damage those tissues [3].

Many studies have been undertaken to assess the features that are salient to the diagnosis of cervical cancer and the factors that affect it and the classification of cervical cancer using cyto-histology images [4-6].

### MINIMUM DISTANCE CLASSIFICATION METHOD

To measure the degree of similarity between two groups of data, one can use minimum distance (MD) method which includes any point belonged to nearest class described by multidimensional space L. Minimum Distance is given by following equations [7]:

$$d(x_h, m_{ih}) = \sqrt{(x_1 - m_{i1})^2 + \dots + (x_L - m_{iL})^2} \quad (1)$$

or

$$d(x_h, m_{ih}) = |x_1 - m_{i1}| + \dots + |x_L - m_{iL}| \quad (2)$$

$x_h$  is a point in space L,  $m_{ih}$  is a vector in dimension L represent class i.

It is same for the distance of j class  $d(x_h, m_{jh})$ . The condition for verifying the minimum distance for all  $j \neq i$  is [8]:

$$d(x_h, m_{ih}) < d(x_h, m_{jh}) \quad (3)$$

**MATERIALS AND METODS**

Samples of slides contain different normal and abnormal cervical tissues were taken by Cyto-Brush and treated with Pap stain as seen in Figure (1), then imaged by microscope with digital camera connected to computer as a system prepared for this goal. Then applying the segmentation technique called adaptive imaging threshold procedure to separate the 100 images of cells [9].

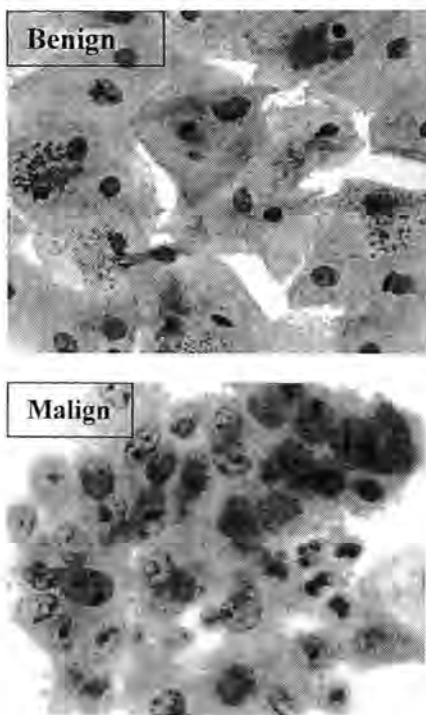


Figure 1: Benign and Malignant cases

**Features**

**Mean:**

The average pixel value taken to be equal to the average brightness or intensity and computed using equation(4), [10]:

$$\mu = \frac{1}{MN} \sum_{x=1}^M \sum_{y=1}^N I(x,y) \tag{4}$$

where M, N are the dimensions of image and I(x,y) is the pixel intensity value (0-255 for a 256 bit image).

**Coefficient of variance:**

Coefficient of variance is defined as the ratio of standard deviation to the mean and calculated from following equation [11]:

$$C_v = \frac{\sigma}{\mu} \times 100\% \tag{5}$$

Sometime  $C_v$  is assumed as a measure to difference in digital image.

**Contrast:**

The term contrast generally refers to the intensity difference between given light and dark values. If the difference is great then the contrast is said to be high; if

small, then the contrast is low. Contrast can be computed in several ways but one of the most common ways is the Michelson formula. The Michelson formula is used to compute the contrast of a periodic pattern, and is defined as [12]:

$$C = \frac{I_{max} - I_{min}}{I_{max} + I_{min}} \tag{6}$$

Where  $I_{max}$  and  $I_{min}$  refer respectively to the maximum and minimum luminance values in the pattern.

**Max P(I):**

When normalized by the size of the image, the histogram yields the (discrete) Probability Density Function P(I) of the gray levels. Thus, measures derived from the normalized histogram of an image of an object provide statistical descriptors characterizing the gray-level distribution of the object [13]. We consider the discrete P(I) [14]:

$$P(I) = \frac{h(I)}{N} \dots\dots\dots 7$$

Where  $h(I)$  is the number of pixels with n value and N is the total number of pixels.  $Max P(I)$  is the upper value of P(I).

**Standard deviation (Std):**

The Standard Deviation is the most commonly used index of variability and is a measure related to the average distance of the scores from their mean value. This is also an indicator of contrast in the image. It is computed using the following result [15]:

$$\sigma = \sqrt{\frac{1}{MN} \sum_{x=1}^M \sum_{y=1}^N (I(x,y) - \mu)^2} \tag{8}$$

The standard deviation is important in identifying the 'details content in an image.

**RESULTS AND DISCUSSION**

Mean quantity in common usage give a measure of centrality. It has widest range and takes in account all pixels of image and gives the average of all values of pixels. It is well known that when the values of pixels increase, the image will be shiner and lighter, therefore our results (Mean) values reflect the fundamental observation (compatible with known information on the samples used), which is that images of malignant cases tend to be lighter and paler than those of benign cells.

The values of Std in benign cells are also smaller than those of malignant cells. Standard deviation is considered as a measure of dispersion. It can therefore be compared with the mean to gain some measure of the degree of spread of the distribution. So the results are compatible with the known nature of cancerous case included more disturbance in structure in malignant than benign cells.

The Coefficient of Variance and Contrast values as measures of difference in digital image are found bigger in malignant than in benign.

Max P(I) values reflect the similarity in images of cells because the repetition of same pixel value in image. The benign cells images have much similarity because they have bigger maximum frequency and the malignant cells images have relatively little similarity because they have smaller maximum frequency. This is compatible with what we guess about the situation in malignancy case, which is characterized by less similarity and this reflects abnormality and disorder state in it.

Tables (1) and (2) of different features explain how these features of both benign and malignant cases overlap with each other in a limited range; also see Figure (2). The overlap ratio between benign and malignant of Mean is 10%, Coef. of variance is 38%, Contrast is 32%, Max P(I) is 8% and Std is 5%.

Minimum Distance method MD is applied to classify cervical cells. It is designed by MATTLAB software version 10, as shown in Algorithm (1).

The input data was subdivided into two subsets: training 50%, and test 50%.

The minimum Euclidean distance is computed between a column vector of test data required to classify and the

collection of column vectors in the features matrix of training data. The algorithm computes the minimum distance and finds the column vector in matrix that is closest to test vector. It gives this closest column vector, its index in matrix which explains the class of vector (benign or malignant)

It is found that the MD investigated was able to give 98% accuracy.

**CONCLUSIONS**

Each feature is not sufficient to differentiate clearly between Benign and Malignant cases. This is noticed in overlap ratio of each feature, there is confusion state in overlap region. But for five group features as combination we get good ability to recognize the class of each data with high accuracy (98%) in classification process altogether with Minimum Distance approach.

Table 1: Statistical features ranges of Benign and Malignant cases

Features	Benign Min- Max	Malignant Min- Max	Overlap Range	Full Range
Mean	57-113	102- 164	102-113	53-164
Coef. of Variance	0.050-0.1519	0.0815-0.2353	0.0815-0.1519	0.050-0.2353
Contrast	0.1084-0.3381	0.2174-0.4895	0.2174-0.3381	0.1084-0.4895
MaxP(I)x10 <sup>-2</sup>	6.30 -23.74	2.01-7.40	6.30-7.40	2.01-23.74
Std	3 - 12	10 - 27	10-12	3-27

**First step:**  
 Determining: the column vector  $x$  included the values of features

**Second step:**  
 Inupt the collection of  $x$  and other column vectors in a matrix represent the classes

**Third step:**  
 Calculating distance between the vector  $x$  and other columns  
 Which represent benign and malignant cases

**Fourth step:**  
 Verifying the minimum distance by two conditions:  
 $d(x_k, m_{ia}) > d(x_k, m_{jb})$  for  $i$  class (benign) or  $d(x_k, m_{ia}) < d(x_k, m_{jb})$  for  $j$  class (malignant)

Algorithm 1: Computing the Minimum Distance of the Two Classes

Table 2: The overlap ratios between benign and malignant features

Features	Overlap Ratio
Mean	10%
Coef. of Variance	38%
Contrast	32%
MaxP(I)x10 <sup>-2</sup>	5%
Std	8%



Figure 2: Overlap ratio

## REFERENCES

- [1] "What You Need To Know About Cervical Cancer", U.S. Department of Health and Human Services, National Institutes of Health (NCI), 2012.
- [2] Munoz N., Bosch FX., de Sanjose S., Herrero R., Castellsagué X., Shah KV., Snijders PJ. and Meijer CJ., "Epidemiologic classification of human papillomavirus types associated with cervical cancer", *N. Engl. J. Med.*, 348(6):518–527, 2003.
- [3] Snijders PJ., Steenbergen RD., Heideman DA. and Meijer CJ., "HPV-mediated cervical carcinogenesis: concepts and clinical implications", *J. Pathol.*, 208(2):152–164, 2006.
- [4] Kim Kwang Baek, "Nucleus Segmentation and Recognition of Uterine Cervical Pap-Smears", LNAI 4482, 2007.
- [5] Walker D., "A Study of the Morphological Parameters of Cervical Squamous Epithelium", IOP, 2003.
- [6] Wang Yin Hai, "Computer Assisted Diagnose of Cervical Intraepithelial Neoplasia Using Histological Virtual Slide", Queen University of Belfast, 2008.
- [7] Umbaugh S. E., "Computer Vision and Image Processing", Prentice-Hall, 1998.
- [8] Richards J. A., "Remote Sensing Digital Image Analysis", Springer-Verlag, 1999.
- [9] Salim J. Attia, "Diagnosis of Breast Cancer Images Using Fuzzy Logic Technique", Ph.D. Thesis Submitted to the council of the College of Science Al – Mustansiriyah University, 2012.
- [10] Gomes, J. and Velho, L., "Image Processing for Computer Graphics", Silvio Levy, New York, Inc., 1997.
- [11] Jain K., "Fundamentals of digital image processing", Prentice Hall, India, 2000.
- [12] Eli Peli, "Contrast in complex images", *J. Opt. Soc. Am.*, 7(10):122-131, 1990.
- [13] John C. Russ, "The Image Processing Handbook", Third Edition, CRC Press LLC, 1998.
- [14] Qiang Wu., Fatima A. Merchant and Kenneth R. Castleman, "Microscope Image Processing", Elsevier Inc., 2008.
- [15] Blackledge J. M. and Dubovitskiy D. A., "Object Detection and Classification with Applications to Skin Cancer Screening", *International Transactions on Intelligent Systems*, 1(1):34-45, 2008.



## Relationship between Some Bacterial Adhesion Ability to Females' Epithelial Cells and Diabetes

Siham Sh. AL-Salihi

Foundation of Technical Education, Medical Lab. Techniques department, College of Technology, Kirkuk, Iraq

### Article info

Received 29/9/2014

Accepted 30/11/2014

Key words:  
UTI,  
bacterial  
adhesion and  
diabetes women

### ABSTRACT

The aim of this research is to determine the relationship between adhesion ability of important bacteria causes urinary tract infection to females' epithelial cells in diabetic and non diabetic women. For this study 135 female were eligible, their ages were 10-60 years old. They were divided into six groups; two of the groups were consist of 15 healthy married and 15 healthy single women whom were used as controls. The other four groups included married and single diabetic women (15 females for each group), married and single diabetic women with other type of diseases (50 and 25 female for each group respectively). The adhesion property of the bacteria (*E. coli*, *Klebsiella pneumoniae*, *Proteus mirabilis*, and *Staphylococcus aureus*) was tested on the females' uroepithelial and buccal cells. Regarding the age group, the significantly highest adhesion rate to uroepithelial cells were in 50-60 years and 40-49 years age groups for all the bacteria, while to buccal cells the highest were in 10-19 years and 50-60 years groups. The bacteria had adhered more significantly to uroepithelial and buccal cells from diabetic than none diabetic women, and even more in married diabetic women than in married none diabetic one. Adding mannose or sucrose to the incubation media had significantly decreased the adhesion ability of *E. coli*, *K. pneumoniae*, and *P. mirabilis* but not affected the *S. aureus*. The mannose was significantly decreased the adhesion ability of the bacteria than sucrose. The adhesion ability of the bacteria was increased to uroepithelial cell in diabetic married and single women with UTIs and kidney problems, while for buccal cells it was increased in influenza suffering patients. Increasing incubation time had increased the adhesion rate of the bacteria, the highest was for 60-75 min. and the lowest was for 15 min. for each of uroepithelial and buccal cells. We can conclude that adhesion ability of bacteria was increased to uroepithelial cell in diabetic married and single women.

### الخلاصة

إن الهدف من هذا البحث هو تحديد العلاقة بين قابلية التصاق أهم أنواع البكتريا المسببة لالتهاب المجاري البولية بالخلايا الظهارية لدى النساء المصابات وغير المصابات بداء السكري. شملت الدراسة 135 أنثى تراوحت أعمارهن بين 10-60 سنة. قسمت الإناث إلى ست مجاميع. تألفت مجموعتين متناهما من 15 أنثى سليمة متزوجة وغير متزوجة اللاتي مثلن مجموعة سيطرة. أما المجاميع الأربعة الأخرى فقد تضمنت 15 أنثى متزوجة وغير متزوجة مصابات بداء السكري و25 و50 أنثى متزوجة وغير متزوجة مصابات بداء السكري مع أمراض أخرى على التوالي لكل مجموعة. اختبرت خاصية الالتصاق لبعض أنواع بكتريا التهاب المجاري البولية (*Escherichia coli*, *Klebsiella pneumoniae*, *Proteus mirabilis* و *Staphylococcus aureus*) على الخلايا الظهارية البولية والفموية للإناث. أثرت المراحل العمرية معنويا على معدل التصاق البكتيريا. وكان المعدل الأعلى للخلايا الظهارية البولية للمراحل العمرية 50-60 و40-49 سنة لكل أنواع البكتيريا، بينما كان المعدل الأعلى للخلايا الظهارية الفموية للمراحل 10-19 و50-60 سنة. بينت النتائج أن التصاق البكتيريا بالخلايا البولية والفموية كان بمعدل أكبر وبفرق معنوي في النساء المصابات بالسكري عنه عند غير المصابات، وبمعدل أكبر في النساء المتزوجات المصابات عنه عند غير المتزوجات المصابات. أدى إضافة سكر المانوز أو السكروز إلى وسط الحضان إلى تقليل قابلية التصاق بكتيريا *E. coli*, *K. pneumoniae* و *P. mirabilis* بينما لم يؤثر على معدل التصاق بكتيريا المكورات العنقودية. وكان معدل التثبيت أعلى في المانوز عنه في السكروز. ازدادت قابلية البكتيريا للالتصاق بالخلايا البولية معنويا لدى النساء المتزوجات وغير المتزوجات المصابات بالسكري والمصابات بإصابات سابقة لالتهاب المجاري البولية أو اللاتي يعانين من مشاكل كلوية بينما ازدادت قابليتها للالتصاق بالخلايا الفموية لدى النساء المصابات بالرشح (الانفلونزا). أدت الزيادة في وقت حضان البكتيريا إلى زيادة قابلية الالتصاق والمعدل الأعلى كان 60-75 دقيقة والأقل كان 15 دقيقة لكل من الخلايا البولية والفموية لكل أنواع البكتيريا. مما سبق يمكن أن نستنتج أن معدل التصاق البكتيريا بالخلايا البولية والفموية لدى النساء المصابات بالسكري المتزوجات وغير المتزوجات يزداد.

## INTRODUCTION

Urinary tract infection (UTI) is one of the most common infections in women [1]. The infection is caused most commonly by *E. coli* and *Staphylococcus* [2], other enterobacteriaceae, such as *Klebsiella* and *Proteus* occasionally cause UTI [1, 3]. Studies showed that approximately one half of all women will have a UTI in their life time [4, 5]. Women with diabetes mellitus (DM) have one increased incidence of UTI compared to healthy women [6, 7]. They are at increased risk for upper tract infection and sever complications occur more frequently [8, 9]. The incidence of UTI was twice in diabetic than in none diabetic women [7]. Diabetes caused several abnormalities of the host defense system that might result in a higher risk of certain infections, including UTI [10]. In addition, a higher glucose concentration in the urine may create culture medium for pathogenic microorganisms [11].

Another factor is the adherence ability of the bacteria; which differs from one to another depending on some factors like the general condition of the person and the sicknesses; studies indicated that the adherence of the microorganisms is better to epithelial cells obtained from patients than those obtained from healthy control subjects [12, 13]. Substance is the Tamm Horsfull Protein (THP), a large glycosylated polypeptide produced by renal tubular cells and excreted via the urine in daily amounts [14], studies have shown that the presences of those (THP) will decrease the binding of bacteria to uroepithelial cells, diabetic patients can have decreased (THP) production [11, 14]. Sever UTI in patients with diabetes mellitus including diabetic cytopathy and glycosuria, abnormal leucocytes function have been recorded [10, 11].

Various substances (glucose, mannose, and albumin) present in the urine of diabetic patients, these substances influence the adherence of bacteria to epithelial cells [14]. Pathogenic microorganism must first enter and adhere to host cell, once attached they become able to proliferate and subsequently cause clinical symptoms [15]. Distinct adherence factors are located on the surface of pathogens mediated attachment to complementary glycoprotein or oligolipids on host tissue [12]. Adhesions are found on the stiff, hair like structures known as fimbriae or pilli that form bonds with a host cell receptors site. Abundant studies suggest that bacterial adherence is mediated by fimbriae which adhere to structures on urinary tract cells and its important contributor to UT colonization [14, 16]. Structural component of p-fimbriae specifically pap E and pap F proteins may promote attachment of fibronectin [17, 18]. Because diabetic women have bacteriuria more often than women without diabetes, and the adherence of microorganisms to host cells is an important step in the pathogenesis of many infections [10], we tried to study the adhesion ability of some UTIs bacteria to human epithelial cells in a group of diabetes and none diabetes women.

## MATERIALS AND METHODS

### Population Study

A total of 135 females were included in this study, their ages were 10- 60 years, and they were divided in to six groups. Two of them 30 females (15 healthy married and

15 healthy single women) were used as controls. The remaining four groups were divided as follows: 15 married diabetic, 15 single diabetic, 50 married diabetic with other types of diseases, 25 single diabetic with other types of diseases.

### Bacterial Isolates

Bacterial isolates (*E. coli*, *K. pneumoniae*, *P. mirabilis*, *S. aureus*) were obtained from culturing urine of patient who was suffering from UTI in Kirkuk and Azadi Teaching Hospitals. The bacteria were isolated, identified by using routine colony characters, staining and biochemical methods [19].

### Bacterial Suspension

Two to three colonies from each bacteria were suspended in normal saline and washed three times, finally the bacteria was diluted in normal saline to a concentration of  $1.5 \times 10^8$  cell/ml by calibrating it with McFarland tube number 4 [14].

### Collections of Epithelial Cells

#### a-Uro epithelial Cells Collection

Thirty ml of urine from the 135 females under the study were collected in clean, dry containers, then centrifuged and washed thrice with saline and finally suspended in about 8 ml saline. The epithelial cells in this suspension were translated on to the surface of cover slips by adding the epithelial cells suspension in a petri dish containing a filter paper No.1 and allowing the cover slips to attach to the filter paper for 10 min. then dried [16].

#### b-Buccal Cells Collection

From the 135 females under the study the buccal cells were collected by scraping the inner side of the cheek with cotton tipped swab, which then immersed in 5ml normal saline to remove the adhered cells from the swab. The cells were washed thrice with saline then suspended in 4ml normal saline. The buccal cells were allowed to adhere to cover slips [13].

### Adherence Assay of Epithelial Cells

For each experiment the air dried cover slips containing the uroepithelial or buccal cells, which incubated with either 1 ml of bacterial suspension or 1 ml phosphate buffer saline (PBS) as negative control, with shaking 350 motilities/ min for 1 hr. at 37°C. After incubation, the suspension was washed four times (250g, 10 min) with PBS to remove any unattached bacteria, then fixed for 15 min in methanol, washed with saline, stained by 3% giemsa stain for 20 min. and washed with saline to remove excess stain. The number of bacteria adhering to each of the first 50 epithelial cells was counted with oil immersion lens light microscopy (1000 X). Epithelial cells that overlapped other cells were excluded from evaluation. The mean number of bacteria per cell was calculated. All experiments were performed in duplicate [14].

### The Effect of Mannose and Sucrose on Adhesion Mean

The same procedure as in step 5 was repeated with addition of 20 µl mannose or sucrose (0.3 3N) to the incubation media, the other steps were completed as in adherence assay of epithelial cells [14, 20, 21].

**The Effect of Time on Adhesion Mean**

The procedure as in adherence assay of epithelial cells [14] was done using different incubation time (15, 30, 60, 75 min.) [22].

**Statistical analysis**

Statistical analyses were performed using Chi-square test, which was used to compare categorical variables. A p-value less than 0.05 were considered significant.

**RESULT AND DISCUSSION**

The adhesion ability of some UTI bacteria (*E. coli*, *K. pneumoniae*, *P. mirabilis*, *S. aureus*) to uroepithelial and buccal cells were studied in 135 females (10-60 years)

whom divided in to six groups as mentioned above. The age group, Table 1 had significantly effected the adhesion ability of bacteria to epithelial cells, the highest was for 50-60 years followed by 40-49 and 30-39 years for uroepithelial, with rate 55.8, 40.4, 35.1, 26.8 bacteria\ cell for each of *E. coli*, *K. pneumoniae*, *P. mirabilis* and *S. aureus* respectively in 50-60 years. The significantly highest adhesion rate in buccal cells was for 50-60 year followed by 10-19, 40-49 year for all bacterial tested types.

The adherence of *E. coli* and *K. pneumoniae* were significantly more than the other two types of bacteria. The adherence property of the bacteria were significantly more strong in diabetic single women than none diabetic single women, Table 2. The highest rate (34.8, 31.6 bacteria\ cell) was for *E. coli* and *K. pneumoniae* respectively for uroepithelial cell, and a rate of 22.7 bacteria\ cell for *E. coli* in buccal cell.

Table 1: Adhesion Mean of Bacteria to Epithelial Cells According to Age Group

Age group	Adhesion mean to uroepithelial cells				Adhesion mean to buccal cells			
	Bacterial type				Bacterial type			
	<i>E. coli</i>	<i>K. pneumoniae</i>	<i>P. mirabilis</i>	<i>S. aureus</i>	<i>E. coli</i>	<i>K. pneumoniae</i>	<i>P. mirabilis</i>	<i>S. aureus</i>
10-19	18.1	18.7	10.3	10.5	29.2	26.9	18.7	15.5
20-29	21.21	23.9	18.6	19.96	15.6	12.4	9.9	7.3
30-39	46.3	39.1	33.3	25.4	18.5	13.6	11.2	9.6
40-49	48.9	33.6	30.6	26.9	22.7	20.1	13.8	12.8
50-60	55.8	40.4	35.1	26.8	31.3	28.9	20.1	18.3

Table 2: Adhesion Mean of Bacteria to Epithelial Cells in Single Women

Bacterial type	Adhesion mean to uroepithelial cells		Adhesion mean to buccal cells	
	Diabetes	None diabetes	Diabetes	None diabetes
<i>E. coli</i>	34.8	25.1	22.7	10.9
<i>K. pneumoniae</i>	31.6	22.4	18.6	8.8
<i>P. mirabilis</i>	24.9	19.7	12.5	6.1
<i>S. aureus</i>	18.3	11.5	8.4	5.6

Table 3: Adhesion Mean of Bacteria to Epithelial Cells in Married Women

Bacterial type	Adhesion mean to uroepithelial cells		Adhesion mean to buccal cells	
	Diabetes	None diabetes	Diabetes	None diabetes
<i>E. coli</i>	50.4	44.9	30.8	12.6
<i>K. pneumoniae.</i>	45.5	38.8	23.3	11.2
<i>P. mirabilis</i>	30.7	25.2	16.8	8.4
<i>S. aureus</i>	28.9	20.3	12.9	7.7

Table 4: Adhesion Mean of Bacteria to Epithelial Cells with Mannose in Single Women

Bacterial type	Adhesion mean to uroepithelial cells				Adhesion mean to buccal cells			
	Diabetes		None diabetes		Diabetes		None diabetes	
	+M	-M	+M	-M	+M	-M	+M	-M
<i>E. coli</i>	20.3	34.8	20.3	25.1	20.2	22.7	5.4	10.9
<i>K. pneumoniae</i>	24.4	31.6	17.5	22.4	12.1	18.6	5.5	8.8
<i>P. mirabilis</i>	19.9	24.9	15.8	19.7	18.2	12.5	6.3	8.1
<i>S. aureus</i>	18.1	18.3	10.8	11.5	8.2	8.4	5.1	5.6

M+ = with mannose, M- = without mannose

Table 5: Adhesion Mean of Bacteria to Epithelial Cells with Mannose in Married Women

Bacterial type	Adhesion mean to uroepithelial cells				Adhesion mean to buccal cells			
	Diabetes		None diabetes		Diabetes		None diabetes	
	+M	-M	+M	-M	+M	-M	+M	-M
<i>E. coli</i>	33.6	50.4	35.1	44.9	25.6	30.8	7.8	12.6
<i>K. pneumoniae</i>	33.3	45.5	30.2	38.8	17.9	23.3	8.8	11.2
<i>P. mirabilis</i>	24.2	30.7	21.1	25.2	10.2	16.6	8.2	10.4
<i>S. aureus</i>	24.4	28.9	19.8	20.3	11.7	12.9	9.2	9.7

+M = with mannose, - M = without mannose.

Table 6: Adhesion Mean of Bacteria to Epithelial Cells with Sucrose in Single Women

Bacterial type	Adhesion mean to uroepithelial cells				Adhesion mean to buccal cells			
	Diabetes		None diabetes		Diabetes		None diabetes	
	+S	-S	+S	-S	+S	-S	+S	-S
<i>E. coli</i>	39.6	34.8	20.6	25.1	19.6	22.7	6.8	10.9
<i>K. pneumoniae</i>	36.2	31.6	18.3	22.4	16.5	18.6	6.6	8.8
<i>P. mirabilis</i>	18.8	24.9	16.9	19.7	8.8	12.5	6.4	8.1
<i>S. aureus</i>	17.8	18.3	10.6	11.5	8.3	8.4	4.9	5.6

+S = with sucrose, -S = without sucrose

Table 7: Adhesion Mean of Bacteria to Epithelial Cells with Sucrose in Married Women

Bacterial type	Adhesion mean to uroepithelial cells				Adhesion mean to buccal cells			
	Diabetes		None diabetes		Diabetes		None diabetes	
	+S	-S	+S	-S	+S	-S	+S	-S
<i>E. coli</i>	44.1	50.4	39.7	44.9	22.2	30.8	10.4	12.6
<i>K. pneumoniae</i>	40.3	45.5	33.6	38.8	18.6	23.3	9.5	11.2
<i>P. mirabilis</i>	27.7	30.7	19.4	25.2	12.7	16.6	7.7	10.4
<i>S. aureus</i>	26.4	28.9	19.8	20.3	10.2	12.9	8.1	9.7

+S = with sucrose, -S = without sucrose

The adherence rate were significantly more strong in married diabetic than married none diabetic women, Table 3. The highest rate was for *E. coli* and *K. pneumoniae* with rate of 50.4, 45.5 bacteria\ cell for uroepithelial cell and 30.8, 23.3 bacteria\ cell for buccal cell for each bacteria respectively, followed by *P. mirabilis* and *S. aureus*. Adding mannose or sucrose to the incubation media had resulted in significantly decreasing the adherence mean of *E. coli*, *K. pneumoniae* and *P. mirabilis* in married or single groups. Adherence mean was constant with *S. aureus* bacteria and not effected with mannose or sucrose addition, Tables (4, 5, 6, and 7).

Regarding the diabetic women suffering from other diseases Tables (8 and 9), the bacteria was adhered significantly more to uroepithelial cells from diabetic women with history of recurrent UTI and kidney problems than other types of diseases. The highest rates (39.9, 31.6, 65.6, 60.4 bacteria\ cell) were for *E. coli* bacteria in both of diabetic single and diabetic married women respectively, while the highest adhesion rate (15.5, 39.9 bacteria\ cell) to buccal cell in both single and married group respectively.

Table 8: Adhesion Means of Bacteria to Epithelial Cells in Diabetic Single Women with other Diseases.

Bacterial type	Group	Adhesion mean to uroepithelial cells in diabetic women with						Adhesion mean to buccal cells in diabetic women with					
		Thyroiditis	Hypertension	Influenza	Kidney problem	UTI	Control	Thyroiditis	Hypertension	Influenza	Kidney problem	UTI	Control
		Bacterial types											
<i>E. coli</i>		25.9	28.3	24.2	31.6	39.9	25.1	9.8	11.1	13.9	13.2	15.5	10.9
<i>K. pneumoniae</i>		22.2	28.9	26.8	30.3	36.4	22.2	8.6	18.7	12.3	11.6	16.1	8.8
<i>P. mirabilis</i>		18.6	22.5	22.6	25.8	29.7	19.7	8.5	9.2	8.7	9.3	10.9	6.1
<i>S. aureus</i>		18.8	18.1	19.5	23.3	20.1	11.5	7.1	7.1	6.6	8.4	10.8	5.6

Table 9: Adhesion Mean of Bacteria to Epithelial Cells in Diabetic Married Women with other Diseases

Bacterial type	Group	Adhesion mean to uroepithelial cells in diabetic women with						Adhesion mean to buccal cells in diabetic women with					
		Thyroiditis	Hypertension	Influenza	Kidney problem	UTI	Control	Thyroiditis	Hypertension	Influenza	Kidney problem	UTI	Control
		Bacterial type											
<i>E. coli</i>		51.5	48.8	51.2	60.4	65.6	44.6	28.9	28.2	30.1	32.8	39.9	12.6
<i>K. pneumoniae</i>		45.8	43.3	46.2	51.4	53.5	38.8	30.7	29.8	27.6	29.2	39.5	11.2
<i>P. mirabilis</i>		29.8	29.2	30.1	31.7	39.8	25.2	18.1	16.8	16.5	17.2	21.3	8.4
<i>S. aureus</i>		25.2	26.6	29.1	32.8	35.3	20.3	13.5	12.1	12.9	13.1	19.7	7.7



Table 10: The Effect of Incubation Time on Adhesion Mean of Bacteria to Epithelial Cells in Single Healthy Women

Bacterial type	Incubation time period in min. in uroepithelial cells				Incubation time period in min. in buccal cells			
	15	30	60	75	15	30	60	75
<i>E. coli</i>	10.8	18.2	25.1	27.7	6.6	8.1	10.9	12.8
<i>K. pneumoniae</i>	10.1	17.3	22.4	25.5	3.9	5.6	8.8	8.9
<i>P. mirabilis</i>	6.2	10.9	19.7	21.2	2.2	4.5	6.1	7.5
<i>S. aureus</i>	5.4	7.7	11.5	13.9	2.8	3.7	5.6	6.6

The effect of incubation time on adherence mean is clear in table 10; the adherence mean had increased with time increasing. The highest was for 60 and 75 min. for both uroepithelial and buccal cells with rate of (25.1, 27.7, 10.9 and 12.8 bacteria\ cell) for each time respectively, in *E. coli*.

Adhesion is believed to be the first step in colonization which mediated by many ways. Adherence requires participation of two factors: host cell receptor and adhesion part on invading microbe [18]. The adhesion ability in this study was affected with age group; high adhesion rate was for cells from older persons. Confirmatory study [23] was found higher incidence of gram positive and negative bacteria in 30-60 age group. In females sexual intercourse is the most important factor predisposing to UTIs, one study demonstrated a 2.6 fold increased risk of UTI in females that have sexual intercourse compared to females that do not have intercourse [24], further more elderly women have decreased Tamm horsfall protein (protective mucoid substance) in urine [25], and decreased estrogen hormone. Tamm-Horsfall protein may prevent one from getting UTI by trapping type 1 fimbriated bacteria and interferes the bacterial adherence to human uroepithelial cells [26, 27]. The role of estrogen in the pathogenesis of UTIs is controversial. *In vitro* studies have demonstrated that estrogen permits adherence of uropathogens to vaginal epithelial cells [28]. Alterations in the vaginal mucosa thought to play an important role for acute disruptions of mucosal barrier that alter normal flora and induce increased receptivity for uropathogens [24]. Host factors that contribute to the disruption of this mucosal barrier are sexual intercourse, diabetes mellitus and non-secretor status these all may lead to increased density of adhesion receptors. Diabetes mellitus, sickle cell disease, hyperphosphataemia, gout and analgesics are also associated with altering the host's natural defense mechanisms. The incidence of pyelonephritis is up to fivefold higher in diabetics compared to non diabetic patients [29]. In fact, a study showed that half of females aged 61 or older had genitourinary symptoms and 29% of this cohort also complained of urinary incontinence. It has also been shown that a greater number of uropathogens attach to epithelial cell surface in females that are older than 65 years of age compared to premenopausal females [30].

Our results had showed that the bacteria were adhered more to cells of married than single women. Married women have sexual activities which may lead to more UTIs infection, and cell surface alteration. Also our results showed that cells from diabetic women have more ability to bacterial adhesion, this could be related to many reasons

as diabetic cytopathy, glycosuria or abnormal leukocyte function or receptors in cells. Various substances present in urine of diabetes [glucose, mannose, albumin, Tamm-horsfall protein] these substance influences the adherence of bacteria to epithelia cells [14]. Bacterial virulence factors play a significant role in determining whether an organism will invade the urinary tract and the level of infection acquired. Uropathogenic *E. coli* is present within bowel flora and pathogenic strains of this microorganism can infect the urinary tract by expressing specific virulence factors that permit adherence and colonization of the lower urinary tract [31, 32].

The mannose or sucrose adding in this study had decreased the adhesion of the bacteria for both uroepithelial and buccal cell in all tested groups. This inhibitory effect depends on the bacteria being mannose depended adhesion or none depended. Type 1 fimbriae bind to mannose containing structure found in many different cell types, including the major protein found in human urine. Adhesions found on the surface of the bacterial membrane are responsible for initial attachment onto urinary tract tissues [21, 26]. Adhesions to uroepithelial cells were inhibited by different types of carbohydrates, [12, 20] were identified a mannose-specific lectin on the surface of adherent strains of *E. coli* and Mannose functions as the primary bladder cell receptor site for uropathogenic *E. coli* (UPEC) to bind. Likewise, [33, 34] were reported that the first step in the adhesion of UPEC to the uroepithelial cells is the binding of Fimbriae H adhesion to the bladder epithelium via interaction with mannose moieties on the host cell surface. Thus the use of mannose or mannose analogs can help to block adhesion of bacteria to the bladder epithelium]. Adherence mean of bacteria in our study was more to cells from diabetic UTI and kidney diseased patients. A previous history of UTI is a strong predictor of having a subsequent UTI. This may be attributable to a host's biological or behavioral features or from persistent colonization of a particular bacterial strain [35]. In healthy patients the epithelium lining the bladder is quiescent as the umbrella cell layer is renewed. However these normally repressed proliferation and differentiation cascades are rapidly activated after the infective process in the murine cystitis model. These proliferation cascades have the potential to induce effective regeneration of an umbrella cell layer within 24 hours of the exfoliation process. In mice has demonstrated that exfoliation of uroepithelial cells prevents uropathogenic *E. coli* from forming clusters [36]. Notably, mice that elicited a mild exfoliation process in response to the uropathogens were more likely to form biofilm that migrated into deeper layers.

Relationships between diseases and the adherence of microorganisms to patient cells have been investigated before, it was found that microorganisms adhere more to buccal epithelial cells isolated from patients who either have a chronic disease or smoke [13, 37]. This is supported by [13] who showed that the receptors on the buccal cells of severely ill patients have a decreased amount of sialic acid and galactose compared with those of healthy control subjects. Other authors suggested that the altered receptor on the epithelial cells of the upper respiratory tract might explain the high prevalence of gram-negative bacterial colonization and pneumonia in the critically ill patients [12, 37]. The same increase has been described in studies on vaginal, buccal, uroepithelial and periurethral cells isolated from patients women with recurrent UTIs [38]. Epithelial cell receptivity plays an important pathogenic role in female patients that are susceptible to recurrent UTI [34]. Buccal cell receptivity is also increased for different strains of *E. coli* in females with increased vaginal cell receptivity. Increasing incubation time had increased the bacterial adherence mean; incubation time increasing will offer better chance for bacterial adherence and colonization [22].

### CONCLUSIONS

The present study found that the adhesion ability of the bacteria was increased to uroepithelial cell in diabetic married and single women, and the bacteria was adhered more to uroepithelial cells from diabetic women with history of recurrent UTI and kidney problems than other types of diseases.

### REFERENCES

1. Medscape, from ACP medicine. "Urinary tract infections". Copyright, 2005.
2. Mahmood AM. "Prevalence and Antimicrobial Susceptibility of Pathogens in Urinary Tract Infections". Journal of Al-Nahrain University, 14 (4); 146- 152, 2011.
3. Semins M. "Medical evaluation and management of urolithiasis". Ther. Adv. Urol, 2(1): 3-9, 2010.
4. Fareid MA. "Frequency and Susceptibility Profile of Bacteria Causing UTIs among women", New York Science Journal,; 5(2):72-80], 2012
5. Abdel Fattah M, Nassser ME, Soliman Y, Baki AH, Gamal MA, Heissein H.A Follow up "Study of Active Urolithiasis at Ain Shams University Hospital- Etiological Factors and Role of Chronic Preventive Strategies". Journal of American Science., 8 (1s), 2012.
6. Fünfstück R, Nicolle LE, Hanefeld M, Naber KG. "Urinary tract infection in patients with diabetes mellitus", Clin. Nephrol., 77(1):40-8, 2012.
7. Geerlings SE, Stolk RP, Camps MJ, Netten PM, Collet JT, Schneeberger PM, Hoepelman AIM: "Consequences of asymptomatic bacteriuria in women with diabetes mellitus. Arch. Intern. Med., 161:1421-1427, 2001.
8. Boroumand MA, Sam L, Abbasi SH: "A symptomatic bacteriuria in diabetic type-2 Iranian diabetic women: a cross sectional study". BMC women's health, 6(4), 2006.
9. Hoepelman AI, Meiland R, Geerlings SE: "Pathogenesis and management of bacterial urinary tract infections in adult patients with diabetes mellitus", J. Antimicrob. Agents, 22 (2): 35-43, 2003.
10. Bonadio M, Costarelli S, Morelli G, Tartaglia T. "The influence of diabetes mellitus on the spectrum of uropathogens and the antimicrobial resistance in elderly adult patients with UTI", BMC Infect. Dis., 6: 54, 2006.
11. Geerlings S E, Meiland R, Hoepelman A I: "Pathogenesis of bacteriuria in diabetes mellitus", Int. J. Antimicrob. Agents, 19 (6): 539-45, 2002.
12. Ghenghesh K S, Elkateb E, Berbash N, Nada R A, Salwa F, Rahouma AA, Seif-Enasser N, Elkhabroun MA, Belresh T and John D: "Diabetic patients in Libya: Virulence factors and phylogenetic group of *Escherichia coli* isolates", J. Med. Microbiol, 58: 1006-1014, 2009.
13. Weinmeister KD, Dal Nogare AR: "Buccal cell carbohydrates are altered during critical illness", Am J Respir Crit Care Med., 150: 131-134, 1994.
14. Geerlings SE, Meiland R, Van lith MC, Brouwer EC, Gaastra W, Hoepelman AIM. "Adherence of type 1-fimbriated *Escherichia coli* to uroepithelial cells more in diabetic women than in control subjects", Diabetes Care, 25:1405-1409. 2002.
15. Wu XR, Sun TT, Medina JJ: "In vitro binding of type 1-fimbriated *Escherichia coli* to uroplakins Ia and Ib: relation to urinary tract infections", Proc Natl Acad Sci U S A, 93: 9630-9635, 1996
16. Geerlings SE, Brouwer EC, Gaastra W, Stolk RP, Diepersloot RJA, Hoepelman AIM: "Virulence factors of *Escherichia coli* isolated from urine of diabetic women with asymptomatic bacteriuria: correlation with clinical characteristics", Antonie van Leeuwenhoek, 80:119-127, 2001.
17. Hull RA, Donovan WH, Terzo MD. "Role of type 1-fimbria and P-fimbria specific adherence in colonization of neurogenic human bladder by *Escherichia coli* IAI", infection and immunity, 70 (11):6481-6484. 2002.
18. Ofek I, Doyle RJ. "Bacterial adhesion to cells and tissue", Champan and hall, p 578, 1994.
19. Colle JG, Miles RS, Watt B. "Tests for the identification of bacteria", In: Mackie and MacCartney Practical Microbiology, 14<sup>th</sup> edn. New York: Churchill Livingstone Inc., 131- 49, 1996.
20. Schaeffer AJ, Mundsden SK, Jones JM. "Effect of carbohydrates on adherence of *Escherichia coli* to human urinary tract epithelial cells". Infect Immun., 1980, 30:531-537, 1980.
21. Hagberg L, Jodal ULF, Korhonen TK, Janson GL, Lindberg, ULF, Catharina SE, "Adhesion , hemagglutination and virulence of *Escherichia coli* causing UTI", Infection and Immunity, 31(2): 564-570, 1981.
22. Lindouist B, Libenthal E, Lee P, Stinson MW, Merrick JM. "Adherence of *Salmonella typhimurium* to small

- intestinal enterocytes of rat", *Infection and Immunity*, 55(12): 3044- 3050, 1987.
23. Enrico M, Vittorio G, Loredana D, Antonia IL, Roberto M, Paolo R, Clementina EC. "Gender and Age-Dependent Etiology of Community-Acquired Urinary Tract Infections", *The Scientific World Journal*, Volume 2012, Article ID 349597, 6 pages, 2012.
  24. Hooton TM, Scholes D, Hughes JP, Winter C, Roberts PL, Stapleton AE, Stergachis A, Stamm WE. "A prospective study of risk factors for symptomatic UTI in young women", *N Engl J Med*, 335(7): 468-74, 1996.
  25. Sobel JD, Kaye D. Reduced uromucoid excretion in the elderly (Letter). *J Infect Dis*, 152:653, 1985.
  26. Orskov I, Ferencz A, Orskov F. "Tamm-Horsfall protein or uromucoid is the normal urinary slime that traps type 1 fimbriated *Escherichia coli*". *Lancet I*, 887- 897, 1980.
  27. Dulawa J, Jann K, Thomsen M, Rambašek M, Ritz E. "Tamm Horsfall glycoprotein interferes with bacterial adherence to human kidney cells". *Eur J Clin Invest*, 18: 87-91, 1988.
  28. Haspels AA, Luisi M and Kicovic PM. "Endocrinological and clinical investigations in post-menopausal women following administration of vaginal cream containing oestriol. *Maturitas*", 3(3-4), 321-7, 1981.
  29. Stapleton A. "Urinary tract infections in patients with diabetes". *Am J Med*, 113 Suppl 1A, 80S-84S, 2002.
  30. Iosif CS and Bekassy Z. "Prevalence of genito-urinary symptoms in the late menopause", *Acta Obstet Gynecol Scand*, 63(3), 257-60, 1984.
  31. Schlager TA, Hendley JO, Bell AL and Whittam TS. "Clonal diversity of *Escherichia coli* colonizing stools and urinary tracts of young girls", *Infect Immun*, 70(3), 1225-9, 2002.
  32. Mulvey MA. "Adhesion and entry of uropathogenic *Escherichia coli*", *Cell Microbiol*, 4(5), 257-71, 2002.
  33. Kau AL, Hunstad DA and Hultgren SJ. "Interaction of uropathogenic *Escherichia coli* with host uroepithelium", *Curr Opin Microbiol*, 8(1), 54-9, 2005.
  34. Lau YE, Rozek A, Scott MG, Goosney DL, Davidson DJ and Hancock R E. Interaction and cellular localization of the human host defense peptide LL-37 with lung epithelial cells", *Infect Immun*, 73(1), 583-91, 2005.
  35. Fowler JE, Jr and Stamey T. A. "Studies of introital colonization in women with recurrent urinary infections. VII. The role of bacterial adherence", *J Urol*, 117(4), 1977.
  36. Anderson GG, Martin SM and Hultgren SJ. "Host subversion by formation of intracellular bacterial communities in the urinary tract", *Microbes Infect*, 6(12), 1094-10, 2004.
  37. El Ahmer OR, Essery SD, Saadi AT, Raza MW, Ogilvie MM, Weir DM, Blackwell CC. "The effect of cigarette smoke on adherence of respiratory pathogens to buccal epithelial cells", *FEMS Immunol Med Microbiol*, 23:27-36, 1999.
  38. Schaeffer AJ, Jones JM, Dunn JK. "Association of vitro *Escherichia coli* adherence to vaginal and buccal epithelial cells with susceptibility of women to recurrent UTI", *N Engl J Med*, 304(18), 1062-6. 1981.



## Evaluation of Vitamin D Status in Patients with Type 1 Diabetes Mellitus

Abdilkarim Yehia J. AL-Sammraie  
National Diabetes Center (NDC)

### Article info

Received 14/9/2014  
Accepted 30/11/2014

### ABSTRACT

Type 1 diabetes mellitus (T1DM) is an autoimmune disease which usually occurs early in life. Some researchers have been interested in a potential link between T1DM and vitamin D due to its ability in making the immune system smarter. The aim of this study is to assert the relationship between the severity and frequency of vitamin D deficiency and risk of developing T1DM in children and adolescents. Eighty (80) T1DM children and adolescents were studied, fasting plasma glucose, HbA<sub>1c</sub>, fasting plasma insulin, serum 25(OH) vit.D<sub>3</sub>, Ca, PO<sub>4</sub>, alkaline phosphatase, in addition to HOMA-IR and BMI were measured for these diabetic patients. These patients were compared with eighty (80) healthy children and adolescents age and sex matched. Thirty two (40%) diabetic patients were 25 (OH) vit.D<sub>3</sub> deficient, forty eight (60%) patients had normal levels, and fifteen (18.75%) of the control group were 25(OH) vit.D<sub>3</sub> deficient, sixty five (81.25%) had normal levels. Vitamin D levels were not significantly lower in diabetic patients compared to control group (23.1±7.2 vs. 24.8 ± 6.9 ng/mL). Serum Calcium of diabetic patients was significantly lower whereas serum phosphorous significantly higher (8.0±1.7 vs. 10.2 ±1.3 mg/dL), (5.2±1.3 vs. 4.0±1.1 mg/dL)(p< 0.01) respectively. Vitamin D levels correlated negatively with BMI (r= - 0.527, p< 0.01) and positively with diabetes duration (r= 0.449, p< 0.01) for those diabetic patients. Vitamin D deficient diabetic patients had significantly higher HOMA-IR and short duration in comparison to patients with normal vitamin D levels (3.3± 0.9 vs. 1.9± 0.5) (10±3.7 vs. 35±12.5 months) (p< 0.01) respectively. The present study show that vitamin D deficiency prevalence was higher in children and adolescent T1DM in comparison to healthy controls.

### الخلاصة

داء السكري النوع الأول هو مرض مناعي ذاتي ويحدث عادة في وقت مبكر من الحياة. يهتم بعض الباحثين بالعلاقة الاحتمالية بين داء السكري النوع الأول وفيتامين (د) وذلك لقابلية الفيتامين في تهيئة جهاز المناعة أكثر الغاية من الدراسة، التحقق من العلاقة بين شدة وتكرار نقص فيتامين (د) وخطر تكوين داء السكري النوع الأول في الأطفال و اليافعين. درس ثمانون (80) طفلاً و يافعا مصابا بداء السكري النوع الأول أذ قيست نسبة السكر و الأنسولين في بلازما الدم و خضاب الدم التراكمي ونسبة 25-(OH) vit.D<sub>3</sub> و الكالسيوم و أنزيم الفوسفات القاعدي بالإضافة إلى HOMA-IR ودالة كتلة الجسم، قورنت هذه النتائج بنتائج ثمانين (80) طفلاً و يافعا من الأصحاء من نفس الفئة العمرية والجنس. أظهرت النتائج أن (40%) أي (32) مريضاً مصاباً بداء السكري لديهم نقص فيتامين (د) وان (60%) أي (48) ليس لديهم نقص فيتامين (د) وان (18,75%) أي (15) من الأصحاء لديهم نقص فيتامين (د) مع (81,25%) أي (65) ليس لديهم نقص فيتامين (د). لم تظهر النتائج وجود نقص نوعي في مستوى فيتامين (د) عند المرضى المصابين بداء السكري عند مقارنة مستواه عند الأشخاص الأصحاء (7,2 ± 23,1 مقابل 6,9 ± 24,8 نانوغرام/مل) أظهرت النتائج وجود نقص نوعي في مستوى الكالسيوم وزيادة نوعية في مستوى الفسفور لدى مرضى السكري عند مقارنة نسبهم مع الأصحاء (8,0 ± 1,7 مقابل 10,2 ± 1,3 ملغم/ دسيليتر) (5,2 ± 1,3 مقابل 4,0 ± 1,1 ملغم/ دسيليتر) (P<0.01) على التوالي. كما أظهرت الدراسة وجود علاقة سالبة بين مستوى فيتامين (د) مع دالة كتلة الجسم (r = - 0.527, p< 0.01) -علاقة موجبة مع مدة المرض عند المرضى المصابين بالسكري (r= 0.449, p< 0.01). أكدت النتائج وجود زيادة نوعية في HOMA-IR و قصر مدة المرض عند مرضى السكري الذين لديهم نقص فيتامين (د) بمقارنة نسبهم مع نفس مرضى السكري الذين ليس لديهم نقص فيتامين (د) (3,3 ± 0,9 مقابل 1,9 ± 0,5) (10 ± 3,7 مقابل 35 ± 12,5 شهر) (p< 0.01) على التوالي. أوضحت الدراسة أن نسبة تكرار نقص فيتامين (د) لدى الأطفال و اليافعين المصابين بداء السكري النوع الأول يكون أكثر عند مقارنته لدى الأشخاص الأصحاء

### INTRODUCTION

There is a growing interest in the extra-skeletal effect of vitamin D in many researches[1]. Type 1 diabetes mellitus (T1DM) is associated with moderate changes in mineral density and strength, beside an increase in the prevalence of fracture risk.

Some studies suggest that vitamin D deficiency has a negative effect on insulin sensitivity and may lead to increase incidence of type 2 DM in adults[2-4]. Several

explanations for reduced bone mineral contents associated with diabetes have been proposed, including advanced glycation end products in bone collagen, inflammatory cytokines, and hypercalciuria associated with glycosuria and diabetic microangiopathy with decrease blood supply to the bone [5].

Significant vitamin D deficiency in children and adolescents with (T1DM) was shown in several recent

studies[6-10]. Other studies suggest that vitamin D deficiency may increase the risk of developing autoimmune disease including T1DM[10,11], and it is emphasized that this situation may have a negative effect on bone health[12-17]. This partly occurs through loss of vitamin D modulation of immune and inflammatory reaction in diabetes [18].

The variable frequency and prevalence of vitamin D deficiency in children and adolescents with T1DM and its effects on metabolic control and insulin requirement, still unexplained fully.

**Aim of study** The aim of this study is to assert the relationship between the severity and frequency of vitamin D deficiency and risk of developing T1DM in children and adolescents.

## MATERIAL & METHODS

A total of eighty (80) type 1 diabetic children and adolescents, (35) boys and (45) girls aged ( $13.7 \pm 1.4$  yrs) with a rang (6-16 yrs) have participated in the study. They attended the pediatric department of National Diabetes Center (NDC), Al-Mustansiriya University/ Baghdad, from January to September 2013. All had no other chronic diseases.

The diabetic subjects were compared with eighty (80) apparently healthy children (36) boys and (44) girls aged ( $13.5 \pm 1.8$  yrs) after taking their medical history as a control group matched for age and sex.

All the study subjects (patients and controls) were excluded from the study, if they had consumed any mineral supplementation, or vitamin D rich foods during the last (3) months from the day of taking blood sample.

Ten (10 mL) of venous blood were collected from 10-12 hrs. fasting diabetic and control groups. The samples were allowed to clot in plain tube at room temperature and serum was aspirated after centrifugation at (3000 rpm) for thirty minutes, divided in plastic tubes and stored at ( $-20^{\circ}\text{C}$ ) until the time of analysis of:

1- Fasting plasma glucose(FPG): was measured directly after separation using Enzymatic method, Biocon Kit, Germany.

2- HbA<sub>1c</sub> using Bio-Rad Laboratories device, program that utilizes principle of ion – exchange high-performance liquid chromatography (HPLC)( Germany).

3- Fasting plasma insulin using ELIZA Kit, DRG Instruments, Germany.

4- Serum Calcium using Teco diagnostic Kit, Anaheim-california,US

5- Serum phosphorus using Randox Kit, UK.

6- Serum alkaline phosphatase using Biolabe Kit, France.

7- Serum 25 (OH) vit.D<sub>3</sub> using de medi tech Kit / Germany.

- Body mass index (BMI) was calculated as the weight in kilogram(Kg) per height in meter squared(m<sup>2</sup>)(National Institute of Health 1998)[19].

**BMI= weight(Kg) / height(m<sup>2</sup>)**

-Homeostatic model assessment (HOMA-IR) insulin resistance was determined using the equation [20,21].

**HOMA-IR= FPI x FPG / 22. 5**

Where FPI is fasting plasma insulin concentration( $\mu$  IU/mL) and FPG is fasting plasma glucose(mmol/L).

Vitamin D status was classified according to the American Academy of Pediatrics (AAP)/L WEPS's recommendation on cut-off levels for status of vitamin D. A 25(OH)D level of ( $<5$  ng/mL) was considered as **sever deficiency**, a level of ( $5 - 15$ ng/mL) as **deficiency**, a level of ( $15-20$  ng/mL) as **insufficiency**, and a level of ( $20-100$  ng/mL) as **normal (sufficient)**.

The patients of this study were divided into two groups according to their vitamin D status.

Those with serum 25(OH)vitamin D levels( $<20$  ng/mL) were grouped as vitamin D **insufficient and deficient**, and those with serum 25(OH)vitamin D levels( $> 20$ ng/mL) as **normal** with regard to vitamin D status[22].

## RESULTS AND DISSCUSSION

Sex (male/ female), age, puberty stage, BMI, waist, hip circumference and waist to hip ratio for T1DM and control subjects are listed in table (1)

Table 1: Clinical Characteristics of Study Subjects

Subject	T1DM	Control	P value
Number	80	80	-
Sex(M/F)	35/45	36/44	-
Age(yrs)(Mean±SD)	$13.7 \pm 1.4$	$13.5 \pm 1.8$	N.S
Prepubertal	37	40	<0.05
Puberty	30	25	<0.05
Young adults	13	15	<0.05
BMI(Kg/m <sup>2</sup> ) (Mean±SD)	$25.7 \pm 1.3$	$24.1 \pm 2.0$	N.S
Waist(cm) (Mean±SD)	$78.2 \pm 2.9$	$76.7 \pm 5.2$	N.S
Hip(cm)(Mean±SD)	$86.9 \pm 2.1$	$89.1 \pm 3.5$	N.S
Waist/ Hip ratio	0.89	0.86	N.S
Disease duration(Months)	21(14-52)	-	

Not significant(> 0.05) =N.S

Table 2: Biochemical Analytics of Study Subjects

Subject	T1DM	Control	P value
FPG(mmol/L) (Mean ± SD)	$14.1 \pm 1.5$	$5.3 \pm 1.1$	<0.01
FPI( $\mu$ IU/mL) (Mean ± SD)	$5.1 \pm 1.6$	$6.2 \pm 2.9$	<0.05
HbA <sub>1c</sub> % (Mean ±SD)	$8.1 \pm 1.1$	$5.2 \pm 0.9$	<0.001
HOMA-IR (Mean ±SD)	$3.3 \pm 0.9$	$1.9 \pm 0.5$	<0.01
S. Ca <sup>2+</sup> (mg/dL) (Mean ±SD)	$8.0 \pm 1.7$	$10.2 \pm 1.3$	<0.01
S. PO <sub>4</sub> (mg/dL) (Mean ±SD)	$5.2 \pm 1.3$	$4.0 \pm 1.1$	<0.01
S. ALP (IU/L) (Mean ±SD)	$220 \pm 50$	$200 \pm 60$	N.S
S.25(OH)vit.D(ng/mL)(Mean ±SD)	$23.1 \pm 7.2$	$24.8 \pm 6.9$	N.S

-Value <0.05 indicates a significant differences.

From a total of eighty (80) T1DM children and adolescents (3, 30, 13), with eighty (80) control subjects (40, 25, 15), are prepubertal, puberty and young adults respectively.

Thirty-two (40%) diabetic patients were vitamin D deficient, while forty-eight (60%) cases had normal vitamin D level. On the other hand, fifteen (12.75 %) of the control group, were vitamin D deficient and sixty-five ( 87.25%) had normal vitamin D level.

Vitamin D levels were not significantly lower in diabetic patients compared to control group.

Serum Calcium levels were significantly lower, while serum phosphorous and fasting plasma glucose levels were significantly higher in T1DM compared to their levels in control group, as shown in table (2) (P<0.01).

In addition to that, vitamin D deficient diabetic patients had significantly higher HOMA –IR and short duration

than those of diabetic patients with normal vitamin D levels ( $P < 0.01$ ).

Beside that serum levels of vitamin D in diabetic patients showed significant negative correlation with BMI ( $r = -0.527$ ,  $P < 0.01$ ) and positive correlation with diabetic duration ( $r = 0.449$ ,  $P < 0.01$ ).

As low vitamin D level is thought to be negatively involved in induced immune mediated  $\beta$ - cell destruction as well as calcium mediated dysfunction leading to onset of clinical diabetes, the level of vitamin D believed to be low at the time of diagnosis.[12-14]

In the present study, in spite of vitamin D levels were lower in diabetic patients compared to that of the control group at the time of the present study ( $23.1 \pm 7.2$  vs.  $24.8 \pm 6.9$  ng/mL), but these levels were not significantly different ( $P > 0.05$ ). The results are disagreed with those of others, whom found that 25(OH)vitamin D levels in new case T1DM were low compared to healthy control ( $P < 0.01$ )[16, 23,24] The small sample size was one of the study limitations and multicenter approaches may be necessary to attain larger sample size.

Some researchers suggested that vitamin D deficiency correlates with severity and frequency of T1DM and that vitamin D supplementation decreases the risk of developing T1DM have been reported.[25-27]

Besides that, some investigators concluded their results, that the frequency of vitamin D deficiency in children and adolescent with T1DM was highly variable and may be high as (90%) or low as (15%)[15-17, 28-30]. The causes of different frequencies could be related to the variability in the definition of vitamin D deficiency. Dietary intake, dark skin color, genetic predisposition, sun avoidance behavior, in addition to latitude and geographical environment may influence this variability[30]. In this study, the prevalence was (40%) which was similar to those of some [14] and disagree with others [15,17,28,31]. Understanding the nature of low vitamin D levels in children with T1DM is important because it may explain the mechanisms of autoimmune  $\beta$ - cell destruction, and may lead to interventions that preventing or delaying insulin dependence by using vitamin D supplementations or its analogues.[30]

Serum calcium levels significantly lower and serum phosphorus levels were significantly higher in T1DM when compared to their levels in control group ( $8.0 \pm 1.7$  vs.  $10.2 \pm 1.3$  mg/dL) ( $5.2 \pm 1.3$  vs.  $4.0 \pm 1.1$  mg/dL) ( $P < 0.01$ ) respectively. This agrees with a study done by [32].

On the other hand, obesity could be a risk factor in term of Hypovitaminosis D in adolescent, so that vitamin supplementation should be administrated to adolescent.[33,34]

The present study, confirms the above fact, that the study showed a significant negative correlation between vitamin D levels with BMI ( $r = -0.527$ ,  $P < 0.01$ ) and positive correlation with diabetes duration ( $r = 0.449$ ,  $P < 0.01$ ) for those diabetic cases. These results concords with the results taken from the 2001-2004 National Nutrition and Health Survey in USA, which indicates that metabolic syndrome prevalence was 3.8 folds higher among obese

adolescents whose 25-(OH)D levels were lower than (15 ng/mL) as compared to those with levels higher than (26 ng/mL).[35]

In addition to that, the study showed that vitamin D deficient in diabetic patients had significantly higher HOMA-IR and short duration than those of diabetic patients with normal vitamin D level ( $3.3 \pm 0.9$  vs.  $1.9 \pm 0.5$ ) ( $10.0 \pm 3.7$  vs.  $35.0 \pm 12.5$  months) ( $P < 0.01$ ) respectively, meanwhile, no significant difference was observed regards HbA<sub>1c</sub> ( $P > 0.05$ ). Those results were in agreement with [35], whom suggested that subjects with Hypovitaminosis D not only displayed impaired  $\beta$ - cell function causing impaired glucose homeostasis, but also were at risk of developing insulin resistance and metabolic syndrome compared with those with normal vitamin D levels.[36]

In the present study, no significant difference was observed between vitamin D deficient cases and those with normal vitamin D levels regarding fasting blood glucose and fasting insulin levels ( $P > 0.05$ ). This results are concordant with those of a report by others whom found that no correlations were found between insulin measurements during oral glucose tolerance test and vitamin D deficiency. They added that mean vitamin D levels were similar in subjects with and without metabolic syndrome. [37-39]

## CONCLUSION

The present study show that vitamin D deficiency prevalence was higher in children and adolescent T1DM in comparison to healthy controls. Even the present study does not show significant association between vitamin D levels and metabolic parameters, vitamin D status of those patients should be assessed in term of bone health. Although in the absence of signs of rickets, vitamin D supplementation should be described to those T1DM children and adolescent with vitamin D deficiency.

## REFERNCES

- [1] Bikle D, " Non-classic action of vit.D ", J.Clin. Endocrinal Metab., 94: 26-34, 2009.
- [2] Chiu KC; Chu A; Go VL; Saad MF, "Hypovitaminosis D is associated with insulin resistance and beta-cell dysfunction", Am J Clin Nutr.,79: 820-825, 2004.
- [3] Zhao G; Ford ES; Li C, " Associations of serum concentration of 25- hydroxyl vitamin D and parathyroid hormone with surrogate markers of insulin resistance among U.S. adults without physician-diagnosed diabetes", Diabetes Care.,33: 344-347, 2010.
- [4] Kayaniyl S; Vieth R; Retnakaran R; Knight JA; Qi Y; Gerstein HC; Perkins BA; Harris SB; Zinman B; Hanley A J, " Association of vit.D with insulin resistance and beta-cell dysfunction in subjects at risk for type 2 diabetes", Diabetes Care,33:1379 – 1381, 2010.
- [5] Ward DI; Yau SK; Mee AP; Mawer EB; Miller CA; Garland HO, " Functional, molecular and biochemical characterization of streptozotocin induced diabetes", J Am SocNephrol, 12: 779 – 790, 2001.

- [6] Green RM; Rogers MA; Bowling FG; Buntain HM; Harris M; Leong GM, "Australian children and adolescents with type 1 diabetes have low vitamin D levels", *Med J Aust.*, 187: 50-60, 2007.
- [7] Svoren BM; Volkening LK; Wood JR; Laffel LM, "Significant vitamin D deficiency in youth with type 1 diabetes mellitus", *J Pediatr.*, 154: 132-134, 2009.
- [8] Reis JP; VonMuhlen D; Miller ER 3<sup>rd</sup>; Michos ED; Appel L J, "Vitamin D status and cardio metabolic risk factor in the United State adolescent population", *Pediatrics*, 124: 371-379, 2009.
- [9] Delvin EE; Lambert M; Levy E, O'Loughlin J; Mark S; Gray-Donald K; Paradis G, "Vitamin D status in mostly associated with glycemia and indicators of lipid metabolism in French-Canadian children and adolescents", *J Nutr.*, 140: 987-991, 2010.
- [10] Holki MF, "Diabetes and vitamin D connection", *Curr Diab Repor.*, 8:393-398, 2008.
- [11] Danescu LG; Levy S; Levy J, "Vitamin D and Diabetes mellitus", *Endocrinology*, 35: 11-17, 2009.
- [12] Pozzilli P; Manfrini S; Crino A; Picardi A; Leomanni C; Cherubini V; Valente L; Khazrai M; Visalli N; IMDIAB group, "Low levels of 25-hydroxy vitamin D<sub>3</sub> and 1,25-hydroxy vitamin D<sub>3</sub> in patients with newly diagnosed type 1 diabetes", *HormMetab Res.*, 37: 680-683, 2005.
- [13] Littorin B; Blom P; Scholin A; Araqvist H J; Blohme; B olinder J; Ekbom-Schnell A; Erikson J W; Gudbjornsdottir S; Nystrom L; Ostman J; Sundkvist G, "Lower levels of plasma 25-hydroxy vitamin D among young adults at diagnosis of autoimmune in T1D compared with control subjects: results from the nationwide Diabetes Incidence study in Sweden(DISS)", *Diabetologia.*, 49:2847-2852, 2006.
- [14] Geer RM; Rogers MA; Bowling FG; Buhtain HM; Harris M; Leong GM; Cotterill AM, " Australian children and adolescents with T1D have low vitamin D levels", *Med J Aust.*, 187:59-60, 2007.
- [15] Svoren BM; Volkening LK; Wood J R; Laffel LM, " Significant vitamin D deficiency in youth with T1D mellitus", *J. Pediatr.*, 154: 132-134, 2009.
- [16] Borkar V V; Devidayal; Verma S; Bhalla AK, " Low levels of vitamin D in North Indian children with newly diagnosed type 1 diabetes", *Pediatr Diabetes*, 11:345-350, 2010.
- [17] Bener A; ALsaied A; AL-Ali M; AL-Kubaisi A; Basha B; Abrahm A; Guter G; Mian M, "High prevalence of vitamin D deficiency in T1D mellitus and healthy children", *Acta Diabetol.*, 46 :183-189, 2009.
- [18] Mathieu C; Van Etten E; Decallonne B; Guilietti A; Gysmans C; Bouillon R; Overbergh, "Vitamin D and 1,25- dihydroxy vitamin D<sub>3</sub> as immunomodulators in the immune system", *J steroid Biochem Mol Bio.*, 89: 449-452, 2004.
- [19] National Institute of Health; National Hearts, Lung, and Blood Institute Clinical, Guideline of the Identification, Evaluation, and Treatment of overweight and Obesity in Adults. The evidence Report, *Obese ,e Res*, 6(Suppl-2): 51S-209 S, 1998.
- [20] Wallace TM; Levy JC; Matthews DR, " Use and abuse of HOMA modeling", *Diabetes Care* ,27(6): 1487-1495, 2004.
- [21] Diabetes Epidemiology Collaborative Analysis of Diagnostic Criteria in Europe Study Group. Will new diagnostic criteria for diabetes mellitus change phenotype of diabetes epidemiology collaborative analysis of diagnostic criteria in Europe study group, glucose tolerance and mortality: comparison of WHO and American Diabetes Association diagnostic criteria. *Lancet*, 354: 617-621, 1999.
- [22] Misra M; Pacaud D; Petriyk A; Collett-Solberg PF; Kappy M, " Drug and therapeutic Committee of the Lawson Wilkins Pediatric Endocrine Society, Vitamin D deficiency in children and its management : review of current Knowledge and recommendations", *Pediatrics*, 122: 398-417, 2008.
- [23] Littorin B; Blom P; Scholin A; Arnquist H J; Blohme G; Bolinder J, " Lower levels of plasma 25-hydroxyvitamin D among young adults at diagnosis of autoimmune type 1 diabetes compared with control subjects", results from nationwide Diabetes Incidence Study in Sweden (DISS) *Diabetologia*, 49: 2847-2852, 2006.
- [24] Pozzilli P; Manfrini S; Crino A; Picardi A; IMIDIAB group, " Low levels of 25-hydroxyvitamin D<sub>3</sub> and 1,25-hydroxyvitamin D<sub>3</sub> in patients with newly diagnosed type 1 diabetes", *Horm Metab Res.*, 37: 680-683, 2005.
- [25] Hypponen E; Reunanen A; Jarvelin MR; Virtanen SM, " Intake of vitamin D and risk of type 1 diabetes: a birth – cohort study", *Lancet*, 358 : 1500-1503, 2001.
- [26] Stene LC; Joner G, "Use of liver oil during the first year of life is associated with risk of children onset type 1 diabetes: a large population-based, case control study", *Am J Clin Nutr.*, 78 : 1128-1134, 2003.
- [27] Gudrun LB; Sonja G; Thomas B; Christa S-N; Peter N John G S, " Prevalence and determination of osteoporosis in patients with type 1 diabetes mellitus", *BMC Endocrine Disorders*, 14: 33-45, 2014.
- [28] Tune O; Cetinkaya S; Kizilgum M, " Evaluation of the relation between vitamin D and insulin requirements and frequency of osteoporosis in children with type 1 diabetes", 49<sup>th</sup> Annual Meeting of ESPE September Espe 290: 22-25, 2010.
- [29] Bener A; Alsaied A; AL-Ali M; AL-Kubaisi A; Basha B; Abraham A, "High prevalence of vitamin D deficiency in type 1 diabetes mellitus and healthy children", *Acta Diabetol.*, 46: 183-189, 2009.
- [30] Bassam S; Bin-Abbas; Moslah A. Jabari; Sharifah D. Issa; Abdullah H; AL-Fares; Seleh AL-Muhsen, " Vitamin D level in Saudi children with type 1 diabetes", *Saudi Med J* , 32(6): 589-592, 2011.
- [31] Janner M; Ballinari P; Mullis EP; Fluck CE, " High prevalence of vit. D deficiency in children and adolescents with type 1 diabetes", *Swiss Med Wkly*, 140: 13091-13091, 2010.
- [32] Hamed EA; Abu Faddan NH; AdbElhafeez; Sayed D, " Parathormone-25(OH)-vitamin D axis and bone

- status in children and adolescents with type 1 diabetes mellitus", *Pediatr Diabetes*, 12: 536-546, 2011.
- [33] Filiz M; Cizmecio LUI; Nilay E; Uzay G; OnurHamzoo LU; Fifukru H, "Hypovitaminosis D in obese and overweight School children", *J.Clin ResPed Endo.*, 1(2): 89-96, 2008.
- [34] Shaum M. Kabadi; Brian K. LE; Longjian Liu," Joint effects of obesity and vitamin D insufficiency on insulin resistance and type 2 diabetes. Result from NHANES. 2001-2006", *Diabetes Care* June 2012.
- [35] Reis J P; Von Muhlen D; Miller ER 3<sup>rd</sup>; Michos ED; Appel L J," Vitamin D status and cardio metabolic risk factor in the United States adolescent population",*Pediatric*, 124: 371-379, 2009.
- [36] Chiu KC; Chu A; GO VLW; Saad MF," Hypovitaminosis D is associated with insulin resistance and B-cell dysfunction", *Am J ClinNutr*, 79 : 820-82, 20045.
- [37] Scraggy R; Holdway I; Singh V; MetclF P; Baker J; Dryson E," Serum 25-hydroxyvitamin D<sub>3</sub> levels decreased in impaired glucose tolerance and diabetes mellitus", *Diabetes Res ClinPract*, 27:181-188, 1995.
- [38] Hypponen E; Power C," Vitamin D status and glucose homeostasis in the 1958 British birth cohort: the role of obesity", *Diabetes Care*, 29:2244-2246, 2006.
- [39] Erdonmez D; Hatun S; Cizmecioglu FM; Keser A," No relationship between vitamin D status and insulin resistance in a group of high school students", *J Clin Res Pediatr En doocrinol* , 3(4): 198- 201, 2011.





## Antibacterial Activity of the Extracts of Chicken Gizzard Membrane Against Some Pathogenic Bacteria Isolated from Urinary Tract Infections

Hannaa Farhan Abbas

Department of biology, College of Science, Al- Mustansiriyah University, Baghdad, Iraq

E- mail: [hannaa\\_f1975@yahoo.com](mailto:hannaa_f1975@yahoo.com)

### Article info

Received 17/9/2014

Accepted 23/2/2015

### ABSTRACT

This study aims to develop a natural antibacterial material with broad spectrum activity against bacteria implicated in stones formation and urinary tract infection. Instead of the use of excessive and non-safe antibiotics and to block the prevalence of multi-drug resistant (MDR) bacterial isolates, which have increased in the last few years.

The aqueous extract of the chicken gizzard membrane was prepared with three different methods and used *in vitro* against some pathogenic bacteria isolated from patient suffering from UTI and urinary stones. The activity of chicken gizzard membrane was determent according to the presence or absence of bacterial growth in cultured plates treated with the aqueous extract.

The present study found that using a cold aqueous extract of the chicken gizzard membrane prepared freshly and used directly without any treatment had remarkable effectiveness compared with other extract, which heat treated and used after one hour or 24 hours of extraction.

We have tested a natural material, which may represent a good candidate for development as an antimicrobial for the most common UTI causative agents in the presence of urinary stones, such as: *E.coli*, *Proteus mirabilis* and *Staphylococcus aureus*.

UT infection associated with the urinary stones remains a major problem, because of the need for treatment with medical drugs (antibiotics) for a long time as well as the possibility of back infection again. The natural antimicrobial material such as the chicken gizzard membrane is an excellent candidate solution to this problem

### الخلاصة

تهدف هذه الدراسة الى تطوير مادة طبيعية ذات فعالية مضادة واسعة الطيف ضد البكتريا المسببة لالتهابات المجاري البولية، بدلا من الاستخدام الواسع وغير الامن لمضادات الحياة، فضلا عن منع ظهور السلالات البكتيرية المتعددة المقاومة للعقاقير والتي بدأت بالتزايد في السنوات القليلة الماضية. حضر المستخلص المائي للغشاء الداخلي لقانصة الدجاج بثلاثة طرق مختلفة واستخدم ضد بعض الاجناس البكتيرية المعزولة من مرضى يعانون من اصابات المجاري البولية. قدرت مدى فاعلية هذا المستخلص بالاعتماد على قياس اقطار مناطق التبيط في اطباق النمو البكتيري. وجدت الدراسة الحالية ان استخدام المستخلص المائي البارد لغشاء القانصة المحضر انيا والمستخدم مباشرة دون اية معاملة قد اظهر فاعلية ملحوظة مقارنة بالمحاليل الاخرى. اخترنا هنا مادة طبيعية قد تمثل منطلقا لتطوير مضادا بكتيريا ناجح لاغلب مسببات التهابات المجاري البولية مثل اشيريشيا القولون، الزانقات الزنجارية والمكورات العنقودية، اذ ان اصابات المجاري البولية تتطلب العلاج بمضادات الحياة لفترة طويلة مع امكانية تكرار الاصابة مجددا، الامر الذي يدفع الى ضرورة وجود مادة طبيعية بديلة ذات فاعلية عالية لحل هذه المشكلة

### INTRODUCTION

Urinary tract infections (UTI) are one of the common chronic and recurrent bacterial infections. Uropathogens, which are able to form biofilm, constitute a major etiological factor in UTI, especially among elder patients who are subject to long-term catheterization. It is caused by the capacity of the microorganisms for efficient and permanent colonization of tissues and also adhesion to diverse polymers used for urological catheter production such as propylene, polystyrene, silicone, polyvinyl chloride or silicone coated latex [1].

Osteopontin production, with associated mucosal damage due to UTI, may allow easier crystal retention and nucleation resulting in stone formation [2].

Attempts to treatment of an infected urinary tract in the presence of stones almost fail. Relapse or reinfection is the rule under these circumstances and this suggests that stones may act as a source of infection in which bacteria are protected from the effect of antimicrobial drugs The Relationship between infection of the urinary tract and urinary stones is well known and has been reported for many years. Stone enhance the susceptibility of the

urinary tract to infection, and infection can predispose to stone formation. [3].

Despite the fact that accurate knowledge of stone composition is of great value when setting up therapeutic advice to prevent stone recurrence, it was not demonstrated until the beginning of 1950 that the structure and internal arrangement of calculi, which is impossible to elucidate using chemical methods, is crucial in determining the mechanism of formation of different kind of stones [4]. Urinary stones may contain a mixed bacterial flora. Two types of *Proteus* (*P. mirabilis* and *P. rettgeri*) were isolated from different parts of a stone isolated from a patient. Also, *Escherichia coli* and *Proteus mirabilis* were isolated from one of the stones.

The bacteria inside urinary bladder stones were shown to survive after exposure of the stones to a 3% solution of iodine in alcohol, or a concentration of an antibiotic excess of that required to inhibit the growth of the isolated organism. Stones were shown in the fluid culture media in which they were incubated, even if they had first been exposed to antimicrobial agents. Moreover, after exposing of stones to bacterial cultures, micro-organisms that eventually penetrated into the stone were protected against high concentrations of antibiotics to which they were otherwise sensitive. The findings may help to explain the reasons of persistence of infection and the ineffectiveness of drugs of urinary tract infection in the presence of urinary tract stones [3].

Antibiotic therapy is the most common treatment for UTI. Fluoroquinolones, nitrofurans, beta-lactams, aminoglycosides, trimethoprim and sulfonamides are used predominantly. However, the biofilm, due to its complex structure, constitutes an effective barrier to the antibiotics used in the treatment of urinary tract infections. In addition, the growing number of multidrug resistant strains limits the usage of many of the currently available chemotherapeutic agents [1]. The etiology of UTI (the pathogens traditionally associated with UTI) are changing many of their features, particularly because of antimicrobial resistance and are also affected by underlying host factors that complicate UTI, such as age, diabetes, spinal cord injury, or catheterization. Consequently, complicated UTI has a more diverse etiology than uncomplicated UTI, and organisms that rarely cause disease in healthy patients can cause significant disease in hosts with anatomic, metabolic, or immunologic underlying disease [5]. Therefore, it seems important to search for new methods of treatment.

The inner lining (membrane) of the chicken gizzard, which has a yellowish-gold color is called *Jineijin* (*ji* = chicken; *nei* = inner; *jin* = gold). This substance has been in use for about 2,000 years. At that time, *jineijin* was described as a treatment for diarrhea [6]. According to Chinese studies, a large dose of *jineijin* could even affect people with normal digestion: 45-60 minutes following ingestion of the roasted *jineijin* powder (5 g) in healthy individuals, the gastric secretion was increased by 30-37% compared with the control group [7]. An additional property of *jineijin* was : breaking down masses, being used for any kind of stagnation in the internal organs, for

lower abdominal masses in women, for gallstones and kidney stones, and for tumors [8].

[9] notes that *jineijin* is effective for treating dyspepsia, food stasis, and infantile malnutrition.

*Jineijin* has trace amounts of digestive enzymes and these enzymes cannot be a major source of the action of this substance because of in our digestive system, there is a release of digestive juices with enzymes in quantities far higher than one would be obtained from *jineijin*. The active component that has been isolated from the *jineijin* is called ventriculin. It had been primarily used to treatment of pernicious anemia, which often resulted from poor absorption of vitamin B12, and for chronic gastritis, one of the main causes of pernicious anemia in adults. Ventriculin was later replaced by other drugs [9].

Because of many of attempts to treatment an infected urinary tract in the presence of stones almost fail, The purpose of the present study is to use the extract of chicken gizzard membrane (*jineijin*) as a new method or drug to the urinary stones and UTI, which is caused by pathogenic bacteria.

## MATERIAL AND METHODS

### Preparing of chicken gizzard membrane powder

After killing a chicken, about 2Kg of fresh and raw chicken gizzard was taken out and cut with a knife to remove the thick inner membrane immediately; then the membranes were washed to clean and dried in the sun then milling to get fine powder, which stored in a cool and dry well-closed container, keep away from moisture and strong light/heat. The general characteristics of the powder are listed in Table 1.

Table 1: General Characteristics for Chicken Gizzard Membrane Powder

Source	Color	Nature/ in flavor	pH after dissolved in water
Chicken	yellow /green	sweet	6.0

### The preparation of the aqueous extract of the chicken gizzard membrane

The aqueous extract of the membranes prepared and used in three different ways:

#### 1- Hot water extract in two ways:

**A:** Dissolve 25 g of powder in 250 ml of hot distilled water and left for 24 hours, then filtrated using filter papers and the filtrate was distributed in the empty dishes and left to dry then we scraped it as powder.

**B:** Dissolve 25 g of powder in 250 ml of distilled water and left for 1 hour in water bath at 60°C, then filtrated using filter papers and the filtrate was distributed in the empty dishes and left to dry then we scraped it as powder.

**2- Cold water extract (C):** Dissolve 20 g of powder in 40 ml of distilled water at room temperature then filtrated using filter papers and the filtrate was used immediately without any treatment.

### Bacterial isolates and growth conditions

Bacterial isolates and their sources are listed in Table 2. Bacteria were grown overnight in Tryptone Soya Broth

(TSB; Oxoid, Basingstoke, UK) and then washed three times in phosphate buffered saline (PBS; NaCl 8 g/l, KCl 0.2 g/l, Na<sub>2</sub>HPO<sub>4</sub> 1.15 g/l, KH<sub>2</sub>PO<sub>4</sub> 0.2 g/l). Bacteria were then resuspended in TSB to an OD<sub>660</sub> nm of 0.5 for all isolates.

**Preparing of nutrient agar plates inoculations**

Nutrient agar plates was inoculated with (1 ml) of bacteria prepared as described above. By using the cork borer wells were made in some of these plates. These plates were used in the next step to determinate the antimicrobial activity of chicken gizzard membrane powder against all bacterial isolates which used in this study.

**Determination of antibacterial activity of chicken gizzard membrane**

5g of the membranes powder A and B was added separately to 10 ml of distilled water (final concentration =0.5g/ml), then filtered and sterilized using millipore filter unit. While the filtrate of powder C was shaking and used directly. 50µl from each filtrate (A,B & C) was transported by micropipette to nutrient agar plates and spread on all the surface of agar, then 0.1ml of bacterial broth for each isolate was spreaded on the surface of the agar and incubated at 37°C for 24 hrs.

In other way 50µl of filtrate was transported to each well in cultured agar plate and incubated at 37°C for 24 hrs. After the end of the incubation period, the presence or absence of bacterial growth in the dishes was investigated. Also the diameters of inhibition zones have been identified.

**RESULTS AND DISCUSSION**

**Bacterial isolates**

Eight samples of urine were collected from patients have turned stones in their urinary tract and the urine culture for these samples was positive. The genus and numbers of the isolated bacteria are listed in table 2. From these readings we see that *Proteus* was prevalent in the events of urinary tract infections, followed by *E. coli* with a slight lead and then finally come genus *Staphylococcus*.

**Antibacterial activity of chicken gizzard membrane powder**

After the end of the incubation period, the growth of bacteria and the diameter of inhibition zones were examined and the results were explained in Table 3. The extract which prepared with method A has not any activity against the tested bacteria, also we can see that the extract B have a little activity. While the cold water extract has a good activity represented by the diameters of inhibition zones.

This study show that infected urinary tract could has one or more of calculi (stones). We conclude from this that the bacterial infection may be one of the reasons for the emergence of calculi. Other study recorded that infection of urinary tract by *Escherichia coli* causes higher than normal expression of promoter protein osteopontin and mucosal damage at renal tubular cells. These suggest that urinary infection may promote stone formation by mucosal damage and elevate promoter protein osteopontin

at tubulus cell, allowing easier crystal retention and nucleation [2].

Table 2: Number, Percentage of Bacterial Isolates and Source of Isolation

Patient has urinary stones	Urine culture	Type of isolate	Serial number	Percentage (%)
1	+	<i>Escherichia coli</i>	1	37.5
2	+	<i>Escherichia coli</i>	2	
3	+	<i>Escherichia coli</i>	3	
4	+	<i>Proteus mirabilis</i>	4	50
5	+	<i>Proteus mirabilis</i>	5	
6	+	<i>Proteus mirabilis</i>	6	
7	+	<i>Proteus mirabilis</i>	7	
8	+	<i>Proteus mirabilis</i>	8	12.5

Table 3:Antibacterial Activity of Extract of Chicken Gizzard Membrane Powder

Type of isolate	Type of extract	Diameters of inhibition zones (Mean±SD)	Growth (Streaking method)
<i>Escherichia coli</i>	A	0±0	+
	B	2±0.1	+
	C	4±0.1	-
<i>Proteus mirabilis</i>	A	0±0	+
	B	2±0.1	+
	C	5±0.1	-
<i>Proteus mirabilis</i>	A	0±0	+
	B	1±0.1	+
	C	4±0.1	-

A: chicken gizzard membrane extract treated with hot water for 24hr. presence of growth

B: chicken gizzard membrane extract treated with hot water for 1hr. +: No growth

C: chicken gizzard membrane extract without any treatment.

In many studies the *Escherichia coli* was the predominant uropathogen (80%) isolated in acute community-acquired uncomplicated infections, followed by *Staphylococcus saprophyticus* (10% to 15%). While *Enterococci*, *Klebsiella*, *Enterobacter* and *Proteus species*, infrequently cause uncomplicated cystitis and pyelonephritis [5].

The current study recorded some different result when it found that the *Proteus species* was dominant causative of UTI, followed by *Escherichia coli* then *Staphylococcus*. [10] observed *Proteus mirabilis* is a pathogenic gram-negative bacterium that frequently causes kidney infection, typically established by ascending colonization of the urinary tract.

Many researches study the urinary tract infections and the effectiveness of the use of antibiotics as a first option in the treatment [11-15].

Microbiological confirmation of a urinary tract infection (UTI) takes 24-48 hrs. In the meantime, patients are usually given empirical antibiotics, sometimes inappropriately [16].

The use of antibiotics for a long time may lead to the emergence of new isolates of antibiotics resistant bacteria, which have been sensitive in the past. Sometimes the use of antibiotics leads to the emergence of side effects, which vary in severity from simple cross to high-risk to human health. Thus there is a need to use an alternative treatment of antibiotic must be effective against bacteria cause UTI

and urinary stones and have few or no side effects at the same time.

Chicken gizzard is the muscular stomach of chicken [17]. In Nigeria, chicken gizzard is a major source of protein to the population and is widely consumed [18]. *Jineiji* has trace amounts of pepsin and amylase. Due to the presence of these enzymes of protein digestion explains why there is remarkable effectiveness of the gizzard membrane against tested bacteria.

Because of these materials affected by heat, this explains the fact that the non-heat treated extract was more effective compared with another which extracted using hot water.

This study advises focusing on the use of fresh cold-aqueous extract of chicken gizzard membrane to treat UTI and stones instead of the extravagant use of antibiotics.

#### REFERENCES

- Ostrowska K, Strzelczyk A, Różalski A. and Stączek P., Bacterial biofilm as a cause of urinary tract infection-pathogens, methods of prevention and eradication, *Postepy Hig Med Dosw (Online)*, 25(67):1027-33, 2013.
- Djojodimedjo T, Soebadi DM., and Soetijipto." *Escherichia coli* infection induces mucosal damage and expression of proteins promoting urinary stone formation," *Urolithiasis*, 41(4):295-301, 2013.
- Rocha H., and Santos CS., "Relapse of Urinary Tract Infection in The Presence of Urinary Tract Calculi: The Role of Bacteria Within The Calculi," *J MED Micr. Biol*, 2:372-375, 1969.
- Grases F., García-Ferragut L. , Costa-Bauzá A., "Analytical study of renal calculi. A new insight," *Recent Res. Devel. in Pure & Applied Anal. Chem.*, 1:187-206, 1998.
- Ronald A., "The etiology of urinary tract infection: traditional and emerging pathogens," *Am J Med*, 8(113):14s-19s, 2002.
- Yang SZ., "The Divine Farmers Materia Medica. A translation of the Shen Nong Ben Cao. Blue Poppy," *Great Masters Series. ebook*. 1998.
- Chan HM., "Pharmacology and Applications of Chinese Materia Medica," *World Scientific*, 1987
- Yang Y., "Chines Herbal Medicines: comparison and characteristics," *Churchill Livingstone. ebook*, 2009.
- Shunpei M., and Shunyi Y., "Textbook on Traditional Chinese Medicine and Pharmacology," *New world press*, 1997.
- Czerwonka G., Arabski M., Wąsik S., Jabłońska-Wawrzycka A., Rogala P., Kaca W., "Morphological changes in *Proteus mirabilis* O18 biofilm under the influence of a urease inhibitor and a homoserine lactone derivative," *Arch Microbiol*, 196(3):169-177, 2014.
- Obi CL. , Tarupiwa A., Simango C., "Scope of urinary pathogens isolated in the Public Health Bacteriology Laboratory, Harare: antibiotic susceptibility patterns of isolates and incidence of haemolytic bacteria," *Cent Afr J Med*, 42(8):244-9, 1996.
- Gupta A., Dwivedi M., Nagana Gowda GA., Ayyagari A., Mahdi, AA., Bhandari M., " (1)H NMR spectroscopy in the diagnosis of *Pseudomonas aeruginosa*-induced urinary tract infection," *NMR Biomed*, 18(5):293-9, 2005.
- Chen PC., Chang LY., Lu CY., Shao PL., Tsai JJ., Tsau YK., et al. , "Drug susceptibility and treatment response of common urinary tract infection pathogens in children," *J Microbiol Immunol Infect*, 13: S1684-1182, 2013.
- Eriksson A., Giske CG., Ternhag A., "The relative importance of *Staphylococcus saprophyticus* as a urinary tract pathogen: distribution of bacteria among urinary samples analysed during 1 year at a major Swedish laboratory," *APMIS*, 121(1):72-8, 2013.
- Lee B., Kang SY., Kang HM., Yang NR., Kang HG., Ha IS., et al. , "Outcome of Antimicrobial Therapy of Pediatric Urinary Tract Infections Caused by Extended-Spectrum  $\beta$ -Lactamase-Producing Enterobacteriaceae," *Infect Chemother*, 45(4):415-21, 2013.
- Burillo A., Rodríguez-Sánchez B., Ramiro A., Cercenado E., Rodríguez-Créixems M., Bouza E., "Gram-Stain Plus MALDI-TOF MS (Matrix-Assisted Laser Desorption Ionization-Time of Flight Mass Spectrometry) for a Rapid Diagnosis of Urinary Tract Infection," *PLoS One*, 9(1):e86915, 2014.
- Giorgio G., "Chicken gizzard," *Anatomy and Embryology*, 171(2):151-162, 1985.
- Iwegbue CMA, Nwajei GE , Iyoha EH., "Heavy metal residues of chicken meat and gizzard and turkey meat consumed in southern Nigeria," *Bulgarian Journal of Veterinary Medicine* 2008;11( 4): 275–280.



## Correlation of Gonadal Hormones and Insulin Resistance with Seminal Fluid in Infertile Males Afflicted with Diabetes Mellitus

Nawal M. J. AL-Shammaa<sup>1</sup>, Amer Hasan Abdullah<sup>2</sup>, and Aufaira Shaker nsaif<sup>3</sup>

<sup>1</sup>Department of Chemistry Ibn- Alhaitham ,College of pure Sciences Education University of Baghdad .

<sup>2</sup>Department of Chemistry, College of Sciences University of AL-Mustansiriyah. E-mail address

<sup>3</sup>Medical laboratory science National diabetes center.

E-mail: nawal.mohammed69@yahoo.com

### Article info

Received 9/9/2014

Accepted 30/11/2014

### ABSTRACT

Male fertility requires normal sperm production and sperm transport, and adequate sexual performance, functions that require normal levels of testosterone. Male infertility could be due to number of factors, including abnormal spermatogenesis; reproductive tract anomalies or obstruction; inadequate sexual and ejaculatory functions; and impaired sperm motility. In this study, fifty men with type 2 diabetic aged under 40 years (31-39) and 50 non diabetic men with same age range as control. The mean age of the controls was (35 ± 3) years and of the diabetic patients (35 ± 4) years. The levels (Mean ± SD) of BMI, FBS, LH, FSH, prolactin, testosterone, C-peptide, IR, IS and seminal fluid count in control and patient groups were determined. A highly significant decrease of BMI in patients ( $p \leq 0.01$ ) compared with the healthy control, and a significant decreased ( $p \leq 0.05$ ) was noticed in seminal fluid count, LH, FSH, IS and testosterone levels, while a significant increase ( $p \leq 0.05$ ) in FBS and C-peptide and IR levels was noticed. There was a no-significant increase in prolactin level in patient group compared with control. A negatively correlation was between seminal fluid count and BMI in control while it was positively correlation in patient group. Also, there was a positive correlation between seminal fluid count and FBS level in control group, while a negatively correlation noticed in patient group. A positively correlation between seminal fluid count and LH, FSH in control and patient groups. There was a positive correlation between seminal fluid count and prolactin control, whereas a negative correlation in patient group. There was a negative correlation between seminal fluid count and serum level C-peptide in each group. A positive correlation between seminal fluid count and IS determined in control and patient groups, while there was a negative correlation between seminal fluid count and IR in both.

### الخلاصة

تتطلب خصوبة الرجال مجموعة من العوامل تتمثل بإنتاج وانتقال حيوانات منوية بشكل طبيعي من خلال أداء جنسي ملائم وهذه الوظائف تتطلب مستويات طبيعية من هرمون التستوستيرون. يحدث العقم في الرجال نتيجة مجموعة من العوامل منها تكون حيوانات منوية غير طبيعية أو ضعيفة أو حصول إعاقة في عملية إيصالها أو عدم كفاءة الوظائف الجنسية. درس في هذا البحث خمسين حالة من الذكور المصابين بمرض السكري النوع الثاني تحت سن الأربعين مع متوسط عمري وانحراف معياري (35±4) سنة ومجموعة سيطرة متطابقة في العمر متمثلة بقياس بخمسين ذكراً غير مصابين بمرض السكري متوسط عمري وانحراف معياري (35±3) سنة، وقياس مستوى كل من مؤشر كتلة الجسم BMI والسكر الصيامي FBS والهرمونات LH وFSH والبرولاكتين والتستوستيرون وسي-بيتايد ومقاومة الأنسولين IR وحساسية الأنسولين IS وعدد الحيوانات المنوية التي عبر مستوياتها بـ (Mean ± SD). أشارت النتائج إلى وجود انخفاض معنوي عالي ( $p \leq 0.01$ ) في مؤشر كتلة الجسم BMI للذكور المصابين بالسكر مقارنة بمجموعة السيطرة، كذلك وجود انخفاض معنوي ( $p \leq 0.05$ ) في مستوى كل من عدد الحيوانات المنوية وهرمونات LH وFSH والتستوستيرون وحساسية الأنسولين عند الذكور المصابين بالسكر مقارنة بمجموعة السيطرة، بينما لوحظ زيادة معنوية ( $p \leq 0.05$ ) في كل من مستوى السكر الصيامي وسي-بيتايد ومقاومة الأنسولين في حين لم تكن هناك زيادة معنوية في مستوى هرمون البرولاكتين عند الذكور المصابين بالسكر مقارنة بمجموعة السيطرة. وجدت علاقة سالبة بين عدد الحيوانات المنوية ومؤشر كتلة الجسم لدى مجموعة السيطرة في حين كانت العلاقة موجبة لدى المصابين بالسكري، ووجدت أيضاً علاقة موجبة بين عدد الحيوانات المنوية ومستوى السكر الصيامي بالنسبة لمجموعة السيطرة في حين كانت العلاقة سالبة لدى المصابين بالسكري، وكما كانت العلاقة موجبة بين عدد الحيوانات المنوية وكل من هرمونات LH وFSH كل من مجموعة السيطرة والمصابين بالسكري وكانت العلاقة موجبة بين عدد الحيوانات المنوية وهرمون البرولاكتين بما يخص مجموعة السيطرة في حين كانت العلاقة سالبة لدى المصابين بالسكري وكانت العلاقة سالبة بين عدد الحيوانات المنوية وهرمون سي-بيتايد عند المجموعتين بينما كانت العلاقة موجبة بين عدد الحيوانات المنوية وحساسية الأنسولين للمجموعتين في حين كانت العلاقة سالبة بين عدد الحيوانات المنوية ومقاومة الأنسولين في كلا المجموعتين.

## INTRODUCTION

**Diabetes mellitus DM**, primary or idiopathic, is a chronic disorder of the carbohydrate, lipid and protein metabolism, characterized by insulin disorders, hyperglycemia and glycosuria. This condition may contribute to microangiopathy, nephropathy and neuropathy [1]. Although most problems due to diabetes have been widely studied, the reproductive system affections are still little understood [2]. The DM has been associated with sexual dysfunction, both in men and women [2-4]. found decreased libido, in addition to the reduced vaginal lubrication and orgasm dysfunctions[5]. associated male infertility with appropriate synthesis of testosterone, caused by molecular changes in the Leydig cells, secondary to diabetes. The narrow relation between the function of Leydig and Sertoli cells could explain the changes found in the spermogram of diabetic patients. The involvement of the pituitary-gonadal system also interferes in these disorders [6]. On the other hand,[7] found that insulin-dependent diabetes is associated with reduced ejaculated semen and decreased vitality and motility of the spermatozoa, with no change in sperm viscosity. However, the relation between male infertility and altered plasma levels of testosterone, follicle stimulating hormone (FSH), luteinizing hormone (LH), and prolactin (PRL) is still obscure[8]. In diabetic patients with organic impotence free testosterone is diminished. This is not found in the non-impotent diabetics and in individuals with psychological impotence, as well as in healthy men [6]. Insulin action in motility and metabolism of human spermatozoa is not defined. Defects in insulin secretion may change testicular and accessory sexual glands function. Usually, the concentration of seminal insulin is higher than that in the serum [9]. The DM is known to cause many systemic complications, male infertility, based on impotence, retrograde ejaculation, and hypogonadism, is not widely recognized to be one of them. Because of the paucity of studies and inconsistencies regarding the impact of DM on semen quality, this disease is seldom looked for in the infertile patient. This view has been challenged by a finding shows that DM induces subtle molecular changes that are important to sperm quality and function. Obesity was the leading contributor of infertility. Other comorbid factors associated with infertility in people with diabetes were hypertension, erectile dysfunction, and varicocele, while insulin action in motility and in the metabolism of human spermatozoa is not defined [10]. Defects in insulin secretion may change testicular and accessory sexual glands function. In 30-40% of men, no cause for infertility is found [11]. Insulin resistance (IR) is an important risk factor for DM (type 2). There is evidence supports the fact that by the time glucose tolerance or fasting glucose levels become impaired, appreciable  $\beta$  cell destruction may have already occurred. Early identification of insulin resistant individuals is important to manage strategies of DM. The euglycaemic insulin clamp method, intravenous glucose tolerance test (IVGTT) and minimal model approximation of the metabolism of glucose (MMAMG) are standard methods to measure of IR in research. Research suggests

that diabetes can hinder the protective effects of male sex hormones such as Testosterone hormone before menopause [8].

## MATERIALS AND METHODS

### Subject:

Fifty of type 2 diabetic men aged under 40 (31-39) and 50 non diabetic men as control who matched age were investigated in this study. Glycemic control sex hormones (prolactin and testosterone) were measured using minividas (Biomerieux,France). Also, serum C-peptide was measured using gamma counter (Wallac) and fasting blood sugar using spectrophotometer, all measurements were done in Al-Yarmok National Diabetes Center in Baghdad. Body mass index (BMI) also estimated, it is defined as the individual's body mass divided by the square of height [12]. In diabetic patients, fasting glucose, glycosilated hemoglobin, testosterone, FSH, LH and PRL were measured [1-3]. The fasting glucose and glycosilated hemoglobin were determined in the same day, thirty minutes after blood was drawn; the diabetic patients fasted for (8 hrs) prior to blood drawing. Glucose level between 60 and 109 mg% and glycosilated hemoglobin up to 8.5 g% were considered normal [4-9]. The reference values were: testosterone: 270 – 1070 ng %; PRL: up to 20 ng/ml; FSH: 1.8 – 9.0 mIU/ml; LH: 0.4 – 5.7 mIU/ml.

### Semen analysis:

The semen sample of male partner was collected after 3-5 days of abstinence by masturbation. The sample was collected in a clean and sterile petridish .The container of each male was labeled with name, age and time of collection. Semen analysis was done according to methodology of WHO manual and involves macroscopic and microscopic examinations [13]. After five days of sexual abstinence, a sperm gram was collected in a sterile vial, which was immediately sealed. The fluid analysis was conducted within the first hour after collection and consisted of evaluation of its physical and chemical characteristics (volume, aspect, odor, viscosity and pH) and of microscopic analysis to observe motility and morphology of the spermatozoa. After semen dilution at 1:20 (0.1 milliliters of semen in 1.9 milliliters of 0.9% saline solution), the spermatozoa were counted in a Neubauer chamber. They were counted in five quadrants, the four lateral ones usually utilized for leukocyte count and the central one for erythrocyte count [14].

### Fasting Insulin calculation:

Insulin was calculated using following formula:  
 Fasting glucose (mg/dl) FBS  $\times$  Fasting Insulin. IR and B% were calculated using an updated HOMA model (HOMA2). The model recalibrated to give these values in normal young adults when using currently available assays for insulin, specific insulin or C-peptide [15].  
 $(\mu\text{U/ml})/405 = \text{IR}$  which used in HOMA-IR we can put:  
 $\text{Insulin } (\mu\text{U/ml}) = \text{IR} \times 405 / \text{FBS}$   
 Optimal level is less than 5. Excess insulin was defined when levels were equal to or higher than 15 $\mu\text{U/ml}$  [16].

**Insulin Resistance (IR), Beta cell function (B %) and Insulin sensitivity (S%) calculation:**

**Statistical analysis:** The data was expressed as mean  $\pm$ SEM, which SEM is standard Error of mean. The comparison between patient group and control group were analyzed using student t-test. Pearson's correlation coefficient was used to compare seminal fluid and sex hormones in patient group. The  $p$ -value of  $\leq 0.05$  was considered highly significant and significant respectively [17].

**RESULTS AND DISCUSSION**

All patients agreed to participate in this study. The mean age of the controls was  $35 \pm 3$  years and of the diabetic patients was  $(35 \pm 4)$  years. The levels (Mean  $\pm$ SD) of BMI, (Mean  $\pm$ SEM) FBS, LH, FSH, PRL, testosterone, C-peptide, IR, IS and seminal fluid count in control and patient groups were determined and are listed in table (1), which shows a highly significant decrease of BMI in male patients compared with the healthy control. There was a significant decrease in each of LH, FSH, testosterone, IS and seminal fluid count levels in patients as compared to healthy control as shown in table (1), while there was a significant increase in FBS, C-peptide, IR levels and also shows non-significant increase in serum prolactin level in patient group comparative with control.

Table 1: Levels (Mean  $\pm$ SD) of BMI, FBS, LH, FSH, prolactin, testosterone, C-peptide, IR, IS and seminal fluid count in control and patient groups

Parameter	Control n=30	Patient n=30	p-value
BMI Kg/m <sup>2</sup>	27.302 $\pm$ 0.928	23.849 $\pm$ 0.928	$p \leq 0.01$
FBS mg/ml	76.6 $\pm$ 1.489	155.25 $\pm$ 8.282	$p \leq 0.05$
LH pmol/L	2.535 $\pm$ 0.254	1.136 $\pm$ 0.185	$p \leq 0.05$
FSH pmol/L	4.165 $\pm$ 0.196	2.415 $\pm$ 0.315	$p \leq 0.05$
Prolactin mol/L	4.165 $\pm$ 0.316	4.195 $\pm$ 0.332	$p \geq 0.05$
Testosterone pmol/L	6.915 $\pm$ 0.500	1.76 $\pm$ 0.268	$p \leq 0.05$
C-Peptide ng/L	2.145 $\pm$ 0.131	4.84 $\pm$ 0.474	$p \leq 0.05$
IR	0.40 $\pm$ 0.025	1.80 $\pm$ 0.170	$p \leq 0.05$
IS	0.454 $\pm$ 0.006	0.332 $\pm$ 0.017	$p \leq 0.05$
Seminal fluid count (ml)	32687500 $\pm$ 3193935.481	70910 $\pm$ 51289.125	$p \leq 0.05$

Significant ( $p \leq 0.05$ ), highly significant ( $p \leq 0.001$ ), non-significant ( $p \geq 0.05$ )

There was a significant negatively correlation (-ve) between seminal fluid count level and BMI in control  $r = -0.150$  and a significant positively correlation (+ve) in patient group  $r = 0.064$  as shown in figure (1).

A significant positively correlation (+ve)  $r = 0.56$  between seminal fluid count level and FBS for control group while a significant negatively correlation (-ve)  $r = -0.332$  in patient group shown in figure (2).

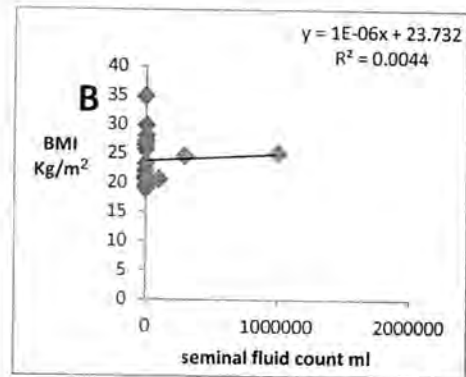
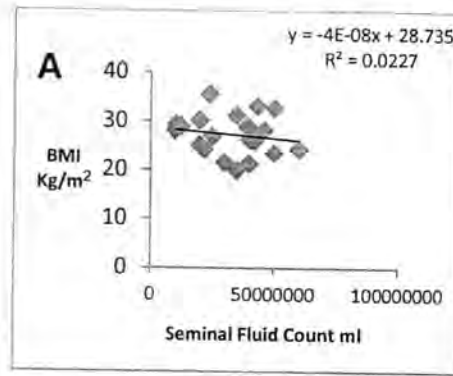


Figure 1: Correlation between serum seminal fluid count and BMI level in control (A) and patient (B) groups.

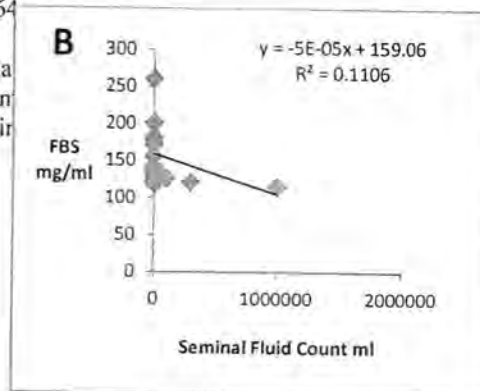
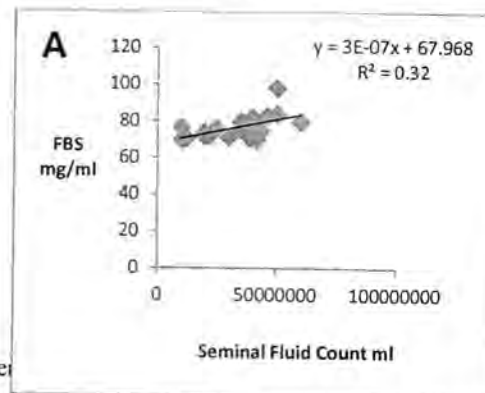


Figure 2: Correlation between serum seminal fluid count and FBS level in control (A) and patient (B) groups.

A significant\* positively correlation (+ve) between seminal fluid count level and LH  $r=0.33$   $r=0.60$ , FSH  $r=0.248$   $r=0.02$  in control and patient groups are shown in figures (3 and 4) respectively. There was a non-significant positively correlation (+ve) between seminal fluid count and prolactin in control  $r=0.295$  and a non-significant negatively , correlation in patient group  $r=-0.179$  as shown in figure (5).

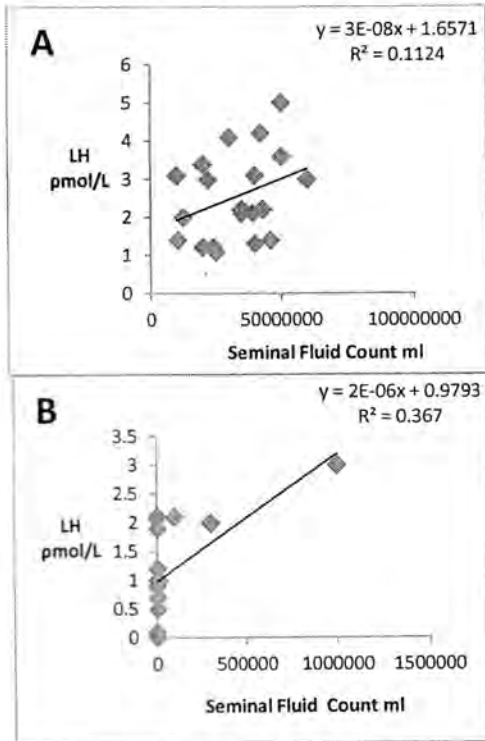


Figure 3: Correlation between serum seminal fluid count and LH level in control (A) and patient(B) groups

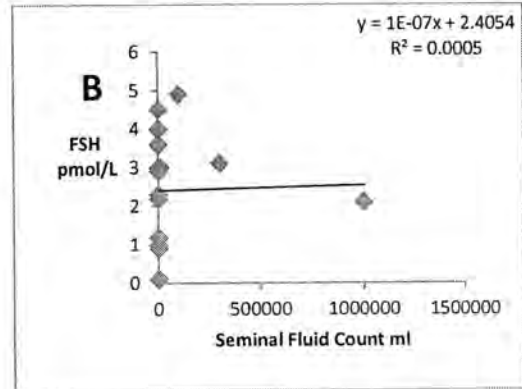
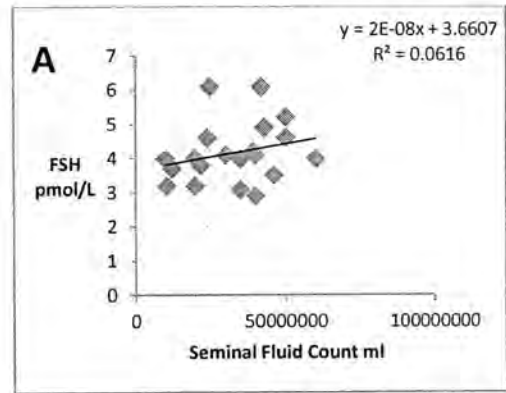


Figure 4: Correlation between serum seminal fluid count and FSH level in control A and patient B group.

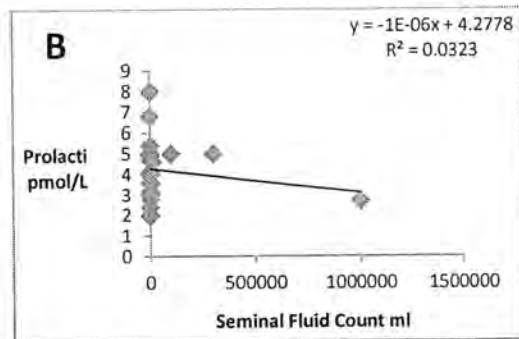
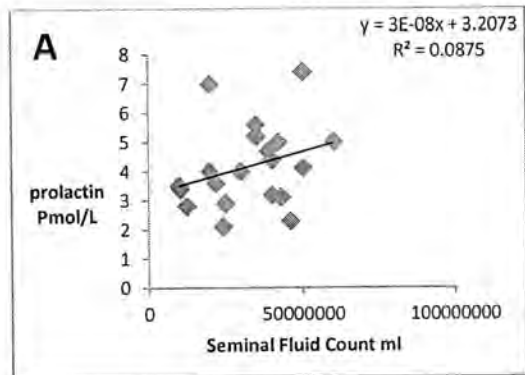


Figure 5: Correlation between serum seminal fluid count and Prolactin level in control (A) and patient (B) group .



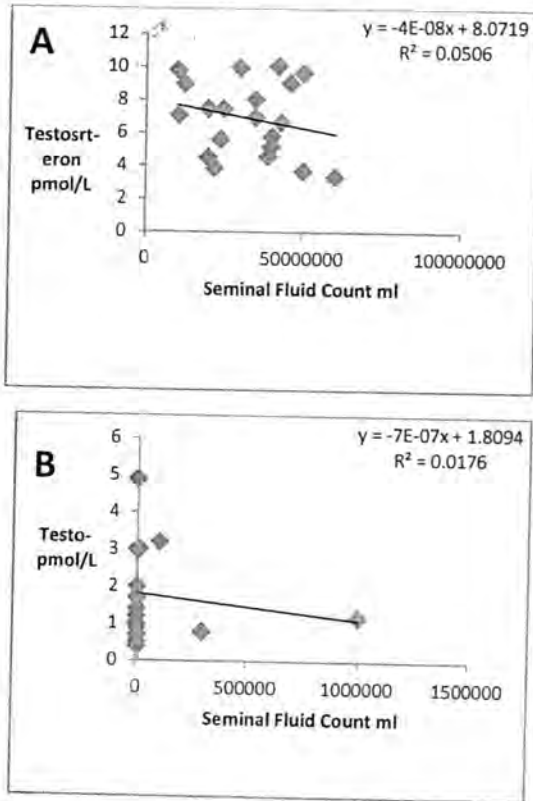


Figure 6: Correlation between serum seminal fluid count and testosterone level in control (A) and patient(B) group .

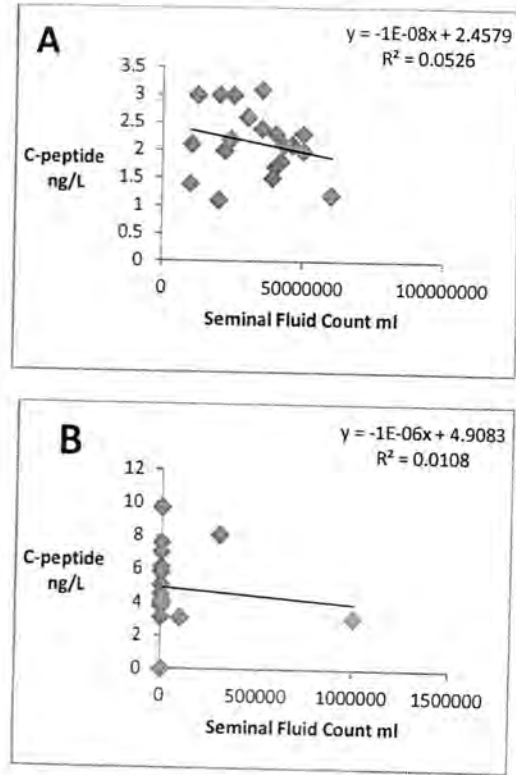


Figure 7: Correlation between serum seminal fluid count and C-peptide level in control (A) and patient(B) group .

Whereas a significant negatively correlation (-ve)  $r = -0.224$ ,  $r = -0.132$  between serum seminal fluid count and testosterone levels in control and patient groups as shown in figure( 6).

There was a significant negatively correlation (-ve)  $r = -0.229$ ,  $r = -0.103$  between serum seminal fluid count and C-peptide level in control and patient groups as shown in figure( 7).

There was a significant negatively correlation (-ve)  $r = -0.04$ ,  $r = -0.25$  between seminal fluid count and IR in control and patient groups as shown figure ( 8).

There was a significant positively correlation(+ve) between serum seminal fluid count and IS  $r = 0.127$  and  $r = 0.175$  in control and patient groups as shown in figure ( 9).

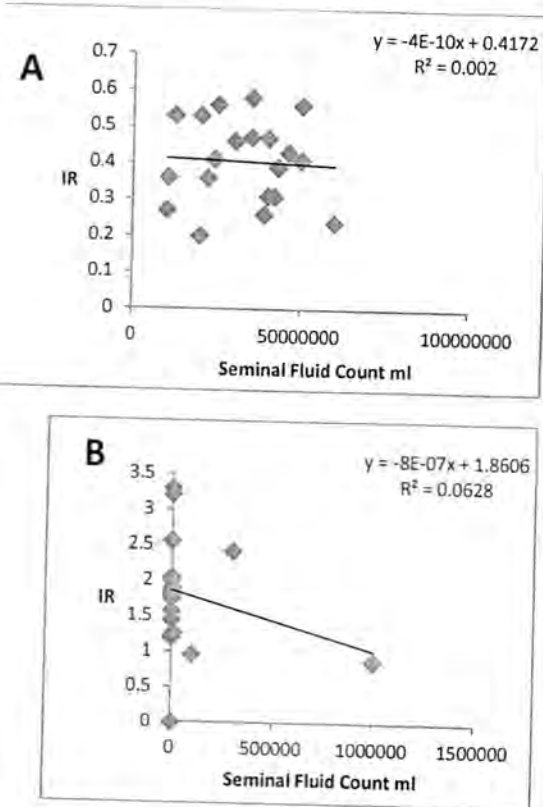


Figure 8: Correlation between serum seminal fluid count and IR level in control (A) and patient (B) group .

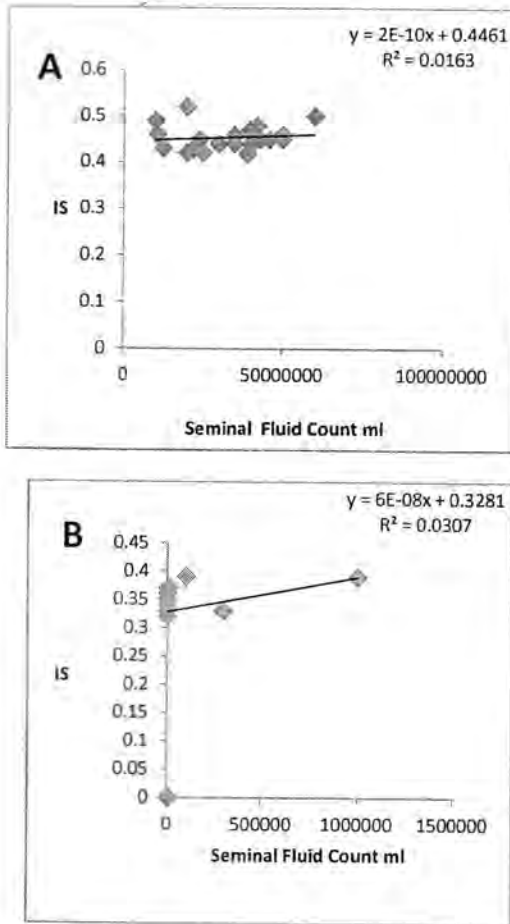


Figure 9: Correlation between serum seminal fluid count and IS level in control (A) and patient (B) group .

A consequence of the hyperbolic relationship is that increased insulin sensitivity is compensated by reduction, or down-regulation, of beta cell function, which may be a mechanism to avoid hypoglycemic episodes. This has been demonstrated as a reduced insulin response to arginine when insulin sensitivity is increased during weight reduction in severely obese subjects undergoing standardized weight reduction by bariatric surgery [18]. That study also demonstrated that the reduction in insulin secretion was quantitatively not as prominent as the increase in insulin sensitivity, which increased the disposition index along with weight reduction. This was followed by improvement of glucose tolerance, in support of the model that glucose tolerance is governed by the hyperbolic relationship between insulin secretion and action. Similarly, in a group of elite sportsmen having extremely high insulin sensitivity, the insulin response to arginine was reduced along a hyperbolic line in comparison with a group of sedentary subjects [19]. Hence, both increases and decreases of insulin sensitivity are associated with compensatory reciprocal changes in insulin secretion.

High levels of C-peptide generally indicate high levels of endogenous insulin production. This may be in

response to high levels of blood glucose caused by glucose intake and/or insulin resistance. Low levels of C-peptide are associated with low levels of insulin production [20]. This can occur when insufficient insulin is being produced by the beta cells or when production is suppressed by exogenous insulin or with suppression tests that involve substances such as somatostatin. Type 2 DM insulin resistance, obesity, and other related comorbidities play the main role in sperm parameter abnormalities and low testosterone levels in patients with diabetes. Both clinical and experimental evidence suggest that sperm parameters are altered in patients with DM. Male infertility, based on impotence, retrograde ejaculation, and hypogonadism, is not widely recognized to be one of them [21]. Because of the paucity of studies and inconsistencies regarding the impact of DM on semen quality, this disease is seldom looked for in the infertile patient. Type 2 DM is characterized by both diminished insulin sensitivity and deficient insulin secretion; these metabolic parameters are important, potentially genetically determined precursors of diabetes [22, 23]. Insulin sensitivity and secretion can be measured by the hyperinsulinemic-euglycemic clamp and the insulin response to intravenous glucose infusion. In non-diabetic subjects, these measures strongly predict the subsequent incidence of diabetes and are often considered the "gold standards" for assessment of insulin sensitivity and secretion [24]. However, as these measures are labor intensive, they are difficult to obtain in the large number of persons typically required for epidemiologic investigations. In such studies, simple indices derived from more easily measured parameters, for example, during an oral glucose tolerance test, would be useful. Several such indices have been proposed, but their utility in epidemiologic studies of diabetes depends on the extent to which they correlate with more sophisticated measures and on whether they predict the incidence of diabetes in a fashion similar to the more sophisticated measures. Male impotence, which consists in difficulty in obtaining or maintaining full erection until the end of coitus, is a common sexual problem in diabetics [25-27]. The prevalence of this complaint ranges from 20 to 50%, increasing with patient age and duration of the disease[28]. The impotence is a multifactorial sexual disorder, secondary to endocrine, vascular, neurological and psychological disorders which act unfavorably on erection. The findings of the present study point to vascular and neuronal anomalies as the major causes of impotence in diabetic patients. On the other hand, hormones did not significantly affect this dysfunction. The general seminal characteristics of color, odor and aspect were similar among all subjects. It could be argued that this occurred probably because of sample selection bias, due to exclusion of controls with signs of lower urinary tract infection, such as prostatitis or cystitis, even in the diabetic group. Earlier studied on the hypothalamic-pituitary-gonadal axis dysfunction and impotence showed conflicting results [29]. The Leydig cell population and testosterone metabolites were reduced, which was inversely related to the increase of insulin resistance [30]. However, other study did not demonstrate altered serum

testosterone levels among diabetics, regardless of their sexual performance [31]. Faerman did not find abnormalities in the number of Leydig cells, neither in testicular morphology in impotent diabetics [32]. Clinical reports prior to the insulin era suggested that insulin deficiency was the cause of impotence in diabetics, since they pointed to erectile dysfunction and testicular atrophy as the most common sexual disorders in poorly controlled diabetics[33]. However, after insulin became available to treat diabetes, there was no change in this problem. The relation between diabetes and male infertility is still being questioned; The type 1 DM (insulin-dependent) lowers seminal fluid volume. The concentration, motility, vitality and the proportion of normal shape spermatozoa is also lower[34]. On the other hand, a study supported the idea that spermatogenic infertility was not common in diabetic men, but in those who had retrograde ejaculation[35]. In the present study, only one patient had seminal fluid changes associated to low serum testosterone and FSH level, with normal LH, suggesting Leydig and Sertoli cell dysfunction. However, the relation between male infertility and altered plasma levels of testosterone, FSH, LH and PRL is still obscure [36]. In diabetic patients with organic impotence free testosterone is diminished. This is not found in the non-impotent diabetics and in individuals with psychological impotence, as well as in healthy men. Insulin action in motility and in the metabolism of human spermatozoa is not defined. Defects in insulin secretion may change testicular and accessory sexual glands function. Usually, the concentration of seminal insulin is higher than that in the serum[36].

### CONCLUSION

This research was performed to discuss the relation between diabetes and male infertility which is still being questioned. In our study we found that there was a decrease in the level of testosterone with an increase in C-peptide and insulin resistance suggesting Leydig and Sertoli cell there was also a decrease in insulin sensitivity that suggests insulin deficiency which was referred to as a cause of impotence in diabetics, also defects in insulin secretion may change testicular and accessory sexual glands function.

### REFERENCES

- [1] Camilleri M., "Clinical practice", Diabetic astroparesis, *N Engl J Med.*, b356(8) :820-9, 2007.
- [2] Miralles-Garcia JM, and Garcia-Diez LC., " Specific aspects of erectile dysfunction in endocrinology", *Int J Impot Res.*, 16(Suppl 2):S10-20, 2004.
- [3] Ballester J, Munoz MC, Dominguez J, Rigau T, Guinovart JJ, and Rodriguez-Gil JE., "Insulin-dependent diabetes affects testicular function by FSH- and LH-linked mechanisms", *J Androl.*, 25(5):706-19, 2004.
- [4] Chandrashekar V, and Bartke A., " The impact of altered insulin-like growth factor-I secretion on the neuroendocrine and testicular functions", *Minerva Ginecol.*, 57(1):87-97, 2005.
- [5] Dinulovic D, and Radonjic G., "Diabetes mellitus/male infertility", *Arch Androl.*, 25(3):277-93, 1990.
- [6] Bhasin S, Enzlin P, Coviello A, and Basson R., " Sexual dysfunction in men and women with endocrine disorders", *Lancet.*, 369(9561):597-611, 2007.
- [7] Miralles-Garcia JM, and Garcia-Diez LC., "Specific aspects of erectile dysfunction in endocrinology", *Int J Impot Res.*, 16(Suppl 2):S10-2, 2004.
- [8] Ballester J, Munoz MC, Dominguez J, Rigau T, Guinovart JJ, and Rodriguez-Gil JE., "Insulin-dependent diabetes affects testicular function by FSH- and LH-linked mechanisms", *J Androl.*, 25(5):706-19, 2004.
- [9] Chandrashekar V, and Bartke A., " The impact of altered insulin-like growth factor-I secretion on the neuroendocrine and testicular functions", *Minerva Ginecol.*, 57(1):87-97, 2005.
- [10] Bener A, Al-Ansari AA, Zirir M, Al-Hamaq AO., " Is male fertility associated with type 2 diabetes mellitus? *Int Urol Nephrol.* , 41:777-784, 2009.
- [11] Dohle GR et al., " Guidelines on male infertility". *European Association of Urology*, 2010.
- [12] "BMI classification, "Global Data base on Body Mass Index", WHO 2006, Retrieved July 27, 2012.
- [13] World Health Organization (WHO), "WHO Laboratory Manual for Examination of Human Semen and Semen Cervical Mucus Interaction". 4th Edition. Cambridge University Press, Cambridge, UK, 1999.
- [14] Petroianu A, Pesquisa em medicina. In: Petroianu A, editor. " Ética, " moral e deontologia médicas", Rio de Janeiro; Guanabara Koogan ., p. 174-8, 2000.
- [15] Wallace TM, Levy JC, Matthews DR." Use and abuse of HOMA modeling", *Diabetes Care.*, 27: 1487-1495, 2004.
- [16] Matsuda M, DeFronzo RA., " Insulin sensitivity indices obtained from oral glucose tolerance testing: comparison with the euglycemic insulin clamp", *Diabetes Care.*, 22: 1462-1470, 1999.
- [17] Sorlie DE., Medical biostatistics: "Examination and board review Norwalk". Connecticut, Appleton and Lang., p:47-88, 1995.
- [18] Guldstrand M, Ahre 'n B & Adamson U., " Improved b-cell function after standardized weight reduction in severely obese subjects. *American Journal of Physiology. Endocrinology and Metabolism insulin clearance in man". Journal of Clinical Endocrinology and Metabolism.*, 88 1264-1270, 2003.
- [19] Porte D Jr., " Beta cells in type II diabetes mellitus", *Diabetes* 40 166-180, 1991.
- [20] Couri CEB, and Foss MC, Voltarelli JC., " Secondary prevention of type I diabetes mellitus: stopping immune destruction and promoting -cell regeneration " .*Braz J Med Biol Res.*, 39(10):1271-1280, 2006.
- [21] Staeva-Vieira T, Peakman M, and von Herrath M., " Translational mini-review series on type-I diabetes:

- immunebased therapeutic approaches for type 1 diabetes", *ClinExp Immunol.*,148(1):17-31, 2007.
- [22] Arap MA et al." Late hormonal levels, semen parameters and presence of antisperm antibodies in patients treated for testicular torsion ", *J Androl*; 28: 528-32, 2007.
- [23] Cherry N et al., " Occupational exposure to solvents and male infertility". *Occup Environ Med*, 58:635-40, 2001.
- [24] Isidori A et al., "Treatment of male infertility". *Contraception* 2005; 72: 314-8. Kunzle R et al." Semen quality of male smokers and nonsmokers in infertile couples", *Fertil Steril*; 79: 287-91, 2003.
- [25] Patki P et al., " Effects of spinal cord injury on semen parameters", *J Spinal Cord Med*; 31: 27-32, 2008.
- [26] Rowe PJ et al., " WHO manual for the standardized investigation and diagnosis of the infertile male" .Cambridge, UK: Cambridge University Press, 2004.
- [27] Shefi S, Turek PJ., " Definition and current evaluation of subfertile men" , *Int Braz J Urol*; 32:385, 2006.
- [28] Boloña ER, Uruga MV, Haddad RM, Tracz MJ, Sideras K, and Kennedy CC, et al., "Testosterone use in men with sexual dysfunction : a systematic review and meta-analysis of randomized placebo-controlled trials", *Mayo Clin Proc.*,82(1):20-8, 2007.
- [29] Chiodini I, Di Lembo S, Morelli V, Epaminonda P, Coletti F, and Masserini B, et al., " Hypothalamic-pituitary-adrenal activity in type 2 diabetes mellitus: role of autonomic imbalance". *Metabolism.*,55(8):1135-40, 2006.
- [30] Pitteloud N, Hardin M, Dwyer AA, Valassi E, Yialamas M, and Elahi D, et al., "Increasing insulin resistance is associated with a decrease in Leydig cell testosterone secretion in men". *J Clin Endocrinol Metab.*,90(5):2636-41, 2005.
- [31] Ballester J, Dominguez J, Munoz MC, Sensat M, Rigau T, and Guinovart JJ, et al., "Tungstate treatment improves Leydig cell function in streptozotocin-diabetic rats", *J Androl.*,26(6):706-15, 2005.
- [32] Faerman I, Vilar O, Rivarola MA, Rosner JM, Jadzinsky MN, and Fox D, et al., "Impotence and diabetes. Studies of androgenic function in diabetic impotent males", *Diabetes.*:21(1):23-30, 1972.
- [33] Bansal TC, Guay AT, Jacobson J, Woods BO, and Nesto RW." Incidence of metabolic syndrome and insulin resistance in a population with organic erectile dysfunction", *J Sex Med.*:2(1):96-103, 2005.
- [34] Garcia-Diez LC, and Corrales-Hernandes JT., " Semen characteristics and diabetes mellitus". *Arch Androl.* 1991;26(2):119-28. *neuroendocrine and testicular functions, Minerva Ginecol.* ;57(1):87-97, 2005.
- [35] Fairburn C., " The sexual problems of diabetic men", *Br J Hosp Med.*:25(5):484, 487, 489-91, 1981.
- [36] Mallidis C, Agbaje I, McClure N, and Kliesch S., " The influence of diabetes mellitus on male reproductive function: a poorly investigated aspect of male infertility", *Urologe A.*:50:33– 37, 2011.



## Synthesis of New 1,3-Oxazole Derivatives

Abdul Jabar Kh. Atia and Ali Abdul waheed

Department of chemistry, college of science, AL- Mustansiriya University

### ABSTRACT

1,3- Oxazole derivatives (2a – d) have been Synthesized by cyclization of hippuric acid with different aromatic aldehydes, hippuric acid was readily obtained by reaction of benzoyl chloride with glycine (2-amino acetic acid). Compounds (2a – d) were converted into a variety of derivatives. All new compounds were characterized by  $^1\text{H}$  NMR, FTIR and UV spectroscopy

### Article info

Received 21/10/2014

Accepted 23/2/2015

### Keywords:

1,3-oxazole-5-one,  
imidazole-5-one,  
pyrazole,  
pyrimidine

### الخلاصة

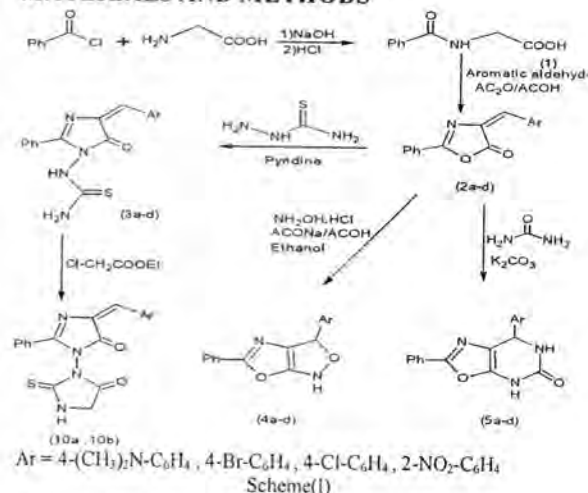
تم في هذا البحث تحضير مركبات (2a-d) من خلال اجراء عملية الغلق الحلقى لحمض الهيبيوريك مع الديهايدات اروماتية مختلفة بينما حضر المركب الاساسي حامض الهيبيوريك من تفاعل المركب benzoyl chloride مع الحامض الاميني (Glycine) ثم بعد ذلك تم تحويل المركبات (2a-d) الى بقية المشتقات. كل المركبات المحضرة تم تشخيصها باستخدام الطرائق الطيفية  $^1\text{H}$  NMR, FTIR and UV

## INTRODUCTION

Oxazoles are a kind of attractive heterocycles not only because of their unique structures and varied applications but also they serve as structural elements for a variety of natural products[1], pharmaceuticals[2] and bioactive compounds[3], A number of synthetic methods to prepare oxazoles have been reported[4]. The typical procedure for the synthesis of oxazoles involves the reaction of readily available substituted urea derivatives with halogenated alkenes or  $\alpha$ -haloketones [5]. Imidazoles are an important class of heterocycles being the core fragment of different natural products and biological systems[6], Compounds containing imidazole moiety have many pharmacological properties and play important roles in biochemical processes [7]. Imidazolones have been associated with several pharmacological activities such as antimicrobial (antifungal, antibacterial and antiviral), anticancer activity, CNS depressant activity[8]. Chalcones are an important class of compounds which are good intermediates for the synthesis of various heterocyclic compounds like flavones, isoxazolines, pyrimidines, quinoxalines, benzalcoumaranones [9]. Chalcones display a wide range of pharmacological properties, including cytotoxicity towards cancer cell lines[10]. Pyrimidine is the most important six membered heterocyclic containing 2 nitrogen atoms at position 1 and 3. It is isomeric with two other forms of diazene[11]. Pyrazole is a five-membered heterocyclic moiety having two adjacent nitrogen atoms within the ring, and It is basic in nature [12], pyrazole is one of the most important one as large variety of biological activities have been reported for various pyrazole derivatives. Conventional method of synthesis of pyrazoles involves the base-catalyzed condensation of aromatic ketones to give  $\alpha$ ,  $\beta$ -unsaturated ketones (also called as chalcones), which undergo subsequent cyclization with hydrazine and hydrazine derivatives[13,14]. The pyrazole nucleus is a ubiquitous

feature of pharmacological interest and has been proven to be a fertile source of medicinal agents, pyrazole derivatives have also exhibited antidiabetic properties, and some of these have biological activities such as anti-inflammatory[15,16].

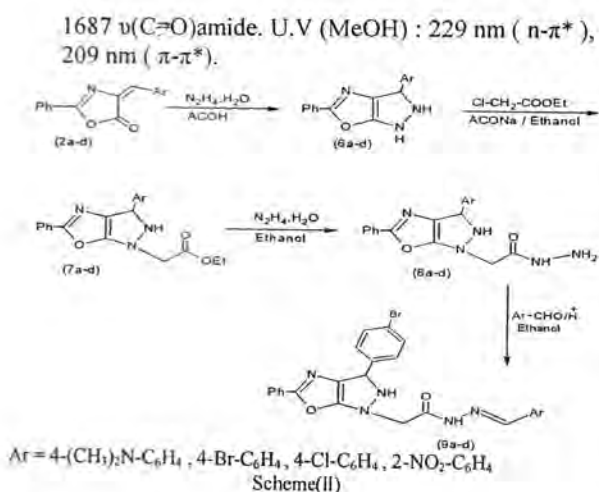
## MATERIALS AND METHODS



### Synthesis of 2-benzamidoacetic acid (1)[17]

To a mixture of glycine (0.18 mole, 13.2 gm) in mixture of sodium hydroxide (60 ml) 10% NaOH was added and stirred for 10 min, then benzoyl chloride (0.18 mole, 25 gm) was added to the mixture, then the reaction mixture was allowed to cool then acidified with conc HCl, ice cooled water was added to the solid product obtained and filtered and recrystallized from appropriate solvent.

(1) :Yield, 74%, m.p. 184-185 °C, IR(cm<sup>-1</sup>): 3342  $\nu$ (NH), 2484-3400  $\nu$ (O-H) 3070  $\nu$ (C-H)aromatic, 2893,2939  $\nu$ (C-H)aliphatic, 1753  $\nu$ (C=O) acid,



### Synthesis of (E)-4-(Arylidene)-2-phenyl-1,3-oxazol-5(4H)-ones(2a-d)[18]

A mixture of (1) (0.02 mole, 3.58 gm) and aromatic aldehydes (0.02 mole) in acetic anhydride (20 ml) and acetic acid (5 ml) was refluxed for 3 hrs, then the reaction mixture was added to ice water and the solid product obtained was filtered and recrystallized from appropriate solvent.

2<sub>a</sub> : Yield, 89 % , m.p. 214-215 C° , IR(cm<sup>-1</sup>): 3016  $\nu(\text{C}-\text{H})$ aromatic , 2812,2899  $\nu(\text{C}-\text{H})$ aliphatic , 1784  $\nu(\text{C}=\text{O})$  lactone , 1645  $\nu(\text{C}=\text{N})$  , (1606,1581)  $\nu(\text{C}=\text{C})$  ar . U.V (MeOH) : 301 nm ( $n-\pi^*$ ), 242 nm ( $\pi-\pi^*$ ).

2<sub>b</sub> : Yield, 75% , m.p. 154-156 C° , IR(cm<sup>-1</sup>): 3057  $\nu(\text{C}-\text{H})$ aromatic , 2839,2985  $\nu(\text{C}-\text{H})$ aliphatic , 1795  $\nu(\text{C}=\text{O})$  lactone , 1653  $\nu(\text{C}=\text{N})$  , (1583,1554)  $\nu(\text{C}=\text{C})$  ar . U.V (MeOH) : 388 nm ( $n-\pi^*$ ), 252 nm ( $\pi-\pi^*$ ).

2<sub>c</sub> : Yield, 83 % , m.p. 116-118 C° , IR(cm<sup>-1</sup>): 3078  $\nu(\text{C}-\text{H})$ aromatic , 2847,2991  $\nu(\text{C}-\text{H})$ aliphatic , 1795  $\nu(\text{C}=\text{O})$  lactone , 1653  $\nu(\text{C}=\text{N})$  , (1556 ,1589)  $\nu(\text{C}=\text{C})$  ar . U.V (MeOH) : 348 nm ( $n-\pi^*$ ), 232 nm ( $\pi-\pi^*$ ). <sup>1</sup>H-NMR (DMSO) (ppm) 7.38 (s, =CH- alkene), 7.60-7.77 (s, 5H for phenyl ring), 8.13-8.34 (dd, 4H for aryl ring).

2<sub>d</sub> : Yield, 70% , m.p. 165-167 C° , IR(cm<sup>-1</sup>): 3070  $\nu(\text{C}-\text{H})$ aromatic , 2839,2985  $\nu(\text{C}-\text{H})$ aliphatic , 1797  $\nu(\text{C}=\text{O})$  lactone , 1654  $\nu(\text{C}=\text{N})$  , (1550, 1599)  $\nu(\text{C}=\text{C})$  ar . U.V (MeOH) : 362 nm ( $n-\pi^*$ ), 245 nm ( $\pi-\pi^*$ ).

### Synthesis of (E)-1-(4-(Arylidene)-5-oxo-2-phenyl-4,5-dihydro-1H-imidazol-1-yl)thiourea(3a-d)[19]

A mixture of (2a-d) (0.02 mole) and thiosemicarbazide (0.02 mole, 0.18 gm) in pyridine (20 ml) was refluxed for 20 hrs, then the reaction mixture was added to ice water and the solid product obtained was filtered and recrystallized from appropriate solvent.

3<sub>a</sub> : Yield, 76 % , m.p. 192-194 C° , IR(cm<sup>-1</sup>): 3412,3466  $\nu(\text{NH}_2)$  , 3075  $\nu(\text{C}-\text{H})$ aromatic , 2858,2906  $\nu(\text{C}-\text{H})$ aliphatic , 1693  $\nu(\text{C}=\text{O})$ lactam , 1633  $\nu(\text{C}=\text{N})$ .

3<sub>b</sub> : Yield, 70% , m.p. 145-147 C° , IR(cm<sup>-1</sup>): 3317,3336  $\nu(\text{NH}_2)$  , 3070  $\nu(\text{C}-\text{H})$ aromatic , 2870,2928  $\nu(\text{C}-\text{H})$ aliphatic , 1708  $\nu(\text{C}=\text{O})$  lactam , 1631  $\nu(\text{C}=\text{N})$ . U.V (MeOH) : 389 nm ( $n-\pi^*$ ), 272 nm ( $\pi-\pi^*$ ).

3<sub>c</sub> : Yield, 67 % , m.p. 135-137 C° , IR(cm<sup>-1</sup>): 3400,3439  $\nu(\text{NH}_2)$  , 3073  $\nu(\text{C}-\text{H})$ aromatic , 2852,2926  $\nu(\text{C}-\text{H})$ aliphatic , 1710  $\nu(\text{C}=\text{O})$ lactam , 1645  $\nu(\text{C}=\text{N})$ .

3<sub>d</sub> : Yield, 74% , m.p. 165-167 C° , IR(cm<sup>-1</sup>): 3375,3444  $\nu(\text{NH}_2)$  3068  $\nu(\text{C}-\text{H})$ aromatic , 2870,2920  $\nu(\text{C}-\text{H})$ aliphatic , 1707  $\nu(\text{C}=\text{O})$  lactame , 1641  $\nu(\text{C}=\text{N})$ . U.V (MeOH) : 315 nm ( $n-\pi^*$ ), 266 nm ( $\pi-\pi^*$ ).

### Synthesis of 3-(Aryl)-5-phenyl-1,3-dihydrooxazol [5,4-c] isoxazol (4a-d)[20]

A mixture of (2a-d) (0.001 mole) and hydroxyl amine hydrochloride (0.003 mole, 0.2 gm) and sodium acetate anhydrous (0.003 mole, 0.24 gm) in (15 ml) ethanol and (5 ml) glacial acetic acid was refluxed for 8 hrs, then the reaction mixture was added to ice water and the solid product obtained was filtered and recrystallized from appropriate solvent.

4<sub>a</sub> : Yield, 70 % , m.p. 147-148 C° , IR(cm<sup>-1</sup>): 3201  $\nu(\text{NH})$  , 2858,2912  $\nu(\text{C}-\text{H})$ aliphatic , 1670  $\nu(\text{C}=\text{N})$  , 1516,1587  $\nu(\text{C}=\text{C})$ aromatic . U.V (MeOH) : 472 nm ( $n-\pi^*$ ), 281 nm ( $\pi-\pi^*$ ).

4<sub>b</sub> : Yield, 84% , m.p. 160-162 C° , IR(cm<sup>-1</sup>): 3151  $\nu(\text{NH})$  , 2816,2912  $\nu(\text{C}-\text{H})$ aliphatic , 1703  $\nu(\text{C}=\text{N})$  , 1560,1583  $\nu(\text{C}=\text{C})$ aromatic . U.V (MeOH) : 387 nm ( $n-\pi^*$ ), 262 nm ( $\pi-\pi^*$ ). <sup>1</sup>H-NMR (DMSO) (ppm) 7.02(-CH-) isoxazole ring , 7.58-8.28 (5H s for phenyl ring , 4H dd for aryl ring), 11.34(1H s, NH).

4<sub>c</sub> : Yield, 62 % , m.p. 170-172 C° , IR(cm<sup>-1</sup>): 3180  $\nu(\text{NH})$  , 2850,2918  $\nu(\text{C}-\text{H})$ aliphatic , 1701  $\nu(\text{C}=\text{N})$ . U.V (MeOH) : 380 nm ( $n-\pi^*$ ), 238 nm ( $\pi-\pi^*$ ).

4<sub>d</sub> : Yield, 57% , m.p. 128-130 C° , IR(cm<sup>-1</sup>): 3178  $\nu(\text{NH})$  , 2870,2987  $\nu(\text{C}-\text{H})$  aliphatic , 1716  $\nu(\text{C}=\text{N})$ .

### Synthesis of 7-(Aryl)-2-phenyl-6,7-dihydrooxazol [5,4-d] pyrimidine-5(4H)-one (5a-d)[21]

A mixture of (2a-d) (0.002 mole) and urea (0.002 mole, 0.12 gm) was dissolved in a mixture of acetone (15 ml) and ethanol (15 ml), then potassium carbonate (0.002 mole, 0.27 gm) was added with vigorous stirring then the mixture was refluxed for 14 hrs, after this the reaction mixture was poured in ice water and the solid product obtained was filtered and recrystallized from appropriate solvent.

5<sub>a</sub> : Yield, 86 % , m.p. 144-145 C° , IR(cm<sup>-1</sup>): 3309  $\nu(\text{NH})$  , 2812,2978  $\nu(\text{C}-\text{H})$ aliphatic , 1707  $\nu(\text{C}=\text{O})$  , 1645  $\nu(\text{C}=\text{N})$ cyclic . U.V (MeOH) : 365 nm ( $n-\pi^*$ ), 234 nm ( $\pi-\pi^*$ ).

5<sub>b</sub> : Yield, 58 % , m.p. 179-181 C° , IR(cm<sup>-1</sup>): 3211  $\nu(\text{NH})$  , 2890,2978  $\nu(\text{C}-\text{H})$  aliphatic , 1716  $\nu(\text{C}=\text{O})$  , 1649  $\nu(\text{C}=\text{N})$  cyclic. U.V (MeOH) : 358 nm ( $n-\pi^*$ ), 292 nm ( $\pi-\pi^*$ ).

5<sub>c</sub> : Yield, 75 % , m.p. 50-52 C° , IR(cm<sup>-1</sup>): 3209  $\nu(\text{NH})$  , 2899,2976  $\nu(\text{C}-\text{H})$ aliphatic , 1718  $\nu(\text{C}=\text{O})$  , 1649  $\nu(\text{C}=\text{N})$  cyclic. U.V (MeOH) : 289 nm ( $n-\pi^*$ ), 228 nm ( $\pi-\pi^*$ ).

5<sub>d</sub> : Yield, 57% , m.p. 150-152 C° , IR(cm<sup>-1</sup>): 3221  $\nu(\text{NH})$  , 2812,2985  $\nu(\text{C}-\text{H})$  aliphatic , 1726  $\nu(\text{C}=\text{O})$  , 1651  $\nu(\text{C}=\text{N})$  cyclic.

**Synthesis of 3-(Aryl)-5-phenyl-2,3-dihydro-1H-pyrazolo [4,3-d] oxazole (6a-d)[22]**

A mixture of (2a-d) (0.005 mole) and hydrazine hydrate (0.005 mole, 0.25 gm) in (20 ml) acetic acid was refluxed for 8 hrs, then the reaction mixture was added to ice water and the solid product obtained was filtered and recrystallized from apposite solvent.

6<sub>a</sub> : Yield, 78 % , m.p. 170-172 C° , IR(cm<sup>-1</sup>):3130  $\nu$ (NH)far from oxazole ring , 3200  $\nu$ (NH)near from oxazole ring , 2848,2943  $\nu$ (C-H)aliphatic , 1662  $\nu$ (C=N)cyclic .U.V(MeOH) : 305 nm(n- $\pi^*$ ), 259 nm ( $\pi$ - $\pi^*$ ).

6<sub>b</sub> : Yield, 68 % , m.p. 211-213 C° , IR(cm<sup>-1</sup>):3201  $\nu$ (NH)far from oxazole ring , 3311  $\nu$ (NH)near from oxazole ring , 2893,2953  $\nu$ (C-H) aliphatic ,1658  $\nu$ (C=N) cyclic. U.V(MeOH) :259 nm(n- $\pi^*$ ) , 228 nm ( $\pi$ - $\pi^*$ ).

6<sub>c</sub> : Yield, 71 % , m.p. 126-128 C° , IR(cm<sup>-1</sup>):3130  $\nu$ (NH)far from oxazole ring , 3209  $\nu$ (NH)near from oxazole ring , 2852,2960  $\nu$ (C-H)aliphatic ,1654  $\nu$ (C=N) cyclic. U.V(MeOH) :284 nm (n- $\pi^*$ ) , 228 nm ( $\pi$ - $\pi^*$ ).

6<sub>d</sub> : Yield, 76% , m.p. 208-210 C° , IR(cm<sup>-1</sup>):2211  $\nu$ (NH)far from oxazole ring , 3258  $\nu$ (NH) near from oxazole ring , 2812,2985  $\nu$ (C-H) aliphatic , 1726  $\nu$ (C=O), 1664  $\nu$ (C=N) cyclic. U.V(MeOH) :258 nm (n- $\pi^*$ ) , 224 nm ( $\pi$ - $\pi^*$ ). <sup>1</sup>H-NMR (DMSO) (ppm) 4.63 (s, NH far from oxazole ring and -CH-), 7.40-8.26 (5H s for phenyl ring , 4H dd for aryl ring), 13.59 (s, NH near from oxazole ring).

**Synthesis of Ethyl 2-(3-(Aryl)-5-phenyl-1H-pyrazolo [4,3-d] oxazol -2 (3H)-yl)acetate (7a-d)[23]**

A mixture of (6a-d) (0.003 mole) and ethyl chloro acetate (0.003 mole,0.36 gm) and sodium carbonate (0.003mole,0.31gm) in ethanol (20 ml) was refluxed for 7 hrs, then the reaction mixture was added to ice water and the solid product obtained was filtered and recrystallized from apposite solvent.

7<sub>a</sub> : Yield, 62 % , m.p. 153-155 C° , IR(cm<sup>-1</sup>):3130  $\nu$ (NH) , 3003  $\nu$ (C-H) aromatic , 2854,2970  $\nu$ (C-H)aliphatic ,1734  $\nu$ (C=O) ,1658  $\nu$ (C=N) . U.V(MeOH) : 306 nm(n- $\pi^*$ ) , 260 nm ( $\pi$ - $\pi^*$ ).

7<sub>b</sub> : Yield, 71 % , m.p. 133-135 C° , IR(cm<sup>-1</sup>):3078  $\nu$ (NH) , 3051  $\nu$ (C-H) aromatic , 2843,2939  $\nu$ (C-H)aliphatic ,1747  $\nu$ (C=O) ,1658  $\nu$ (C=N) . U.V(MeOH) : 269 nm(n- $\pi^*$ ) , 253 nm ( $\pi$ - $\pi^*$ ).

7<sub>c</sub> : Yield, 60 % , m.p. 123-125 C° , IR(cm<sup>-1</sup>):3203  $\nu$ (NH) , 3073  $\nu$ (C-H) aromatic , 2864,2978  $\nu$ (C-H)aliphatic ,1737  $\nu$ (C=O) ,1664  $\nu$ (C=N) . U.V(MeOH) : 229 nm(n- $\pi^*$ ) , 214 nm ( $\pi$ - $\pi^*$ ).

7<sub>d</sub> : Yield, 71% , m.p. 100-102 C° , IR(cm<sup>-1</sup>):3080  $\nu$ (NH) , 3001  $\nu$ (C-H) aromatic , 2912,2951  $\nu$ (C-H)aliphatic ,1749  $\nu$ (C=O) ,1656  $\nu$ (C=N) . U.V(MeOH): 306 nm(n- $\pi^*$ ) , 260 nm ( $\pi$ - $\pi^*$ ). <sup>1</sup>H-NMR (DMSO) (ppm) 1.21-1.25 (triplet -CH<sub>3</sub>) , 4.17 - 4.24 (quartate , -CH<sub>2</sub>-O-) , 4.68 (-CH<sub>2</sub>-C=O) , 4.98 (s, NH and -CH-), 7.42-8.28 (5H s for phenyl ring , 4H dd for aryl ring) .

**Synthesis of 2-(3-(Aryl)-5-phenyl-1H-pyrazolo[4,3-d]oxazol-2(3H)-yl)acetohydrazide(8a-d)[24]**

A mixture of (7a-d) (0.002 mole) and hydrazine hydrate (0.002 mole , 0.1 gm) in ethanol (20 ml) was refluxed for 10 hrs, then the reaction mixture was added to ice water and the solid product obtained was filtered and recrystallized from apposite solvent.

8<sub>a</sub> : Yield, 56 % , m.p. 187-189 C° , IR(cm<sup>-1</sup>): 3252,3288  $\nu$ (NH<sub>2</sub>) , 3034  $\nu$ (C-H)aromatic , 2850,2920  $\nu$ (C-H) aliphatic , 1651  $\nu$ (C=O) amide . U.V (MeOH) : 304 nm (n- $\pi^*$ ) , 244 nm ( $\pi$ - $\pi^*$ ).

8<sub>b</sub> : Yield, 77% ,m.p. 182-184 C° , IR(cm<sup>-1</sup>): 3290,3296  $\nu$ (NH<sub>2</sub>) , 3070  $\nu$ (C-H) aromatic , 2854,2929  $\nu$ (C-H) aliphatic , 1658  $\nu$ (C=O) amide . U.V (MeOH) : 228 nm (n- $\pi^*$ ) , 213 nm ( $\pi$ - $\pi^*$ ).

8<sub>c</sub> : Yield, 60 % , m.p. 128-130 C° , IR(cm<sup>-1</sup>): 3294,3317  $\nu$ (NH<sub>2</sub>) , 3067  $\nu$ (C-H) aromatic , 2848,2916  $\nu$ (C-H) aliphatic , 1629  $\nu$ (C=O) amide . U.V (MeOH) :385 nm (n- $\pi^*$ ) , 236 nm ( $\pi$ - $\pi^*$ ). Mass Spectra( 367 g / mole) .

8<sub>d</sub> : Yield, 64% , m.p. 178-180 C° ,IR(cm<sup>-1</sup>): 3311,3319  $\nu$ (NH<sub>2</sub>) ,3061  $\nu$ (C-H) aromatic , 2848,2918  $\nu$ (C-H) aliphatic , 1683  $\nu$ (C=O) amide . U.V (MeOH) : 260 nm (n- $\pi^*$ ) , 226 nm ( $\pi$ - $\pi^*$ ).

**Synthesis of (E)-N-(4-bromobenzyl)-2-(3-(Aryl)-5-phenyl-1H-pyrazolo [4,3-d]oxazol-2(3H)-yl)acetohydrazide (9a-d)[25]**

A mixture of aromatic aldehydes (0.001 mole) was dissolved in (20 ml) ethanol with (3 drops) from glacial acetic acid, then added (0.001 mole , 0.41 gm) from the compounde (8b) to the mixture and refluxed for 6 hrs, then the reaction mixture was added to ice water and the solid product obtained was filtered and recrystallized from apposite solvent.

9<sub>a</sub> : Yield, 75 % , m.p. 135-136 C° , IR(cm<sup>-1</sup>): 3244  $\nu$ (NH) , 3059  $\nu$ (C-H) aromatic , 2854,2922  $\nu$ (C-H) aliphatic , 1681  $\nu$ (C=O) amide , 1666  $\nu$ (C=N) . U.V (MeOH) : 341 nm (n- $\pi^*$ ) , 229 nm ( $\pi$ - $\pi^*$ ).

9<sub>b</sub> : Yield, 70% ,m.p. 295 C° decomposition , IR(cm<sup>-1</sup>): 3134  $\nu$ (NH) , 3066  $\nu$ (C-H) aromatic , 2852,2924  $\nu$ (C-H) aliphatic , 1660  $\nu$ (C=O) amide , 1629  $\nu$ (C=N) . U.V (MeOH) : 288 nm (n- $\pi^*$ ) , 227 nm ( $\pi$ - $\pi^*$ ).

9<sub>c</sub> : Yield, 68 % , m.p. 173-175 C° , IR(cm<sup>-1</sup>): 3130  $\nu$ (NH), 3049  $\nu$ (C-H) aromatic , 2881,2929  $\nu$ (C-H) aliphatic , 1681  $\nu$ (C=O) amide , 1624  $\nu$ (C=N) . U.V (MeOH) : 260 nm (n- $\pi^*$ ) , 227 nm ( $\pi$ - $\pi^*$ ).

9<sub>d</sub> : Yield, 68% , m.p. 268-270 C° ,IR(cm<sup>-1</sup>): 3213  $\nu$ (NH) , 3068  $\nu$ (C-H) aromatic , 2852,2924  $\nu$ (C-H) aliphatic , 1654  $\nu$ (C=O) amide , 1639  $\nu$ (C=N) . U.V (MeOH) : 260 nm (n- $\pi^*$ ) , 227 nm ( $\pi$ - $\pi^*$ ).

**Synthesis of (E)-4-(Arylidene)-1-(5-oxo-2-thioxoimidazolidin-1-yl)-2-phenyl-1H-imidazol-5(4H)-one (10 a,b)[23]**

A mixture of (3a,b) (0.001 mole) and ethyl chloro acetate (0.001 mole , 0.122 gm) in ethanol (20 ml) was refluxed for 10 hrs, then the reaction mixture was added to ice water and the solid product obtained was filtered and recrystallized from apposite solvent.

10<sub>a</sub> : Yield, 76 % , m.p. 123-125 C° , IR(cm<sup>-1</sup>): 3300 ν(NH) , 3086 ν(C-H) aromatic, 2858,2910 ν(C-H) aliphatic , 1720 ν(C=O) *New imidazole ring* . U.V (MeOH) : 354 nm ( n-π\* ), 269 nm ( π-π\* ).

10<sub>b</sub> : Yield, 72% ,m.p. 130-132 C° , IR(cm<sup>-1</sup>): 3318 ν(NH) , 3077 ν(C-H) aromatic, 2850,2949 ν(C-H) aliphatic , 1714 ν(C=O) *New imidazole ring* . Mass Spectra ( 442 g /mole ).

## RESULTS AND DISCUSSION

Schemes (I - II) were summarized the synthesis of different derivatives of hippuric acid (1) which was synthesized by treatment of benzoyl chloride with glycine. The reaction is followed by the appearance of the new (C=O) band at (1687 Cm<sup>-1</sup>) due to carbonyl of amide and band at 1753 for (C=O acid) and bands at (2484-3400 Cm<sup>-1</sup>) for stretching vibration of (acidic OH). λ<sub>max</sub> (MeOH) at (229 nm) responsible for (n → π\*) transition of (N and O) atoms and at (209 nm) due to (π → π\*). Compounds (2a - d) have been synthesized by the reaction of compound (1) with different aromatic aldehydes in acetic anhydride and acetic acid, the reaction proceeds by elimination of H<sub>2</sub>O molecule. The reaction is followed by appearance of the new (C=O) band at (1784-1797 Cm<sup>-1</sup>) for lactone ring which showed the increase of frequency of carbonyl and band at (1645-1654 Cm<sup>-1</sup>) for stretching vibration of (C=N). The λ<sub>max</sub> (MeOH) at (301-388 nm) responsible for (n → π\*) transition of (N and O) atoms and at (232-252 nm) due to (π → π\*). <sup>1</sup>H-NMR (DMSO)(ppm) for compound (2c) shows appearance asinglet band at (7.38) due to proton of (-CH=) and many signals at (7.60-8.34) due to aromatic protons (5H s for phenyl ring , 4H dd for aryl ring ). The treatment of compound (2a - d) with Thiosemicarbazide led to the formation of (3a - d). Compound (3a - d) have been identified by IR spectrum which it shows the appearance of the new two bands (asymmetric & symmetric at (3466-3336 Cm<sup>-1</sup>) and (3412-3317 Cm<sup>-1</sup>) and band at (1693-1710 Cm<sup>-1</sup>) for stretching vibration of (C=O lactam). The λ<sub>max</sub> (MeOH) at (315-389 nm) responsible for (n→π\*) transition of (N and O) atoms and at (272-266 nm) due to (π→ π\* ). Compounds (4a - d) have been obtained by the reaction of hydroxyl amine hydrochloride and sodium acetate anhydrous with compounds (2a - d) in ethanol and glacial acetic acid. The reaction is followed by the appearance of the new band at (3201-3151 Cm<sup>-1</sup>) due to (N-H) group and disappearance the band of (C=O) for lactone ring. The λ<sub>max</sub> (MeOH) at (472-387 nm) responsible for (n→ π\*) transition of (N and O) atoms and at (281-262 nm) due to (π → π\*). <sup>1</sup>H-NMR (DMSO) (ppm) for compound (4b) shows appearance asinglet band at (7.02) due to proton of (-CH-) isoxazole ring and many bands at (7.5-8.2) due to aromatic protons (5H s for phenyl ring , 4H dd for aryl ring) and other singlet band at(11.34) due to proton of (NH) group .

The treatment of compounds (2a - d) with urea in a mixture of ethanol and acetone and K<sub>2</sub>CO<sub>3</sub> led to the formation of (5a - d). The reaction is followed by show appearance of the new (C=O) band at (1726-1707 Cm<sup>-1</sup>) due to urea moiety in pyrimidine ring , and appearance a new band at

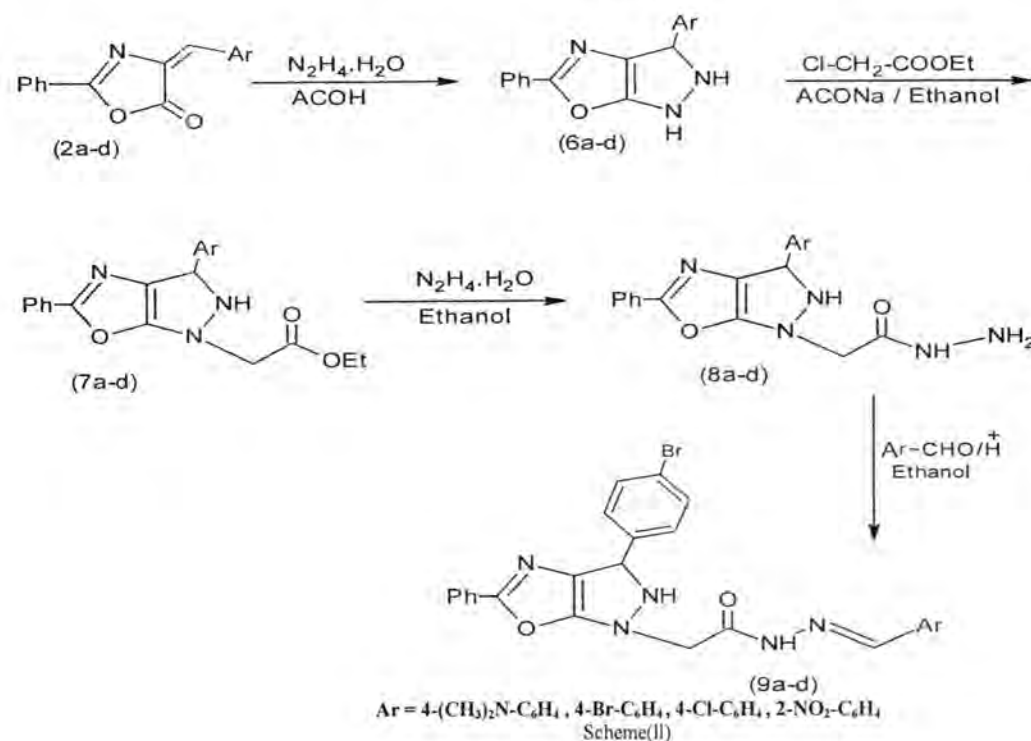
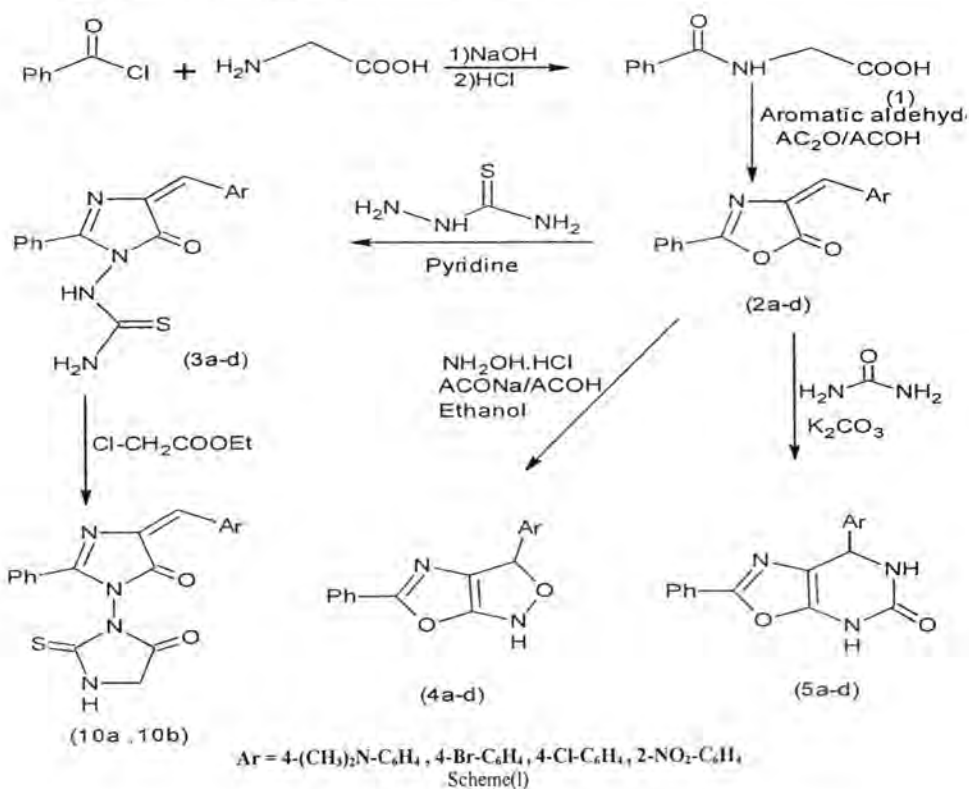
(3309-3209 Cm<sup>-1</sup>) due to (N-H) which near from oxazole ring , and other band at (3273-3155 Cm<sup>-1</sup>) due to (N-H) which far from oxazole ring .The λ<sub>max</sub> (MeOH) at (365-289 nm) responsible for (n→ π\*)transition of (N and O)atoms and at (292-228 nm) due to (π → π\* ) . Compounds (10a,b) have been synthesized by the reaction of compounds (3a,b) with chloro ethyl acetate in ethanol .The reaction is followed by the appearance of the new (C=O) band at(1720,1714 Cm<sup>-1</sup>) for the new imidazole ring , and shows the disappearance the bands of (NH<sub>2</sub>) group.The λ<sub>max</sub>(MeOH) for compound(10a) at(354 nm) responsible for (n→ π\*)transition of (N and O)atoms and at (269 nm)due to (π → π\* ). Mass Spectra for compound (10b) shows identical the experimental molecular weight with theoretical molecular weight which equal to (442 g/mole).

Scheme (II) Compounds (6a-d) have been synthesized by the reaction of hydrazine hydrate with compounds (2a-d) in acetic acid. The reaction is followed by the appearance of two new bands at (3311-3200 Cm<sup>-1</sup>) and (3211-3130 cm<sup>-1</sup>)due to two (N-H)group pyrazole ring and disappearance the band of (C=O) for lactone ring . The λ<sub>max</sub> (MeOH) at (305-258 nm) responsible for (n→ π\*) transition of (N and O) atoms and at (259-224 nm) due to (π → π\* ) . <sup>1</sup>H-NMR (DMSO)(ppm) for compound (6d) shows appearance asinglet band at (4.63) due to proton of (NH) group far from oxazole ring which overlapped with proton of (-CH-) pyrazole ring and many bands at(7.40-8.26) due to aromatic protons (5H s , 4H d,d) and asinglet band at (13.59) due to proton of (NH) group which near from oxazole ring . The treatment of compounds (6a - d) with Chloro ethyl acetate led to the formation of (7a - d) . Compounds (7a - d) have been identified by IR spectrum which it show appearance of the new (C=O) band at (1749-1734 Cm<sup>-1</sup>)for ester group . The λ<sub>max</sub> (MeOH) at (306-229 nm) responsible for (n→π\*) transition of (N and O)atoms and at (260-214 nm) due to (π → π\* ) . <sup>1</sup>H-NMR (DMSO)(ppm) for compound (7d) shows appearance a triplet band at (1.21-1.25) due to protons of (-CH<sub>3</sub>) , and a quartate band at (4.17-4.24) due to two protons of (-CH<sub>2</sub>-O) and asinglet band at (4.68) due to two protons of (-CH<sub>2</sub>-C=O) , and other singlet band at (4.98) due to proton of (NH) group which overlapped with proton of (-CH-) pyrazole ring , and many bands at (7.42-8.28) due to aromatic protons (5H s for phenyl ring , 4H dd for aryl ring) . Compounds (8a-d) have been synthesized by the reaction of Compounds (7a-d) with hydrazine hydrate in ethanol, the reaction proceeds by elimination of (C<sub>2</sub>H<sub>5</sub>OH) molecule. The reaction is followed by appearance of the new two bands (asymmetric & symmetric) at (3319-3252 Cm<sup>-1</sup>) and (3311-3288 Cm<sup>-1</sup>) due to (NH<sub>2</sub>) group ,and anew (C=O) band at (1683-1629 Cm<sup>-1</sup>) for amide which shows decrease of frequency of carbonyl .The λ<sub>max</sub> (MeOH) at (385-228 nm) responsible for (n→ π\* )transition of (N and O)atoms and at (244-213 nm) due to (π → π\* ) . Mass Spectra for compound (8c) shows identical the experimental molecular weight with theoretical molecular weight which equal to (367 g/mole) . Schiff bases (9a-d) have been obtained by reaction of compound (8b) with different aromatic aldehydes in



ethanol and glacial acetic acid. The reaction is followed by disappearance the band of (NH<sub>2</sub>) group and appearance anew band at (3331-3150 Cm<sup>-1</sup>) due to (NH amide) . The λ<sub>max</sub> (MeOH) at (341-260 nm) responsible for (n → π\*)

transition of (N and O)atoms and at (229-227 nm) due to (π → π\*).



## REFERENCES

- [1] I.J.Turchi , M.J.S.Dewar . Chemistry of oxazoles ., Chem Rev 75: 389–437 (1975).
- [2] A.Nishida ,M.Fuwa ,S.Naruto , Y.Sugano , H.Saito and M.Nakagawa . Solid-phase Synthesis of 5-(3-indolyl) Oxazoles that Inhibit lipid Peroxidation .. *Tetrahedron Lett.* 41 4791 (2000) .
- [3] Y.Li , F.Guo , Z.Zha and Zhiyong Wang. Metal-free synthesis of polysubstituted oxazoles via a decarboxylative cyclization from primary  $\alpha$ -amino acids. *Sustainable Chemical Processes* ., 1:8 (2013) .
- [4] R.Nesi , S.Turchi , D.Giomi ., New perspectives in oxazole chemistry: synthesis and cycloaddition reactions of a 4-nitro-2-phenyl Derivative1. *J.Org. Chem.* 61:7933–7936 (1996) .
- [5] K. M. Gokhale ,O.Wagal and Aashish Kanitkar. Synthesis of Di and Trisubstituted Oxazoles in Nonionic Liquid Under Catalyst Free Conditions ., *Int.J.Pharm.Phytopharmacol.Res.*, 1(4): 156-160(2012) .
- [6] S.R.Ranabir , L.K.Neil , C.M.Jill , T.W.Christopher . In vivo processing and antibiotic activity of microcin B17 analogs with varying ring content and altered bisheterocyclic sites, *Chemistry & Biology* ., 6, 5, 305-318(1999).
- [7] A. A. Marzouk, V. M. Abbasov, A. H. Talybov and S.K.Mohamed . Synthesis of 2,4,5-Triphenyl Imidazole Derivatives Using Diethyl Ammonium Hydrogen Phosphate as Green, Fast and Reusable Catalyst. *World Journal of Organic Chemistry* ., Vol. 1, No. 1, 6-10(2013).
- [8] C.h.Voosala , N. S. Yarla, M. Nakka and Siddaiah Vidavaluri (Facile Synthesis of 1-(substituted phenyl)-2-phenyl-4-(substitutedbenzylidene)-imidazole-5-ones and Antifungal Activity Studies against Phytopathogens . Voosala et al., *Med chem* , 4:1(2013).
- [9] S.S.Shah and K.Goswami . Synthesis, characterization and anti microbial activity of some novel chalcone compounds having benzyloxymonochloro resacetophenone moiety ., *Der Pharma Chemica*, 5(1):75-80(2013).
- [10] R.Ravichandran , M.Rajendran , D.Devapiriam .Studies on Chalcone Derivatives Antioxidant and Stability Constant., *J.of Chem, Bio and Physical Sciences* ., Vol. 3, No. 4; 2446-2458(2013) .
- [11] S.D.Arikkatt , B.Mathew , J.Joseph , M.Chandran , A.R. Bhat , K. Krishnakumar . Pyrimidine Derivatives and Its Biological Potential – A Review . *Int.J. of Org and Bio Chemistry.*, ISSN 2249 – 0345(2014) .
- [12] N.Malik , P.Dhiman , A.Khatkar , N.Redhu , D.P.Singh . Pyrazole Derivatives : A Worthy Insight Into Potent Biological Activities: A Review., *IJPRBS*, Volume 2(4): 415 -427(2013).
- [13] J.T.Li , X.H.Zhang and Z.P.Lin. An improved synthesis of 1, 3, 5-triaryl- 2- pyrazolines in acetic acid aqueous solution under ultrasound irradiation , *B. J. Org. Chem* ., 3: 1860-5397(2007).
- [14] B.M.Rao , S.Ramesh , D. Bardalai, H. Rahman and H.A.Shaik. Synthesis , characterization and evaluation of anti-epileptic activity of four new 2-pyrazoline derivatives compounds ., *Sch. J. App. Med. Sci.*, 1(1):20-27(2013).
- [15] A.Budakoti , A.R.Bhat , F.Athar , A.Azam . Synthesis and evaluation of 3-(3- bromo phenyl)-5-phenyl-1-(thiazolo [4,5-b] quinoxaline-2-yl)-2-pyrazoline Derivatives, *Eur. J. Med. Chem.*, 43: 1749-1757(2008) .
- [16] P. Jayaroopa , G. V.Kumar , N. Renuka , M.A. H. Nayaka , K. Ajay Kumar. Evaluation Of New Pyrazole Derivatives For Their Biological Activity: Structure-Activity Relationship. *IJPRIF.*, Vol.5, No.1, pp 264-270(2013).
- [17] Abdul Jabar Kh. Atia . Molecules ,Synthesis and Antibacterial Activities of New Metronidazole and Imidazole Derivatives .,14(17) 2431-2446 (2009) .
- [18] F.C.Savariz , M.A.Foglio , J. E.de Carvalho , A.L.T.G. Ruiz , M.C. T. Duarte , M.F. da Rosa , E. Meyer and M.H.Sarragiotto , Synthesis and Evaluation of New  $\beta$ -Carboline-3-(4-benzylidene)-4H-oxazol-5-one Derivatives as Antitumor Agents ., *Molecules* , 17, 6100-6113 (2012) .
- [19] A.K.AL. Abodi , N.Majed , S.A.Kadhem and R.H.Al-Bayati . Synthesis and Characterization of New 1,3-Oxazol-5-(4H)-one Derivatives . *American Journal of Organic Chemistry* ., 2, 6, 143-150 (2012).
- [20] H.H.Sayed , A.H.Shamroukh and A.E.Rashad . Synthesis and biological evaluation of some pyrimidine, pyrimido[2,1-b][1,3]thiazine and thiazolo[3,2-a]pyrimidine derivatives ., *Acta Pharm.*, 56, 231-244, (2006).
- [21] S.Y .Hassan . Synthesis, Antibacterial and Antifungal Activity of Some New Pyrazoline and Pyrazole Derivatives ., *Molecules* ., 18 , 2683-2711 (2013) .
- [22] W.S.Loh ,C.K.Quah ,T.S.Chia ,H.F.Sapnakumari, B. Narayana and B.K.Sarojini . Synthesis and Crystal Structures of N-Substituted Pyrazolines ., *Molecules*, 18, 2386-2396 (2013).
- [23] J.H.Tomma . Synthesis of New Schiff Bases and 2,3-Disubstituted -1,3-Thiazolidin-4-one Derivatives Containing Benzothiazole Moiety Ibn- AL-haitham J. For Pure & Appl . Sci., V.24, 2 (2011).
- [24] M.M.Abdulrasool , A.H.Jawad and J.K.Shneine . Synthesis , Characterization and Evaluation of Biological Activity of New Heterocyclic Compounds Containing 1,2,4-Triazole and 1,3,4-Thiadiazole Rings .*International Journal of Applied Science and Technology* .,Vol 2 , No 10 (2012) .
- [25] H. N.Kim , H.K.Lee ,and S.W. Lee Bull . A Novel Linking Schiff-Base Type Ligand (L: py-CH=N-C<sub>6</sub>H<sub>4</sub>-N=CH-py) and Its Zinc Coordination Polymers: Preparation of L, 2-Pyridin-3-yl-1H-benzimidazol, trans-[Zn(H<sub>2</sub>O)<sub>4</sub>L<sub>2</sub>](NO<sub>3</sub>)<sub>2</sub>(MeOH)<sub>2</sub>, [Zn(NO<sub>3</sub>)(H<sub>2</sub>O)<sub>2</sub>(L)](NO<sub>3</sub>)(H<sub>2</sub>O)<sub>2</sub>, and [Zn(L)(OBC)(H<sub>2</sub>O)] (OBC = 4,4'-Oxybis(benzoate)) ., *Korean Chem. Soc.*,Vol. 26, 892 ( 2005).



## Flow Injection- Spectrophotometric Determination of Clonazepam Based On Its Oxidative Condensation with Promethazine Hydrochloride

Mouayed Q. Al-Abachi, and Hind Hadi

Department of Chemistry, College of Science, University of Baghdad, Baghdad-Iraq

### Article info

Received 30/9/2014

Accepted 30/11/2014

### ABSTRACT

Simple methods were proposed for the spectrophotometric determination of clonazepam (CLO) in pharmaceutical formulations. The methods were based on the reaction of CLO with promethazine hydrochloride (PMH) in the presence of potassium periodate. The green water soluble product was measured at  $\lambda_{max}$  606 nm using both batch and flow injection analysis (FIA) approach. The effect of chemical and physical parameters was investigated by univariate method. Under the optimum conditions, calibration graphs were observed linear from 0.5-25 and 5-120  $\mu\text{g mL}^{-1}$  CLO with detection limits of 0.23 and 1.38  $\mu\text{g mL}^{-1}$  CLO by batch and FIA procedure respectively. The relative standard deviations of the proposed methods were less than 1.03 and 1.64 by batch and FIA procedure respectively. The FIA sample throughput was 120 sample per hour. The proposed methods were successfully applied to the determination of CLO in its pharmaceutical preparations.

### الخلاصة

يتضمن البحث تطوير طريقة طيفية جديدة وبسيطة للتقدير الكمي للمقادير الضئيلة من الكلونازيبام في المحاليل المائية والمستحضرات الصيدلانية باستعمال المطياف الضوئي-الحقن الجرياني. تعتمد الطريقة على تفاعل الأزواج التأكسدي بين الكلونازيبام مع كاشف بروميتازين هيدروكلورايد بوجود بيرايودات الصوديوم، إذ يتكون ناتج أخضر مستقر وذائب في الماء يعطي أعلى قمة امتصاص عند طول موجي 606 نانومتر. تشير منحنيات الامتصاص مقابل التركيز بأن قانون بير ينطبق ضمن مدى التركيز 0.5-25 و 5-120 مايكروغرام مل-امن الكلونازيبام ويحد كشف 0.23 و 1.38 مايكروغرام مل-امن الكلونازيبام لطريقتي الدفعة والحقن الجرياني على التوالي. قيم الانحراف القياسي النسبي للطرق المقترحة كانت أقل من 1.03 و 1.64 لطريقتي الدفعة والحقن الجرياني على التوالي. وبمعدل نمذجة 120 نموذج بالساعة. درست الظروف المثلى للتفاعل وجميع المتغيرات الكيميائية والفيزيائية بدقة وطبقت الطريقتين بنجاح على المستحضرات الصيدلانية الحاوية على الكلونازيبام.

### INTRODUCTION

Clonazepam (CLO; 5-(o-chlorophenyl) -1,3-dihydro-7-nitro-2H-1,4-benzodiazepin- 2-one), a benzodiazepine with prominent anticonvulsant, anxiolytic properties Figure(1). It has been most effective in treating typical and atypical absence, myoclonic and akinetic seizures, and infantile spasms. Coadministration of a barbiturate may exacerbate the drowsiness caused by clonazepam [1, 2].

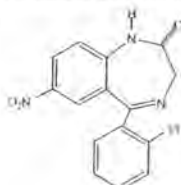


Figure 1- Clonazepam

A literature survey revealed that clonazepam is official in the Indian, British, American, European and Japanese Pharmacopeia. IR spectroscopy method has been reported for identification and potentiometric and HPLC methods have been reported for assay [3-7]. Different HPLC and GC methods that have been reported for the determination of Clonazepam in biological fluids [8-13].

Among various methods available for trace analysis, FIA-spectrophotometry continues to be one of the most popular

because of its simple and cost effectiveness. There are few FIA- spectrophotometric methods available for the determination of CLO and these methods were not completely satisfactory as they either require temperature or pH control. The present study describes the development of a batch and FIA methods based on oxidative coupling reaction between CLO and PMH in presence of sodium periodate in neutral medium. The green product was spectrophotometrically measured at 606 nm.

### METHODS AND MATERIALS

#### Apparatus

All spectral and absorbance measurements were carried out on Shimadzu UV-Visible 260 digital double beam recording spectrophotometer. A flow cell with 50  $\mu\text{L}$  internal volume and 1cm bath length was used to measure absorbance. A two-channel manifold (Figure 2) was employed for the FIA spectrophotometric determination of CLO drug. A peristaltic pump (Ismatec, Labortechnik-Analytik, CH-8152, and Glatbrugg - Zurich-Switzerland) was used to transport the carriers' solutions. (Rheodyne, Altex 210, Supelco-USA) injection valve was employed to provide appropriate injection volumes of standard solutions and samples. Flexible vinyl tubing of

0.5 mm internal diameter was used for the peristaltic pump. Reaction coil (RC) was of Teflon with internal diameter of 0.5 mm. Channel (A) was used to transport PMH, and channel (B) to transport oxidant solution (sodium periodate). The sample solution was injected into the stream of PMH, through the injection valve, which then combined at T-link with stream of sodium periodate and mixed in reaction coil. Solutions were propelled by peristaltic pump with total flow rate of 4.5 mL min<sup>-1</sup>. The absorbance was measured at 606 nm.

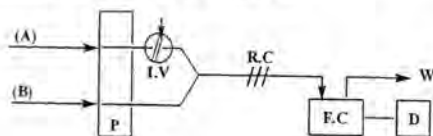


Figure 2. Manifold Employed for FIA-Spectrophotometric Determination of CLO with PMH and NaIO<sub>4</sub> where: A, 10 mM of PMH Solution; B, 0.1M of Sodium Periodate Solution; I.V, Injection Valve; RC, Reaction Coil; S, Sample; P, Peristaltic Pump; F.C, Flow Cell; D, Detector; W, Waste Reagent and Materials

Analytical reagent grade chemicals and distilled water were used throughout. Pure CLO drug sample was kindly provided from State Company of Drug Industries and Medical Appliances, SDI, Samara, Iraq. Pharmaceutical tablets were obtained from commercial sources.

#### Clonazepam (CLO) Reduction Solution (500 µg mL<sup>-1</sup>)

This was prepared by dissolving 0.0500 g of CLO in ethanol. It was transferred into 50 mL volumetric flask, and diluted to the mark with the same solvent. The solution was transferred into beaker of 125 mL. A 20 mL of distilled water, 20 mL of hydrochloric acid (11.64 N), and then 3 g of zinc powder were added. The beaker was allowed to stand for 15 min at room temperature (25 °C), then the solution was filtered into 100 mL volumetric flask, washed the residues with distilled water, and finally the volume was diluted to the mark with distilled water to obtain 500 µg mL<sup>-1</sup> of CLO reduction solution [14]. More dilute solution was prepared daily by appropriate dilution using distilled water.

#### Promethazine Hydrochloride (PMH) Solution (1.5 and 10mM)

It was freshly prepared by dissolving 0.0481 g and 0.3209 g of PMH and diluting it to 100 mL with distilled water in volumetric flask.

#### Sodium Periodate Solution (0.1M and 0.2M)

It was prepared by dissolving 2.1360 g and 4.2720 g of SPI and diluting it to 100 mL with distilled water in a volumetric flask.

#### Solutions of Pharmaceutical Tablets

Tablets samples: Twenty tablets were accurately weighed and finely powdered. An amount of the powder equivalent to 50 mg of CLO was dissolved in 30 mL of ethanol. The solution was filtered into 50 mL volumetric flask, the residue was washed with ethanol and finally the volume was diluted to the mark with the same solvent to obtain 1000 µg mL<sup>-1</sup> of CLO. This solution was transferred into 125 mL beaker and was reduced as previously described. Further appropriate solutions of pharmaceutical tablets were made using distilled water.

#### Reaction Mechanism of the Method

The reduced drug of CLO, by virtue of their strong electron donating ability, coupling with PMH (oxidized by sodium periodate), leading to the formation of oxidative coupled product, as shown in Figure (3) [15].

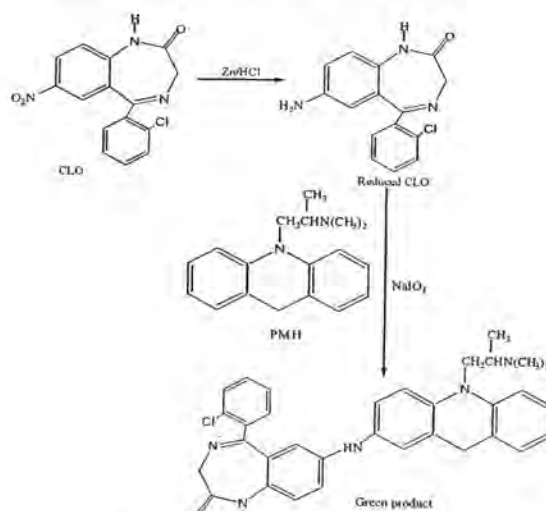


Figure 3: Mechanism of Reaction Product

Based on the observed molar reactivity of the reaction between CLO and PMH in the presence of sodium periodate to yield a green product ( $\lambda_{max}$  of 606 nm with a molar absorption coefficient of 10607.5 L.mole<sup>-1</sup>.cm<sup>-1</sup>), the reaction given in Figure 3 was postulated.

#### Procedures

##### • General Batch Procedure:

An aliquot of sample containing 12.5-625 µg of CLO was transferred into a series of 25 mL standard flasks. A volume of 4.0 mL of 1.5 mM PMH solution, and 1.0 mL of 0.2M sodium periodate solution were added. The contents of the flasks were diluted to the mark with distilled water, mixed well and left for 25 min. The absorbance was measured at 606 nm (at room temperature 25°C) against reagent blank containing all materials except CLO. A calibration graph was drawn and the regression equation calculated. For the optimization of conditions and in all subsequent experiments, a solution of 500 µg was used in a final volume of 25 mL (i.e. 20 ppm).

##### • General FIA Procedure

Working solutions of CLO in the range 5-120 µg mL<sup>-1</sup> were prepared from stock solutions. A 200 µL portion of CLO was injected into the stream of 10 mM PMH which then mixed with the oxidant solution (sodium periodate of 0.1M), with a flow rate of 2.25 mL min<sup>-1</sup> in each channel (Figure 1). The resulting absorbance of the green product was measured at 606 nm and a calibration graph was shown in Table 1. Optimization of conditions was carried out on 100 µg mL<sup>-1</sup> of CLO.

#### RESULTS AND DISCUSSION

The factors affecting the sensitivity and stability of the coloured product resulting from the oxidative of CLO with PMH and sodium periodate in neutral medium were

carefully studied. A typical spectrum for CLO reaction product against reagent blank is shown in Figure 4.

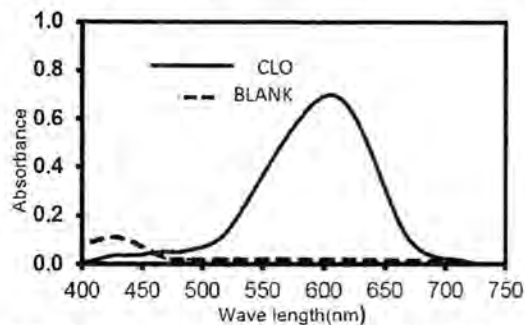


Figure 4: Absorption Spectra of 20 µg/mL of CLO Treated as Described Under Procedure and Measured Against Blank and the Reagent Blank Measured Against Distilled Water.

#### Batch Spectrophotometric Determination Chemical Variables, Time of Reaction, and Compositions of the Product and Temperature of Reaction

The best experimental conditions for the determination of CLO were established for PMH 1.5 mM (from 0.5 to 5 mL), NaIO<sub>4</sub> 0.2M (from 0.75 to 3 mL) by adding various volumes of their solutions to a fixed concentration of CLO and measuring the absorbance at 606 nm. The results obtained (Figure 5) showed that 4.0 mL of 1.5 mM PMH and 1 mL of 0.2M NaIO<sub>4</sub> gave the maximum color intensity and led to the maximum color stability of the dye product for 500 µg of CLO in a final volume of 25 mL.

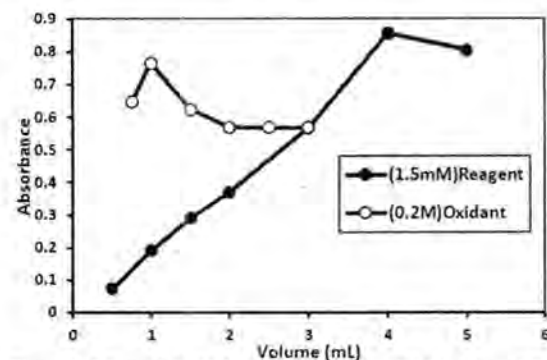


Figure 5: Effect of the Volume of Reagent (PMH 1.5mM) and Oxidant (NaIO<sub>4</sub> 0.2M)

Experimental results revealed that the colour intensity reaches a maximum level after the drug solution had been reacted with PMH and sodium periodate in a neutral medium for 25 min, therefore, a 25 min development time was suggested as the optimum reaction time and remain stable for 120 min. The order of adding reagents is an essential part of the experiment, it was found that the order of adding reagent cited under general procedure (Drugs+Reagent+Oxidant) gave a maximum color intensity and a minimum absorbance of the blank and was used in all subsequent experiments. The effect of temperature on the colour intensity of the dye was studied. In practice, a higher absorbance was obtained when the colour was developed at room temperature (25°C) than

when the calibrated flasks were placed in an ice-bath at (0°C) or in a water bath at (60 °C).

The composition of the formed complex between CLO and PMH in the presence of sodium periodate has been established under the recommended optimum conditions by using mole ratio method. The stoichiometry of the reaction was studied using equimolar concentrations (1.584 × 10<sup>-3</sup> M) of the CLO and PMH at constant sodium periodate concentration, adopting mole ratios' method, a molar ratio of 1:1 drug to PMH was obtained by the applied method as shown in Figure 6.

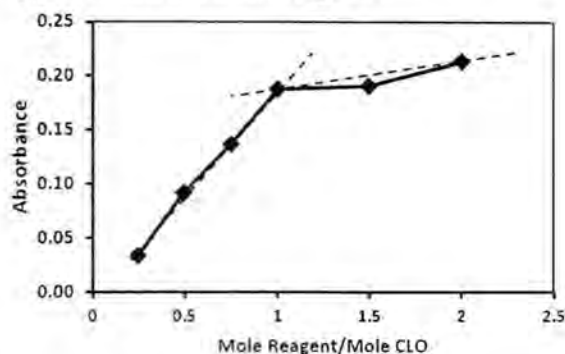


Figure 6: Mole Ratio Plot

The regression equation obtained, from a series of CLO standards, and the analytical features of this procedure are summarized in Table 1 in which the main performance of the flow procedure developed for CLO determination in order to make an effective comparison between the two approaches are also summarized.

Table 1: Analytical Characteristics of the Procedures Developed for the Determination of CLO

Parameter	Batch procedure	FIA procedure
Regression equation	$y = 0.0336x + 0.0374$	$y = 0.0115x - 0.0488$
Linear range (µg mL <sup>-1</sup> )	0.5-25	5-120
Correlation coefficient (R <sup>2</sup> )	0.9985	0.9991
Limit of detection (s/n=3) µg mL <sup>-1</sup>	0.23	1.38
Reproducibility %	<1.03	<1.18
Average of recovery, %	99.525	100.855
Through-put (sample per hour)	2	120

#### FIA-Spectrophotometric Determination

The batch method of determining CLO was adopted as a basis to develop FIA procedure. The manifold used to determine CLO was so designed to provide different reaction conditions to magnify the absorbance signal generated by the reaction of CLO drug with PM and sodium periodate. Maximum absorbance intensity was obtained when the sample was CLO was injected into the stream of 10 mM PMH which then mixed with the oxidant solution (sodium periodate of 0.1M) in reaction coil as given in Figure 1. The influence of different chemical and physical FIA parameters on the absorbance intensity of the colored product was optimized as follows:

#### Optimization of Chemical Parameters

The effects of various concentrations of PMH were investigated. A concentration of 10 mM gave the highest absorbance and was chosen for further use. The results are shown in Figure 7. It was observed that the reaction between CLO and PMH depends on the oxidation process with sodium periodate. Various concentrations of NaIO<sub>4</sub>

were investigated; the optimum concentration of 0.1M gave the best results and minimum blank value as shown in Figure 7 and was considered as optimum value.

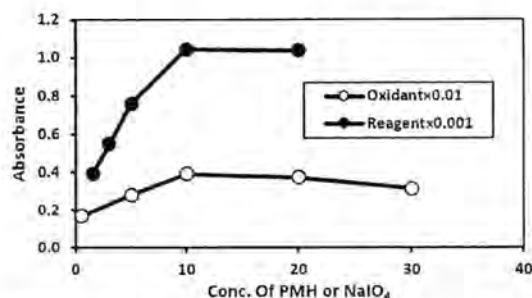


Figure 7: Effect of the Concentration of Reagent and Oxidant Optimization of Manifold Parameters

The variables studied under the optimized reagent concentrations are the flow rate, the injected sample volume and the reaction coil length. The effect of injected sample volume was investigated using three injected volumes 150, 200 and 250  $\mu\text{L}$ . The results obtained showed that injected sample of 150  $\mu\text{L}$  gave the lower absorbance between them, while the injected sample of 250  $\mu\text{L}$  gave unstable response; therefore a 200  $\mu\text{L}$  was chosen because it gave a good absorbance and a stable response. The effect of total flow rate on the sensitivity of the coloured reaction product was investigated in the range of 0.25-6  $\text{mL min}^{-1}$ . The results obtained showed that a total flow rate of 4.5  $\text{mL min}^{-1}$  (2.25  $\text{mL min}^{-1}$  in each line) gave the highest absorbance as shown in Figure 8 and was used in all subsequent experiments.

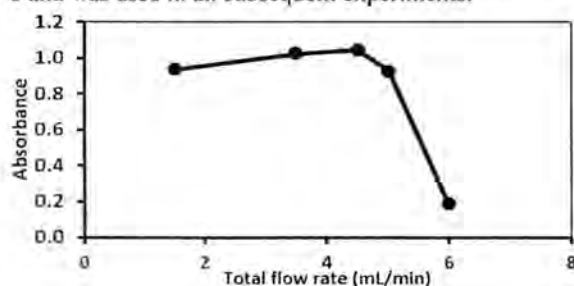


Figure 8: Effect of Total Flow Rate

Coil length is an essential parameter that affects the sensitivity of the coloured reaction product and was investigated in the range of 25-150 cm. The results obtained showed that a coil length of 50 cm gave the

highest absorbance as shown in Figure 9 and was used in all subsequent experiments.

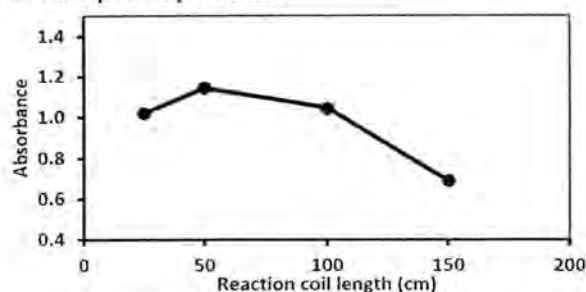


Figure 9: Effect of Reaction Coil Length

The reaction time is also an important parameter that affects the sample throughput and was investigated by calculating the interval time between the sample injection and the appearance end of signal. The reaction time for each sample was 30 sec, therefore, the sample throughput was 120 samples per hour.

#### Analytical Characteristics

Analytical characteristics such as sampling rate, detection range, correlation coefficient and relative standard deviation (RSD) of each method were determined for the above optimized conditions as shown in Table 1. In comparison of the batch with FIA procedure, the later is more convenient than the former method because of its speed (sample throughput of 120 injections per hour) and wider linear range of calibration graph. In addition the precision of the methods was evaluated by analyzing pure sample of CLO and a good recovery was obtained Table 2.

Table 2: Accuracy and Precision of the Proposed Methods

Method	Conc. of CLO, $\mu\text{g mL}^{-1}$		E%*	Rec.%*	RSD%*
	Present	Found			
Batch	5.00	5.03	0.64	100.64	1.03
	10.00	9.92	-0.79	99.21	0.49
FIA	50.00	50.39	0.78	100.78	0.11
	70.00	70.65	0.93	100.93	1.18

\*Average of four determinations.

#### Analysis of Pharmaceutical Samples

The suggested method was applied to the quantitative determination of CLO in pharmaceutical formulations. Two types of tablets containing CLO have been analyzed and they gave a good accuracy and precision as shown in Table 3. The proposed methods were compared successfully with the British pharmacopeia's standard method [16], since F-test and T-test showed that there were no significant differences between the proposed and the official methods Table 4.

Table 3: Application of the Proposed Methods for Determination of CLO in Pharmaceutical Forms

Proposed method	Drug form	Conc. of CLO, $\mu\text{g mL}^{-1}$		E%*	Rec.%*	RSD%*
		Present	Found			
Batch	0.5mg	5.00	4.92	-1.59	98.40	1.73
		10.00	9.91	-0.87	99.13	1.14
	2mg	5.00	4.96	-0.75	99.25	3.91
		10.00	9.99	-0.13	99.87	0.57
FIA	0.5mg	20.00	19.97	-0.15	99.86	1.00
		30.00	30.13	0.42	100.42	0.20
	2mg	20.00	19.94	-0.29	99.71	1.46
		30.00	29.61	-1.29	98.71	0.75

\*Average of four determinations

Table 4: The Comparison of the Proposed Methods with Standard Method Using t- and F-Statistical Tests

Drug form	Proposed method				Standard method	
	Batch		FIA		Rec. (Xi) <sub>2</sub>	(Xi - X̄) <sub>2</sub> <sup>2</sup>
	Rec.% (Xi) <sub>1</sub>	(Xi - X̄) <sub>1</sub> <sup>2</sup>	Rec.% (Xi) <sub>1</sub>	(Xi - X̄) <sub>1</sub> <sup>2</sup>		
CLO pure	99.925	0.258	100.855	0.619	100.500	0.322
0.5mg	98.765	0.425	100.140	0.005	99.800	0.018
2mg	99.560	0.020	99.210	0.736	99.500	0.188
S**	0.555 (S <sub>1</sub> <sup>2</sup> =0.352)		(S <sub>2</sub> <sup>2</sup> =0.687)		(S <sub>2</sub> <sup>2</sup> =0.263)	
t (2.776)*	1.318		0.278		(n <sub>1</sub> + n <sub>2</sub> - 2) = 4	
F (19.000)*	1.336		2.584		n <sub>1</sub> = 3, n <sub>2</sub> = 3	

\*Table value.

$$**s = \text{pooled standard deviation} = \sqrt{\frac{(n_1-1)S_1^2 + (n_2-1)S_2^2}{n_1+n_2-2}}, t = \frac{|\bar{X}_1 - \bar{X}_2|}{s \sqrt{\left(\frac{1}{n_1} + \frac{1}{n_2}\right)}}, S_1^2 = \text{variation} = \frac{\sum(X_i - \bar{X})^2}{n_1 - 1} \text{ and } S_2^2 = \frac{\sum(X_i - \bar{X})^2}{n_2 - 1}$$

## CONCLUSION

The analytical procedure is simple, fast and accurate. It has been satisfactorily applied to determine CLO in pure and dosage forms. The reaction can be carried out in batch and FIA and in this paper both approaches were compared. Although very few methods are available for determining CLO by FIA-spectrophotometer based on oxidative coupling reaction, the suggested method, which is simple, rapid, offers the advantages of sensitivity more than the reported methods, and a wide range of determination without the need for extraction or heating. The wide applicability of the new method for routine quality control is well established by the assay of CLO at concentration level of trace (ppm) in pharmaceutical formulations.

## REFERENCES

- Parker WA Epilepsy," In: Herfindal ET, Gourley DR, Hart LL (Eds) Clinical pharmacy and therapeutics". Williams and Wilkins, Maryland:585-586, 1988.
- Martindale: "The Complete Drug Reference", Pharmaceutical press, 36<sup>th</sup> Edition: 478-479, 2009.
- The Indian Pharmacopoeia, The Indian Pharmacopoeia commission, Ghaziabad, 6th edition, Vol.-II :1111-1114, 2010.
- British Pharmacopoeia, British Pharmacopoeia Commission, Vol I:546. Vol III:2444-2445, 2007.
- United state pharmacopoeia, Rockville, USP convention, Inc, 30th edition:1795-1797, 2007.
- European Pharmacopoeia monograph: Clonazepam available online at <http://www.sinoapi.com/pharmacopoeia/pharmacopoeia-ep6.asp?cas=1622-61-3> (Accessed on 24/07/2011).
- Japanese Pharmacopoeia monograph: Clonazepam available online at <http://www.sinoapi.com/pharmacopoeia/pharmacopoeia-jp15.asp?cas=1622-61-3>.
- Christopher J and James TS," Analysis of Clonazepam in a tablet dosage form using small bore HPLC", Journal of Pharmaceutical and Biomedical Analysis, 18: 453-460, 1998.
- Isabelle F. B., Fabienne P. and Christian J., "Development of a rapid RP-HPLC method for the determination of clonazepam in human plasma", Journal of Pharmaceutical and Biomedical Analysis, 36: 865-869, 2004.
- Mistsuhrio N., Kana F., Tadashi S. and Yoshihiro K., "High-Performance Liquid Chromatographic Assay of Clonazepam in Human Plasma Using a Non-porous Silica Column", Biol. Pharm. Bull, 27: 893-895, 2004.
- Min, B.H. and Garland, W.A., "Determination of Clonazepam and its 7-Amino Metabolite in Plasma and Blood by Gas Chromatography- Chemical Ionization Mass Spectrometry", Journal of Chromatography, 139:121-133, 1977.
- Wang Z., Zhu G. and Li G., "Determination of Phenobarbital, phenytoin, Carbamazepine and Clonazepam in serum by HPLC", The Chinese Journal of Modern Applied Pharmacy, 2: 155-156, 2002.
- Arthur F.S., Carl V.P., and Nancy M., "Determination of Clonazepam and flunitrazepam in blood and urine by electron-capture GLC", Journal of Pharmaceutical Sciences, 63: 520-527, 1974.
- Hassan, S. M., Belal, F., El-Din, M. S., and Sultan, M., " Spectrophotometric determination of some pharmaceutically important nitro compounds in their dosage forms. Analyst, 113 (7): 1087-1089, 1988.
- Alhemiary, N.A .F. and Saleh, M. H. A., "Spectrophotometric Determination of Tinidazole Using Promethazine and Ethyl Vanillin Reagents in Pharmaceutical Preparations", Der Pharma Chemica, , 4(6):2152-2160, 2012.
- British Pharmacopoeia , H . M . Stationary Office , crown copyright, London , 1993 .



### Synthesis and Characterization of 2-Hydrazinyl 3H-imidazol[4,5b]Pyridine Derivatives

Nisreen Kais Abood

Department of Chemistry, College of Science, Al-Mustansiriyah University Baghdad, Iraq.

Email :serein\_82@yahoo.com

#### Article info

Received 21/9/2014

Accepted 30/11/2014

#### Keywords:

Pyrazoline,  
Traizine, Triazole  
and Tetrazole.

#### ABSTRACT

New series of 2-hydrazinyl-3H-imidazol[4,5b]pyridine derivatives were prepared by reacting the 2-mercapto-3H-imidazol[4-5b]pyridine A with hydrazine hydrate give compound (1), which reacted with aromatic aldehyde, benzyl, nitrous acid, ethyl cyanoacetate, acetylacetone, formic acid, benzoylchloride, chloroacetic acid, benzalacetophenone and Glucose, to give new derivatives of pyrazoline, triazine, triazole and tetrazole, compounds (2-11), some new N(5-(aryl phenyl)-H-tetrazolo-yl)-3H-imidazo[4,5b]pyridine-2-amine, derivatives (12a, b-14a, b) have been prepared by reaction of 2-hydrazinyl-3H-imidazo [4,5b] pyridine (1) with various aromatic acid chloride and sodium azide., the prepared compounds were confirmed by techniques FT-IR spectrum and Elemental Analysis and some of them confirmed by <sup>1</sup>HNMR spectrum.

#### الخلاصة

حضرت سلسلة جديدة من مشتقات 2-هيدرازين-3-اميدازول بيريدين من تفاعل 2-مركبتو-3-اميدازول بيريدين مع الهيدرازين اللاماني الذي اعطى المركب (1) والذي تفاعل بدوره مع بعض المواد العضوية والالديهيدات الاروماتية والبنزائل وحمض النتروزواثيل سيانواستيت، استايل اسيتون وحمض الفورمك وبنزويل كلورايد وكلورو حامض الخليك وبنزل اسيتوفينون والكلكوز لتعطي مشتقات جديدة من البايروزول و ترايزين وترايازول وتترازول 11-2. حضرت مركبات جديدة 14a-b من تفاعل المركب 2-هيدرازين-3-اميدازول بيريدين مع مختلف معوضات حامض الكلوريد الاروماتي وصوديوم ازايد لتعطي مشتقات التترازول، وشخصت هذه المركبات بواسطة الطرائق الطيفية FT-IR و Elemental Analysis وبعضها شخص بأطياف <sup>1</sup>HNMR.

#### INTRODUCTION

The wide field of applying hydrazine derivatives is attractive to synthesize compounds that combine versatility of the hydrazide chemistry, which have specific advantage various host structure [1]. Hydrazide derivatives are used in the synthesis of pharmaceutical bulk drugs [2], agrochemicals, polymers and dye industries[3]. In addition, some hydrazides show neuroprotective properties and are used as antidepressant drugs [4]. The importance of imidazole in biological system has attracted much interested due to their involvement in the chemical and biochemical processes[5], like anti-cancer, anti-viral, anti-inflammatory [6] anti-histaminic, anti-oxidant, anti-hypertensive and anti-coagulant [7]. Pyrazoles are chemical compounds of synthetic origin that have five-membered heterocyclics with two nitrogen atoms and three adjacent carbons[8]. Pyrazoline derivatives possess a broad spectrum of biological activities such as antifungal[9], antidepressant, anticovulsant [10], antibacterial, anticancer, antipyretic[11] anti-neoplastic activities, antiamebic and anticholinergic[12]. Tetrazole derivatives have attracted large attention because of their unique structure and applications [13] as antihypertensive, antialergic, anticonvulsant agent [14]. In the present work we have synthesised new heterocyclic compounds derivatives from 2-hydrazinyl-3H-imidazol[4,5b]pyridine which containing pyrazoline, triazine, triazole and tetrazole moieties with predictable biological activities.

#### MATERIALS AND METHODS

Melting points were determined in open capillaries and were uncorrected. The purity of the synthesized compounds was routinely checked by TLC on silica gel. FTIR spectra on a Perkin Elmer 1600 FT spectrometer, Elemental Analysis%, <sup>1</sup>HNMR was recorded on a Varian-Mercury300MHz spectrometer.

**Synthesis 2-hydrazinyl-3H-imidazo[4,5-b]pyridine(1):** A mixture of 3H-imidazo[4,5-b]pyridine-2-thiol A (0.01mole) and (98%)hydrazine hydrate (10ml) was refluxed for 3hrs., ethanol (15ml) was added and refluxed for 4hrs. The reaction was monitored by TLC after completion of reaction. Separated precipitate was filtered and washed with cold water and recrystallized from ethanol

**General procedure of synthesizing 2-(2-(3,4,5-trimethoxy benzy lidene) hydrazinyl)-3H-imidazo[4,5-b]pyridine (2), and 2-(2-(3H-imidazo[4,5-b] pyridin-2-yl)hydrazono)-1,2-diphenylethanone(3):**

A solution of compound (1) (0.01mole) and 3,4,trimethoxybenzaldehyde or benzyl (0.01) in ethanol was refluxed for 15hrs. The reaction was monitored by TLC after completion of reaction. The solid separated by cooling, and was recrystallized from ethanol.

**Synthesis of N-(3H-imidazo)tetrazolo[4,5b]pyridine (4):**

An aqueous solution of sodium nitrite (0.03mole) in 10ml of H<sub>2</sub>O was added dropwise with stirring to a solution of



compound (1) (0.01mole) in acetic acid (10ml) the solution left stirring for 24hrs. The reaction was monitor by TLC after completion of reaction. The obtained solid product during stirring was filtered off and recrystallized from ethanol.

**General procedure of synthesizing 3-amino-1-(3H-imidazo[4,5-b]pyridin-2-yl)-1H-pyrazol-5(4H)-one (5) and 2-(3,5-dimethyl-1H-pyrazol-1-yl)-3H-imidazo[4,5-b]pyridine (6), 2(3-H-imidazo-[1,2,4] triazolo[4,5b]pyridine(7):** To a solution of compound (1) in absolute ethanol (30ml), ethyl cyano acet and acetyl acetone or formic acid (0.01mole) was added and the reaction mixture was refluxed for 10-15 hrs. The reaction was monitored by TLC after completion of reaction. The obtained solid product after concentrating and cooling and recrystallization from ethanol.

**Synthesis of 2(3-H-imidazo-3-phenyl[1,2,4] triazolo[4,5b]pyridine (8)**

To a solution of compound (1) (0.01mole) in pyridine (30ml) benzoyl chloride (0.01mole) was added and the reaction was monitored by TLC after completion of reaction. The obtained solid product, recrystallized from ethanol.

**Synthesis of N-(3H-imidazo [4,5b] pyridine [1,2,4] triazin-4-ol (9), 2-(3,5-diphenyl-4,5-dihydro-1H-pyrazol-1-yl) -3H-imidazo [4,5-b] pyridine (10), 6-(2-(3H-imidazo[4,5-b]pyridin-2-yl) hydrazono) hexane-1,2,3,4,5pentaol (11):**

To a solution of (0.01mole) in xylene or ethanol (20ml), (0.01mole) of chloro acetic acid, benzalacetophenon or glucose was added and the reaction mixture was refluxed for 2-5hrs. A few drops of acetic acid was added in case of reaction glucose. The reaction was monitored by TLC after completion of reaction. The solid product was filtered off and recrystallized from ethanol.

**Synthesis of 3H-imidazo [4,5-b]pyridin-2-yl) - arylbenzohydrazide (12a-b):**

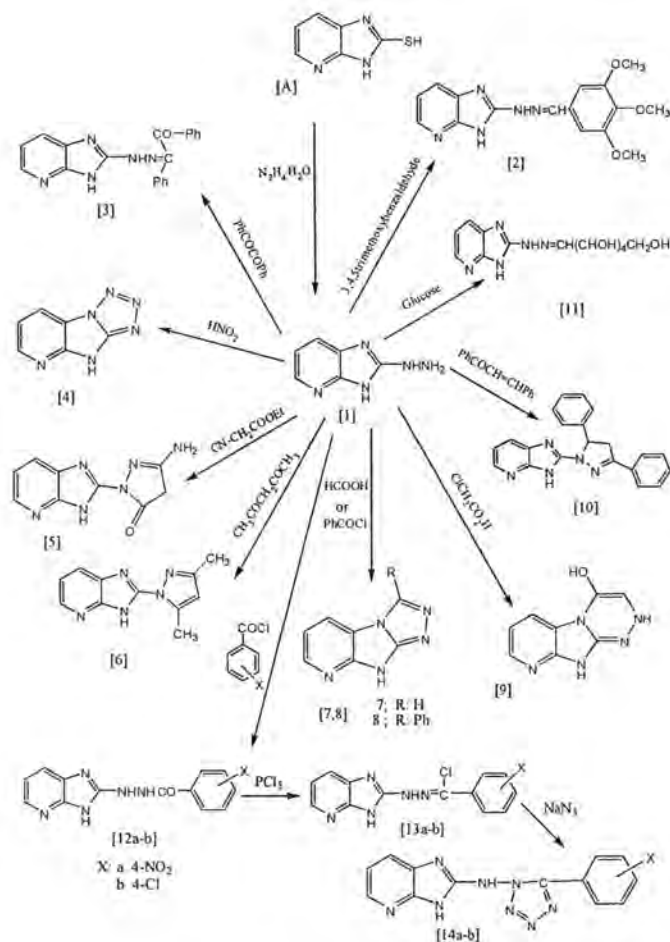
To a solution of compound (1) (0.01mole), (0.01mole) aryl acid chloride in pyridine with constant shaking, after the addition was complete the mixture left at room temperature for 2 hrs. The solid product was filtered and recrystallized from ethanol.

**Synthesis of N'(3H-imidazo[4,5-b] pyridin-2-yl) arylbenzo hydrazonoylchloride(13a-b):**

A mixture of compound (12a-b) (0.004mole) and  $\text{PCl}_5$  (0.004mole) was heated at  $100^\circ\text{C}$  for 1hr., when the evolution of fumes of HCl was ceased  $\text{POCl}_3$  was removed under reduce pressure.

**Synthesis of N'(3H-imidazo(substitutedphenyl)-1H-tetrazolo[4,5b] pyridine(14a-b):**

The residual of compound (13a-b) was treated with an ice cold solution of sodium azide (0.01mole) the excess of the sodium acetate in water (25ml) and acetone (30ml) were added with stirring and which continued over night. Acetone was removed under reduce pressure, remaining aqueous portion was extracted by chloroform the solid product was obtained by moving the solvent.



Scheme 1: Synthesis of new compounds

## RESULTS AND DISCUSSION

The new derivatives were prepared following the reaction sequences in scheme 1. Treatment of 3H-imidazo[4,5-b]pyridine-2-thiol with hydrazine hydrate in boiling ethanol gave compound (1) indicated by appearance  $\text{NH}_2$  at the (3383-3205)  $\text{cm}^{-1}$  and disappearance of SH, shown in table (1)  $^1\text{H NMR}$  (DMSO- $d_6$ ) of compound (1): 12.2 (s, 1H, NH imidazol) 9.4 (s, 1H, C-NH), 4.7 (s, 2H,  $\text{NHNH}_2$ ), 7.7-8.7 (m, 5H, CH pyridine). Table 2. Reaction of compound (1) with 3,4,5-trimethoxy benzaldehyde and benzil produced (2,3) respectively, through the nucleophilic attack of the nitrogen of the hydrazine moiety of the carbon of the carbonyl followed by elimination of one molecule of water, then the IR of compound (2) show that appearance  $\nu\text{C}=\text{N}$  1600  $\text{cm}^{-1}$  table (1).  $^1\text{H NMR}$  (DMSO- $d_6$ ) of compound (2): 12.2 (s, 1H, NH imidazol) 10.5 (s, 1H, CNH), 3.9 (s, 3H,  $\text{OCH}_3$ ), 7-8 proton of heterocyclic table 2, compound (3) show  $\nu\text{C}=\text{N}$  1600  $\text{cm}^{-1}$ ,  $\text{C}=\text{O}$  1678  $\text{cm}^{-1}$ , Table (1). Reaction compound (1) with nitrous acid to give tetrazole derivatives 4, the IR show  $\nu\text{C}=\text{N}$  1599  $\text{cm}^{-1}$ , tetrazol ring 1188  $\text{cm}^{-1}$  table (1), as show in the mechanism below [15].

The binucleophilic centers ( $\text{NHNH}_2$ ) of the hydrazino moiety can be used to synthesize new heterocyclic rings

through its reaction with ethyl cyanoacetate and acetylacetone. Thus, reaction of (1) with ethyl cyanoacetate gave the pyrazolone derivative 5, through the nucleophilic attack of the nitrogen of the hydrazino moiety to the cyano group followed by rearrangement of afford amino derivative (not isolated), then the attack of the second nitrogen to the carbonyl of the ester with elimination of one molecule of ethanol. However, the reaction of (1) with acetyl acetone gave the pyrazole derivative (6), through the sequence attack of the two nucleophilic centers of the hydrazino moiety to the two carbonyl group of acetyl acetone. The IR spectrum of (5) exhibited bands for  $\nu\text{CO}$  at 1745,  $\nu\text{C}=\text{N}$  at 1614,  $\nu\text{NH}$  at 3373 and  $\nu\text{NH}_2$  at 3277  $\text{cm}^{-1}$  (broad) table (1).  $^1\text{H NMR}$  (DMSO- $d_6$ ) of compound (5): 12.2 (s, 1H, NH imidazol), 6.3 (s, 2H,  $\text{NH}_2$ ), 2.1 (s, 2H,  $\text{CH}_2$  methylene), 7.7-8.3 proton of heterocyclic table 2, while that of (6) exhibited bands for  $\nu\text{C}=\text{N}$  at 1616 and  $\nu\text{NH}$  at 3286  $\text{cm}^{-1}$  table (1).  $^1\text{H NMR}$  (DMSO- $d_6$ ) of compound (6): 13 (s, 1H, NH imidazol), 6.1 (s, H, CH pyrazol), 2.3 (s, 3H,  $\text{CH}_3$ ), 7-8 proton of heterocyclic table 2. Preparation new triazole derivatives have also taken into consideration due to the wide range of the applications, then the triazole prepared from reaction compound (1) with formic acid

and benzoyl chloride, the IR spectrum show the  $\nu$  C=N 1616, 1618, NH 3304, 3342, (N=N=N-) 1491, 1485 respectively, compound (7-8) table(1). The reaction of (1) with chloroacetic acid in boiling dry xylene gave the triazine derivative (9). Its IR spectrum exhibited bands for  $\nu$  C=N at 1612,  $\nu$  OH and  $\nu$  NH at 3402 and 3171  $\text{cm}^{-1}$  (broad) table(1)  $^1\text{H-NMR}$  (DMSO- $d_6$ ) of compound 9: 12.2 (s, 1H, NH imidazol), 7.2 (s, 1H, CNH), 4.1 (s, 1H, NH), 5.4 (s, 1H, C=CH), 1.2 (s, 1H, OH), 6-7 proton of heterocyclic table 2. Compound (1) reacts with benzalacetophenone to produce the pyrazoline derivative (10). The reaction proceed through condensation reaction, to afford intermediate compound (not isolated), that underwent cyclization to give compound (10). Its IR spectrum exhibited bands for  $\nu$  C=N at 1616 and  $\nu$  NH at 3240  $\text{cm}^{-1}$   $^1\text{H-NMR}$  (DMSO- $d_6$ ) of compound (10): 12.1 (s, 1H, NH imidazol), 5.4 (s, 1H, CH methine), 3.9 (d, 2H, CH-CH<sub>2</sub>),

7.2-8.4) proton of heterocyclic table (2), while Reaction of (1) with glucose gave compound (11). Its IR spectrum exhibited bands for  $\nu$  C=N at 1560 and,  $\nu$  NH and OH at 3443  $\text{cm}^{-1}$  (broad), table(1). N-(3H-imidazo (substituted phenyl-1H-tetrazolo[4,5b] pyridine (14a-b) was prepared by the reaction between compound (1) and aroylchloride derivatives give compound (12a-b) then react with  $\text{PCl}_5$  to give (13a-b). Tetrazole were synthesized under mild conditions in a short reaction time with good overall yield as outlined in Scheme 1, the IR spectrum of compound (14a): 1616  $\nu$  C=N, 3117 NH, 1583  $\text{NO}_2$  asym., 1365  $\text{NO}_2$  sym, 1188 (tetrazol ring), 1491 (N=N=N-), (14b): 1616  $\nu$  C=N, 3304 NH, 1130 (tetrazol ring), 1438 (N=N=N-) table(1),  $^1\text{H-NMR}$  (DMSO- $d_6$ ) of compound (14a): 12.2 (s, 1H, NH imidazol), 4 (s, 1H, C-NH) 7.2-8.8 (m, H proton of heterocyclic), table (2).

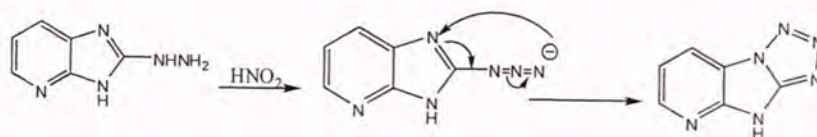


Table 1: Physical Properties and Spectral Data of Compounds

Com. NO.	Formula	M.Wt	Yield%	m.p C°	FT-IR(KBr) $\text{cm}^{-1}$	Elemental Analysis calculated/found %
1	C <sub>6</sub> H <sub>7</sub> N <sub>5</sub>	149	60	200-202	3383-3205 NH, 3057 CH ar. 1616 $\nu$ C=N, 1558 C=C	C 48.32/48.30, H 4.73/4.31 N 46.95/46.90
2	C <sub>16</sub> H <sub>17</sub> N <sub>5</sub> O <sub>3</sub>	327	65	238-240	3315 NH, 3051 CH ar., 1600 $\nu$ C=N, 1568 C=C	C 58.71/58.70, H 5.23/5.20 N 21.39/21.37
3	C <sub>20</sub> H <sub>15</sub> N <sub>5</sub> O	341	70	185-187	3360 $\nu$ NH, 1678 $\nu$ CO, 1600 $\nu$ C=N, 1494 C=C	C 70.37/70.35, H 4.43/4.41 N 20.52/20.51
4	C <sub>6</sub> H <sub>7</sub> N <sub>6</sub>	160	60	164-166	3352 $\nu$ NH, 1599 $\nu$ C=N, 3080 CH ar., 1489 (N=N=N-), 1188 tetrazole ring.	C 45.10/45.00, H 2.52/2.50 N 52.48/52.46
5	C <sub>9</sub> H <sub>8</sub> N <sub>6</sub> O	216	62	190-192	3373 $\nu$ NH, 3277 NH, 1745 $\nu$ CO 1614 $\nu$ C=N, 1558 C=C	C 50.11/50.00, H 3.73/3.70 N 38.87/38.77
6	C <sub>11</sub> H <sub>11</sub> N <sub>5</sub>	213	66	210-112	3286 NH, 1616 $\nu$ C=N, 1433 C=C, 3080 CH ar., 2924 CH aliphatic.	C 61.96/61.93, H 5.20/4.85 N 32.84/32.80
7	C <sub>7</sub> H <sub>5</sub> N <sub>5</sub>	159	70	175-177	3304 NH, 1616 $\nu$ C=N, 1491 (N=N=N) 3076 CH ar., 2939 CH aliphatic	C 52.75/52.73, H 3.16/3.15 N 44.11/44.10
8	C <sub>13</sub> H <sub>9</sub> N <sub>5</sub>	235	70	230-232	3342 NH, 1618 $\nu$ C=N, 1485 (N=N=N) 3053 CH ar., 2852 CH aliphatic	C 66.34/66.32, H 3.76/3.75 N 29.77/29.75
9	C <sub>8</sub> H <sub>7</sub> N <sub>5</sub> O	189	73	237-239	3402 OH, 3171 NH, 1612 $\nu$ C=N, 3007 CH ar., 2928 CH aliphatic	C 50.78/50.77, H 3.73/3.72 N 37.23/37.22
10	C <sub>21</sub> H <sub>17</sub> N <sub>5</sub>	339	60	223-225	3240 NH, 1616 $\nu$ C=N, 1560 C=C, 3051 CH ar., 2987 CH aliphatic	C 74.32/74.22, H 5.05/5.03 N 20.64/20.63
11	C <sub>12</sub> H <sub>17</sub> N <sub>5</sub> O <sub>5</sub>	311	57	198-200	3443 NH and OH (broad), 1560 $\nu$ C=N, 3051 CH ar., 2987 CH aliphatic	C 46.32/46.30, H 5.31/5.30 N 22.53/22.52
12a	C <sub>13</sub> H <sub>10</sub> N <sub>6</sub> O <sub>3</sub>	298	65	210-212	3400 $\nu$ NH, 1695 CO, 3090 CH ar. 1442 C=C, 1523 $\text{NO}_2$ asym, 1344 $\text{NO}_2$ sym	C 52.36/52.35, H 3.39/3.38 N 28.19/28.18
12b	C <sub>13</sub> H <sub>10</sub> ClN <sub>5</sub> O	287	65	195-197	3417 $\nu$ NH, 1687 $\nu$ CO, 3009 CH ar. 1442 C=C, 765 Ar-Cl	C 54.27/54.26, H 3.49/3.48 N 25.31/25.30
13a	C <sub>13</sub> H <sub>9</sub> N <sub>6</sub> O <sub>2</sub> Cl	316	60	228-230	3120 $\nu$ NH, 1606 $\nu$ C=N, 3020 CH ar. 1450 C=C, 1535 $\text{NO}_2$ asym, 1317 $\text{NO}_2$ sym	C 49.32/49.30, H 2.89/2.86 N 26.34/26.32
13b	C <sub>13</sub> H <sub>9</sub> N <sub>5</sub> Cl <sub>2</sub>	306	55	214-216	3240 $\nu$ NH, 1616 C=N, 1530 C=C, 750 Ar-Cl	C 51.01/51.00, H 2.98/2.96 N 22.89/22.88
14a	C <sub>13</sub> H <sub>9</sub> N <sub>9</sub> O <sub>2</sub>	323	70	225-227	3117 NH, 1616 $\nu$ C=N, 1583 $\text{NO}_2$ asym, 1365 $\text{NO}_2$ sym., 1188 tetrazol ring, 1491 (N=N=N-).	C 48.31/48.30, H 2.84/2.81 N 35.35/35.33
14b	C <sub>13</sub> H <sub>9</sub> N <sub>8</sub> Cl	312	66	245-247	3304 NH, 1616 $\nu$ C=N, 1130 tetrazol ring, 1438 (N=N=N-), 760 Ar-Cl	C 49.92/49.90, H 2.93/2.90 N 30.25/30.24

Table 2: Chemical Schiff's  $^1\text{H-NMR}$  Spectra

Comp. No.	$^1\text{H-NMR}$ (DMSO $d_6$ ) $\delta$ ppm
1	12.2 (s, 1H, NH imidazol), 9.4 (s, 1H, C-NH), 4.7 (d, 2H, NHNH <sub>2</sub> ), 7.7-8.7 (m, 5H, CH pyridine).
2	12.2 (s, 1H, NH imidazol), 10.5 (s, 1H, CNH), 3.9 (s, 3H, OCH <sub>3</sub> ), 7-8 proton of heterocyclic
5	12.2 (s, 1H, NH imidazol), 6.3 (s, 2H, NH <sub>2</sub> ), 2.1 (s, 2H, CH <sub>2</sub> methylene), 7.7-8.3 proton of heterocyclic
6	13 (s, 1H, NH imidazol), 6.1 (s, 1H, CH pyrazol), 2.5 (s, 3H, CH <sub>3</sub> ), 7-8 proton of heterocyclic
8	12.2 (s, 1H, NH imidazol), 7.2 (s, 1H, CNH), 4.1 (s, 1H, NH), 5.4 (s, 1H, C=CH), 1.2 (s, 1H, OH), 6-7 proton of heterocyclic.
9	12.1 (s, 1H, NH imidazol), 5.4 (s, 1H, CH methine), 3.9 (d, 2H, CH-CH <sub>2</sub> ), 7.2-8.4) proton of heterocyclic
14a	12.2 (s, 1H, NH imidazol), 4 (s, 1H, C-NH), 7.2-8.8 (m, H proton of heterocyclic)

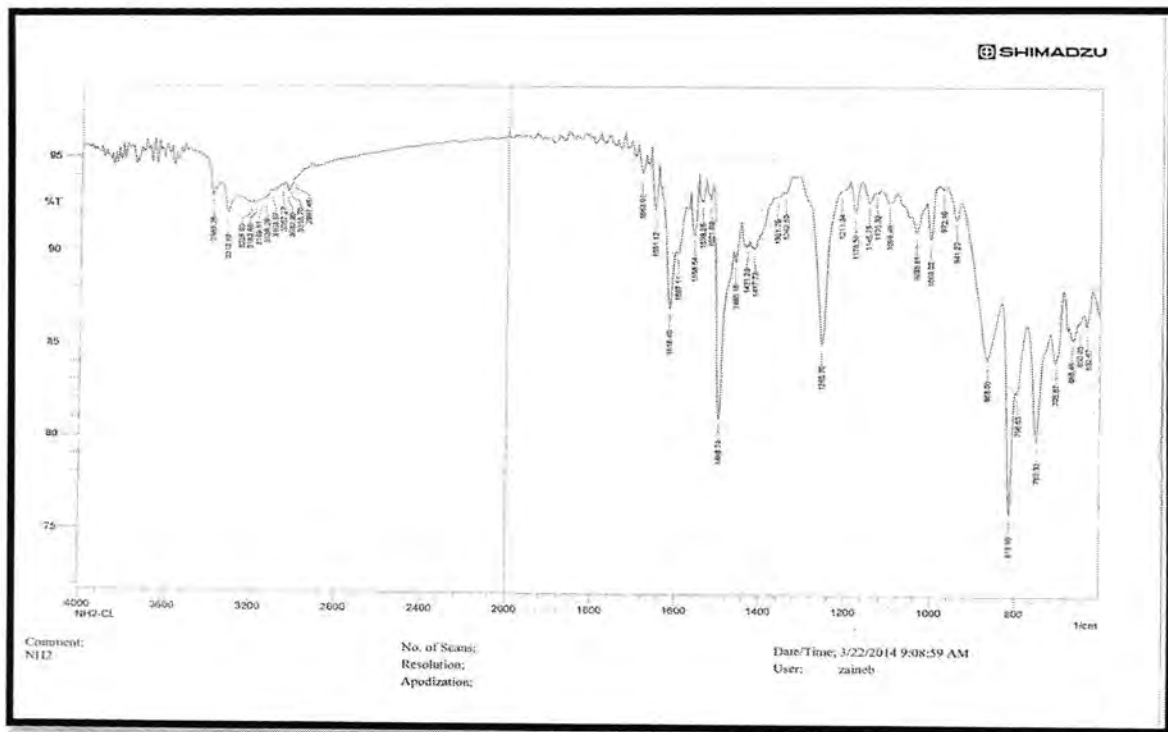


Figure 1: FT-IR Spectrum of compound (1)

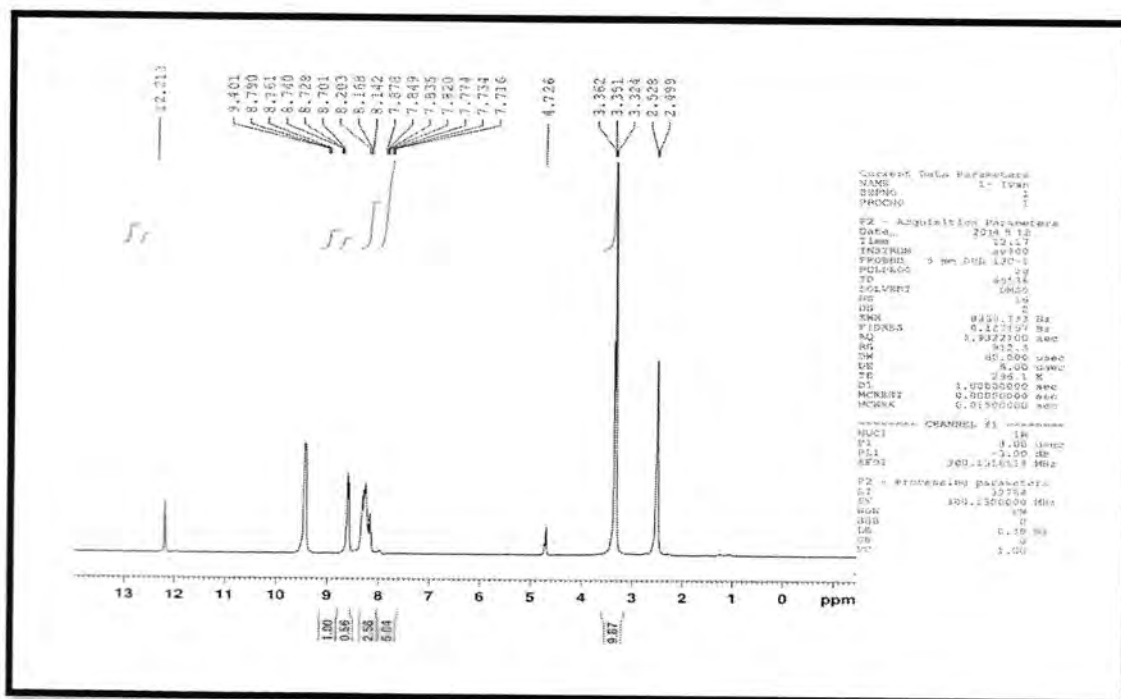


Figure 2: <sup>1</sup>H-NMR Spectrum of compound (1)

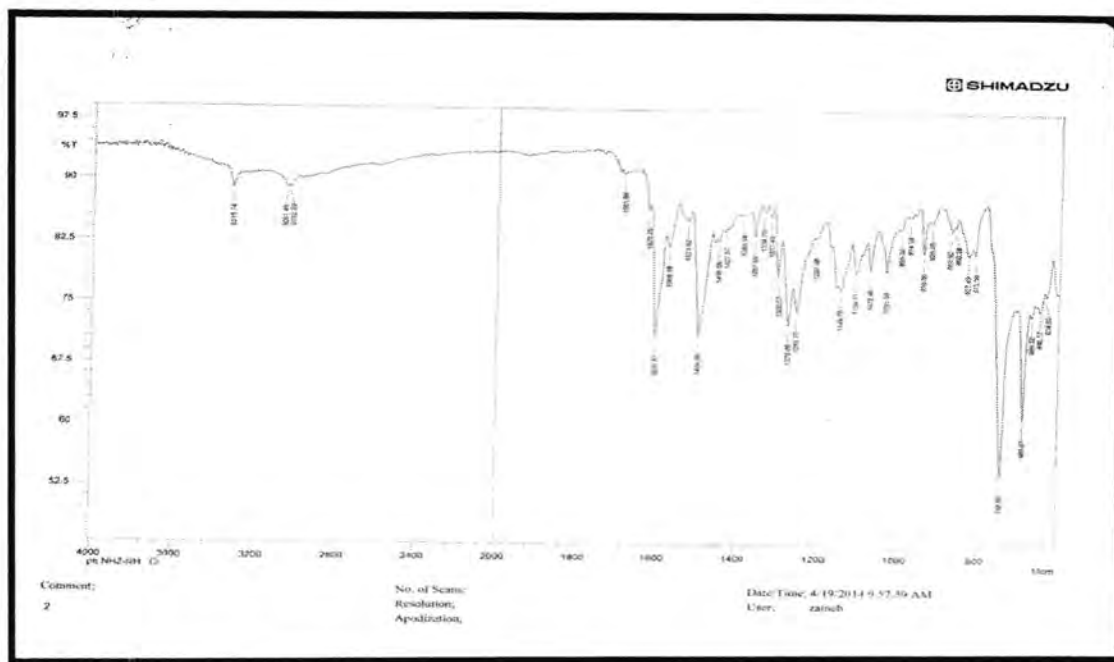


Figure 3: FT-IR Spectrum of compound (2)

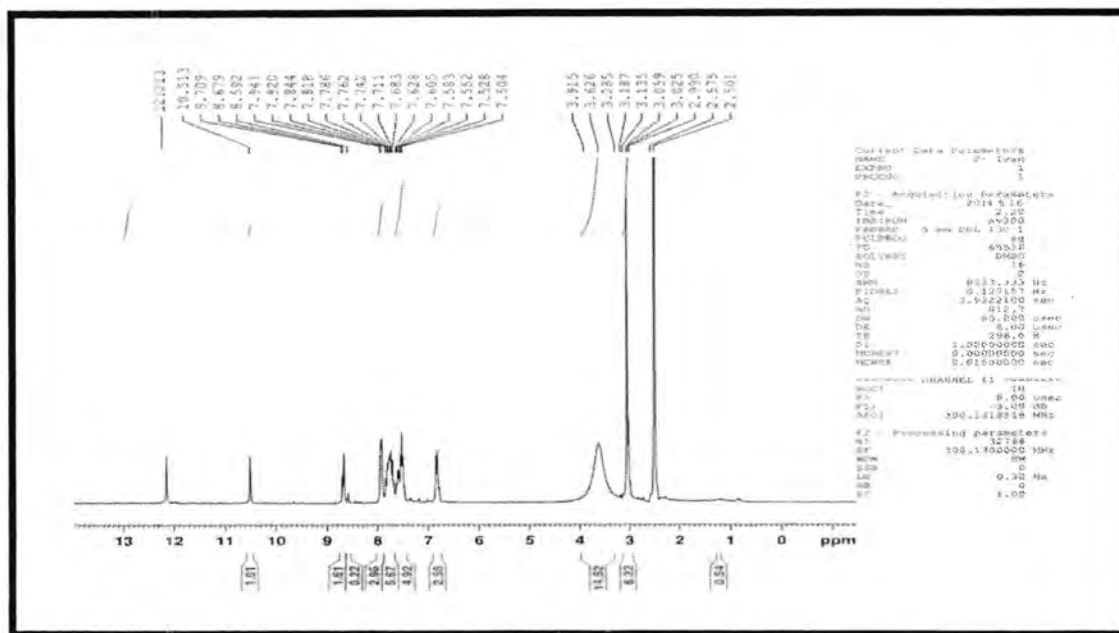


Figure 4: <sup>1</sup>H-NMR Spectrum of compound (2)

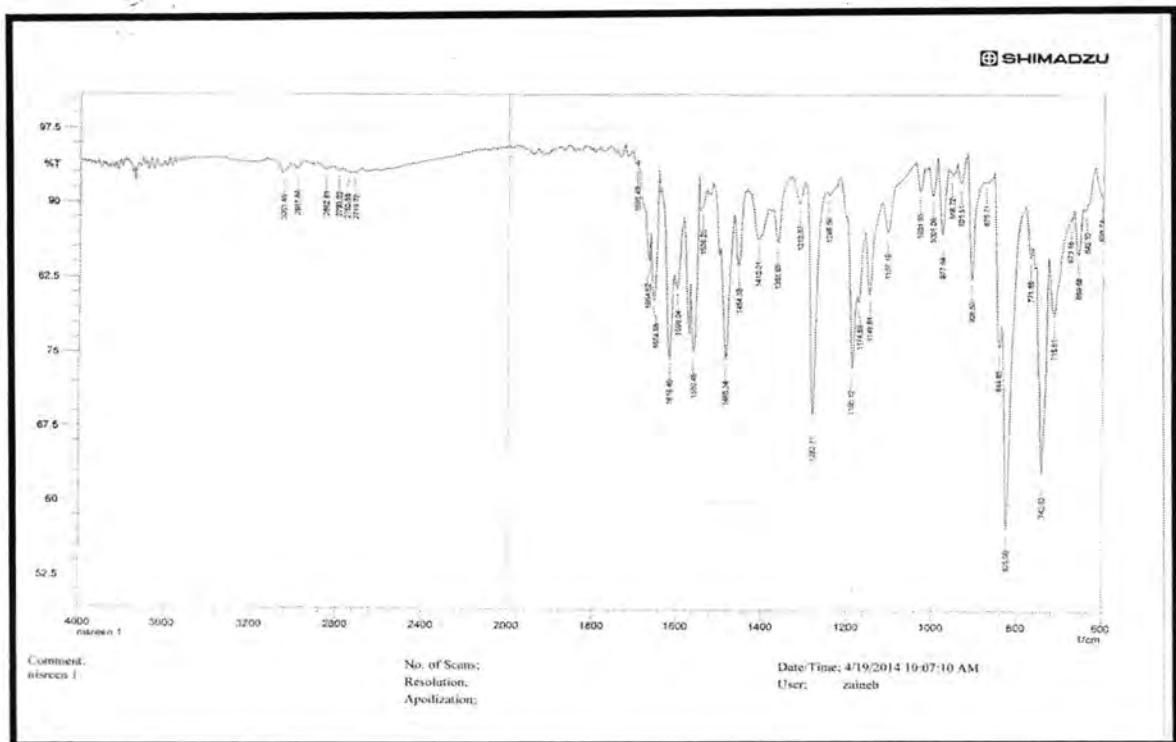


Figure 5: FT-IR Spectrum of compound (9)

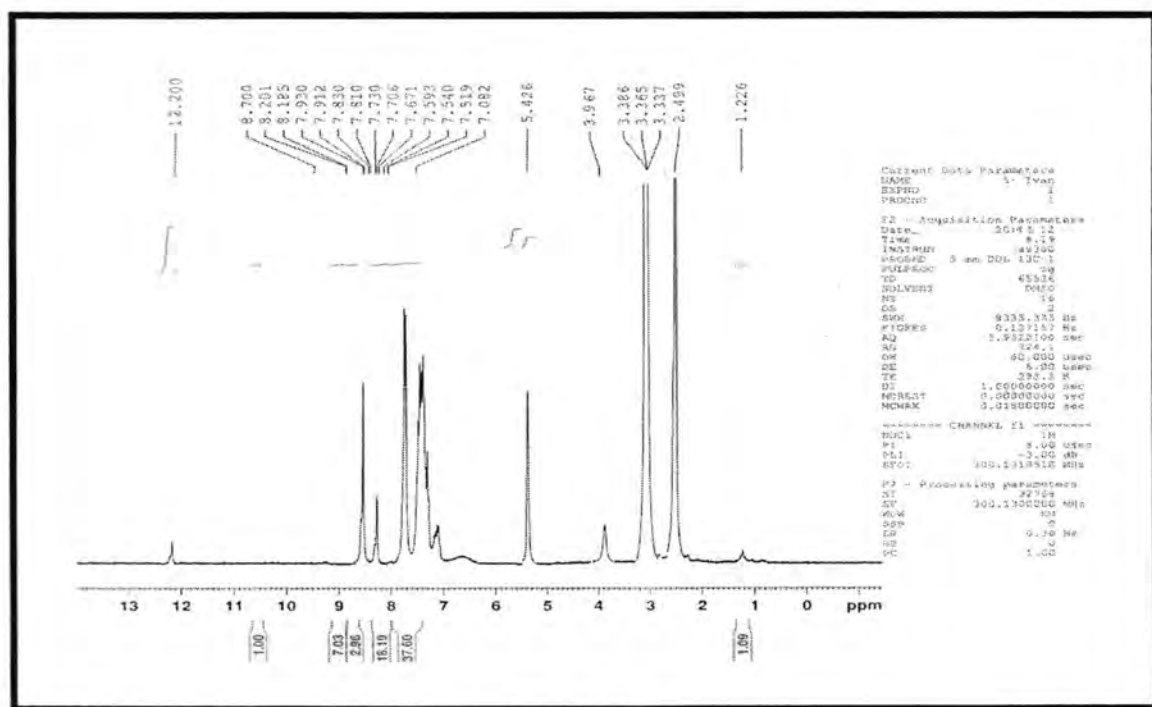


Figure 6: <sup>1</sup>H-NMR Spectrum of compound (9)

REFERENCES

- [1] Britvin S.N., Spiridonova D.V., Siidra O.I., Lotnyk A., Kienle L., Krivovichev S.V., and Depmeier W., "Synthesis, structure and properties of hydrazinium germanate pharmacosiderite,  $(N_2H_5)_3 Ge_7O_{15}(OH) \cdot 2.5H_2O$ " Microporous and Mesoporous Materials 131:282–288, 2010.
- [2] Jagota N.K., Chetram A.J., and Nair J.B., "Determination of trace levels of hydrazine in the penultimate intermediate of a novel anti-infective agent" Journal of Pharmaceutical and Biomedical Analysis 16:1083–1087, 1998.
- [3] Badgujar D. M., Talawar M. B., and Mahulika P. P., "Biological Evaluation of 1, 2-bis (2, 4, 6-Trinitrophenyl) Hydrazine," Indian J. Pharm. Biol. Res. 1(4):25-29, 2013.
- [4] Leetw C.M., Huitema C., Liu J., James K.E.J.C., and Eltis L.D., "Crystal structure of the main peptidase from the SARS coronavirus inhibited by substrate like azo-peptide epoxide," J. Mol. Biol. 354:1137-1151, 2005.
- [5] Ambadkar D.S. and mkedar R. "Synthesis of new 2(substituted phenyl) 4-(4-methoxy phenyl)-5(phenyl)-1H-Imidazoles from 4-methoxybenzil in the absence of catalyst" International journal of scientific and research publication 3,2250-3153(2013).
- [6] kas L., Brukstus L.K., Gaidelis A.B., and Buchinskaite P.G, Udrenaitė V.A. and Dauksas V.K., "Synthesis and anti-inflammatory activity of new derivatives of 6-benzoyl-1-4-benzodioxane" ,pharm.chem. J.34:353-355,2000.
- [7] Ranza A., Elaryess, Ghareb N., Azab M.M. and Said M.M., "Synthesis and antimicrobial activities of some novel benzimidazol and benzotriazole derivatives containing  $\beta$ Lactam," life science journal 10(3):1784-1793, 2013.
- [8] Kuidu, Yi-Jia Me, Xiam-Ting Cao, Peng-Fei zhang and Hui Zheng "the synthesis of pyrazole derivatives based on glucose", International Journal of chemical Engineering and application.; 4:238-240, 2013.
- [9] Gomha S.M., and Abdel-Aziz H.A. "Synthesis and antimicrobial activity of some pyrazolo[3',4':4,5]pyrimido[1,2-b][1,2,4]triazino[5,4-f][1,2,4,5]tetrazinone derivatives", International Journal of Advanced Research; 1: 450-457, 2013.
- [10] Dasary K., Lavania A., Yadav M. and Anand A.V., "Synthesis, characterization and study of antioxidant activities of some new pyrazoline derivatives containing isatin moiety," International Journal of Research in Engineering and science; 7:8-13, 2013.
- [11] Baria B., Viradiya D., Kotadiya V., and Anamik shah R.K., "Acid -promoted synthesis of imidazolopyrazole derivative Via Multi compound reaction using ultra sound irradiation", International Letters of Chemistry .Physics and Astronomy; 11:277-283, 2014.
- [12] Jagadte S.D., Mulik A.G., Chandam D.R., Patil P.P., Sankpal S.A., Sawant A.D. and Deshmukh M.B., "Synthesis of some novel 3,5-diaryl pyrazole derivatives dibenzo -18-crown-6-ether", Indian Journal of Chemistry ;52B:1352-1356, 2013.
- [13] Varadaraji D.A., Suban S.S., Ramasamy V.R., Kubendiran K., Raguraman J.S., Nalilu S.K. and Pati H.N., "synthesis and evaluation of series of 1-substituted tetrazole derivatives as antimicrobial agent" ,Org. Commun ;3:3,45-56, 2010.
- [14] Koppula P. and Purohit N., " synthesis of new biological active triazolo, tetrazolo and coumarinoly derivatives of iso coumarins", .Org. Commun; 6:4,148-161, 2013.
- [15] Abd-elghaffar N.F., Kadah M.S., Sayed G.H., Radwan A.M., and Abd-ela S.N., "synthesis and anti-tumor activity of some novel heterocyclic compounds prepared from hydrazinopyridazine derivatives ", Australian Journal of basic and applied science, 7(8):968-973, 2013.



## Study of Cloud Shortwave Radiative Properties

Abdulwahab Husain Alobaidi

Middle Technical University, Institute of Technology, Department of Electronic Techniques

Email: awhalobaidi@yahoo.com

### Article info

Received 16/9/2014

Accepted 30/11/2014

### ABSTRACT

Clouds play a major role in radiative balance of Earth's atmosphere due to their scattering and absorption of shortwave radiation. The aim of this research is to study these processes. A model was developed in terms of cloud liquid water path, cloud effective radii, and single scattering albedo. Computation was made for different liquid paths and effective radii. The results indicated that for a given liquid water path, scattering increases with decreasing cloud effective radius and water clouds scatter more and absorb less radiation.

### الخلاصة

تلعب الغيوم دوراً رئيسياً في التوازن الإشعاعي للغلاف الجوي للأرض بسبب قيامها باستطارة وامتصاص الإشعاع قصير الموجة. ويهدف البحث دراسة هذه العمليات. إن الانموذج طور في حدود مسار الماء السائل للغيمة، نصف قطر الغيمة الفعال واستطارة الألبيدو الأحادية. الحساب أعد لسائل مختلف المسارات ونصف القطر الفعال. تشير نتائج مسار الماء السائل المعطى إلى زيادة الاستطارة مع نقصان نصف القطر الفعال للغيمة وإن الغيوم المائية أكثر استطارة وأقل امتصاصاً للإشعاع.

### INTRODUCTION

The study of clouds, where they occur, and their characteristics, play a key role in understanding of climate change. Low, thick clouds primarily reflect solar radiation and cool the surface of the Earth. High, thin clouds primarily transmit incoming solar radiation; at the same time, they trap some of the outgoing infrared radiation emitted by Earth and radiate it back downward, thereby warming the surface of Earth. Whether a given cloud will heat or cool the surface depends on several factors, including the cloud's altitude, size, and the make-up of the particles that form the cloud. The balance between cooling and warming actions of clouds is very close although, overall, averaging the effects of all the clouds around the globe, cooling predominates [1].

Cloud particles are largely composed of liquid water or ice. The microphysical properties of clouds, such as, cloud droplet size, liquid water content, vertical extent, determine the precipitation efficiency as well as the radiative properties of clouds [2]. Cloud shortwave radiative properties are usually parameterized as a function of the liquid water content and the effective radius of the cloud droplet size distribution [3-5]. Early model of the radiative properties of clouds was proposed by [6]. [7] developed a simple model of cloud radiative forcing. The aim of this work is to study the effect of cloud liquid water path and effective radius of cloud droplet on the shortwave radiative properties of clouds.

### THEORITICAL PART

For a given type of particles characterized by the size distribution  $n(r)dr$ , the volume extinction coefficient (in units length<sup>-1</sup>)  $k_{ext}$  is determine as [6]:

$$k_{ext} = \int_{r_1}^{r_2} \sigma_{ext} n(r) dr \quad (1)$$

$$k_{ext} = \pi \int_{r_1}^{r_2} Q_{ext} r^2 n(r) dr \quad (2)$$

Where  $\sigma_{ext}$  is the extinction efficiency and  $Q_{ext}$  is the extinction cross section. Cloud droplet sizes vary from a few microns to 100 microns with average diameter of 10 to 20 microns. Therefore  $\chi = \frac{2\pi r}{\lambda}$  is much greater than 1 for shortwave radiation wavelengths  $\lambda$ . In this case  $Q_{ext} = 2$  and equation (2) becomes:

$$k_{ext} = 2\pi \int_{r_1}^{r_2} r^2 n(r) dr \quad (3)$$

The cloud liquid water content,  $LWC$ , is defined as [8]:

$$LWC = \frac{4}{3} \pi \rho_l \int_{r_1}^{r_2} r^3 n(r) dr \quad (4)$$

where  $\rho_l$  is the density of water.

Using the definition of the effective radius,  $r_e$ , [6]:

$$r_e = \frac{\int r^3 n(r) dr}{\int r^2 n(r) dr} \quad (5)$$

equation (4) becomes:

$$LWC = \frac{4}{3} \pi \rho_l r_e \int_{r_1}^{r_2} r^2 n(r) dr \quad (6)$$

Combining equations (3) and (6) gives:

$$k_{ext} = \frac{3 LWC}{2 \rho_l r_e} \quad (7)$$

The extinction optical depth,  $\tau_{ext}$ , is defined as [9]:

$$\tau_{ext} = \int k_{ext} dz \approx k_{ext} \Delta z \quad (8)$$

where  $\Delta z$  is the cloud depth. And using the definition of cloud liquid water path  $LWP = LWC \Delta z$ , equation (7) becomes:

$$\tau_{ext} = \frac{3 LWP}{2 \rho_l r_e} \quad (9)$$

Now the cloud transmittance, which is defines as  $T = \exp(-\tau_{ext})$ , can be expressed in terms of the cloud liquid water path as:

$$T = \exp\left(-\frac{3 LWP}{2 \rho_l r_e}\right) \quad (10)$$

The transmittance (T) is related to the scattering (S) and absorption (A) is given by [9]:

$$T + S + A = 1 \quad (11)$$



Because most water clouds are both optically thick and are only weakly absorbing, multiple scattering cannot be neglected [9]. However, multiple scattering cannot be computed from a simple formula. To simplify the calculation, we use the definition of the single scattering albedo [6]:

$$\omega = \frac{S}{S+A} \quad (12)$$

Table 1 gives the single scattering albedo for various values of effective radius. The parameters needed for computing scattering and absorption for different cloud types are given in Table 2 [10].

Table 1: Single Scattering Albedo of Various Values of Effective Radius

$r_e$ (micron)	2	4	8	16
$\omega$	0.93	0.92	0.90	0.85

Table 2: Parameters for three Type of Clouds

Cloud Type	Effective radius (micron)	Cloud liquid water path ( $g/m^2$ )	Single scattering albedo
Stratocumulus (Sc)	10	50-250	0.888
Cumulus (Cu)	12	100-300	0.875
Cumulonimbus (Cb)	18	200-1000	0.828

### RESULTS AND DISCUSSION

Figure 1 shows the shortwave scattering as a function of liquid water path for four values of mean effective radius. Scattering is calculated using equations 10, 11, and 12; and single scattering albedo given in table 1. Scattering increases as liquid water path increases and has strong dependence on liquid water path for low values of liquid water path. This dependency depends on the value of the effective radius of cloud droplet. For instance, when the effective radius is 2  $\mu m$ , the strong dependency holds for values of liquid water path less than 60  $g m^{-2}$ , while for effective radius of 16  $\mu m$ , the strong dependency holds for liquid water path values less than 200  $g m^{-2}$ . The results also indicates that for a given liquid water path, scattering increases with decreasing the effective radius. When the liquid water path is 10  $g m^{-2}$  the scattering is 50% for effective radius of 2  $\mu m$ , compared with 7.6% for effective radius equal to 16  $\mu m$ .

Figure 2 illustrates the shortwave absorption by water cloud a function of liquid path for four different values of cloud mean effective radius. It is seen that the variation of absorption with mean effective radius depends on the value of the liquid water path. For liquid water paths less than 70  $g m^{-2}$ , absorption increases with decreasing the cloud mean effective radius for a given value of liquid water path while this behavior changes to the opposite when liquid water path is greater than 70  $g m^{-2}$ . It is also noted that beyond the 70  $g m^{-2}$  liquid water path, the dependence of absorption on liquid water path becomes stronger with increasing mean effective radius. Comparing figure 2 with figure 1 shows that absorption is notably smaller than scattering, which indicates that scattering is dominant in water clouds.

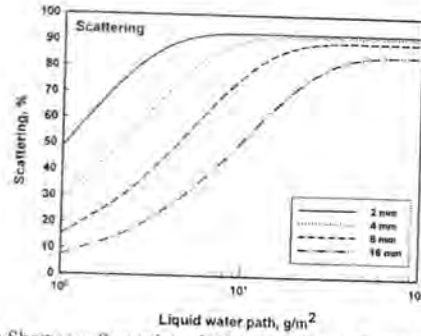


Figure 1: Shortwave Scattering of Water Clouds as a Function of Liquid Water Path for Different Values of Cloud Mean Effective Radius.

The model also was used to compute the scattering and absorption for three different types of clouds; cumulus (Cu) stratocumulus (Sc), and cumulonimbus (Cb). The parameters of these types of clouds are listed in table 2. Figures 3 and 4 shows the results of these computations. It is evident that scattering increases with increasing liquid water path for all types of clouds and the Sc and Cu clouds scatter more radiation than Cb clouds due to their relatively small effective radii. The relatively large amount of liquid water path of Cb clouds is due to their vertical extent. The absorption is notably much lower than scattering of all types of clouds. The Cb clouds absorbs more radiation than the other types of clouds. This is because Cb contains larger drops.

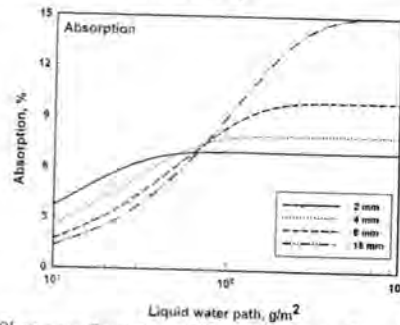


Figure 2: Shortwave Absorption of Water Clouds as a Function of Liquid Water Path for Different Values of Cloud Mean Effective Radius.

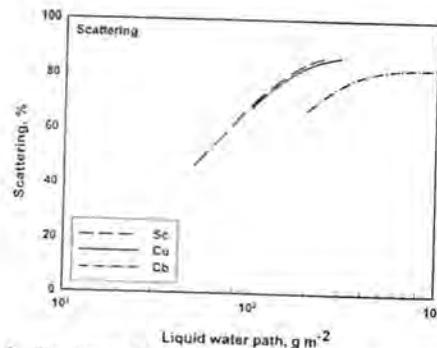


Figure 3: Shortwave Scattering of Cumulus, Stratocumulus, and Cumulonimbus Clouds as a Function of Liquid Water Path.

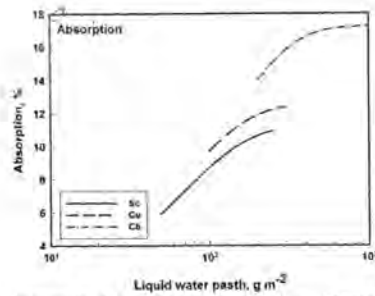


Figure 4: Shortwave Absorption of Cumulus, Stratocumulus, and Cumulonimbus Clouds as a Function of Liquid Water Path.

## CONCLUSIONS

The radiative properties of water clouds depend on the characteristics of the cloud such as type, size, concentration number of cloud droplets. Using simple model, it was found that scattering and absorption of shortwave radiation increases with increasing liquid water path. The dependence of scattering and absorption on what becomes weaker at relatively high values of liquid water path. Scattering is much higher than absorption for all types of water clouds. Cb clouds scatter less and absorb more radiation than Cu and Sc clouds due to their larger radii and large liquid path.

## References

- [1] Wallace J. and Hobbs P. "Atmospheric Science An Introductory Survey", Elsevier, 2006
- [2] Andrews D. G. "An Introduction to Atmospheric Physics", 2<sup>nd</sup> Edition, Cambridge University Press, 2010.
- [3] Fouquart Y., and Bonnel B. "Computation of solar heating of the Earth's atmosphere: A new parameterization", Beitr. Phys.Atmos., 53: 35-62, 1980.
- [4] Slingo A., and Shrescker H. M. "On the shortwave radiative properties of stratiform clouds", Quart. J. Roy. Meteor. Soc., 108: 407-426, 1982.
- [5] Stephens G. L. "The parameterization of radiation for numerical weather prediction and climate models", Mon. Wea. Rev., 112: 826-867, 1984.
- [6] Damiano P., and Chylek P. "Shortwave radiative properties of clouds: Numerical Study", J. Atmos. Sc., 51: 1223-1233, 1994.
- [7] Corti T., and Peter T. "A simple model for radiative cloud forcing", Atmos. Chem. Phys., 5751-5758, 2009.
- [8] Rogers R. R., and Yau M. K. "A Short Course in Cloud Physics", 3<sup>rd</sup> Edition, Elsevier, 1989.
- [9] Liou K. N. "An Introduction to Atmospheric Radiation, 2<sup>nd</sup>. Edition", Elsevier, 2002.
- [10] Linacre E. and Geerts B. "Cloud liquid water content, drop sizes, and number of droplets", 1999.
- [11] [http://www-das.uwyo.edu/~geerts/cwx/notes/chap08/moist\\_cloud.html](http://www-das.uwyo.edu/~geerts/cwx/notes/chap08/moist_cloud.html).



### Bases in the Space of Vector Valued Analytic Multiple Dirichlet Series

Mushtaq Shakir A. Hussein and Nagem R. Nagem

Department of Mathematics, College of Science, Mustansiriyah University, Baghdad, IRAQ

#### Article info

Received 16/9/2015

Accepted 11/1/2015

#### ABSTRACT

In this paper, we consider the space  $Y$  of all functions represented by vector valued multiple Dirichlet series and analytic in a half plane equipped with various topologies. The main result of this paper is concerned with finding the conditions for a base in  $Y$  to become a proper base and certain continuous linear operators which are used to determine the proper bases in  $Y$ .

#### الخلاصة

تُعد دراستنا في هذا البحث بالاعتماد على الفضاء  $Y$  الذي يمثل فضاء جميع الدوال الممتلئة بواسطة متجه القيم لسلسلة درشلت ذات المتغيرات المعقدة المتعددة والذي صيغتها

$$f(s_1, s_2) = \sum_{m,n=1}^{\infty} a_{m,n} e^{s_1 \lambda_m + s_2 \mu_n}, s_j = \sigma_j + it_j, j = 1, 2, \quad (\sigma_j, t_j \text{ هي متغيرات حقيقية})$$

و  $a_{m,n}$  تنتمي الى بنائخ الجبر  $E$  وتكون هذه الدوال تحليلية في نصف المستوى المعقد، وان الفضاء المعتمد مع توبولوجي معين سيكون فضاء فرشت وفي هذا الفضاء وصفنا شكل المؤثر الخطي المستمر  $F$  من  $Y$  الى  $Y$  وأعطينا أيضاً توصيفاً للأساس الفعلي بواسطة استخدام فضاء دوال درشلت التحليلية لمتجه القيم وحصلنا على خواص لفضاءات توبولوجية متعددة.

#### INTRODUCTION

Consider the series

$$f(s_1, s_2) = \sum_{m,n=1}^{\infty} a_{m,n} e^{(s_1 \lambda_m + s_2 \mu_n)}, s_j = \sigma_j + it_j, j = 1, 2 \quad (\sigma_j, t_j \text{ are real variables}), \quad (1)$$

Such that  $a_{m,n} \in E$  belong to a commutative  $E$  with identity element  $\chi$  with  $\|\chi\|=1$  and  $\lambda_m \in R$  satisfying the condition

$$0 < \lambda_1 < \lambda_2 < \lambda_3 \dots < \lambda_m \dots, \lambda_m \rightarrow \infty \text{ as } m \rightarrow \infty$$

and  $\mu_n \in R$  satisfying the condition

$$0 < \mu_1 < \mu_2 < \mu_3 \dots < \mu_n \dots, \mu_n \rightarrow \infty \text{ as } n \rightarrow \infty$$

Further, suppose S.B. Hazem [1]

$$\lim_{m,n \rightarrow \infty} \frac{\log(m+n)}{\lambda_m + \mu_n} = 0 \quad (2)$$

and

$$\limsup_{m,n \rightarrow \infty} \frac{\log^+ \|a_{m,n}\| + A_1 \lambda_m + A_2 \mu_n}{\lambda_m + \mu_n} = 0$$

$A_1 > 0$  and  $A_2 > 0$ . Here we take  $\log^+ x = 0$  if  $x \leq 1$  and  $\log^+ x = \log x$  if  $x > 1$ . The maximal abscissas of convergence are equal to  $A_1$  and  $A_2$  respectively, i.e. the series of function  $f(s_1, s_2)$  converges in the domain

$$d = \{(\sigma_1 + it_1, \sigma_2 + it_2) \in C^2; \sigma_1 < A_1, \sigma_2 < A_2, -\infty < t_1, t_2 < \infty\}$$

Suppose that a vector valued Dirichlet series (1) absolutely convergent in a left half plane

$\sigma_1 < A_1, \sigma_2 < A_2$ . Then the given series represents vector valued analytic function in the half plane  $\sigma_1 < A_1, \sigma_2 < A_2$  and the series is also called vector valued analytic Dirichlet series.

The growth properties order and lower order, type and lower type of the vector valued analytic Dirichlet series [2] taking  $E$  to be Banach space.

B.L. Srivastava [2] defined obtained the coefficient characterization of order and type.

By giving different topologies on the set of analytic function defined by Dirichlet series of one complex variable, Kamthan and Gautam [3] obtained various topological properties. G.S.Srivastava and Archana Sharma [4] have been considered the space of vector valued analytic Dirichlet series and obtained these properties.

In this paper, we have extended and improve the above results to the space of vector valued analytic Dirichlet series of several complex variables. For the sake of simplicity, we consider the functions of two complex variables. Though our result can be easily extended to functions of several complex variables.

Consider  $\Psi$  be the class of functions  $f$  given by (1) satisfying

$$\limsup_{m,n \rightarrow \infty} \frac{\log^+ \|a_{m,n}\| + A_1 \lambda_m + A_2 \mu_n}{\lambda_m + \mu_n} = 0. \quad (3)$$

For all  $f \in \Psi$ , let us define

$$\|f\|_{\sigma_1, \sigma_2} = \sum_{m,n=1}^{\infty} \|a_{m,n}\| e^{\sigma_1 \lambda_m + \sigma_2 \mu_n}, \text{ for } \sigma_1 < A_1, \sigma_2 < A_2.$$

Thus in view of (3)  $\|f\|_{\sigma_1, \sigma_2}$  is well defined and for each  $\sigma_1 < A_1, \sigma_2 < A_2$  introduces a norm on  $\Psi$ . We denote by  $\Psi(\sigma_1, \sigma_2)$ , the space  $\Psi$  equipped with the norm  $\|\cdot\|_{\sigma_1, \sigma_2}$ . Let  $\rho$  be the topology generated by the family of norms  $\{\|f\|_{\sigma_1, \sigma_2} : \sigma_1 < A_1, \sigma_2 < A_2\}$  which is equivalent to the topology generated by the invariant metric  $d$ , where

$$d(f, g) = \sum_{m,n=1}^{\infty} \frac{1}{2^{m+n}} \frac{\|f-g\|_{\sigma_{m,n}}}{1+\|f-g\|_{\sigma_{m,n}}},$$

Such that  $\{\sigma_{m,n}\}$  is a sequence

$$\sigma_1 < \sigma_2 < \dots < \sigma_m < \dots, \sigma_m \rightarrow A_1 \text{ as } m \rightarrow \infty$$

$$\sigma_1 < \sigma_2 < \dots < \sigma_n < \dots, \sigma_n \rightarrow A_2 \text{ as } n \rightarrow \infty.$$

Throughout this paper we shall assume that the space  $\Psi$  is equipped with the topology generated by the metric  $d$ .

A sequence  $\{\alpha_{m,n}\} \subseteq \Psi$  is said to be linearly independent if for any sequence  $\{c_{m,n}\}$  of complex

number for which  $\sum_{m,n=1}^{\infty} c_{m,n} \alpha_{m,n}$  converges in  $\Psi$ ,

$$\sum_{m,n=1}^{\infty} c_{m,n} \alpha_{m,n} = 0 \text{ implies that } c_{m,n} = 0 \forall m, n. \text{ A}$$

subspace  $\Psi_0$  of  $\Psi$  is said to be spanned by a sequence  $\{\alpha_{m,n}\} \subseteq \Psi$  if  $\Psi_0$  consists of all linear combinations

$$\sum_{m,n=1}^{\infty} c_{m,n} \alpha_{m,n} \text{ such that } \sum_{m,n=1}^{\infty} c_{m,n} \alpha_{m,n} \text{ converges in}$$

$\Psi$ . A sequence

$\{\alpha_{m,n}\} \subseteq \Psi$  which is linearly independent and spans a closed subspace  $\Psi_0$  of  $\Psi$  is said to be a base in  $\Psi_0$ .

In particular,

if

$$e_{m,n} \in \Psi, e_{m,n}(s_1, s_2) = \omega e^{s_1 \lambda_m + s_2 \mu_n}, m, n \geq 1,$$

then  $\{e_{m,n}\}$  is a base in  $\Psi$ . A sequence  $\{\alpha_{m,n}\} \subseteq \Psi$  will be called a proper base if it is a base and it satisfies the following condition:

" For all sequences  $\{a_{m,n}\} \subseteq E$ , convergence of

$$\sum_{m,n=1}^{\infty} a_{m,n} \alpha_{m,n} \text{ in } \Psi \text{ implies the convergence of}$$

$$\sum_{m,n=1}^{\infty} a_{m,n} e_{m,n} \text{ in } \Psi "$$

### Main Results

We shall prove the following result.

**Theorem (1):** The space  $\Psi$  is a Frechet space.

Here, as defined above,  $\Psi$  is a normed linear metric space. For showing that  $\Psi$  is a Frechet space, we need to show that  $\Psi$  is complete. Let  $\{f_\alpha\}$  be a Cauchy sequence in  $\Psi$ . Hence it is a Cauchy sequence in  $\Psi(\sigma_1, \sigma_2)$  for each real  $\sigma_1 < A_1, \sigma_2 < A_2$ . Therefore, for any given  $\varepsilon > 0$  there exists a positive integer  $Q_0 = Q_0(\varepsilon, \sigma_j), j = 1, 2$  such that

$$\|f_\alpha - f_\beta\|_{\sigma_1, \sigma_2} < \varepsilon \quad \forall \alpha, \beta \geq Q_0, \sigma_1, \sigma_2 \geq 1.$$

$$\text{Denoting by } f_\alpha(s_1, s_2) = \sum_{m,n=1}^{\infty} a_{m,n}^{(\alpha)} e^{s_1 \lambda_m + s_2 \mu_n},$$

$$f_\beta(s_1, s_2) = \sum_{m,n=1}^{\infty} a_{m,n}^{(\beta)} e^{s_1 \lambda_m + s_2 \mu_n}, \text{ we have therefore}$$

$$\sum_{m,n=1}^{\infty} \|a_{m,n}^{(\alpha)} - a_{m,n}^{(\beta)}\| e^{\sigma_1 \lambda_m + \sigma_2 \mu_n} < \varepsilon, \text{ for all } \alpha, \beta \geq Q_0 \quad (4)$$

Therefore for each fixed  $m, n = 1, 2, \dots, \{a_{m,n}^{(\alpha)}\}$  is a Cauchy sequence in the Banach space  $E$ . Hence there exists a sequence  $\{a_{m,n}\} \subseteq E$  such that

$$\lim_{\alpha \rightarrow \infty} a_{m,n}^{(\alpha)} = a_{m,n}, m, n \geq 1.$$

Now letting  $\beta \rightarrow \infty$  in (4), we have for  $\alpha \geq Q_0$

$$\sum_{m,n=1}^{\infty} \|a_{m,n}^{(\alpha)} - a_{m,n}\| e^{\sigma_1 \lambda_m + \sigma_2 \mu_n} \leq \varepsilon. \quad (5)$$

Let us denote by  $f = \sum_{m,n=1}^{\infty} a_{m,n} e_{m,n}$ . Now it

remains to show that  $f \in \Psi$ . We choose  $\sigma_{i,1}, \sigma_{i,2}$  such that  $A_1 < \sigma_{i,1} + \varepsilon$  and  $A_2 < \sigma_{i,2} + \varepsilon$ . From (5) we have

$$\sum_{m,n=1}^{\infty} \|a_{m,n}^{(\alpha)} - a_{m,n}\| e^{\sigma_{i,1} \lambda_m + \sigma_{i,2} \mu_n} \leq \varepsilon \quad \alpha \geq Q_1, \quad (6)$$

where  $Q_1 = Q_1(\varepsilon, \sigma_{i,j}), j = 1, 2$ . Keeping  $\alpha$  as fixed in (6) and in view of (3), we observe that

$$\|a_{m,n}^{(\alpha)}\| \leq e^{(\sigma - A_1) \lambda_m + (\varepsilon - A_2) \mu_n} \quad \forall m, n \geq Q_2$$

$Q_2 = Q_2(\varepsilon, \alpha)$ . Then

$$\|a_{m,n}\| \leq \|a_{m,n}^{(\alpha)} - a_{m,n}\| + \|a_{m,n}^{(\alpha)}\|$$

$$\|a_{m,n}\| \leq \varepsilon e^{-(\sigma_{i,1} \lambda_m + \sigma_{i,2} \mu_n)} + e^{(\varepsilon - A_1) \lambda_m + (\varepsilon - A_2) \mu_n}$$

$$\|a_{m,n}\| < 2e^{(-A_1 + \varepsilon) \lambda_m + (-A_2 + \varepsilon) \mu_n}$$

$$\forall m, n > M = \max\{Q_1, Q_2\}$$

Now by taking log to the above inequality, we get that

$$\log \|a_{m,n}\| < (-A_1 + \varepsilon)\lambda_m + (-A_2 + \varepsilon)\mu_n$$

$$\log \|a_{m,n}\| + A_1\lambda_m + A_2\mu_n < \varepsilon(\lambda_m + \mu_n)$$

Thus

$$\limsup_{m,n \rightarrow \infty} \frac{\log^+ \|a_{m,n}\| + A_1\lambda_m + A_2\mu_n}{\lambda_m + \mu_n} = 0$$

Thus  $\sum_{m,n=1}^{\infty} a_{m,n} e_{m,n} \in \Psi$ . Therefore  $f_{\alpha} \rightarrow f \in \Psi$ .

Hence  $\Psi$  is complete. This proves Theorem 1.

**Theorem (2):** A necessary and sufficient condition for the linear transformation  $F: \Psi \rightarrow \Psi$  with  $F(e_{m,n}) = \alpha_{m,n} \in \Psi$ ,  $m = 1, 2, \dots$ ,  $n = 1, 2, \dots$  to be continuous is that for each  $\sigma_1 < A_1, \sigma_2 < A_2$

$$\limsup_{m,n \rightarrow \infty} \frac{\log^+ \|\alpha_{m,n}\|_{\sigma_1, \sigma_2} - A_1\lambda_m - A_2\mu_n}{\lambda_m + \mu_n} \leq 0. \quad (7)$$

**Proof.** Let  $F$  be a continuous linear transformation from  $\Psi$  into  $\Psi$  with  $F(e_{m,n}) = \alpha_{m,n}$ ,  $m = 1, 2, \dots$

$n = 1, 2, \dots$ . Then for any given  $\sigma_1$  there exists a  $\sigma'_1$

( $\sigma_1, \sigma'_1 < A_1 + \varepsilon$ ) and a finite constant  $K_1$  and for

any given  $\sigma_2$  there exists a  $\sigma'_2$  ( $\sigma_2, \sigma'_2 < A_2 + \varepsilon$ )

and a finite constant  $K_2$  such that

$$\|F(e_{m,n})\|_{\sigma_1, \sigma_2} \leq K_1 K_2 \|e_{m,n}\|_{\sigma'_1, \sigma'_2}$$

$$\Rightarrow \|\alpha_{m,n}\| \leq K_1 K_2 e^{\sigma'_1 \lambda_m + \sigma'_2 \mu_n} \quad m, n \geq 1$$

Now by taking log to the above inequality, we get that

$$\log \|\alpha_{m,n}\| \leq \sigma'_1 \lambda_m + \sigma'_2 \mu_n < (A_1 + \varepsilon)\lambda_m + (A_2 + \varepsilon)\mu_n$$

$$\log \|\alpha_{m,n}\| - A_1\lambda_m - A_2\mu_n < \varepsilon(\lambda_m + \mu_n).$$

Thus

$$\Rightarrow \limsup_{m,n \rightarrow \infty} \frac{\log^+ \|\alpha_{m,n}\| - A_1\lambda_m - A_2\mu_n}{\lambda_m + \mu_n} < 0.$$

Conversely. Let the sequence  $\{\alpha_{m,n}\}$  satisfies (7)

and let  $\alpha(s_1, s_2) = \sum_{m,n=1}^{\infty} a_{m,n} e_{m,n} \in \Psi$ . Then there

exists an  $\varepsilon > 0$  such that

$$\frac{\log^+ \|\alpha_{m,n}\| - A_1\lambda_m - A_2\mu_n}{\lambda_m + \mu_n} \leq -\varepsilon \text{ for all } Q \geq Q_1(\varepsilon).$$

$$\log \|\alpha_{m,n}\| - A_1\lambda_m - A_2\mu_n \leq -\varepsilon(\lambda_m + \mu_n),$$

$$\log \|\alpha_{m,n}\| < (A_1 - \varepsilon)\lambda_m + (A_2 - \varepsilon)\mu_n.$$

Now by taking exponential to the above inequality, we get that

$$\|\alpha_{m,n}\|_{\sigma_1, \sigma_2} < e^{(A_1 - \varepsilon)\lambda_m + (A_2 - \varepsilon)\mu_n}.$$

Further, for a given  $\nu > 0$  such that  $\nu < \varepsilon$

$$\|\alpha_{m,n}\| \leq e^{(-A_1 + \nu)\lambda_m + (-A_2 + \nu)\mu_n} \text{ for all } Q \geq Q_2(\nu).$$

Hence

$$\|\alpha_{m,n}\| \|\alpha_{m,n}\|_{\sigma_1, \sigma_2} \leq e^{(-A_1 + \nu)\lambda_m + (-A_2 + \nu)\mu_n} e^{(A_1 - \varepsilon)\lambda_m + (A_2 - \varepsilon)\mu_n}$$

for all  $Q \geq \max(Q_1, Q_2)$

$$= e^{(\nu - \varepsilon)\lambda_m + (\nu - \varepsilon)\mu_n}.$$

Hence the series  $\sum_{m,n=1}^{\infty} \|\alpha_{m,n}\| \|\alpha_{m,n}\|_{\sigma_1, \sigma_2}$  is convergent.

As  $\sigma_1 < A_1, \sigma_2 < A_2$ , therefore  $\sum_{m,n=1}^{\infty} a_{m,n} \alpha_{m,n}$  is

convergent in  $\Psi$ . Hence there exists a linear transformation  $F: \Psi \rightarrow \Psi$  such that

$$F(\alpha) = \sum_{m,n=1}^{\infty} a_{m,n} \alpha_{m,n} \text{ and } F(e_{m,n}) = \alpha_{m,n}, \text{ for}$$

each  $\alpha_{m,n} \in \Psi$ . Now we prove the continuity of  $F$ .

Given  $\sigma_1 < A_1, \sigma_2 < A_2$ , there exists  $\nu > 0$  such that

$$\frac{\log^+ \|\alpha_{m,n}\| - A_1\lambda_m - A_2\mu_n}{\lambda_m + \mu_n} \leq -\nu \text{ for all } m, n \geq N$$

$$\log \|\alpha_{m,n}\| - A_1\lambda_m - A_2\mu_n \leq -\nu(\lambda_m + \mu_n),$$

$$\log \|\alpha_{m,n}\| < (A_1 - \nu)\lambda_m + (A_2 - \nu)\mu_n.$$

Now by taking exponential to the above inequality, we get that

$$\|\alpha_{m,n}\|_{\sigma_1, \sigma_2} \leq e^{(A_1 - \nu)\lambda_m + (A_2 - \nu)\mu_n}.$$

$$\Rightarrow \|\alpha_{m,n}\|_{\sigma_1, \sigma_2} \leq K_1 K_2 e^{(A_1 - \nu)\lambda_m + (A_2 - \nu)\mu_n} \text{ for all}$$

$m, n \geq 1$ .

Now,

$$\|F(\alpha)\| \leq K_1 K_2 \sum_{m,n=1}^{\infty} \|\alpha_{m,n}\| e^{(A_1 - \nu)\lambda_m + (A_2 - \nu)\mu_n} = K_1 K_2 \|\alpha\|_{(A_1 - \nu, A_2 - \nu)}$$

Hence  $F$  is continuous. Since  $\sigma_1 < A_1, \sigma_2 < A_2$  is arbitrary, it shows that  $F$  is continuous. This proves Theorem 2.

We now give the characterization of proper bases. First we prove

**Theorem (3):** Let  $\{a_{m,n}\} \subseteq E$  and  $\{\alpha_{m,n}\} \subset \Psi$  be given sequences. The following three conditions are equivalent:

(i) Convergence of  $\sum_{m,n=1}^{\infty} a_{m,n} e_{m,n}$  in  $\Psi$  implies the

convergence of  $\sum_{m,n=1}^{\infty} a_{m,n} \alpha_{m,n}$  in  $\Psi$ .

(ii) The convergence of  $\sum_{m,n=1}^{\infty} a_{m,n} e_{m,n}$  in  $\Psi$  implies that

$$\lim_{m,n \rightarrow \infty} a_{m,n} \alpha_{m,n} = 0 \text{ in } \Psi.$$

(iii)  $\limsup_{m,n \rightarrow \infty} \frac{\log^+ \|\alpha_{m,n}\|_{\sigma_1, \sigma_2} - A_1 \lambda_m - A_2 \mu_n}{\lambda_m + \mu_n} < 0$ , for all

$$\sigma_1 < A_1, \sigma_2 < A_2.$$

**Proof.** First suppose that (i) hold. Then for any sequence  $\{a_{m,n}\}$ , where  $a_{m,n}$ s belong to Banach algebra  $E$ ,

$\sum_{m,n=1}^{\infty} a_{m,n} e_{m,n}$  converges in  $\Psi$  implies that

$\sum_{m,n=1}^{\infty} a_{m,n} \alpha_{m,n}$  converges in  $\Psi$  which in turn implies

that  $a_{m,n} \alpha_{m,n} \rightarrow 0$  as  $m, n \rightarrow \infty$ . Hence (i)  $\Rightarrow$  (ii).

Now we assume that (ii) is true but (iii) is false. This implies that for some  $\sigma'_1 < A_1, \sigma'_2 < A_2$

$$\limsup_{m,n \rightarrow \infty} \frac{\log^+ \|\alpha_{m,n}\| - A_1 \lambda_m - A_2 \mu_n}{\lambda_m + \mu_n} \geq 0.$$

Hence there exists a sequence  $\{m_k\}$  and  $\{n_k\}$  of positive integers, such that

$$\frac{\log^+ \|\alpha_{m_k, n_k}\| - A_1 \lambda_{m_k} - A_2 \mu_{n_k}}{\lambda_{m_k} + \mu_{n_k}} \geq -k^{-1}, \forall m_k \text{ and } n_k, k = 1, 2, \dots$$

We define a sequence  $\{a_{m,n}\} \subseteq E$ , as

$$a_{m,n} = \begin{cases} \omega e^{-((A_1 - k^{-1})\lambda_{m_k} + (A_2 - k^{-1})\mu_{n_k})} & \forall m = m_k, n = n_k, k = 1, 2, \dots \\ 0 & m \neq m_k, n \neq n_k \end{cases}$$

Then, we have

$$\begin{aligned} \|a_{m_k, n_k}\| e^{\sigma_1 \lambda_{m_k} + \sigma_2 \mu_{n_k}} &= e^{-((A_1 - k^{-1})\lambda_{m_k} + (A_2 - k^{-1})\mu_{n_k})} e^{\sigma_1 \lambda_{m_k} + \sigma_2 \mu_{n_k}} \\ &= e^{-((A_1 - k^{-1}) - \sigma_1)\lambda_{m_k} + (A_2 - k^{-1} - \sigma_2)\mu_{n_k}} \end{aligned}$$

For large  $K$ ,  $(A_1 - \sigma_1 - k^{-1}) > 0$  and  $(A_2 - \sigma_2 - k^{-1}) > 0$ .

Hence  $\sum_{k=1}^{\infty} \|a_{m_k, n_k}\| e^{\sigma_1 \lambda_{m_k} + \sigma_2 \mu_{n_k}}$  converges in  $\Psi$  for

all  $\sigma_1 < A_1, \sigma_2 < A_2$ .

On the other hand, for all  $k = 1, 2, \dots$

$$\begin{aligned} \|a_{m_k, n_k}\| \|\alpha_{m_k, n_k}\| &\geq \\ e^{-((A_1 - k^{-1})\lambda_{m_k} + (A_2 - k^{-1})\mu_{n_k})} & \\ e^{(A_1 - k^{-1})\lambda_{m_k} + (A_2 - k^{-1})\mu_{n_k}} &= 1. \end{aligned}$$

Therefore the sequence  $\{a_{m,n} \alpha_{m,n}\}$  does not tend to zero as  $m, n \rightarrow \infty$  and this contradicts (ii). Hence (ii)  $\Rightarrow$  (iii). Lastly we show that (iii)  $\Rightarrow$  (i).

In course of the proof of Theorem 2 above, we have already proved that if (iii) holds then there exists a linear continuous transformation  $F: \Psi \rightarrow \Psi$  with

$F(e_{m,n}) = \alpha_{m,n} \in \Psi, m = 1, 2, \dots, n = 1, 2, \dots$ . By continuity of  $F$ ,

$$\begin{aligned} F\left(\sum_{m,n=1}^{\infty} a_{m,n} e_{m,n}\right) &= F\left(\lim_{m,n \rightarrow \infty} \sum_{k=1}^{m,n} a_{k,k} e_{k,k}\right) \\ &= \lim_{m,n \rightarrow \infty} \left\{ \sum_{k=1}^{m,n} a_{k,k} F(e_{k,k}) \right\} = \sum_{m,n=1}^{\infty} a_{m,n} \alpha_{m,n}. \end{aligned}$$

Thus the proof of Theorem 3 is complete.

**Theorem (4):** Let  $\{a_{m,n}\} \subseteq E$  and  $\{\alpha_{m,n}\} \subseteq \Psi$ .

The following three properties are equivalent:

(a)  $\lim_{m,n \rightarrow \infty} (a_{m,n} \alpha_{m,n}) = 0$  in  $\Psi$  implies that

$\sum_{m,n=1}^{\infty} a_{m,n} e_{m,n}$  converges in  $\Psi$ .

(b) Convergence of  $\sum_{m,n=1}^{\infty} (a_{m,n} \alpha_{m,n})$  in  $\Psi$  implies

that  $\sum_{m,n=1}^{\infty} a_{m,n} e_{m,n}$  converges in  $\Psi$ .

(c)

$$\lim_{\sigma_1, \sigma_2 \rightarrow A_1, A_2} \left\{ \liminf_{m,n \rightarrow \infty} \frac{\log^+ \|\alpha_{m,n}\|_{\sigma_1, \sigma_2} - A_1 \lambda_m - A_2 \mu_n}{\lambda_m + \mu_n} \right\} \geq 0$$

**Proof.** Obviously (a)  $\Rightarrow$  (b). We now prove that (b)  $\Rightarrow$  (c). to prove this, we suppose that (b) holds but (c) does not hold. Therefore

$$\lim_{\sigma_1, \sigma_2 \rightarrow A_1, A_2} \left\{ \liminf_{m,n \rightarrow \infty} \frac{\log^+ \|\alpha_{m,n}\|_{\sigma_1, \sigma_2} - A_1 \lambda_m - A_2 \mu_n}{\lambda_m + \mu_n} \right\} < 0$$

Since  $\|\cdot\|_{\sigma_j}$  increases as  $\sigma_j$  increases, this implies

that for each  $\sigma_1 < A_1, \sigma_2 < A_2$

$$\liminf_{m,n \rightarrow \infty} \frac{\log^+ \|\alpha_{m,n}\|_{\sigma_1, \sigma_2} - A_1 \lambda_m - A_2 \mu_n}{\lambda_m + \mu_n} < 0, \text{ for}$$

all  $\sigma_1 < A_1, \sigma_2 < A_2$ .

Hence if  $\nu > 0$  is a fixed small positive number, then for each  $r > 0$ , we can find a positive numbers  $m_r, n_r$  such that  $\forall r$ , we have  $m_{r+1} > m_r, n_{r+1} > n_r$  and

$$\frac{\log^+ \|\alpha_{m_r, n_r}\| - A_1 \lambda_{m_r} - A_2 \mu_{n_r}}{\lambda_{m_r} + \mu_{n_r}} < -\nu \tag{8}$$

$$\log \|\alpha_{m_r, n_r}\| - A_1 \lambda_{m_r} - A_2 \mu_{n_r} \leq -\nu(\lambda_{m_r} + \mu_{n_r}),$$

$$\log \|\alpha_{m_r, n_r}\| \leq (A_1 - \nu)\lambda_{m_r} + (A_2 - \nu)\mu_{n_r}.$$

Now by taking exponential to the above inequality, we get that

$$\Rightarrow \|\alpha_{m_r, n_r}\|_{\sigma_1, \sigma_2} \leq e^{(A_1 - \nu)\lambda_{m_r} + (A_2 - \nu)\mu_{n_r}}.$$

Now we choose a positive number  $\nu_1 < \nu$  and define a sequence  $\{\alpha_{m,n}\} \subseteq E$  as

$$\alpha_{m,n} = \begin{cases} \omega e^{-(A_1-\nu_1)\lambda_{m_r} + (A_2-\nu_1)\mu_{n_r}} & \forall m = m_r, n = n_r, r = 1, 2, \dots \\ 0 & m \neq m_r, n \neq n_r \end{cases}$$

Then, for any  $\sigma_1 < A_1, \sigma_2 < A_2$

$$\sum_{m,n=1}^{\infty} \|\alpha_{m,n}\|_{\sigma_1, \sigma_2} = \sum_{r=1}^{\infty} \|\alpha_{m_r, n_r}\|_{\sigma_1, \sigma_2} \quad (9)$$

Omit from the above series those finite number of terms, which correspond to those number  $m_r, n_r$  for which  $1/r > \nu_1$ . The remainder of the series in (9) is dominated by  $\sum_{r=1}^{\infty} \|\alpha_{m_r, n_r}\|_{\sigma_1, \sigma_2}$ . Now by (8) and (9), we find that

$$\begin{aligned} \sum_{m,n=1}^{\infty} \|\alpha_{m,n}\|_{\sigma_1, \sigma_2} &\leq \sum_{r=1}^{\infty} \|\alpha_{m_r, n_r}\|_{\sigma_1, \sigma_2} \leq \\ &\sum_{r=1}^{\infty} e^{(A_1-\nu_1)\lambda_{m_r} + (A_2-\nu_1)\mu_{n_r}} e^{-(A_1-\nu_1)\lambda_{m_r} + (A_2-\nu_1)\mu_{n_r}} \\ &= \sum_{r=1}^{\infty} e^{(\nu_1-\nu)\lambda_{m_r} + (\nu_1-\nu)\mu_{n_r}} \end{aligned}$$

Since  $\nu_1 < \nu$ , above series is convergent. For this sequence  $\{\alpha_{m,n}\}$  as defined above,  $\sum_{m,n=1}^{\infty} \|\alpha_{m,n}\|_{\sigma_1, \sigma_2}$  converges in  $\Psi(\sigma_1, \sigma_2)$  and hence converges in  $\Psi$ . But we have

$$\begin{aligned} \sum_{m,n=1}^{\infty} \|\alpha_{m,n}\| e^{\sigma_1 \lambda_m + \sigma_2 \mu_n} &= \sum_{r=1}^{\infty} \|\alpha_{m_r, n_r}\| e^{\sigma_1 \lambda_{m_r} + \sigma_2 \mu_{n_r}} \\ &= \sum_{r=1}^{\infty} e^{-(A_1-\nu_1)\lambda_{m_r} - (A_2-\nu_1)\mu_{n_r}} e^{\sigma_1 \lambda_{m_r} + \sigma_2 \mu_{n_r}} \\ &= \sum_{r=1}^{\infty} e^{(\sigma_1 + \nu_1 - A_1)\lambda_{m_r} + (\sigma_2 + \nu_1 - A_2)\mu_{n_r}} \end{aligned}$$

Now given  $\nu_1$  choose  $\sigma_1 < A_1, \sigma_2 < A_2$  such that  $\sigma_1 + \nu_1 > A_1, \sigma_2 + \nu_1 > A_2$ , then the above series is divergent for this  $\sigma_1, \sigma_2$ . Hence  $\sum_{m,n=1}^{\infty} \alpha_{m,n} e_{m,n}$  does not converge in  $\Psi$  and this is a contradiction. Therefore (b)  $\Rightarrow$  (c).

Now we prove that (c)  $\Rightarrow$  (a). we assume (c) is true but (a) does not hold. Then there exists a sequences  $\{\alpha_{m,n}\}$ , where  $\alpha_{m,n}$  belongs to Banach space  $E$ , for which  $\|\alpha_{m,n}\|_{\sigma_{m,n}} \rightarrow 0$  in  $\Psi$ , but  $\sum_{m,n=1}^{\infty} \alpha_{m,n} e_{m,n}$  does not converge in  $\Psi$ . This implies that

$$\limsup_{m,n \rightarrow \infty} \frac{\log^+ \|\alpha_{m,n}\| + A_1 \lambda_m + A_2 \mu_n}{\lambda_m + \mu_n} > 0.$$

Hence there exists a positive number  $\varepsilon$  and a sequence  $\{m_k\}, \{n_k\}$  of positive integers such that

$$\frac{\log^+ \|\alpha_{m_k, n_k}\| + A_1 \lambda_{m_k} + A_2 \mu_{n_k}}{\lambda_{m_k} + \mu_{n_k}} \geq e^{(-A_1 + \varepsilon)\lambda_{m_k} + (-A_2 + \varepsilon)\mu_{n_k}} \quad (10)$$

We choose a positive numbers  $\nu$  such that  $\nu < \varepsilon/2$ , by assumption we can find a positive number  $\sigma_1 = \sigma_1(\nu), \sigma_2 = \sigma_2(\nu)$  such that

$$\liminf_{m,n \rightarrow \infty} \frac{\log^+ \|\alpha_{m,n}\| - A_1 \lambda_m - A_2 \mu_n}{\log(\lambda_m^{\sigma_1} \cdot \mu_n^{\sigma_2})} \geq -\nu.$$

Hence there exists  $N = N(\nu)$ , such that

$$\frac{\log^+ \|\alpha_{m,n}\| - A_1 \lambda_m - A_2 \mu_n}{\lambda_m + \mu_n} \geq -2\nu \quad \forall m, n \geq N. \quad (11)$$

$$\log \|\alpha_{m,n}\| - A_1 \lambda_m - A_2 \mu_n \leq -2\nu(\lambda_m + \mu_n)$$

$$\log \|\alpha_{m,n}\| \leq (A_1 - 2\nu)\lambda_m + (A_2 - 2\nu)\mu_n$$

$$\|\alpha_{m,n}\| \leq e^{(A_1 - 2\nu)\lambda_m + (A_2 - 2\nu)\mu_n}$$

Therefore,

$$\begin{aligned} \|\alpha_{m_k, n_k}\|_{\sigma_1, \sigma_2} &\geq e^{(-A_1 + \varepsilon)\lambda_{m_k} + (-A_2 + \varepsilon)\mu_{n_k}} e^{(A_1 - 2\nu)\lambda_{m_k} + (A_2 - 2\nu)\mu_{n_k}} \\ &= e^{(\varepsilon - 2\nu)\lambda_{m_k} + (\varepsilon - 2\nu)\mu_{n_k}} \rightarrow \infty \quad \text{as} \\ &k \rightarrow \infty, \text{ since } \varepsilon > 2\nu \end{aligned}$$

Thus  $\{\|\alpha_{m,n}\|_{\sigma_1, \sigma_2}\}$  does not tend to zero in  $Y(\sigma_1, \sigma_2)$  for the  $\sigma_j, j = 1, 2$  chosen above and this is a contradiction. Thus (c)  $\Rightarrow$  (a) is proved. This completes the proof of Theorem 4.

**Corollary (5):** A base  $\{\alpha_{m,n}\}$  in a closed subspace  $\Psi_0$  of  $\Psi$  is proper if and only if it satisfies the condition (iii) and (c) of Theorem (3) and Theorem (4).

## REFERENCES

1. Behnam.H.S and Srivastava.G.S : Growth of analytic Dirichlet functions of two complex variables, Indian J. Math., Vol. 40, No.3, 269-281,(1998).
2. Srivastava.B.L.: A study of spaces of certain classes of vector valued Dirichlet series, Thesis, I.I.T Kanpur, (1983).
3. Kamthan.P.K and Singh Gautam.S.K : Bases in a certain space of functions analytic in the half plane, Indian J. pure Appl. Math., 24, 1066-107, (1975).
4. Srivastava.G.S and Archana Sharma : Bases in the space of vector valued analytic Dirichlet series, International Journal of pure and app. Math., Vol.70, No.7, 993-1000, (2011)



**Direct and Inverse Theorems for the Bezier Variant of Operators  $M_n$  in  $L_{\delta,p}$ -Spaces**

Lekaa Abdulkareem Hussein

Al-Mustansiriyah University, College of Science, Physics Department

**Article info**

Received 10/11/2014  
Accepted 11/1/2015

**ABSTRACT**

In this paper we found better estimation for the rate of convergence in locally global norms of bounded measurable functions by the Bezier variant of the operators  $M_n$  in terms of average modulus of smoothness.

**الخلاصة**

في بحثنا هذا قمنا بحساب درجة أفضل تقريب للدوال المقيدة القابلة للقياس في الفضاءات  $L_{\delta,p}[a,b]$  في بحثنا هذا قمنا بحساب درجة أفضل تقريب للدوال المقيدة القابلة للقياس في الفضاءات  $L_{\delta,p}$  باستخدام معدل مقياس النعومة Bezier variant للمؤثرات  $M_n$  بواسطة  $(1 \leq p < \infty)$

$$\tau_{\phi^\lambda}(f, x)_{\delta,p}$$

**INTRODUCTION**

There are many scientist study the approximation by the Bezier variant of some well known operators such as Nurhayatfspir and Ismetyuksel in (2005) [4] introduced the Bezier variant of a general sequence of linear positive operators and estimate the rate of convergence of these operators for functions of bounded variation and such as Asha Ram Gairola and p. N. Agrawal in (2010) [1] studied the approximation by the Bezier variant of the operators  $M_n$  in  $L_\infty$ -space

In our paper we will study the approximation of bounded measurable function by the Bezier variant of operators  $M_n$  in  $L_{\delta,p}$ -space  $(1 \leq p < \infty)$

Now let as list some deffinitions that we will use throughout our work

Let  $X = [1, \infty)$ , we denote by  $L_{\delta,p}(X)$  the space of all bounded measurable functions such that  $\|f\|_{\delta,p} < \infty$  is defined by

$$\|f\|_{\delta,p} = \left( \int_x \left( \sup \{ |f(y)| : y \in [x - \frac{\delta}{2}, x + \frac{\delta}{2}] \} \right)^p dx \right)^{\frac{1}{p}}, x \in X$$

Let  $\phi(x) = \sqrt{x(1+cx)}$ ,  $0 \leq \lambda \leq 1$ , then

$$w_{\phi^\lambda}(f, t) = \sup_{0 < \lambda \leq t} \sup_{x - h\phi^\lambda(x) \geq 0} \left| f\left(x + \frac{h\phi^\lambda(x)}{2}\right) - f\left(x - \frac{h\phi^\lambda(x)}{2}\right) \right|$$

Where  $\phi(x)$  is an admissible weight function of Ditzan-Totik modulus of smoothness  $w_{\phi^\lambda}(f, t)$  and the corresponding K-functional is defined as  $K_{\phi^\lambda}(f, t) = \inf_{g \in W_\lambda} \{ \|f - g\| + t \|\phi^\lambda g'\| \}$ ,  $t \in (0, \infty)$

where  $W_\lambda = \{g : g \in AC[0,1], \|\phi^\lambda g'\| < \infty\}$

$g \in AC[0,1]$  means that  $g$  is absolutely continuous on  $[0,1]$

The average modulus of smoothness for  $f \in L_{\delta,p}$  is defined by:

$$\tau_{\phi^\lambda}(f, t)_{\delta,p} = \|w_{\phi^\lambda}(f, t)\|_{\delta,p}$$

And corresponding K-functional is defined by:

$$K_{\phi^\lambda}(f, t)_{\delta,p} = \inf_{g \in W_\lambda} \{ \|f - g\|_{\delta,p} + t \|\phi^\lambda g'\|_{\delta,p} \}, t \in (0, \infty)$$

The operators:

$$M_n(f, x) = \sum_{K=0}^{\infty} P_{n,K}(x, c) \int_0^{\infty} b_{n,K}(t, c) f(t) dt \dots (1)$$

Considered by Gupta and Mohapatra [3] for Lebesgueintegrable function on the interval  $[0, \infty)$ , where

$$P_{n,K}(x, c) = (-1)^K \frac{x^K}{K!} \phi_{n,c}^{(K)}(x),$$

$$b_{n,K}(t, c) = (-1)^{K+1} \frac{t^K}{K!} \phi_{n,c}^{(K+1)}(t) \text{ and}$$

For  $c > 0$ ,  $\phi_{n,c}(x) = (1+cx)^{-\frac{n}{c}}$  and  $x \in [0, \infty)$ ,

And for  $c = 0$ ,  $\phi_{n,c}(x) = e^{-nx}$  and  $x \in [0, \infty)$ ,

We observe that for the case  $c > 0$ , the operators  $M_n$  reduce Baskakov-Durrmeyer operators and when  $c = 0$  these become Szasz-Durrmeyer type operators.

For  $\alpha \geq 1$ , the Bezier variant  $M_{n,\alpha}$  of the operators  $M_n$  is defined by:

$$M_{n,\alpha}(f, x) = \sum_{K=0}^{\infty} Q_{n,K}^\alpha(x, c) \int_0^{\infty} b_{n,K}(t, c) f(t) dt \dots (2)$$

Where:

$$Q_{n,K}^\alpha(x, c) = J_{n,K}^\alpha(x, c) - J_{n,K+1}^\alpha(x, c)$$

$$\text{with } J_{n,K}(x, c) = \sum_{v=K}^{\infty} P_{n,v}(x, c)$$

For  $\alpha = 1$ , the operators  $M_{n,\alpha}$  reduce to the operators  $M_n$

**MAIN RESULTS**

**Theorem:**

Let  $f \in L_{\delta,p}[1, \infty)$ ,  $\phi(x) = \sqrt{x(1+cx)}$ ,  $0 \leq \lambda \leq 1$ ,  $C \geq 0$  and  $0 < \beta < 1$ , then the following statements are equivalent:

$$(i) |M_{n,\alpha}(f, x) - f(x)| = O\left(\frac{\alpha^{\frac{1}{2}} \phi^{1-\lambda}(x)}{\sqrt{n}}\right)$$

$$(ii) \tau_{\phi^\lambda}(f, x)_{\delta,p} = O(x^\beta)$$



**Corollary:**

Let  $f \in L_{\delta,p}[1, \infty)$ ,  $\vartheta(x) = \sqrt{x(1+cx)}$ ,  $0 \leq \lambda \leq 1, C \geq 0$  then

$$|M_{n,\alpha}(f, x) - f(x)| \leq \tau_{\vartheta^\lambda} \left( f, \frac{\alpha^{\frac{1}{2}} \vartheta^{1-\lambda}(x)}{\sqrt{n}} \right)_{\delta,p}$$

**AUXILIARY RESULTS**

We can use some lemmas and corollaries to solve our problem.

**Lemma (1) [3]:**

For  $m \in \mathbb{N} \cup \{0\}$ , if we define the  $m$ -th order moment for the operators  $M_n$  by:

$$\mu_{n,m}(x, c) = \sum_{k=0}^{\infty} P_{n,k}(x, c) \int_0^{\infty} b_{n,k}(t, c) (t-x)^m dt$$

Then

$$\mu_{n,0}(x, c) = 1, \quad \mu_{n,1}(x, c) = \frac{1+cx}{n-c}$$

and

$$\mu_{n,2}(x, c) = \frac{2cx^2(n+c) + 2x(n+2c) + 2}{(n-c)(n-2c)}$$

Also, there holds the following recurrence relation

$$\begin{aligned} [n-c(m+1)]\mu_{n,m+1}(x, c) &= x(1+cx)[\mu_{n,m}^{(1)}(x, c) \\ &+ 2m\mu_{n,m-1}(x, c)] \\ &+ [(1+2cx)(m+1) \\ &- cx]\mu_{n,m}(x, c), \quad n > c(m+1) \end{aligned}$$

**Corollary (1):**

If  $c \geq 0$  and  $K > 2$ , then for sufficiently large  $n$ , we have:

$$\mu_{n,2}(x, c) \leq \frac{K\vartheta^2(x)}{n} \dots \dots \dots (3)$$

**Lemma (2) [1]:**

For the functions  $J_{n,K}(x, c)$  and  $Q_{n,K}^\alpha(x, c)$ , we have:

$$1 = J_{n,0}(x, c) > J_{n,1}(x, c) > \dots > J_{n,K}(x, c) > J_{n,K+1}(x) \dots \dots \dots (4)$$

$$0 < \vartheta_{n,K}^\alpha(x, c) \leq \alpha P_{n,K}(x, c), \alpha \geq 1$$

$$M'_{n,\alpha}(1, x) = 0 \dots \dots \dots (5)$$

$$\begin{aligned} |M'_{n,\alpha}(f, x)| &\leq \alpha \left| \sum_{k=0}^{\infty} (J_{n,k}^{\alpha-1}(x, c) - J_{n,k+1}^{\alpha-1}(x)) J'_{n,k+1}(x) \right. \\ &+ \int_0^{\infty} f(t) b_{n,k}(t, c) dt \\ &\left. + M'_n(f, x) \right| \dots \dots \dots (6) \end{aligned}$$

**Corollary (2):**

From (3) and (5), it follows that:

$$M_{n,\alpha}((t-x)^2, x) \leq \alpha \frac{c\vartheta^2(x)}{n}, c > 2$$

**Lemma (3):**

For  $f \in L_{\delta,p}[1, \infty)$ ,  $\vartheta(x) = \sqrt{x(1+cx)}$ ,  $0 \leq \lambda, t, x > 0$ , we have:

$$\left| \int_x^t f'(u) du \right| \leq 2 \left( x^{-\frac{\lambda}{2}} (1+ct)^{\frac{\lambda}{2}} + \vartheta^{-\lambda}(x) \right) |t-x| \|\vartheta^\lambda f'\|_{\delta,p}$$

**Proof:**

By using Holder's inequality, we have:

$$\begin{aligned} \left| \int_x^t f'(u) du \right| &\leq \|\vartheta^\lambda f'\| \left| \int_x^t \frac{du}{\vartheta^\lambda(u)} \right| \leq \|\vartheta^\lambda f'\| |t-x|^{1-\lambda} \left| \int_x^t \frac{du}{\vartheta(u)} \right|^\lambda \\ &\leq \|\vartheta^\lambda f'\|_{\delta,p} |t-x|^{1-\lambda} \left| \int_x^t \frac{du}{\vartheta(u)} \right|^\lambda \end{aligned}$$

$$\text{Since } \left| \int_x^t \frac{du}{\vartheta(u)} \right| \leq \left| \int_x^t \frac{du}{\sqrt{u}} \right| \left( \frac{1}{\sqrt{1+cx}} + \frac{1}{\sqrt{1+ct}} \right)$$

$$\text{and } \left| \int_x^t \frac{du}{\sqrt{u}} \right| \leq \frac{2|t-x|}{\sqrt{x}}$$

using the inequality  $|a+b|^p \leq |a|^p + |b|^p, 0 \leq p \leq 1$ , we get

$$\begin{aligned} \left| \int_x^t f'(u) du \right| &\leq \|\vartheta^\lambda f'\|_{\delta,p} |t-x| \frac{2^\lambda}{x^{\lambda/2}} \left| \frac{1}{\sqrt{1+cx}} + \frac{1}{\sqrt{1+ct}} \right|^\lambda \\ &\leq \|\vartheta^\lambda f'\|_{\delta,p} |t-x| \frac{2^\lambda}{x^{\frac{\lambda}{2}}} \left( (1+ct)^{-\frac{\lambda}{2}} + (1+cx)^{-\frac{\lambda}{2}} \right) \end{aligned}$$

$$\begin{aligned} \left| \int_x^t f'(u) du \right| &\leq \|Q^\lambda f'\|_{\delta,p} |t-x| \frac{2^\lambda}{x^{\lambda/2}} \left| \frac{1}{\sqrt{1+cx}} + \frac{1}{\sqrt{1+ct}} \right|^\lambda \\ &\leq \|\vartheta^\lambda f'\|_{\delta,p} |t-x| \frac{2^\lambda}{x^{\frac{\lambda}{2}}} \left( (1+ct)^{-\frac{\lambda}{2}} + (1+cx)^{-\frac{\lambda}{2}} \right) \end{aligned}$$

Hence, the lemma follows:

**Lemma (4) [1]:**

For any non-negative real number  $m$ , there holds the inequality:

$$M_{n,\alpha}((1+ct)^{-m}, x) \leq K_m (1+cx)^{-m},$$

Where  $K_m$  is a constant depending on  $m$  only.

**Lemma (5) [1]:**

For the functions  $J_{n,K}(x, c)$  and  $P_{n,K}(x, c)$ , there hold the relations:

$$(i) \vartheta^2(x) \sum_{v=K}^{\infty} P'_{n,v}(x) = \sum_{v=K}^{\infty} (v-nx) P_{n,v}(x, c)$$

$$(ii) (1+cx) J'_{n,K}(x, c) + n J_{n,K}(x, c) = n J_{n,K-1}(x, c) + cx J'_{n,K-1}, \text{ where } c \geq 0, \vartheta^2(x) = x(1+cx)$$

**Corollary (3):**

From (i), we get:

$$\begin{aligned} x(1+ct) J'_{n,K}(x, c) &= \sum_{v=K}^{\infty} (v-nx) P_{n,v}(x, c) \\ &= \sum_{v=K+1}^{\infty} (v-nx) P_{n,v}(x, c) \\ &+ K P_{n,K}(x, c) - nx P_{n,v}(x, c) \\ &= cx^2 J'_{n,K}(x, c) + K P_{n,v}(x, c) \text{ using (ii)} \end{aligned}$$

Hence we have,

$$J'_{n,K}(x, c) = \frac{K}{x} P_{n,v}(x, c)$$

**Lemma (6):**

The following statements are hold for the operators  $M_{n,\alpha}$ :

- (i)  $|\vartheta^\lambda(x)M'_{n,\alpha}(f, x)| \leq C\alpha \|\vartheta^\lambda f'\|_{\delta,p}$
- (ii)  $|\vartheta^\lambda(x)M'_{n,\alpha}(f, x)| \leq C\alpha \vartheta^{\lambda-1}(x)\sqrt{n}\|f\|_{\delta,p}$

Where  $\lambda \geq 1$

**Proof:**

**Part (i)**

From (5) and (6), we get:

$$\begin{aligned} M'_{n,\alpha}(f, x) &= M'_{n,\alpha}(f, x) - f(x)M'_{n,\alpha}(1, x) \\ &= M'_{n,\alpha}\left(\int_x^t f'(u)du, x\right) \\ &\leq \alpha \left| \sum_{K=0}^{\infty} (J_{n,K}^{\alpha-1}(x, c) - J_{n,K+1}^{\alpha-1}(x)) J'_{n,K+1}(x) \right. \\ &\quad \left. * \int_0^{\infty} \left( \int_x^t f'(u)du \right) b_{n,K}(t, c) dt \right| \\ &\quad + \left| M'_n\left(\int_x^t f'(u)du, x\right) \right| \\ &=: S_1 + S_2 \dots \dots \dots (7) \end{aligned}$$

Now, we find estimates for  $S_1$  and  $S_2$  separately as follows:

By using the inequality

$$|a^\alpha - b^\alpha| \leq \alpha|a - b| \text{ with } 0 \leq a, b \leq 1 \text{ and } \alpha \geq 1, [3]$$

and corollary (3) we have:

$$\begin{aligned} S_1 &= \alpha \left| \sum_{K=0}^{\infty} (J_{n,K}^{\alpha-1}(x, c) - J_{n,K+1}^{\alpha-1}(x)) J'_{n,K+1}(x) \int_0^{\infty} \left( \int_x^t f'(u)du \right) b_{n,K}(t, c) dt \right| \\ &\leq \frac{\alpha}{x} \sum_{K=0}^{\infty} K P_{n,K}(x, c) \int_0^{\infty} \left| \int_x^t f'(u)du \right| b_{n,K}(t, c) dt \end{aligned}$$

From lemma (3), we have:

$$\begin{aligned} S_1 &\leq \frac{2\alpha}{x} \sum_{K=0}^{\infty} K P_{n,K}(x, c) * \\ &\int_0^{\infty} \left( x^{-\frac{\lambda}{2}} (1+ct)^{-\frac{\lambda}{2}} \right. \\ &\quad \left. + \vartheta^{-\lambda}(x) |t - x| \|\vartheta^\lambda f'\|_{\delta,p} \right) b_{n,K}(t, c) dt \\ &\leq \frac{2\alpha \|\vartheta^\lambda f'\|_{\delta,p}}{x^{1+\frac{\lambda}{2}}} \sum_{K=0}^{\infty} K P_{n,K}(x, c) \int_0^{\infty} (1+ct)^{-\frac{\lambda}{2}} |t - x| b_{n,K}(t, c) dt \\ &\quad + \frac{2\alpha \|\vartheta^\lambda f'\|_{\delta,p}}{x \vartheta^\lambda(x)} \sum_{K=0}^{\infty} K P_{n,K}(x, c) \int_0^{\infty} |t - x| b_{n,K}(t, c) dt \\ &=: S_{11} + S_{12} \dots \dots \dots (8) \end{aligned}$$

By Holder's inequality, we get:

$$\begin{aligned} &\int_0^{\infty} (1+ct)^{-\frac{\lambda}{2}} |t - x| b_{n,K}(t, c) dt \leq \\ &\left( \int_0^{\infty} (1+ct)^{-\lambda} b_{n,K}(t, c) dt \right)^{\frac{1}{2}} \left( \int_0^{\infty} (t-x)^2 b_{n,K}(t, c) dt \right)^{\frac{1}{2}} \end{aligned}$$

then

$$\begin{aligned} S_{11} &\leq \frac{2\alpha \|\vartheta^\lambda f'\|_{\delta,p}}{x^{1+\frac{\lambda}{2}}} \sum_{K=0}^{\infty} K P_{n,K}(x, c) * \\ &\left( \int_0^{\infty} (1+ct)^{-\lambda} b_{n,K}(t, c) dt \right)^{\frac{1}{2}} \left( \int_0^{\infty} (t-x)^2 b_{n,K}(t, c) dt \right)^{\frac{1}{2}} \end{aligned}$$

Now, it can be easily shown that:

$$\int_0^{\infty} (t-x)^2 b_{n,K}(t, c) dt = 0(x^2)$$

Therefore, by using lemma(4) we get the following estimate for  $S_{11}$ :

$$\begin{aligned} S_{11} &\leq \frac{2\alpha \|\vartheta^\lambda f'\|_{\delta,p}}{x^{\frac{\lambda}{2}}} \sum_{K=0}^{\infty} K P_{n,K}(x, c) \left( \int_0^{\infty} (1+ct)^{-\lambda} b_{n,K}(t, c) dt \right)^{\frac{1}{2}} \\ &\leq \frac{2\alpha \|\vartheta^\lambda f'\|_{\delta,p}}{x^{\frac{\lambda}{2}}} \left( \sum_{K=0}^{\infty} K^2 P_{n,K}(x, c) \right)^{\frac{1}{2}} \left( \sum_{K=0}^{\infty} P_{n,K}(x, c) \int_0^{\infty} (1+ct)^{-\lambda} b_{n,K}(t, c) dt \right)^{\frac{1}{2}} \\ &\leq \frac{2\alpha \|\vartheta^\lambda f'\|_{\delta,p}}{x^{\frac{\lambda}{2}}} \frac{1}{(1+ct)^{\frac{\lambda}{2}}} \end{aligned}$$

Next, using corollary (2) and Holder's inequality for summation, we get:

$$\begin{aligned} S_{12} &\leq \frac{2\alpha \|\vartheta^\lambda f'\|_{\delta,p}}{x \vartheta^\lambda(x)} \left( \sum_{K=0}^{\infty} K^2 P_{n,K}(x, c) \right)^{\frac{1}{2}} \left( \sum_{K=0}^{\infty} P_{n,K}(x, c) \int_0^{\infty} (t-x)^2 b_{n,K}(t, c) dt \right)^{\frac{1}{2}} \\ &\leq \frac{2\alpha \|\vartheta^\lambda f'\|_{\delta,p}}{\vartheta^\lambda(x)} \end{aligned}$$

Combining the estimates of  $S_{11}$  and  $S_{12}$ , we obtain:

$$S_1 \leq \frac{C\alpha \|\vartheta^\lambda f'\|_{\delta,p}}{\vartheta^\lambda(x)} \dots \dots \dots (9)$$

Again, the estimate of  $S_2$  we obtained along the lines of  $S_1$  for  $\alpha = 1$ .

Hence, we get (i).

**Part (ii)**

From part (i) we have:

$$\begin{aligned} M'_{n,\alpha}(f, x) &\leq \alpha \left| \sum_{K=0}^{\infty} (J_{n,K}^{\alpha-1}(x, c) - J_{n,K+1}^{\alpha-1}(x)) J'_{n,K+1}(x) \right. \\ &\quad \left. * \int_0^{\infty} f(t) b_{n,K}(t, c) dt \right| + |M'_n(f(t), x)| \\ &=: T_1 + T_2 \dots \dots \dots (10) \end{aligned}$$

For  $T_1$ , we get the estimate by using corollary(1):

$$\begin{aligned} T_1 &\leq \alpha \|f\| \left| \sum_{K=0}^{\infty} (J_{n,K}^{\alpha-1}(x, c) - J_{n,K+1}^{\alpha-1}(x)) J'_{n,K+1}(x) \right| \\ &\leq \alpha \|f\|_{\delta,p} \frac{n}{\vartheta^2(x)} \sum_{v=K}^{\infty} \left| \frac{v}{n} - x \right| P_{n,v}(x, c) \\ &\leq \alpha \|f\|_{\delta,p} \frac{\sqrt{n}}{\vartheta(x)} \dots \dots \dots (11) \end{aligned}$$

Similar estimate is established for  $T_2$  as it is obtained by putting  $\alpha = 1$  in the estimate of  $T_1$ .

Hence, the lemma is established from (7) to (11).

**Lemma (7):**

If  $f \in L_{\delta,p}[a, b]$ ,  $a, b \in R$ ,  $1 \leq p < \infty$ , we have

$$\omega_K(f, x)_{\delta,p} \leq \tau_K(f, x)_{\delta,p}$$

**Proof:**

$$\begin{aligned} \omega_K(f, x)_{\delta, p} &= \text{Sup}_{|h| \leq \delta} \{ \|\Delta_h^K f(\cdot)\|_{\delta, p} \} \\ &= \text{Sup}_{|h| \leq \delta} \left\{ \left( \text{Sup} \left\{ |\Delta_h^K f(y)|, y \in \left[ x - \frac{k\delta}{2}, x + \frac{k\delta}{2} \right] \right\} \right)^p dx \right\}^{\frac{1}{p}} \\ &\leq \text{Sup}_{|h| \leq \delta} \left\{ \int_a^b \left( \omega_K(f, y + \frac{kh}{2}, \delta) : y \in \left[ x - \frac{k\delta}{2}, x + \frac{k\delta}{2} \right] \right)^p dx \right\}^{\frac{1}{p}} \\ &= \text{Sup}_{|h| \leq \delta} \left\{ \int_{a+\frac{kh}{2}}^{b+\frac{kh}{2}} \left( \omega_1(f, y, \delta), y \right. \right. \\ &\quad \left. \left. \in \left[ x - \frac{k\delta}{2}, x + \frac{k\delta}{2} \right] \right)^p dx \right\}^{\frac{1}{p}} \end{aligned}$$

$$= \tau_K(f, x)_{\delta, p}$$

**Proof of the Main Theorem:**

Let  $g = g_{n, x, \lambda} \in w_\lambda$  where  $n, x, \lambda$  fixed

From the definition of  $K_{\phi^\lambda}(f, t)_{\delta, p}$  we get:

$$\begin{aligned} \|f - g\|_{\delta, p} + \frac{\alpha^{\frac{1}{2}} \phi^{1-\lambda}(x)}{\sqrt{n}} \|\phi^\lambda g'\|_{\delta, p} \\ \leq 2K_{\phi^\lambda} \left( f, \frac{\alpha^{\frac{1}{2}} \phi^{1-\lambda}(x)}{\sqrt{n}} \right)_{\delta, p} \dots \dots \dots (12) \end{aligned}$$

Since  $M_{n, \alpha}$  is constant preserving, we can write:

$$\begin{aligned} |M_{n, \alpha}(f, x) - f(x)| &\leq 2\|f - g\|_{\delta, p} \\ &+ |M_{n, \alpha}(g, x) - g(x)| \dots \dots \dots (13) \end{aligned}$$

Using the representation  $g(t) = g(x) + \int_x^t g'(u) du$

And lemma (3), we have:

$$\begin{aligned} |M_{n, \alpha}(g, x) - g(x)| &= \left| M_{n, \alpha} \left( \int_x^t g'(u) du \right) \right| \\ &\leq 2\|\phi^\lambda g'\|_{\delta, p} \left[ \phi^\lambda(x) M_{n, \alpha}(|t-x|, x) + x^{-\frac{\lambda}{2}} M_{n, \alpha} \left( \frac{|t-x|}{(1+ct)^{\frac{\lambda}{2}}}, x \right) \right] \\ &:= 2\|\phi^\lambda g'\|_{\delta, p} [H_1 + H_2] \dots \dots \dots (14) \end{aligned}$$

By using Schwarz's inequality and corollary (2), we get:

$$\begin{aligned} H_1 &= \phi^\lambda(x) \sum_{K=0}^{\infty} Q_{n, K}^\alpha(x, c) \int_0^{\infty} b_{n, K}(t, c) |t-x| dt \\ &\leq \alpha^{\frac{1}{2}} \phi^{-\lambda}(x) \left( \sum_{K=0}^{\infty} Q_{n, K}^\alpha(x, c) \int_0^{\infty} b_{n, K}(t, c) dt \right)^{\frac{1}{2}} \times \\ &\quad \left( \sum_{K=0}^{\infty} Q_{n, K}^\alpha(x, c) \int_0^{\infty} b_{n, K}(t, c) (t-x)^2 dt \right)^{\frac{1}{2}} \\ &\leq \alpha^{\frac{1}{2}} \frac{K \phi^{1-\lambda}(x)}{\sqrt{n}} \dots \dots \dots (15) \end{aligned}$$

Also by using Schwarz's inequality, corollary (2) and lemma (4), we get the following estimation for  $H_2$ :

$$\begin{aligned} H_2 &= x^{-\frac{\lambda}{2}} M_{n, \alpha} \left( \frac{|t-x|}{(1+ct)^{\frac{\lambda}{2}}}, x \right) \\ &\leq M_{n, \alpha}((t-x)^2, x)^{\frac{1}{2}} \left( M_{n, \alpha}((1+ct)^{-\lambda}, x) \right)^{\frac{1}{2}} \\ &\leq x^{-\frac{\lambda}{2}} \alpha^{\frac{1}{2}} (1+cx)^{-\frac{\lambda}{2}} \frac{\phi(x)}{\sqrt{n}} \\ &= c \alpha^{\frac{1}{2}} \frac{\phi^{1-\lambda}(x)}{\sqrt{n}} \dots \dots \dots (16) \end{aligned}$$

By (17) and (18), we have the estimate:

$$\begin{aligned} |M_{n, \alpha}(g, x) - g(x)| \\ \leq C \alpha^{\frac{1}{2}} \frac{\phi^{1-\lambda}(x)}{\sqrt{n}} \|\phi^\lambda g'\|_{\delta, p} \dots \dots \dots (17) \end{aligned}$$

Thus, from (14)-(17) we get (ii)  $\Rightarrow$  (i):

Now, to prove (i)  $\Rightarrow$  (ii), we have:

$$\begin{aligned} |\bar{\Delta}_{\lambda \phi^\lambda(x)} f(x)| &\leq |M_{n, \alpha}(z) - f(z)| + |M_{n, \alpha}(x) - f(x)| \\ &\quad + |\bar{\Delta}_{\lambda \phi^\lambda(x)} M_{n, \alpha} f(x)| \\ &\leq 2C \gamma_{x, h}^\beta + |\bar{\Delta}_{\lambda \phi^\lambda(x)} M_{n, \alpha} f(x)| \end{aligned}$$

where  $\gamma_{x, h} = \max\{y, z\}, y = x - \frac{h\phi^\lambda(x)}{2}, \text{ and } z = x + h\phi^\lambda(x)/2$

define a weighted Steklov type average function  $g$  as:

$$g(x) := \frac{1}{\gamma \phi^\lambda(x)} \int_{-\frac{\gamma}{2} \phi^\lambda(x)}^{\frac{\gamma}{2} \phi^\lambda(x)} f(x-u) du, \quad \lambda \geq 0$$

So, we get:

$$\begin{aligned} (g - f)(x) &= \frac{1}{\gamma \phi^\lambda(x)} \int_{-\frac{\gamma}{2} \phi^\lambda(x)}^{\frac{\gamma}{2} \phi^\lambda(x)} [f(x-u) - f(x)] du \\ &\leq C \omega_{\phi^\lambda(x)}(f, \gamma) \end{aligned}$$

then:

$$\begin{aligned} |g'(x)| &= \left| \frac{1}{\gamma \phi^\lambda(x)} \left( f \left( x + \frac{\gamma}{2} \phi^\lambda(x) \right) \right. \right. \\ &\quad \left. \left. - f \left( x - \frac{\gamma}{2} \phi^\lambda(x) \right) \right) \right| \\ &\leq \frac{1}{\gamma \phi^\lambda(x)} \omega_{\phi^\lambda(x)}(f, \gamma) \end{aligned}$$

Then we get:

$$\|g'(\cdot)\|_{\delta, p} \leq \frac{1}{\gamma \delta} \tau_{\phi^\lambda(x)}(f, \gamma)_{\delta, p} \dots \dots \dots (18)$$

From lemma 6(i), we have:

$$|M'_{n, \alpha}(g, x)| \leq C \frac{\alpha}{\gamma \delta} \tau_{\phi^\lambda(x)}(f, \gamma)_{\delta, p} \dots \dots \dots (19)$$

By using Bernstein type inequalities, and then using (18) and (19), we get the estimate:

$$\begin{aligned} |\bar{\Delta}_{\lambda \phi^\lambda(x)} M'_{n, \alpha}(f, x)| \\ \leq h \phi^\lambda(x) (|M'_{n, \alpha}(f - g, x)| \\ + |M'_{n, \alpha}(g, x)|) \\ \leq Cah \phi^\lambda(x) (\phi^{-1}(x) \sqrt{n} \|f - g\|_{\delta, p} + \|g'\|_{\delta, p}) \\ \leq Cah \left( \phi^{\lambda-1} \sqrt{n} + \frac{1}{\gamma} \right) \tau_{\phi^\lambda(x)}(f, \gamma)_{\delta, p} \end{aligned}$$

Then, we have:

$$\tau_{h\phi^\lambda(x)}(f, \gamma)_{\delta, p} \leq 2C\gamma_{x,h}^\beta + C\alpha h \left( \phi^{\lambda-1}\sqrt{n} + \frac{1}{\gamma} \right) \tau_{\phi^\lambda(x)}(f, \gamma)_{\delta, p}$$

Choosing  $\gamma_{x,h} = \gamma$  and using the argument of [2] we get (i)  $\Rightarrow$  (ii) ■

**Proof of the Corollary:**

From (12)-(17), we have:

$$|M_{n,\alpha}(f, x) - f(x)| \leq CK_{\phi^\lambda} \left( f, \frac{\alpha^{1/2}\phi^{1-\lambda}(x)}{\sqrt{n}} \right)_{\delta, p}$$

Since,  $K_{\phi^\lambda}(f, x)_{\delta, p} \leq \omega_{\phi^\lambda}(f, x)_{\delta, p}$

Then

$$|M_{n,\alpha}(f, x) - f(x)| \leq C\omega_{\phi^\lambda} \left( f, \frac{\alpha^{1/2}\phi^{1-\lambda}(x)}{\sqrt{n}} \right)_{\delta, p}$$

By lemma (7)  $\omega_{\phi^\lambda}(f, x)_{\delta, p} \leq \tau_{\phi^\lambda}(f, x)_{\delta, p}$

Then, we get:

$$|M_{n,\alpha}(f, x) - f(x)| \leq C\tau_{\phi^\lambda} \left( f, \frac{\alpha^{1/2}\phi^{1-\lambda}(x)}{\sqrt{n}} \right)_{\delta, p}$$

**REFERENCES**

[1] Asha R. G., and Agrawal P. N., "Direct and Inverse Theorems for the Bezier Variant of Certain Summation-Integral Type Operators", Turk J. Math., 34 :221-234, 2010.

[2] Berens H., and Lorentz G. G., "Inverse Theorem for Bernstein Polynomials", Indiana Univ. Math. J., 21 :693-708, 1972.

[3] Gupta V., and Mohapatra R., "On the Rate of Convergence for Certain Summation-Integral Type Operators", Math. Ineq. Appl., 9(3) :465-472, 2006.

[4] Nurhayat I., and Ismet Y., "on the Bezier variant of srivasTava-Gupta operators" Applied mathematics E-Notes, 5, 129-137, 2005.



## Some Bayes Estimators for Maxwell Distribution with Conjugate Informative Priors

Tasnim H.K. Al-Baldawi  
Dept. of Math, College of Science, University of Baghdad  
tasnim@csbaghdad.edu.iq

### Article info

Received 10/4/2012  
Accepted 11/1/2015

### Key words:

Maxwell distribution, Bayes Estimators, informative prior, conjugate prior, squared and modified squared error loss functions.

### ABSTRACT

In this article, we propose to obtain Bayesian and non-Bayesian estimators for the shape parameter of Maxwell distribution. We consider a class of informative priors, namely; inverted gamma prior information and inverted Chi square prior information. The Bayes estimators are obtained under two different loss functions; the squared error loss function and the modified squared error loss function. Based on a Monte Carlo simulation study, those estimators are compared to the corresponding maximum likelihood estimator. The performance of these estimators was numerically explored under different conditions. The comparison criteria are the mean square error MSE.

Comparison shows that Bayes estimators of the shape parameter with the inverted Chi square prior have less MSE for small  $\theta$  and hyper-parameter  $\alpha$ . And the MSE of the maximum likelihood estimator was very close to the MSE of Bayesian estimators only under the squared error loss function.

### الخلاصة

في هذه الدراسة، استخرجت مقدرات بيزية ولا بيزية لمعلمة الشكل لتوزيع ماكسويل. فيما يتعلق بمقدرات بيز، استعملت دوال أسبقية معلوماتية وهي بالتحديد دالة أسبقية معكوس كاما ودالة أسبقية معكوس مربع كاي. استخرجت مقدرات بيز وفقاً لدالة الخسارة التربيعية ودالة الخسارة التربيعية المعدلة. أجريت مقارنة مقدرات بيز المستخرجة مع مقدر الأرجحية العظمى من خلال أسلوب المحاكاة إذ أجري استطلاع أداء هذه المقدرات عند حالات مختلفة باستعمال متوسط مربعات الخطأ (MSE) بوصفه معياراً للمقارنة.

أظهرت المقارنة أن مقدرات بيز المستندة إلى دالة أسبقية معكوس مربع كاي كان لها أقل متوسط مربعات خطأ في حالة  $\theta$  صغيرة ومعلمة أسبقية  $\alpha$  صغيرة. كما أظهرت النتائج تقارب كبير في قيم متوسط مربعات الخطأ فيما يخص مقدرات بيز ومقدر الأرجحية العظمى تحت دالة الخسارة التربيعية فقط.

### INTRODUCTION

Maxwell distribution was first introduced by J. C. Maxwell (1860) and then described by Boltzmann (1870) with a few assumptions [1].

Maxwell distribution plays an important role in Physics and chemistry. It gives the distribution of speeds of molecules in thermal equilibrium as given by statistical mechanics. For example, this distribution explains many fundamental gas properties in kinetic theory of gases, distribution of energies and moments, ...etc [2].

[3] considered Maxwell distribution as a lifetime model for the first time. [4] generalized Maxwell distribution by introducing one more parameter. [5] studied Empirical Bayesian estimation for Maxwell distribution. [6] discussed Bayesian estimation for two component mixture of Maxwell distribution, assuming type I censored data.

The Bayesian deduction requires appropriate choice of priors for the parameters. In the last several decades, Bayesian analysis focused on priors that are uninformative. But if we have enough information about the parameter, then it is better to make use of the informative priors. The parameters of the prior distribution are called hyper-parameters [7].

In this paper, we derive Bayes estimators of the parameter  $\theta$  for the Maxwell distribution along with maximum likelihood estimator. Since the Maxwell model is skewed, there should be a skewed prior for this model. We use the inverted gamma as a natural conjugate prior for the Maxwell model. The inverted Chi square which is another form of the inverted gamma distribution is also considered as a prior.

The estimators are derived in the following order: Maximum likelihood estimator, Bayes estimators with inverted gamma prior under squared and modified squared error loss functions, and the inverted Chi square prior under the squared and modified squared error loss functions. Comparison was made through a Monte Carlo simulation study on the performance of these estimators. The results are summarized in tables and followed by the conclusions.

### MAXWELL DISTRIBUTION

A random variable X, follow the Maxwell (or Maxwell-Boltzmann) distribution if its pdf is given by:

$$f(x|\theta) = \frac{4}{\sqrt{\pi}} \frac{1}{\theta^{3/2}} x^2 \exp\left[-\frac{x^2}{\theta}\right] \quad 0 < x < \infty; \theta > 0 \quad (1)$$

where  $\theta$  is the shape parameter.

The cumulative distribution function (cdf) in its simplest form, is given by:

$$F(x|\theta) = \frac{1}{\Gamma(\frac{3}{2})} \Gamma\left(\frac{x^2}{\theta}, \frac{3}{2}\right)$$

where  $\Gamma(x, \alpha) = \int_0^x u^{\alpha-1} e^{-u} du$

Alternative forms of the cdf found in [8]. The  $r^{\text{th}}$  moment is given by:

$$E(X^r) = \frac{2}{\sqrt{\pi}} \theta^{r/2} \Gamma\left(\frac{r+3}{2}\right); r > -3$$

In particular;

$$E(X) = 2 \sqrt{\frac{\theta}{\pi}}$$

and

$$\text{Var}(X) = \frac{\theta}{2\pi} (3\pi - 8) = 0.2268 \theta$$

The Maxwell distribution is positively skewed and had leptokurtic distribution with

$$\text{Mode} = +\sqrt{\theta}$$

and

$$\text{Median} = \sqrt{\frac{\theta}{\pi}} \left( \frac{\sqrt{\pi} + 4}{4} \right) = 1.0856\sqrt{\theta}$$

### MAXIMUM LIKELIHOOD ESTIMATOR

Let  $X_1, \dots, X_n$  be a set independent identically distributed random variables from Maxwell distribution with parameter  $\theta$ . The likelihood function for Maxwell pdf is given by:

$$L(x_i; \theta) = \left(\frac{4}{\sqrt{\pi}}\right)^n \frac{1}{\theta^{3n/2}} \prod_{i=1}^n x_i^2 \exp\left[-\frac{\sum_{i=1}^n x_i^2}{\theta}\right]$$

By taking the log and differentiating partially with respect to  $\theta$ , we get:

$$\frac{\partial \ln L(x_i; \theta)}{\partial \theta} = n \ln\left(\frac{4}{\sqrt{\pi}}\right) + \sum_{i=1}^n \ln x_i^2 - \frac{3n}{2} \ln \theta - \frac{\sum_{i=1}^n x_i^2}{\theta^2} \quad (2)$$

Then the MLE of  $\theta$  is the solution of equation (2) after equating the first derivative to zero. Hence:

$$\hat{\theta} = \frac{2 \sum_{i=1}^n x_i^2}{3n} \quad (3)$$

### BAYES ESTIMATORS

To obtain Bayes estimators, we assume that  $\theta$  is a real valued random variable with probability density function  $\pi(\theta)$ . The posterior distribution of  $\theta$  is the conditional probability density function of  $\theta$  given the data. A loss function is used to represent a penalty associated with each estimate. The loss should be zero if and only if

$$\hat{\theta} = \theta. \text{ We consider two loss functions}$$

#### 1- The squared error loss function

In most cases the researchers use the squared error loss function which is symmetrical, and associates equal importance to the losses, and obtain the posterior mean as the Bayesian estimate. By using the squared error loss function, we have:

$$L_1(\hat{\theta}, \theta) = (\hat{\theta} - \theta)^2$$

Bayes estimator will be the estimator that minimizes the posterior risk given by:

$$R_1(\hat{\theta} - \theta) = E[L_1(\hat{\theta}, \theta)] = \int_0^\infty (\hat{\theta} - \theta)^2 h(\theta|x) d\theta$$

which is minimized when

$$E(\theta|x) = \int_0^\infty \theta h(\theta|x) d\theta \quad (4)$$

#### 2- The modified squared error loss function

This loss function is considered by [9] with the exponential distribution Here we employ this loss function with the Maxwell distribution. It is given by:

$$L_2(\hat{\theta} - \theta) = \theta^r (\hat{\theta} - \theta)^2$$

And Bayes estimator will be the estimator that minimizes the posterior risk given by:

$$R_2(\hat{\theta} - \theta) = E[L_2(\hat{\theta}, \theta)] = \int_0^\infty \theta^r (\hat{\theta} - \theta)^2 h(\theta|x) d\theta$$

which is minimized when

$$\hat{\theta} = \frac{E(\theta^{r+1}|x)}{E(\theta^r|x)} \quad (5)$$

where

$$E(\theta^r|x) = \int_0^\infty \theta^r h(\theta|x) d\theta$$

### INFORMATIVE PRIOR INFORMATIONS

Bayes estimators for the parameter  $\theta$ , is considered with informative prior information. An informative prior expresses specific information about a variable. In this case, the use of prior information is equivalent to adding a number of observations for a given sample size, and therefore leads to the reduction of the variance or the posterior risk of the Bayes estimates. A conjugate prior distribution is such that the posterior distribution and the prior are members of the same family of distributions [10]. The conjugate prior, inverted gamma distribution is a two parameter continuous probability distribution, which is the reciprocal of a variable distributed according to the gamma distribution. The inverted Chi square distribution is the distribution of a random variable whose reciprocal divided by its degrees of freedom is a Chi square distribution [6]. Following is the derivation of these estimators:

#### i) Inverted Gamma prior information under squared error loss function

This conjugate prior distribution is the distribution of the reciprocal of a variable distributed according to gamma distribution.

$$\pi_3(\theta) = \frac{\beta^\alpha e^{-\frac{\beta}{\theta}}}{\Gamma(\alpha) \theta^{\alpha+1}}; \alpha, \beta, \theta > 0. \quad (6)$$

The posterior distribution for the parameter  $\theta$  given the data  $(x_1, x_2, \dots, x_n)$  is:

$$h(\theta|x) = \frac{\prod_{i=1}^n f(x_i|\theta)\pi(\theta)}{\int_0^\infty \prod_{i=1}^n f(x_i|\theta)\pi(\theta) d\theta} = \frac{e^{-\frac{(\sum_{i=1}^n x_i^2 + \beta)}{\theta}} \theta^{-\frac{3n-2\alpha-2}{2}}}{\int_0^\infty e^{-\frac{(\sum_{i=1}^n x_i^2 + \beta)}{\theta}} \theta^{-\frac{3n-2\alpha-2}{2}} d\theta}$$

$$\text{Let } y = \frac{\sum_{i=1}^n x_i^2 + \beta}{\theta},$$

then

$$h(\theta|\mathbf{x}) = \frac{y^{\frac{3n+2\alpha+2}{2}} e^{-y}}{-(\sum_{i=1}^n x_i^2 + \beta) \int_0^\infty y^{\frac{3n+2\alpha-2}{2}} e^{-y} dy}$$

And the posterior distribution becomes as follows:

$$h(\theta|\mathbf{x}) = \frac{-(\sum_{i=1}^n x_i^2 + \beta)^{\frac{3n+2\alpha}{2}} e^{-\frac{(\sum_{i=1}^n x_i^2 + \beta)}{\theta}}}{\theta^{\frac{3n+2\alpha+2}{2}} \Gamma(\frac{3n+2\alpha}{2})} \quad (7)$$

According to the squared error loss function, the corresponding Bayes' estimator for the parameter  $\theta$  with the posterior distribution (7) is such that:

$$\theta_1^* = E(\theta|\mathbf{x}) \quad (8)$$

Substituting (7) in (8), we get:

$$E(\theta|\mathbf{x}) = \frac{-(\sum_{i=1}^n x_i^2 + \beta)^{\frac{3n+2\alpha}{2}}}{\Gamma(\frac{3n+2\alpha}{2})} \int_0^\infty \theta^{-\frac{3n-2\alpha}{2}} e^{-\frac{(\sum_{i=1}^n x_i^2 + \beta)}{\theta}} d\theta$$

Let

$$y = \frac{(\sum_{i=1}^n x_i^2 + \beta)}{\theta}$$

Then

$$E(\theta|\mathbf{x})$$

$$= \frac{-(\sum_{i=1}^n x_i^2 + \beta)^{\frac{3n+2\alpha}{2}}}{\Gamma(\frac{3n+2\alpha}{2})} \int_0^\infty e^{-y} \left( \frac{\sum_{i=1}^n x_i^2 + \beta}{y} \right)^{-\frac{3n-2\alpha}{2}} \frac{-(\sum_{i=1}^n x_i^2 + \beta)^{\frac{3n+2\alpha}{2}}}{y^2} dy$$

And after few steps

$$E(\theta|\mathbf{x}) = \frac{\sum_{i=1}^n x_i^2 + \beta}{\Gamma(\frac{3n+2\alpha}{2})} \int_0^\infty e^{-y} y^{\frac{3n+2\alpha-4}{2}} dy = \frac{(\sum_{i=1}^n x_i^2 + \beta) \Gamma(\frac{3n+2\alpha-2}{2})}{\Gamma(\frac{3n+2\alpha}{2})}$$

Hence,

$$\theta_1^* = \frac{2(\sum_{i=1}^n x_i^2 + \beta)}{3n+2\alpha-2} \quad (9)$$

**ii) Inverted Gamma prior information under modified squared error loss function**

Now, according to the modified squared error loss function, the corresponding Bayes estimator for  $\theta$  with the posterior distribution (7) is such that:

$$\theta_2^* = \frac{E(\theta^{r+1}|\mathbf{x})}{E(\theta^r|\mathbf{x})} \quad (10)$$

Substituting (7) in (10), we get:

$$E(\theta^r|\mathbf{x}) = \frac{-(\sum_{i=1}^n x_i^2 + \beta)^{\frac{3n+2\alpha}{2}}}{\Gamma(\frac{3n+2\alpha}{2})} \int_0^\infty \theta^{-\frac{3n-2\alpha+2r}{2}} e^{-\frac{(\sum_{i=1}^n x_i^2 + \beta)}{\theta}} d\theta$$

Let

$$y = \frac{\sum_{i=1}^n x_i^2}{\theta}$$

Then

$$E(\theta^r|\mathbf{x})$$

$$= \frac{-(\sum_{i=1}^n x_i^2 + \beta)^{\frac{3n+2\alpha}{2}}}{\Gamma(\frac{3n+2\alpha}{2})} \int_0^\infty e^{-y} \left( \frac{y}{\sum_{i=1}^n x_i^2 + \beta} \right)^{\frac{3n+2\alpha-2r}{2}} \frac{-(\sum_{i=1}^n x_i^2 + \beta)}{y^2} dy$$

Hence,

$$E(\theta^r|\mathbf{x}) = (\sum_{i=1}^n x_i^2 + \beta)^{r+1} \frac{\Gamma(\frac{3n+2\alpha-2r-2}{2})}{\Gamma(\frac{3n+2\alpha}{2})} \quad (11)$$

In the same manner, we find the numerator of  $\theta_2^*$  which become:

$$E(\theta^{r+1}|\mathbf{x}) = (\sum_{i=1}^n x_i^2 + \beta)^{r+2} \frac{\Gamma(\frac{3n+2\alpha-2r-4}{2})}{\Gamma(\frac{3n+2\alpha}{2})} \quad (12)$$

And from (11) and (12), we get:

$$\theta_2^* = \frac{2(\sum_{i=1}^n x_i^2 + \beta)}{(3n+2\alpha-2r-4)}$$

**iii) Inverted Chi square prior information under squared error loss function**

The inverted Chi square distribution is the distribution of a random variable whose reciprocal divided by its degrees of freedom is a Chi square distribution.

$$\pi_3(\theta) = \frac{\beta^{\alpha/2} e^{-\frac{\beta}{2\theta}}}{\Gamma(\frac{\alpha}{2}) \theta^{\frac{\alpha+1}{2}}}; \alpha, \beta, \theta > 0. \quad (13)$$

The posterior distribution for the parameter  $\theta$  given the data  $(x_1, x_2, \dots, x_n)$  is:

$$h(\theta|\mathbf{x}) = \frac{\prod_{i=1}^n f(x_i|\theta)\pi(\theta)}{\int_0^\infty \prod_{i=1}^n f(x_i|\theta)\pi(\theta)d\theta} = \frac{e^{-\frac{(\sum_{i=1}^n x_i^2 + \beta)}{\theta}}}{\theta^{\frac{3n+\alpha-2}{2}}}$$

$$\text{Let } y = \frac{(\sum_{i=1}^n x_i^2 + \beta)}{\theta}, \text{ then}$$

$$h(\theta|\mathbf{x}) = \frac{y^{\frac{3n+\alpha+2}{2}} e^{-y}}{-(\sum_{i=1}^n x_i^2 + \frac{\beta}{2}) \int_0^\infty y^{\frac{3n+2\alpha-2}{2}} e^{-y} dy}$$

And the posterior distribution becomes as follows:

$$h(\theta|\mathbf{x}) = \frac{-(\sum_{i=1}^n x_i^2 + \frac{\beta}{2})^{\frac{3n+\alpha}{2}} e^{-\frac{(\sum_{i=1}^n x_i^2 + \frac{\beta}{2})}{\theta}}}{\theta^{\frac{3n+\alpha+2}{2}} \Gamma(\frac{3n+\alpha}{2})} \quad (14)$$

According to the squared error loss function, the corresponding Bayes estimator for the parameter  $\theta$  with the posterior distribution (14) is such that:

$$\theta_3^* = E(\theta|\mathbf{x}) \quad (15)$$

Substituting (14) in (15), we get:

$$E(\theta|\mathbf{x}) = \frac{-(\sum_{i=1}^n x_i^2 + \frac{\beta}{2})^{\frac{3n+\alpha}{2}}}{\Gamma(\frac{3n+\alpha}{2})} \int_0^\infty \theta^{-\frac{3n-\alpha}{2}} e^{-\frac{(\sum_{i=1}^n x_i^2 + \frac{\beta}{2})}{\theta}} d\theta$$

Let

$$y = \frac{(\sum_{i=1}^n x_i^2 + \frac{\beta}{2})}{\theta}$$

Then

$$E(\theta|\mathbf{x})$$

$$= \frac{-(\sum_{i=1}^n x_i^2 + \frac{\beta}{2})^{\frac{3n+\alpha}{2}}}{\Gamma(\frac{3n+\alpha}{2})} \int_0^\infty e^{-y} \left( \frac{\sum_{i=1}^n x_i^2 + \frac{\beta}{2}}{y} \right)^{-\frac{3n-\alpha}{2}} \frac{-(\sum_{i=1}^n x_i^2 + \frac{\beta}{2})}{y^2} dy$$

And after few steps

$$E(\theta|\mathbf{x}) = \frac{\sum_{i=1}^n x_i^2 + \frac{\beta}{2}}{\Gamma(\frac{3n+\alpha}{2})} \int_0^\infty e^{-y} y^{\frac{3n+\alpha-4}{2}} dy = \frac{(\sum_{i=1}^n x_i^2 + \frac{\beta}{2}) \Gamma(\frac{3n+\alpha-2}{2})}{\Gamma(\frac{3n+\alpha}{2})}$$

Hence,

$$\theta_3^* = \frac{2\sum_{i=1}^n x_i^2 + \beta}{3n+\alpha-2} \quad (16)$$

vi) *Inverted Chi square prior information under modified squared error loss function*

Now, according to the modified squared error loss function, the corresponding Bayes estimator for  $\theta$  with the posterior distribution (14) is such that:

$$\theta_4^* = \frac{E(\theta^{r+1}|\mathbf{x})}{E(\theta^r|\mathbf{x})} \tag{17}$$

Substituting (4) in (17), we get:

$$E(\theta^r|\mathbf{x}) = \frac{-(\sum_{i=1}^n x_i^2 + \frac{\beta}{2})^{\frac{3n+\alpha}{2}}}{\Gamma(\frac{3n+\alpha}{2})} \int_0^\infty \theta^{\frac{-3n-\alpha+2r}{2}} e^{-\frac{(\sum_{i=1}^n x_i^2 + \frac{\beta}{2})}{\theta}} d\theta$$

Let

$$y = \frac{\sum_{i=1}^n x_i^2 + \frac{\beta}{2}}{\theta}$$

Then

$$E(\theta^r|\mathbf{x}) = \frac{-(\sum_{i=1}^n x_i^2 + \frac{\beta}{2})^{\frac{3n+\alpha}{2}}}{\Gamma(\frac{3n+\alpha}{2})} \int_0^\infty e^{-y} \left(\frac{y}{\sum_{i=1}^n x_i^2 + \frac{\beta}{2}}\right)^{\frac{3n+\alpha-2r}{2}} \frac{-(\sum_{i=1}^n x_i^2 + \frac{\beta}{2})}{y^2} dy$$

Hence,

$$E(\theta^r|\mathbf{x}) = \left(\sum_{i=1}^n x_i^2 + \frac{\beta}{2}\right)^r \frac{\Gamma(\frac{3n+\alpha-2r}{2})}{\Gamma(\frac{3n+\alpha}{2})} \tag{18}$$

In the same manner, we find the numerator of  $\theta_6^*$  which becomes:

$$E(\theta^{r+1}|\mathbf{x}) = \left(\sum_{i=1}^n x_i^2 + \frac{\beta}{2}\right)^{r+1} \frac{\Gamma(\frac{3n+\alpha-2r-2}{2})}{\Gamma(\frac{3n+\alpha+2}{2})} \tag{19}$$

And from (18) and (19), we get:

$$\theta_4^* = \frac{2 \sum_{i=1}^n x_i^2 + \beta}{(3n + \alpha - 2r - 4)}$$

**RESULTS AND DISCUSSION**

In order to investigate the performance of the derived estimators, samples of size  $n=20, 50$  and  $100$  were generated from Maxwell distribution. To generate a sample from Maxwell distribution, we applied an

algorithm suggested by [8]. The algorithm involves the following steps:

- 1- To generate two random numbers  $X_1$ , and  $X_2$  from uniform distribution  $U(0, 1)$ .
- 2- To obtain two standard normal variates  $Y_1$ , and  $Y_2$  using the transformation

$$Y_1 = \sqrt{-2\log(x_1)} \cos 2\pi(x_2), \quad Y_2 = \sqrt{-2\log(x_1)} \sin 2\pi(x_2)$$

and find  $Z = \frac{Y_1 + Y_2}{2}$  which is  $N(0, 1)$ .

- 3- To repeat steps 1 and 2 three times to generate a Chi square variate,  $\chi_3^2$  using:

$$T = \sum_{i=1}^3 Z_i^2, \text{ which is gamma variate } G\left(\frac{1}{2}, \frac{3}{2}\right).$$

- 4- Using the transformation  $V = \sqrt{\frac{T\theta}{2}}$ , we get a

random number generated from Maxwell variate.

In our simulation study, we generated samples of size  $n = 20, 50$ , and  $100$  from Maxwell distribution with  $\theta = 0.5, 1$ , and  $2$ . The following pairs of values of the parameters  $\alpha$  and  $\beta$  are chosen  $\{(\alpha, \beta) = (0.5, 1), (1, 1), (1.5, 0.5), (2, 2), (1, 5), (5, 2), (2, 3)\}$  and four values of  $r$  ( $r = -1, 1, 3$ , and  $5$ ). The process was repeated 2000 times and the expected values for the maximum likelihood estimates and Bayes estimates of the parameter  $\theta$  are obtained along with their mean square error (MSE), where

$$MSE(\hat{\theta}) = \frac{\sum_{i=1}^R (\hat{\theta}_i - \theta)^2}{R}$$

The results are summarized and tabulated in the following tables for each estimator and for all sample sizes. The entries within parentheses represent the corresponding MSE.

Table 1: Expected Values of Parameter  $\theta$  and MSE with  $\theta=0.5, \alpha=0.5, \beta=1$

n	$\hat{\theta}$	$\theta_1^*$	$\theta_2^*$			$\theta_3^*$	$\theta_4^*$		
			r=1	r=3	r=5		r=1	r=3	r=5
20	.4997 (.0083)	.5421 (.0103)	.5815 (.0165)	.6271 (.0276)	.6805 (.0461)	.5296 (.0096)	.5685 (.0147)	.6135 (.0245)	.6663 (.0414)
50	.4997 (.0033)	.5164 (.0036)	.5307 (.0045)	.5457 (.0058)	.5617 (.0078)	.5114 (.0035)	.5256 (.0042)	.5406 (.0054)	.5564 (.0072)
100	.4997 (.0016)	.5080 (.0017)	.5149 (.0019)	.5220 (.0023)	.5293 (.0027)	.5055 (.0017)	.5124 (.0019)	.5195 (.0022)	.5267 (.0026)



Table 2: Expected Values of Parameter  $\theta$  and MSE with  $\theta=0.5, \alpha=1, \beta=1$

n	$\tilde{\theta}$	$\theta_1^*$	$\theta_2^*$			$\theta_3^*$	$\theta_4^*$		
			r=1	r=3	r=5		r=1	r=3	r=5
20	.4997 (.0083)	.5664 (.0127)	.6068 (.0209)	.6535 (.0345)	.7079 (.0561)	.5421 (.0103)	.5815 (.0091)	.6271 (.0276)	.6805 (.0460)
50	.4997 (.0033)	.5263 (.0040)	.5407 (.0052)	.5559 (.0068)	.5721 (.0091)	.5164 (.0036)	.5307 (.0045)	.5457 (.0058)	.5616 (.0077)
100	.4997 (.0016)	.5130 (.0018)	.5199 (.0021)	.5271 (.0025)	.5344 (.0030)	.5080 (.0017)	.5149 (.0020)	.5220 (.0023)	.5293 (.0027)

Table 3: Expected Values of Parameter  $\theta$  and MSE with  $\theta=0.5, \alpha=1.5, \beta=0.5$

n	$\tilde{\theta}$	$\theta_1^*$	$\theta_2^*$			$\theta_3^*$	$\theta_4^*$		
			r=1	r=3	r=5		r=1	r=3	r=5
20	.4997 (.0083)	.5079 (.0080)	.5436 (.0110)	.5846 (.0177)	.6323 (.0299)	.5123 (.0085)	.5492 (.0121)	.5919 (.0196)	.6417 (.0333)
50	.4997 (.0033)	.5029 (.0033)	.5166 (.0037)	.5311 (.0046)	.5464 (.0060)	.5047 (.0034)	.5185 (.0039)	.5332 (.0048)	.5487 (.0063)
100	.4997 (.0016)	.5013 (.0017)	.5081 (.0018)	.5150 (.0020)	.5222 (.0023)	.5022 (.0017)	.5090 (.0018)	.5160 (.0020)	.5231 (.0024)

Table 4: Expected Values of Parameter  $\theta$  and MSE with  $\theta=0.5, \alpha=2, \beta=2$

n	$\tilde{\theta}$	$\theta_1^*$	$\theta_2^*$			$\theta_3^*$	$\theta_4^*$		
			r=1	r=3	r=5		r=1	r=3	r=5
20	.4997 (.0083)	.5481 (.0100)	.5859 (.0162)	.6293 (.0269)	.6796 (.0441)	.5330 (.0093)	.5711 (.0145)	.6151 (.0242)	.6663 (.0405)
50	.4997 (.0033)	.5194 (.0036)	.5334 (.0045)	.5482 (.0059)	.5639 (.0079)	.5129 (.0035)	.5270 (.0042)	.5419 (.0054)	.5576 (.0072)
100	.4997 (.0016)	.5096 (.0017)	.5164 (.0019)	.5235 (.0023)	.5307 (.0027)	.5063 (.0017)	.5132 (.0019)	.5202 (.0022)	.5274 (.0026)

Table 5: Expected Values of Parameter  $\theta$  and MSE with  $\theta=1, \alpha=1, \beta=5$

n	$\tilde{\theta}$	$\theta_1^*$	$\theta_2^*$			$\theta_3^*$	$\theta_4^*$		
			r=-1	r=1	r=3		r=-1	r=1	r=3
20	.9994 (.0330)	1.1161 (.0606)	1.1161 (.0606)	1.2494 (.0100)	1.3455 (.1633)	1.1011 (.0444)	1.1011 (.0444)	1.1812 (.0721)	1.2738 (.1207)
50	.9993 (.0132)	1.0660 (.0176)	1.0660 (.0176)	1.0952 (.0230)	1.1260 (.0306)	1.0396 (.0150)	1.0396 (.0150)	1.0682 (.0188)	1.0985 (.0247)
100	.9994 (.0067)	1.0327 (.0078)	1.0327 (.0078)	1.0467 (.0091)	1.0610 (.0108)	1.0194 (.0071)	1.0194 (.0071)	1.0332 (.0080)	1.0474 (.0094)

Table 6: Expected Values of Parameter  $\theta$  and MSE with  $\theta = 1, \alpha = 5, \beta = 2$

n	$\hat{\theta}$	$\theta_1^*$	$\theta_2^*$			$\theta_3^*$	$\theta_4^*$		
			r = -1	r = 1	r = 3		r = -1	r = 1	r = 3
20	.9994 (.0330)	.9407 (.0292)	.9407 (.0292)	.9995 (.0290)	1.0661 (.0374)	.9836 (.0302)	.9836 (.0302)	1.0502 (.0367)	1.1266 (.0553)
50	.9993 (.0132)	.9740 (.0126)	.9740 (.0126)	.9993 (.0126)	1.0260 (.0139)	.9928 (.0128)	.9928 (.0128)	1.0194 (.0138)	1.0476 (.0164)
100	.9994 (.0067)	.9864 (.0065)	.9864 (.0065)	.9994 (.0065)	1.0127 (.0069)	.9961 (.0066)	.9961 (.0066)	1.0094 (.0068)	1.0231 (.0066)

Table 7: Expected Values of Parameter  $\theta$  and MSE with  $\theta = 2, \alpha = 2, \beta = 3$

n	$\hat{\theta}$	$\theta_1^*$	$\theta_2^*$			$\theta_3^*$	$\theta_4^*$		
			r = -1	r = 1	r = 3		r = -1	r = 1	r = 3
20	1.9988 (.1321)	2.0311 (.1246)	2.0311 (.1246)	2.1712 (.1706)	2.3320 (.2733)	2.0488 (.1344)	2.0488 (.1344)	2.1952 (.1897)	2.3640 (.3083)
50	1.9986 (.0530)	2.0118 (.0517)	2.0118 (.0517)	2.0662 (.0588)	2.1235 (.0727)	2.0186 (.0533)	2.0186 (.0533)	2.0739 (.0613)	2.1323 (.0766)
100	1.9987 (.0268)	2.0054 (.0265)	2.0054 (.0265)	2.0323 (.0282)	2.0599 (.0315)	2.0087 (.0269)	2.0087 (.0269)	2.0359 (.0288)	2.0638 (.0324)

The results of this study are stated in the following points:

- 1- The comparison shows that Bayes estimators of parameter  $\theta$  of Maxwell distribution based on Inverted Chi square prior with respect to the squared error loss function gives less MSE only when  $\theta$  is small.
- 2- The comparison shows that Bayes estimators with informative priors gave almost close values of MSE with the maximum likelihood estimator under the squared error loss function, while values of MSE of estimators under the modified squared error loss function, increases notably with the increase of  $r$ .
- 3- Under the modified squared error loss function one can easily observe that the parameters are generally overestimated with the increase of  $r$ . The extent of overestimation is higher for small  $n$ .
- 4- It is obvious that MSE of all estimates of  $\theta$  are reduced with the increase in the sample size.
- 5- Finally, from the results, we can conclude that the suitable prior depends on the appropriate values of  $\theta$ , and the hyper-parameters  $\alpha$  and  $\beta$ , specifically; the inverted Chi square prior is preferable for small values of  $\alpha$  and large values of  $\beta$ , while the use of the inverted gamma prior is better when  $\theta$  and  $\alpha$  become large.

**REFERENCES**

[1] Kasmi A. S. M., Aslam M., and Ali S., "A note of Maximum likelihood estimator for the mixture of Maxwell distributions using type I censored scheme". The open stat. and prob. Journal, (3): 31-35, (2011).  
 [2] Johnson L.N., Kota S., and Balakrishnan n., "Continuous Univariate Distributions", Vol. 1, Second Edition, John Wiley & Sons (1994).

[3] Tyagi R.K., and Bhattacharya S.K., "Bayes estimation of the Maxwell's velocity distribution function", Statistica, 29.(4): 563-7, (1989).  
 [4] Chaturvedi A., and Rani U., "Classical and Bayesian reliability estimation of the generalized Maxwell failure distribution", Journal of Statistical Research, 32: 113-120, (1998).  
 [5] Bekker A., and Roux J.J., "Reliability characteristics of the Maxwell distribution: A Bayes estimation study", Comm. Stat. (Theory & Math.), 34(11): 2169-2178, (2005).  
 [6] Kasmi A.S.M., Aslam M., and Ali S., "On the Bayesian estimation for two component mixture of Maxwell distribution, assuming type I censored data", Int. J. of Applied Science and Technology, 2(1): 197- 218, (2012).  
 [7] Tahir M., and Saleem M., " On relationship between some Bayesian and classical estimators", Pakistan Journal of Life and Social Science, 8(2): 159-161, (2010).  
 [8] Krishna H., and Malik M., "Reliability estimation in Maxwell distribution -with Type-II censored data", International Journal of Quality and Reliability management, 26(2): 184-195, (2009).  
 [9] Al Kutubi H.S., and Ibrahim N. A., "Bayes estimator for Exponential distribution with extension of Jeffrey prior information", Malaysian Journal of mathematical Sciences, 3(2): 297-313, (2009).  
 [10] Tahir M., and Saleem M., " A comparison of priors for the parameter of the time-to-failure model", Pakistan Journal of science, 63(1): 49-52, (2011).



## A New Method for Optimizing Security Site Using Dual Homed Host

Raghad Mohammed Hadi

Management and Economy Collage / University of All mustansuraia.

### Article info

Received 19/1/2014

Accepted 11/5/2014

### ABSTRACT

Recently, there has been an increased request for working in networks and especially the networks that connect with the internet because of the benefits of these networks and especially in transporting information, exploring, exchange messages, marketing, ...etc. But, there are many problems, as information security relates to the need to keep information from falling in the wrong hands. Failure to follow good security practices may lead to unauthorized use of information, fraud and identity theft. Normal flow of information in a business context is not an example of lax security practices and does not lead to unauthorized use and fraud associated with bad security. The policy issues relating to information security differ markedly from the policy issues relating to information sharing. So, the proposed system presents the protection system as one of these mechanisms. The study depends on building the system on the packet filtering mechanism, uses the single box (dual home host) as architecture and detecting viruses, which have specified as signatures, worms and Trojan horse. Depending on intranet that contains four personal computers, one is the server, and the second is the client connected to this server, the third is branch of the site, and the fourth is hacker computer.

### الخلاصة

في الآونة الأخيرة، أصبح هناك زيادة في الطلب على العمل في الشبكات وخصوصاً الشبكات التي تربط مع شبكة الانترنت بسبب الفوائد من هذه الشبكات وخصوصاً في نقل المعلومات والتصفح وتبادل الرسائل والتسويق... الخ. هناك العديد من المشاكل التي تتعلق بأمن المعلومات منها الحاجة إلى الحفاظ على المعلومات من الوقوع في الأيدي المغرصة وعدم اتباع الممارسات الأمنية الجيدة الأمر الذي قد يؤدي إلى استعمال المعلومات على نحو غير مصرح به، مثل العنث وسرقة الهوية. إن التدفق الطبيعي للمعلومات في سياق الأعمال ليس مثالا على الممارسات الأمنية المترسخة ولا يؤدي إلى الاستعمال غير المصرح به والاحتيال المرتبط بالأمنية السيئة. إن قضايا السياسات المتعلقة بأمن المعلومات تختلف بشكل ملحوظ عن قضايا السياسة العامة المتصلة بتقاسم المعلومات. لذلك قدم النظام المقترح احد طرق السرية المعتمدة على packet filter واستعمل single box مع كشف الفايروسات (Trojan horse و Worms و Signiture) بالإعتماد على اربعة حواسيب، الأولى للخادم والثانية للزبون والثالثة مربوطة بالموقع والرابعة حاسبة المخترق.

### INTRODUCTION

Computer network has become an infrastructure resource for businesses, corporations, government agencies, and academic institutions. There are many different models of security that people use to protect their data and resources on internet for example authentication, auditing, encryption methods, and firewalls. A firewall is a combination of hardware and software used to implement a security policy governing network traffic between two or more networks, some of them may be under user's administrative control and the others may be out of his control (e.g. the internet). When we need to build any type of security model we must process the packet of connection to make security of the site work in the right place, as there are no controls on all ports of connection because they are very large, and when any software scan for large number of ports, this would make the connection very slow [1-3].

### PROBLEM STATEMENT

The problem in security policy is that it must attempt to protect the privacy of users and their data, to control

access to restricted data and resources and to prevent fraudulent transactions. Because of the previous reasons, many protections systems appeared to protect the sensitive sites on the Internet from many and different types of penetrations and attacks. These attacks may be: **Interception:** an unauthorized part gains access to an asset, and attacks on confidentiality. **Modification:** an unauthorized party does not gain access to but tampers with an asset, and attacks integrity [4, 5]. To protect our networks and computer systems against security attacks, many security services are needed in the network and server system, such as authentication, access control, confidentiality, and integrity. Among them, authentication service is to make sure whether a client is authentic or not, by using user's ID, password or internet address,...etc. Integrity is used to prevent unauthorized modification of resources and it includes the integrity of system resources, information, and personnel [6, 7]. There are many ways to protect information from eavesdropping as it travels through a network: • physically secure the network, so that

eavesdropping is impossible. Hide the information that you wish to secure within information that appears innocuous. • Encrypt the information so that it cannot be decoded by any party who is not in possession of the proper key [8,9]

#### OBJECTIVE OF RESEARCH AND MOTIVATION TOWARDS RESEARCH

The paper aims to protect the Internet Website by use of mixing or merging packet filtering mechanism and use of the single box (dual home host), in addition to detecting the viruses which have specified signatures, worms and Trojan horse, from unauthorized user who wants to see or damage the private information that put in Internet Website, by using the Intranet zone as case study of the proposed system. The later examines each packet that is sent by or received to website and to ensure fulfillment of all security policy of the web site.

#### SECURE DATA COMMUNICATION

The transaction and communication on the internet involve more than just a user computer and the server of the website that the users are dealing with. Each message back and forth goes through several computers along the way, and the user can not even predict which computers are involved.

The information on the Internet sites is readily available to any user, but in fact there is sensitive information that must be protected. So, data security on Internet site must attempt to protect the privacy of users and their data, control access to restricted data and resources and fraudulent transaction. An *attack* is generally unwanted intrusion, whose strategies often concentrate on vulnerabilities (also called holes or backdoors) of specific operating systems of networks or hardware of network. Following are the major risks involved in any internet transaction:

- **Eavesdropping:** any information that user transmits may be overheard by other computer, for example, credit card number.
- **Manipulation:** the information that user sends or receives may be altered by third parties, for example, the delivery address of his shipment might be altered.
- **Impersonation:** the user might not be dealing with the entity that he thinks he is dealing with. [10,11]
- **Malware:** Any program that is purposefully created to harm the computer system operations or data that is termed as malicious programs.
- **Computer Viruses:** is a self-replicating code (including possibly evolved copies of it) that infects other executable programs. Viruses usually need human intervention for replication and execution.
- **Worm:** Computer worm is a self-replicating standalone program that spreads on computer networks. Worms usually do not need any extra help from the user to replicate and execute [12].
- **Trojan:** Trojan horses or simply Trojans are programs that perform some malicious activity under the guise of some normal programs.
- **Spyware:** is computer software that is installed surreptitiously on a personal computer to intercept or take

partial control over the user's interaction with the computer, without the user's informed consent [12].

#### RELATIVE WORK IN PAST SYSTEMS

For all above mentioned types of protection systems that appeared in past systems such as:

**1-Firewall Protection System;** it has many types of firewalls that can be installed on many types of configuration, it tends to differ in its approach but can be characterized as firewalls block traffic and firewall permits traffic. **2- Intruder Detection;** it tends to monitor and audit the behavior of the user to detect whether he was an author or an intruder. **3-Anti viruses,** some characterize viruses by their "signatures". The others called heuristic scanners and they are generally working with specific types of viruses, and have no signature [12].

#### THE PROPOSED SYSTEM PLATFORM REQUIREMENTS

The platform is the foundation of the software solution and should be presented first. The core component will be indicted, piecing it all together in overall architecture, with some though about communication, **figure (1)** shows the proposed platform system.

The proposed system consists of the following parts:

**a) Client :** The proposed system is a secure system, to run must have a hardware, the hardware is different types of device, recommendation should run at the following device: 1. Personal computer or laptop with at least the following specifications or higher: • Microsoft windows XP

- IIS which provide basic HTTP
- TCP/IP protocol
- HTTP protocol
- Web browser
- LAN Cart type Ethernet bases 10 Mbps.
- 512 RAM
- 1.7 CPU

**b) Server:** These four computers are distributed between two servers and two clients as shown in figure (1), one of these is the server of protected system and the other is internet server, the server of the protected system uses two LAN cards type Ethernet base 10 Mbps; one card is connected to client (peer to peer connection), and the other is connected to the hub. This principle makes the protected server to working as single box structure (dual home host). All four computers transmit data using Shield Twisted Pair (STP). And the recommend system is as web application so that proposed depends and uses web server feature like:

- **IIS (Internet Information Services):** it provides basic HTTP, FTP and SMTP Service.
- **ADO.NET (Active Data Objects):** it provides robust development platform for building web application, which OLE DB provider (ODEDB) and can be connected to any Microsoft tool and interface with underlay databases.
- c) Branch computer:** it works as client computer but in unprotected site.

**d) Hacker computer:** it uses the IP Address Spoofing Attack to make authorized access to the protected site, and it is able to insert any malicious programs in any packet, without any changes to these files especially their sizes.

The result will determine the holes and vulnerabilities of the protection system to penetrate the security in simple and efficient way. And makes Denial-of-Service attack to the authorized machine (client in protected site). Denial-of-Service Attack means the attacker floods the server with requests to connect to other servers that don't exist.

**e) Hub:** is used to connect the protected server with the internet server, branch computer, and hacker or cracker computer, so to connect with client in protected site it uses the second LAN card.

### THE PROPOSED SYSTEM IN DESIGN PROCESS

The proposed system in the designing phase contains two parts the first part is the traditional protection but it provides good access control mechanism at IP and TCP layers and either accept or reject packets; the second part is detecting the computer viruses, and then sends to the second LAN card (to client) of the website what is explained below the:

**The first part (access control):** is constructed using packet filtering mechanism by applying the single box structure (dual homed host), because this structure provides best isolation between the internet and the protected network. The packet filtering is used because it is the basic rule to construct all types of security mechanisms like NAT, proxy, and VPN and all these mechanisms are using the packets in its work. Moreover, the proposed system starts collecting information about users connected to the network using the NetBIOS names and packet capturing technique. The information about the user will detect and analyze to accept the authorized users and refuse unauthorized users as detailed below:

**a) Packet analysis:** Generally all attack types and protection system types on Internet depend on packet analysis. The analysis may focus on the data in the packets or on specific fields of the TCP/IP protocols headers such IP, TCP, UDP, ICMP headers. As shown in figure (2).

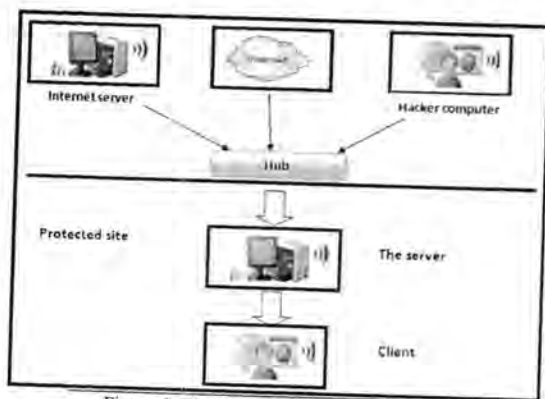


Figure 1: The Proposed System Structure

**b) Receiving packet from first LAN card:** the proposed system works by receiving packet from the first LAN card that connects to internet and from the ports that the system scans.

**c) Send packet to a buffer:** the system will examine each packet in the buffer by comparing the IP address of the source computer and destination computer of packet with authorized IPs table. Therefore the number of ports and the IP of source and destination computer determine the level of security.

**d) Rejected or accepted the packet:** Whereas the IP of the source or destination computer is unauthorized the packet is rejected, access is denied and sends message to the request owner (source computer) about this situation. When the IP of the source and destination address is authorized it is accepted.

**e) The authentication level:** When the IP of the source and destination address is authorized, the proposed system will ask the user about his name and password to login inside the protected network. If the first name and password of the user do not match the proposed system will reject this request until the user enter the exact name and password or cut the connection. But when the users enter the true name and password the protection system send the packet to the second part.

### Scanning

Scanning is the most widely used industry standard. Scanning involve searching for strings in files. The strings being searched are pre-defined virus signatures and support exact matching as well as wildcards to look for variants of a virus.

### Activity Monitoring

Activity Monitoring is the latest trend in virus research where a file execution is monitored for traces of malicious behavior.

### Integrity Checking

Integrity Checking creates a cryptographic checksum for each file on a system and periodically monitors for any variation in that checksum to detect possible changes caused by viruses.

### Data Mining

Data Mining involves applying a full suite of statistical and machine learning algorithms on a set of features derived from malicious and clean programs, all of these methods involve matching/mismatching criteria to work. The method can be classified as anomaly, misuse, or a hybrid detection method. Anomaly Detection involves creating a normal profile of the system or programs and checking for any deviation from that profile. Misuse Detection involves creating a malicious profile in the form of an exact or heuristic signature and checking for that signature in the programs. Hybrid Detection uses data from both clean and malicious programs to build classifiers.

### j) Packet Send or not to the Second LAN Card:

If there is a virus in the data, then the session destroyed and assign that session as malicious one then put all the information related to it (such as user name and its password and source and destination IP addresses, ports, protocol type and statues) as unauthorized packets that would be as updating for protection system rules. But if there is no virus then send packet to second LAN card which is connected to protected network. When the request is addressed to the web server this server response to request and sends the home page of web site to the source computer, and then the user enters the name and the password to complete display of his private information. The flowcharts shown in figures 3 and 4 represent the mechanism of the proposed system.

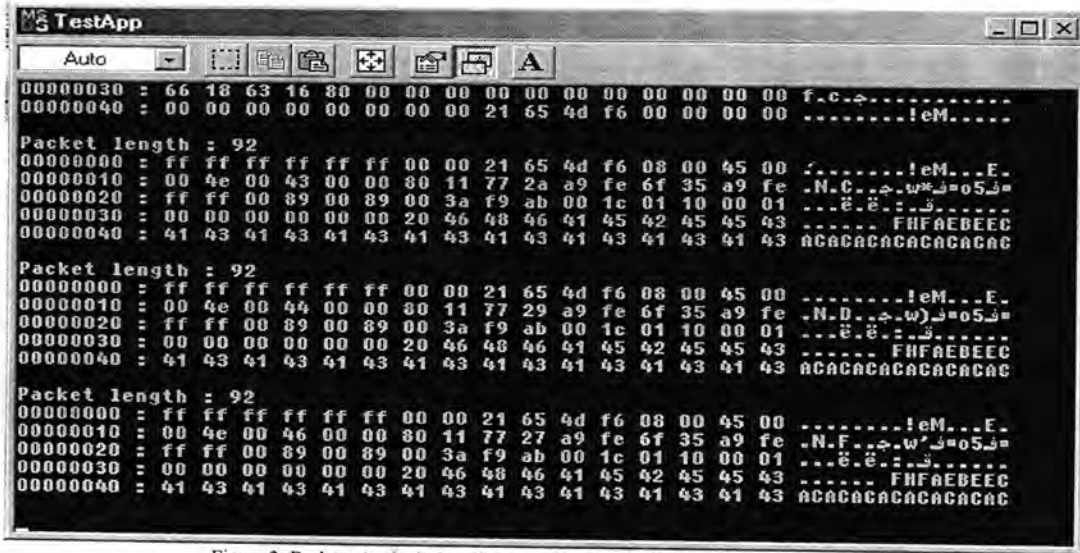


Figure 2: Packets Analysis from Proposed System by Packet Capture Software

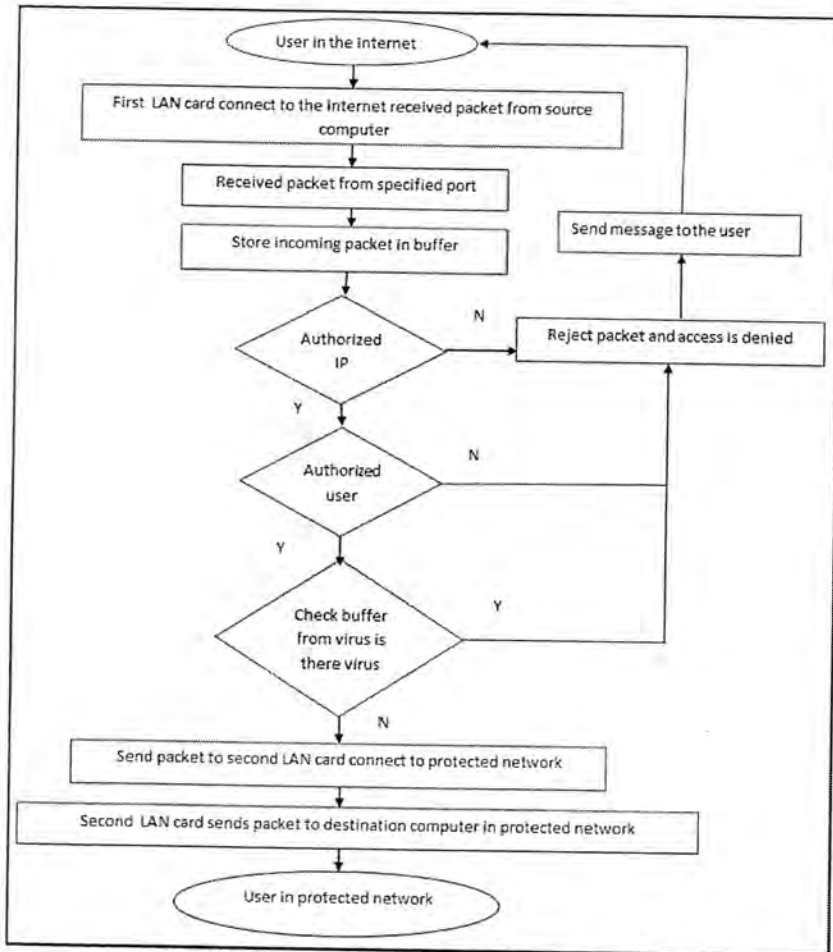


Figure 3: Incoming Packet to the Protected System from Internet

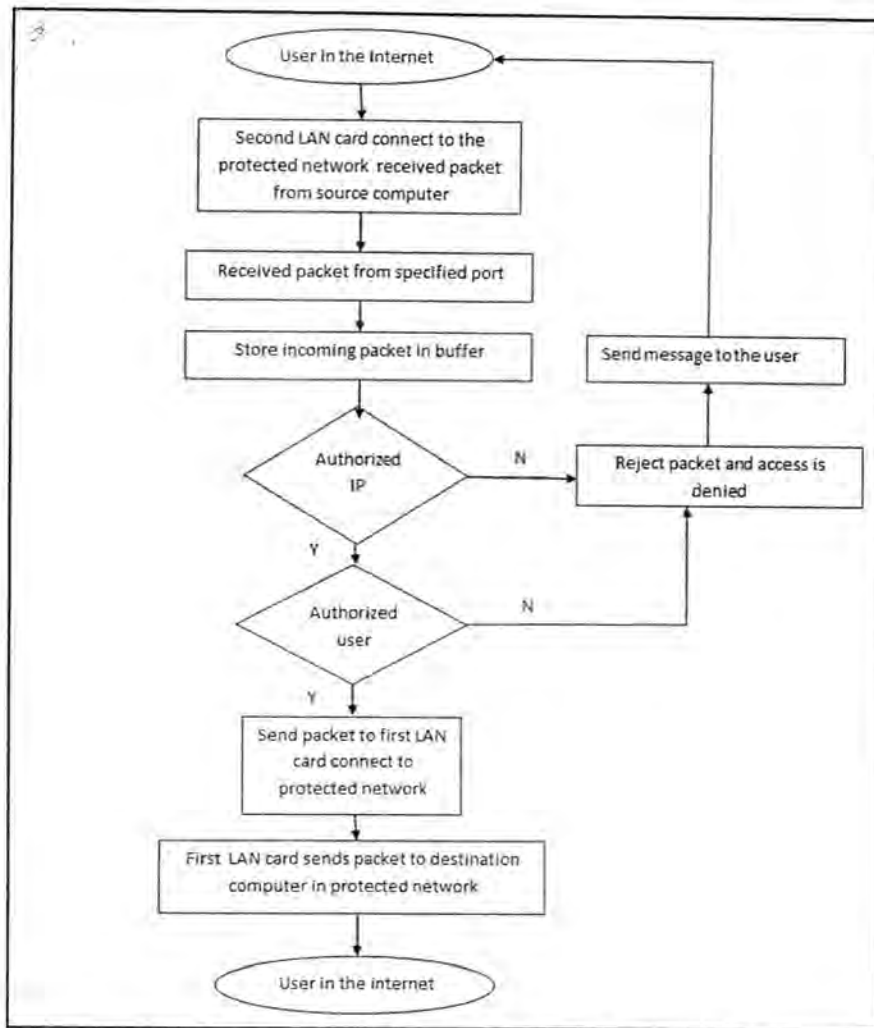


Figure 4: Incoming Packet to the Protected System from Protected Network

### TABLES

System database tables are stored in the server and are controlled by administrator; access to database in server using ADO.NET, the database contains three tables represent the system.

- User login table: Content two fields, user name and password, the structure of this table is shown in table (1).
- Client database table: comprises several fields as name, job, address, Mail and these field depend on application type, the structure of this table is shown in table(2).
- Detection results of new & unknown tables, which comprise classifier, variables, detection rate, and false rate, the structure of this table is shown in table (3).

### SERVER TOOLS

The server is designed as administrator to client accounts in protected site. However, controlling the administrator tools can be shown in figure (5), the tools consist of:

- **Key selector:** this operation was performed when we create account to use system for the first time.
- **Add/remove account:** in this operation, adding and removing account is done by the server through administrative tools.
- **Authentication check:** in this operation the server can check whether the user is authorized to enter system by password in login table.

Table 1: User Login Database

NAME	TYPE	LENGHT
User name	Text	256 Bytes
Password	Text	8 Bytes

Table 2: Client Database

NAME	TYPE	LENGHT
Name	Text	20 Bytes
Job	Text	15 Bytes
Address	Text	50 Bytes
Mali	Text	15 Bytes

Table 3: Detection Results of New & Unknown Malware

Classifier	Variables	Detection Rate	False Alarm Rate
Random Forest	All	93.1%	6.3%
Random Forest	RF	92.4%	9.2%
Random Forest	PCA	89.7%	10.1%
Bagging	All	91.1%	7.4%
Bagging	PCA	91.1%	9.6%

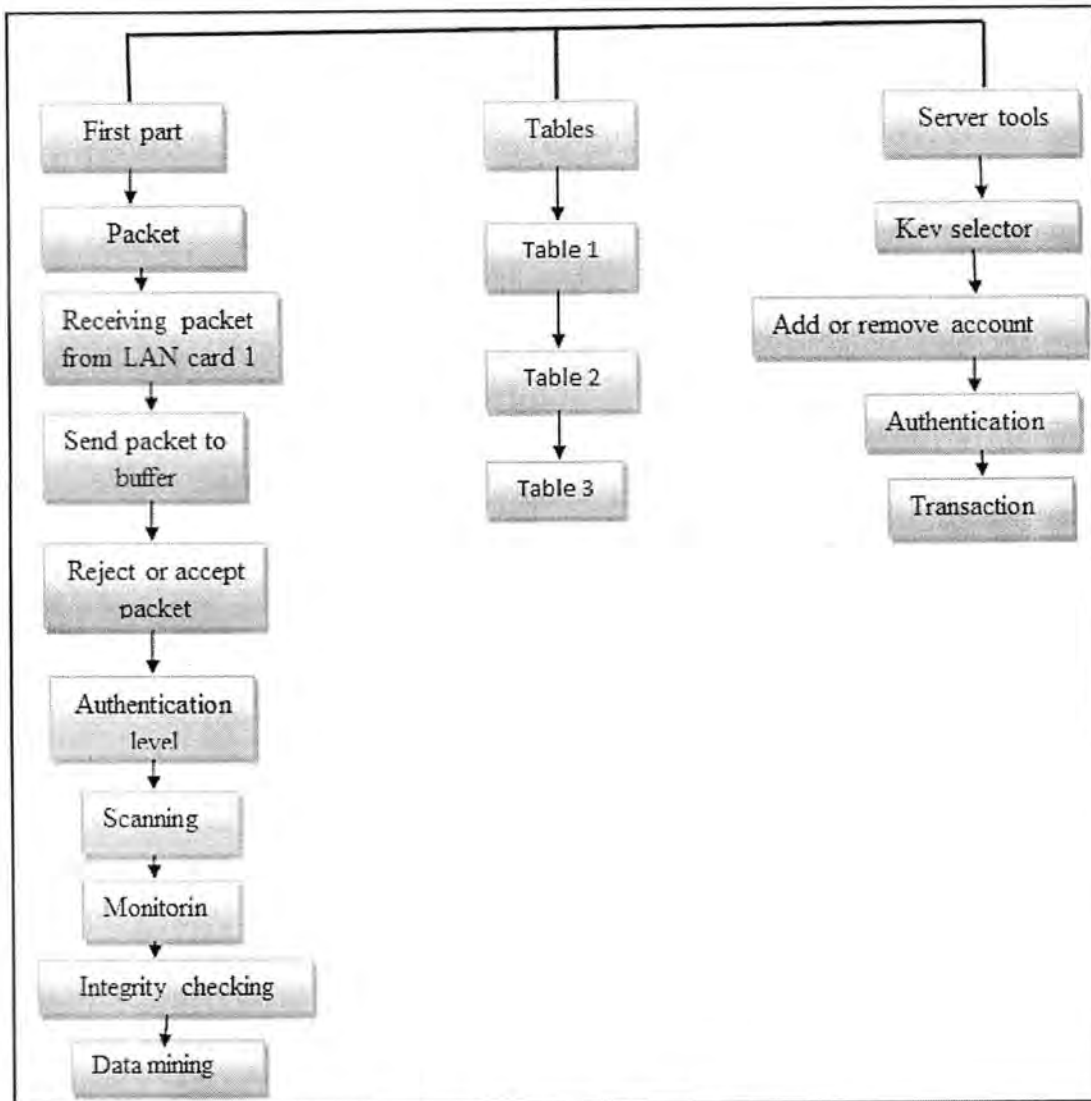


Figure 5: Block Diagram of System Parts



- Step 1: The user sends request to the system.
- Step 2: The server responses to user's request by receiving Special information to enter the system.
- Step 3: The user sends data.
- Step4: The server receives put data in buffer, open database of information about computers.
- Step5: the server loads IP, subnet mask, user name, password, and ports that permit to pass to protected network through the proposed system.
- Step6: listen to the port.

End.

#### RECEIVED PACKET FROM THE LAN CARD ALGORITHM:

- Step 1: Get packet from LAN card buffer.
- Step2: transfer the packet to specified buffer.
- Step 3: check the IP address sender.
- Step 4: check the IP address receiver.
- Step 5: check the user name and password.
- Step 6: if the user name and IPs are authorized then  
Send the packet to detection phase.  
If there is no malware then go to step 7.  
Else  
Close the connection and send message " Access is Denied"
- Step 7: send the packet to the second LAN card.

End.

#### CONCLUSIONS:

- 1) There is no perfect security method because always there are intruders and new types of different attacks and malicious code. But since all the attacks can be pass the proposed system as packets, so the proposed protection system aim to achieved by the denial of all incoming requests from unauthorized user to web server using ports that are scanned by the proposed program, and at the same time allowing authorized user's incoming requests.
- 2) Using the dual homed host architecture helped us increasing the protection, because it isolates the protected network from the internet and all traffic must pass through this host.
- 3) All types of security methods, in past, depend on packet capture processing. When we need to build any type of security we must process the packet of connection to make the security site work in the right place for this reason, we depend on packet filtering methods.
- 4) One of the major and the simple attack approaches from hacker computer is by trying several attempts to login in the system, the enhancement system control on this approach by making the authentication monitors, and count the number of the login attempts to distinguish the legal and illegal ones and then make a decision to block the system.
- 5) The proposed algorithm is implemented as a software in terminal devices by simplifying the process

operations and reducing the consumed time based on partitioning the block itself to achieve the task of multiprocessing and use a new technique of detecting viruses with data mining, because the cost of using hardware is expensive.

- 6) When we are using more than one technique of protection, this would minimize the probability of attack. Therefore, in our research we use authentication and detection viruses.

#### REFERENCES

- [1] Schuba C. L., "On the modeling, design, and implementation of firewall technology", Ph.D. thesis. Purdue university, December 2000.
- [2] William R. Cheswick and Steven M. Bellovin. "firewalls and internet security". At&T Bell laboratories, November 2005.
- [3] William F., Julia A., and Ed Stoner, "Deploying firewalls", paper. Carnegie Mellon University, May 2006.
- [4] McNulty F. L., "Security on The Internet", Associate Director For Computer Security National Institute of Standards and Technology U.S. Department of Commerce, Before the Subcommittee on Science, Space, and Technology U.S. House of Representative, March 22, 1994.
- [5] Killers B., "A new Generation of Antivirus Software offer Maximum Protection", Pc Magazine, February, 4(2), 2004. [www.Pcmag.mideast.com](http://www.Pcmag.mideast.com)
- [6] Cross M., "Security+ Study Guide and DVD Training System", Syngress Publishing, Inc., 2010.
- [7] Garfinkel S. & Eugene H. Spafford, "Web Security & Commerce", ISBN: 1-56592-269-7, 1<sup>st</sup> Edition, June 1997.
- [8] Stallings W., "Network Security Essentials: Application and Standards", Prentice Hall, 2002.
- [9] Diffie W. and Hellman M., "New Directions in Cryptography", IEEE Transactions on Information Theory, IT-22(6):644-654, 1976
- [10] Binnion R., Ltd T. D., "Network and Internet Security Issue and Solutions", Town send, Taphouse, 1999.
- [11] ZDNet Research center Business and Technology, White Papers, "Intrusion Detection-Deploying The Shomiti Century Tap", METAS, ZCInc.ZDNet. 2001. <http://WWW.ZDnet.com>.
- [12] Arnold W. and Tesauo G., "Automatically Generated Win32 Heuristic Virus Detection." In Virus Bulletin Conference, pp. 123-132, 2000.



## Modifying Steganography in Android Mobile Image Based on ECC Algorithm

Zainab Khyioon Abdalrdha and Mushtaq Talib Ajjah

Computer Science Department, University of Mustansiriyah

E-mail: [zainabkhyioon83@yahoo.com](mailto:zainabkhyioon83@yahoo.com)

### Article info

Received 5/4/2014

Accepted 30/11/2014

Keywords:  
Cryptography,  
ECC Algorithm,  
Steganography, and  
Android Operating  
System.

### ABSTRACT

Due to wide spread use of mobile phone and more available applications like internet and because internet is unsecure way of data transmission, Therefore , it is very necessary to protect the data especially sensitive data. One of the better ways to protect the data is using cryptography and steganography.

In this paper, we used steganography method that based on Least Significant Bit (LSB). The techniques that are optimized by XOR method, which increases the security of the text before being sent across the medium by hiding messages with in an image, and increases the confidentiality by using ECC (Elliptic Curve Cryptography) algorithm to provide cipher text that can be recovered. It was designed for color images which were sent by Viber,WhatsApp, and E-mail programs, so it will be difficult by unauthorized people to extract the original messages. The proposed approach is tested using different types of mobile types(Galaxy S3, Galaxy S4, and HTC).

### الخلاصة

أن الانتشار الواسع لاستعمال النقال وتوفر التطبيقات الكثيرة مثل الانترنت وبما أن الإنترنت هو طريقة غير آمنة لنقل البيانات لذلك أصبح من الضروري حماية البيانات خصوصا البيانات الحساسة. واحد من افضل الطرق في حماية البيانات هو استخدام التشفير والأخفاء.

أستعملنا في هذا البحث طريقة Steganography المعتمدة على تقنية البتات الأقل أهمية "LSB" المحسنة باستعمال طريقة XOR تزيد سرية وتعقيد الرسالة قبل الإرسال عن طريق إخفاءها في الصورة، وزيادة السرية باستعمال خوارزمية المنحنى الأهليجي (ECC) لتوفير نص مشفر يمكن استرجاعه. هذا النظام صمم للصور الملونة التي أرسلت عبر برامج البريد الإلكتروني والواتس اب والفايبر، أعطيت عمليات الإرسال هذه نتائج جيدة لم تتأثر نوعية الصورة بهذه العمليات. اختبر النظام المقترح على انواع مختلفة من الهواتف النقالة مثل جالكسي اكس 3 وجلكسي اس 4 و HTC.

### INTRODUCTION

The idea of Information Hiding can be traced back to a few thousand years ago. In many Competition environments, hide the presence of communication is desirable to avoid suspicion from adversaries [1]. They represent a class of operation used to embed data into different forms of media such as images, sound, or text. The embedded data should be invisible to any observer [2]. In the past few years there has been growing interest in ways to quickly hide the information with other information. The fact that an unspecified number of copies can be produced illegally, Led to a study of ways to embed copyright information hidden serial the preparation of audio and video data; the concern that privacy could be eroded led to the retransmission of unknown services systems, and techniques for making laptops difficult for a third party to track. Restrictions on some governments provide encryption to drive people to study and find ways to services for those who communicate secretly [3]. Hide information is technology include confidential information to data covering, make confidential information invisible or inaudible to any observer [4]. The cryptography and steganography both give the total security to a data or information, thus we need to apply both techniques to achieve essential security. There are number of ways can be done, but here we will concern

with methods of altering the information contained in such a way that the recipient can undo the alteration and discover the original data [5]. Steganography and cryptography are two related areas. Cryptography dissolves the message so it cannot be understood; As long as the secret key is unknown, so it cannot recover the original message. Steganography hides the message so that we cannot see them or detected [6].

### MOBILE TELEPHONE

Mobile phones or hand phone is a form of communication that relies on wireless connectivity through a network of distributed transmission towers inside secure area. The hand phones evolution has meant her to be not only a way voice communication [7]. However, they have begun be used as minimal computer machine to send and receive emails messages, designation, and surfing web. Also, the best developed and capable of capturing images that are compared with high- precision cameras. Hand phone have become a way to boost advertising, because of competition from the service provider to increase mobile phones, communication has become the price of using these telephone at high price and a wide range of human [8].

**CRYPTOGRAPHY**

Process of concealing information and the operation of camouflage it, is known as encryption. The encrypted original text is called the cipher text and a collection of rules used to encrypt information from the ordinary is encryption algorithm. Usually run this algorithm based on the key of encryption, which is a contribution to the algorithm along with the letter. In order to enable the receiver to get the letter of the cryptogram there has a decryption algorithm which, when used with the suitable key of decryption, return the original text of the cipher text [9]. The cipher system is shown in figure (1).

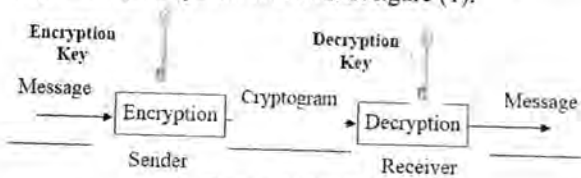


Figure 1: Cipher System

The encryption is the best effective way to accomplish security of data means. Encryption method hides the contents of the original letter can be retrieved through the decryption method [10]. The primary purpose from encryption is to prevent unauthorized from seeing or modify data. Algorithms depend on key use key to encrypt the letter. There are two general categories depend on encryption key :

**symmetric encryption** which work with a single key to encryption and decryption the letter, and **asymmetric encryption** which work with two contrast keys: two public and private keys one for encoding letter, and other for decoding it [11]. In this paper we encryption using Elliptic Curve cryptography is asymmetric encryption which depends on the complication of elliptic curve distinct logarithm of its safety. Elliptic curve cryptography (ECC) is a method to asymmetric encryption depends on the fatalistic framework from elliptic of curves over finite fields [12]. ECC delivers very high force per bit of any known common-key system because of the complication difficult problem, (Elliptic Curve distinct logarithm Problem (ECDLP)), which means that littler key sizes produce equivalent standard from security [13]. Elliptic Curve Cryptography (ECC) works to use of variables and parameters in elliptic curve only limited elements of finites fields. To introduce the principle of attracting ECC compared with RSA is that it shows seems to be equal to the size of the security bit is much smaller, and thus reduces Processing overhead. On the other hand, despite the fact that ECC theory about for some time, it is too soon begun to show products and there was sustained interest in the investigation of the encryption weakness [14].

One family elliptic of curves uses in cryptographic applications: Primes curves on  $R_q$ . For Prime of the curve on the  $R_q$ . We are using a cube the equation that all changes and parameters take the values the scope of valid numbers as of 0 to  $q-1$ ,

The calculations are performed with respect to modulo  $q$  [15]. The computations of the ECC are defined over the elliptic curve Equation (1).

$$y^2 \text{ mod } p = x^3 + ax + b \text{ mod } p \dots\dots (1)$$

Where:

$a, b, x,$  and  $y$  are the real numbers, the elliptic curve changes with various choices of  $a$  and  $b$ .

Can prove that the Abelian group is limited and can be defined based on the equation group  $E_q(a,b)$  provided  $x^3 + ax + b \text{ mod } q$  which has no recurrent factors that is equivalent to the condition.

$$4a^3 + 27b^2 \text{ mod } p \neq 0 \text{ mod } p \dots\dots (2)$$

Where:

$4a^3 + 27b^2 \text{ mod } p \neq 0 \text{ mod } p$  each value of "a" & "b" give a dissimilar elliptic curve. Every point  $(x, y)$  that meets on top of equation plus point in infinity lie on the elliptic curve [15].

**MATHEMATICAL PROCESSES IN ELLIPTIC CURVE CRYPTOSYSTEM**

Addition rules over  $E_q(a,b)$ , Agree with algebraic technique described elliptic curves specified on the real numbers. For all the points of  $P, Q \in E_p(a, b)$  [14]:

1.  $P+Q=P$ .
2. If  $P=(X_p, Y_p)$  then  $p+(X_p, -Y_p)=O$ . Then point  $(X_p, -Y_p)$  is negative of  $p$ , denoted as  $-p$ .
3. If  $p=(x_p, y_p)$  and  $Q=(x_q, y_q)$  with  $p \neq Q$ , then  $R=P+Q=(x_r, y_r)$  is

Determined by the following rules:

$$X_R = (\lambda^2 - X_p - X_q) \text{ mod } p$$

$$Y_R = (\lambda (X_p - X_R) - Y_p) \text{ mod } p$$

Where:  $\lambda = \left( \frac{Y_q - Y_p}{X_q - X_p} \right) \text{ Mod } p$  if  $P \neq Q$

And

$$\lambda = \left( \frac{3X_p^2 + a}{2Y_p} \right) \text{ Mod } p$$
 if  $P = Q$

4. Multiplication is defined as repeated addition; for example,  $4P=P + P + P + P$ .

This paper describes the logical design of the proposed system through presenting the ECC algorithm, which will be implemented by encrypting text then hiding it with in an image of mobile depending on android operating system.

**STEGANOGRAPHY**

Steganography is derived from two words "Steganos" and "Graphia" means "covered" or "hidden" and "written" respectively (16). The main purpose of this technique is using for hiding data in a cover media therefore data is undetectable by anyone else. The simple implementation method of this technique is use to hide text data in cover image file. The cover media for a steganography technique can be

a text, audio, image or video. Mostly text steganography is not used as it contributes in increasing the difficulty level of detecting of hidden bits, while text cover data offers smaller memory occupation and is simpler to communicate [17].

Steganography add another layer of secrecy **undetectability** over cryptography **confidentiality** (18). The individuals can not notice the presence of confidential information if steganography is used, while they can observe the encoded secret information if cryptography is used [19]. Three factors were used in design method of steganography: perceptual robustness, transparency, and the ability to hide. These requisites are known as “magic triangle” and contradictory [20].

Primary objectives to hide information are transparency, transparency perception. Therefore, the methods of concealment of information, If someone knows there are parts of the hidden information can be easily draws. The main difference among steganography from other methods of hiding exchanged information. In cryptography, human can be conscious of the presence of the information mode note encrypted information, even though it will not be able to understand the information. However, but in the hide, the information will be invisible and cannot be observed from anyone [21]. In history, the Greeks wrote the text on the tablets enclosed with wax to conceal information .Another was an innovative method for shaving chief of an apostle and tattoos a letter or picture on the apostle’s head. After the hair has grown again, the letter undetected even have been shaved his head again. In the electronic era, is increased incentive to hide message excreted in the field of various multimedia, and secure communication over the Internet [22].

Steganography different from cryptography in the feel that that wherever concentrates cryptography to keep secret of message contents, steganography focused on maintaining a secret message. Each of steganography and coding is a way to safeguard the information as of unauthorized persons, but technology alone is not ideal, so need to can be unwound. Once revealed the existence of hidden information, and defeated the purpose of concealing information partially [23].

The power of steganography can amplify through a combination of it with encryption. A basic model for steganography as offer in Figure (2), consists of the following [24, 25]:



Figure 2: The basic model to hide

- Cover file (Carrier): is the original file that an integral part of the secret message required. It is known as host file.
- Payload (Secret Message): Message is a secret that should be an integral part of the inside cover of a file in a specific steganography model. Load can be text, sound, image [26].
- Stego file (stego-object): is obtained on end file after load included to cover a particular file..
- Stegokey: is the key that might use to code of confidential information for additional level of safety.

## ANDROID OPERATION SYSTEM

Android is operating system open source of mobile using for all phones and devices that contain personal computers. Factory can be used a telephone Android if followed the Convention on which came in the field of software development Kit. There are no limitations or conditions on the manufacturers of the telephone company for the exchange their extensions with anyone else, as there are in of other

open source programs, and if the departure of the Linux kernel as it is. The Linux kernel is under various authorization and more restrictions from Android. Android is a software an environment the hardware a platform, which Contains the operating system, and was built on Linux kernel running on the host-based Dalvik default machine system. Running Dalvik default machine Android apps cases the virtual machine instances. Android has a rich user interface, the application window, the Java class libraries, and multimedia support. Android also comes with an built-in communication applications such short message service job features (messages); Android software environment is shown in figure (3) [27].



Figure 3: Android Software Environment

## RELATED WORK

**1. Kaisa Nyberg, [2004][28].** The aim of this paper is for discussing the design strategies to cryptographic algorithms and at the third-generation of cellular networks. Particularly, he considers how to address the problems found in the design of GSM 3GPP specifications of the Universal Mobile Telecommunications System (UMTS) networks.

**2.Ritesh Pratap Singh, etal, [2010][29].** In the present paper, the expansion in the mobile phone use, and the added advantage of telecommunications companies Such as MMS (multi) media the message service to lure more customers.

## AIM OF THIS WORK

The aim of this work is to increase the information that will be transported through the mobile application through to hide information and coding together in order to hide the text in the image using the mobile Android operating system for building security software. Using ECC algorithm to encrypt text Security will provide

information in motion picture and documentation to the sender to hide the text in the image depending on the source Android operating system.

**THE PROPOSED APPROACH**

This section illustrates the proposed Approach of the system.

**THE PROPOSED APPROACH ALGORITHM TO HIDE INFORMATION**

This section illustrates the Proposed Approach Algorithm to hide information for approach. It is shown in algorithm (1).

<p><b>Input:</b> Message (Plain text)  <b>Output:</b> Cipher text hidden in an Image</p>
<p>Process:  <b>Step1:</b> Enter the text  <b>Step2:</b> Encryption text using ECC algorithm.  <b>Step3:</b> The result from encryption operation is then embedded in the image using XOR method then Perform XOR operation on bits stored at part alpha location in pixel  <b>Step4:</b> Save image after embedding the cipher text in image.  <b>Step5:</b> send image over commutation channel e.g. (viber,yahoo mail or web site).  <b>Step6:</b> The message receivers apply operation decryption of the message.  <b>Step7:</b> Extract the result from the image saved in embedding operation that the cipher text uses XOR operation and information hidden is executed from image.  <b>Step8:</b> After extracting cipher text from image, decryption operation using ECC algorithm starts working.  <b>Step7:</b> The result of decrypting is a plaintext  <b>Step8:</b> End.</p>

Algorithm 1: The Proposed Approach Algorithm to hide information

**THE PROPOSED ALGORITHM TO ENCRYPT A TEXT**

In this stage the entered text will be encrypted using ECC algorithm. The ECC encryption can be used in a wide range of applications, involving the security of the network, ECC is a public-key encryption and security of ECC based on the difficulty in finding value of R for given value of Rp, the parameters of elliptic curve schemes encryption here are carefully chosen in order to resist all attacks known of Elliptic Curve Discrete Logarithmic Problem. Each character in the message space is mapped onto two different points on the elliptic curve. Moreover, s is different for different characters. With this the same character of the message space is mapped for various characters in the codes space. In this paper we used ECC Algorithm to encryption message.

**THE PROPOSED XOR METHOD TO HIDE A TEXT**

XOR is operator very common ingredient in more complex ciphers. In itself, using a constant repeating key, a simple XOR codes can trivially be broken by using hesitate analyze. If the content of any message can be guessed or otherwise known then the key can be detect. In steganography the hidden information is important,

Steganography is to conceal the message in such a method that no one but the sender and the receiver knows of the survival of the letter. An approach is different from the encoder, which aims to make the information not readable. The embedding process is achieved by converting cipher text "the result of encryption operation" to binary and then using password (As the key to the way XOR) and repeat the password on the length of the cipher text. XOR method test of cipher text and then decides 0 or 1 to be an integral part. XOR is known as 'Exclusive-OR' and it is a bitwise operator from binary mathematics. Uses operator XOR for "flip" bits (zeroes and ones) in a piece of regular text to create a encrypted text. Return XOR operators (1) when the value of either the bit the first or second bit is (1). The XOR operators return (0) when either or both of the bits are (1).

The XOR operator is a very common ingredient in more complex ciphers. A simple repetition XOR codes is therefore sometimes used to hide information. Eventual embedding starts by embedding the result from XOR operation into the image and beginning from location 100 of pixel by using Least Significant Bit (LSB). LSB inclusion is a combined and easy way to embed information in the lid photo in the sequence. The message stored in the LSB is pixel of the RGB value.

The main difference of the proposed code is the fact that data is now one dimensional array of integer. One integer from this array is associated with each pixel. This integer is 32 bits wide, so it has the capacity to hold the 8-bit red, green and blue components of a pixel value. The remaining 8 bits are used for the alpha component, which represents pixel transparency, and this part of alpha is used to hide information inside the proposed system. The ordering of red, green, blue and alpha is shown in Figure (4).

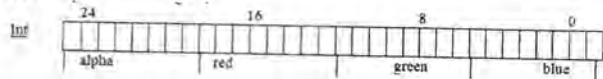


Figure 4: Red, Green, Blue and Alpha Values of Digital Image

**EXPERIMENTAL WORK**

Each step in algorithm (1) Will be shown in the following example the main interface of the proposed system contains two parts (Encryption & Hidden Information, Decryption) as shown in figure (5).



Figure 5: the Main Interface of the Proposed System

**Step1:** Choosing the Encryption & Hidden Information will appear interface that include ECC algorithm as shown in figure (6).



Figure 6: The Main Interface of Encryption & Hidden Information

**Step 2:** The message is "AL- Mustansiriyah University will evaluate scientific conference in 10/4/2014" is entered using ECC algorithm and the result of encryption of message is

"]7f@?>4U^b7c=[2@e>?8IH\_9Ce@;?B\_>UF=b@Ua@Hc;8CCg]e]MVAXFZcS\_eTFgUh[ha<;A5?QNEACWGGC\\_J4^egYN7=L]ZMULAFB2AR^RCLWT4@^PZ5g>666GXeWIU@AQ];aU7TC\@c^VIZaCQSEP>AT?ET", the Cipher text is illustrated in Figure (7).



Figure 7: Encryption of Message Using ECC Algorithm

**Step 3:** choosing hide information to hide the message that encrypted by ECC Algorithm, and then choosing a picture Gallery then Hiding message by XOR Method then save picture, as illustrated in Figure (8).

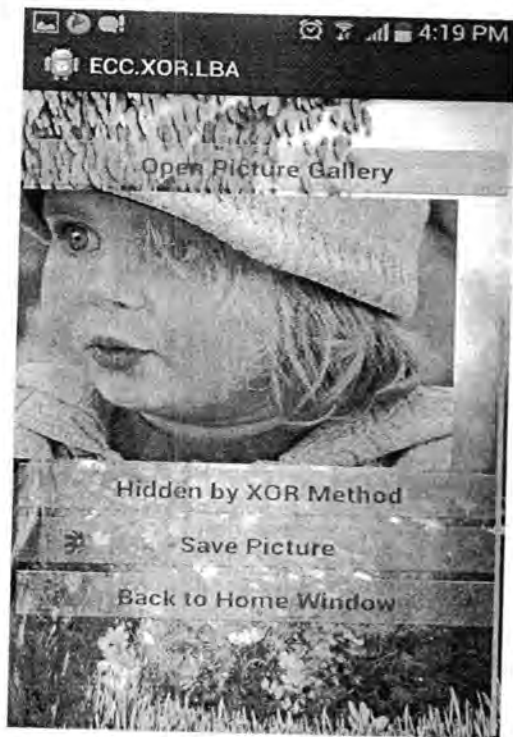


Figure 8: Load the Image

**Step 5:** After accessing the message, the receiver will make decryption on the message by clicking on “back to Home window”, then open picture and upload the picture that hide the message then clicking on “Extract info from picture”, the result of Extract is illustrated in Figure (9).



Figure 9: Decryption using ECC Algorithm

**Step 7:** End.

### EXPERIMENT TEXT OF THE PROPOSED SYSTEM

This section illustrates the results that obtained by executing the proposed system, and its testing results using PSNR and MSE. The tests were applied to color images with format (BMP) and size (256\*256) to select the highest (PSNR) value with its minimum value of (MSE). For all the experiments presented the following tables compare the maximum PSNR and minimum MSE of ECC algorithm of the proposed system. As shown in figures (10) & (11) the images before embedding text and after embedding a text.



The result of test, after apply encryption on a text using ECC algorithm and embedding the text in the image, found that the image cover child, and Lena are the best using the image format (Bmp) as shown in table (1).

Table 1: Values of PSNR and MSE after Using Algorithm of BMP Images

	PSNR Value	MSE Value
Image Cover	ECC Algorithm	ECC Algorithm
Apple	54.0445	2.1148
Child	62.0242	0.1445
Lena	61.1834	0.1356
Horses	55.7725	3.1436

### CONCLUSIONS

1. This paper presents a method of encrypting messages of mobile in the android operating system environment using ECC algorithm.
2. ECC algorithm is a public key encryption system, which is safe for the much smaller size of the key. Which reduces processing overhead, and the analysis and description in this paper has vast significance.
3. This paper gives a brief description and analysis of ECC encryption and availability some help in improving the coding systems for network security.
4. This proposed system can be used in all types of JAVA enabled mobile devices that is compatible with any type of mobile phone, and tablet devices that use Android operating system.
5. Hiding the text into the image using LSB technique with the help of XOR operation gives more security and complexity

6. The approach is compatible with any type of mobile phone that uses Android operating system.
7. Using steganography and cryptography together provides strong security and invisible communication.
8. From experimental results, it was seen that the proposed method is effective because the result for PSNR and MSE, and no difference is found Among the original photo and the stego image when ECC algorithm is used.

## REFERENCES

1. Min's, "Multimedia Data Hiding", Ph. D.Thesis. Dissertation, Princeton University, April 2001.
2. Bender W., Gruhal D., Morimoto N. and A.L.U. , "Techniques for Data Hiding", IBM System Journal, 35, (3 &4), 1996.
3. Richard P., "An Analysis of Steganographic Techniques", Dept. of Computer Science and Software Engineering, Faculty of Automatics and Computer, University of Politehnica, Timisoara,1998.
4. InoueS., MakinoK. and TakizawaO., "A proposal on Information Hiding Methods using XML", Yokohama National University2001. <[http://www.takizawa.ne.jp/nlp\\_xml.pdf](http://www.takizawa.ne.jp/nlp_xml.pdf)>
5. Samir K. and Somaditya R., "Information Security through Data Encryption and Data Hiding", International Journal of Computer Applications (0975 – 8887),4,(12), August 2010.
6. Samer A. ,"A New Steganographic Algorithm for Hiding A Plain Text in Gray Images Using Blocks", Information Technology & National Security Conference, 2007.
7. Roceanu I., "Knowledge Anywhere, Anytime Based on the Wireless Devices" in Proceedings of the 5th Scientific Conference eLearning and Software for Education, Bucharest: 68-72, 2009.
8. Schiffman J., Zhang X., Gibbs S., Kunjithapa A., and Jeong S., "Securing Elastic Applications on Mobile Devices for Cloud Computing" in *ACM Cloud Computing Security Workshop*, USA,:127-134, 2009.
9. Kumar M. and Lal S., "A Cryptographic study of some digital signature scheme", Ph.D.Thesis, Formerly Agera University, 2003.
10. Piper F. and Murphy S., "Cryptography: A very short introduction", Oxford university press, 2002. [http://www.PJoks24x7.com/Referenceware\\_for\\_professionals.htm](http://www.PJoks24x7.com/Referenceware_for_professionals.htm).
11. Wikipedia, "Encryption", <http://en.wikipedia.org/wiki/Encryption>, modified on 13December 2006.
12. Martin Leslie," Elliptic Curve Cryptography", paper , June 5, 2006.
13. McLeman C. , " Hyper elliptic Curves ", 2001 , A Whitepaper available at <http://Crypto.Math.Hmc.edu/>
14. William Stallings," Cryptography and Network Security Principles and Practices", Fourth Edition, Prentice Hall,2005.
15. William Stallings," Cryptography and Network Security Principles and Practices", fifty Edition, Prentice Hall ,2011.
16. HoffsteinJ., Lieman D., Silverman J. " Polynomial Rings and Efficient Public KeyAuthentication", Proceeding of the International Workshop on Cryptographic Techniques and E-Commerce (CrypTEC '99), M. Blum and C.H. Lee, eds., City University of Hong Kong Press,1999.
17. Cox I. J., et al. "Digital Watermarking and Steganography", 2<sup>nd</sup> Edition, Morgan Kaufmann Publishers, Elsevier Inc.(2008).
18. Shirali- Shahreza M. H. and Shirali- Shahreza M., "A New Approach to Persian/Arabic Text Steganography", 5th IEEE/ACIS International Conference on Computer and Information Science, 310- 315. (2006)
19. Bohme R. "Advanced Statistical Steganalysis", Springer-Verlag, Berlin, 2010.
20. CvejicN., Algorithms for Audio Watermarking and Steganography. Finland: Oulu University Press, 2004.
21. JudgeJ. C., "Steganography: Past, Present, Future", SANS white paper, 2001. URL: <http://www.sans.org/rr/papers/index.php?id=552>, last visited: 31 March 2008.
22. Ahmed Ch.," Steno Encrypted Message in Any Language for Network Communication Using Quadratic Method", Journal of Computer Science 6 (3): 320-322, 2010 ISSN 1549-3636 © 2010 Science Publications.
23. Wang H.& Wang S., "Cyber warfare: Steganography vs. Steganalysis", Communications of the ACM, 47:10, October 2004.
24. seddik A. H.," Enhancing the (MSLDIP) Image steganographic method (ESLDIP Method) ", International Conference on Graphicand Image Processing (ICGIP 2011), Proc. of SPIE 8285, 82853I, © 2011 SPIE.
25. Abdul A. I., "Hiding Data Using LSB - 3", J.Basrah Researches (Sciences), 33, (4), (81-88), December, 2007.
26. Swain, G. and Lenka, S. K., "A Novel Approach to RGB Channel Based Image Steganography Technique ", International Arab Journal of e-Technology, 2, (4), June 2012.
27. Android. "What is Android " <http://developer.android.com/guide/basics/what-isandroid.html>, retrieved March 4, 2010.
28. Kaisa Nyberg , Cryptographic Algorithms for UMTS, 2004.
29. Ritesh Pratap Singh, Mohd. AftabAlam Khan, Mehwash Khan, and Neha Singh," Spread Spectrum Image Steganography in Multimedia Messaging Service of Mobile Phones", International Journal of Electronics Engineering, 2 (2), 2010, pp. 365 – 369.





## Detecting Cancer Cells of Mammographic Images Based on Top-Hat Transformation

Layla Hussein

Al-Mustensiriyh University, College of Science, Department of Computer Science.

E-mail:laylahussain.abaas@yahoo.com

### Article info

Received 22/10/2011

Accepted 11/1/2015

### ABSTRACT

Mammography breast cancer images assist detecting disease caused by cells normal growth and have the ability physicians. Software use to analyze these images may also use for assist physicians in their daily Mathematical Morphology is a theory which provides a number of useful tools for image analysis. In our proposed approach the Top-Hat transform is used to extract cancer cells from Mammography breast cancer images. Top-Hat transformation operated in morphology which is used for extracting small or narrow, bright or dark features in an image. This paper have been proposed an approach to extract cancer cells by using Top-Hat filtering with circular structuring element with different diameter (10, 20, 30, 40, and 50). This approach applies on three different mammography cancer images with properties. Image 1 Type: JPEG Image Size: 556200 bytes Class: unit 8 Dimension: 618px\*300px x3. Image 2 Type: JPEG Image Size: 283500 bytes Class: unit 8 Dimensions: 350px \* 270 px x33- image 3 Type: JPEG Image Size: 359976 bytes Class: unit 8 Dimensions: 424px \* 283 px x3. The experimental results show how the different in circular structuring element are affected extracting the cancer cells of images. And we applied some post-processing after top-hat filtering by using an adaptive mask to enhance the resultant images.

### الخلاصة

صور السرطان المأخوذة بجهاز Mammography تساعد الاطباء في اكتشاف المرض الناتج عن خلايا ذات نمو طبيعي. ان البرامجيات المستعملة في تحليل هذه الصور يمكن ايضا ان تستعمل في التشخيص الطبي في وقتنا الحالي. التشكل الرياضي هو نظرية تجهز عدد من الادوات المفيدة لتحليل الصور. في بحثنا المقترح استعمل تحويل Top-Hat الذي يعمل في علم التشكل على تحديد الخلايا السرطانية في الصور وتحديد التفاصيل الصغيرة او الضيقة في الصورة. في هذا البحث استخدمت طريقة لتحديد الخلايا السرطانية في الصور الناتجة من جهاز Mammography باستعمال تحويل Top-Hat على صور ملونة unit 8 Image 1 Type: JPEG Image Size: 556200 bytes Class: unit 8 dimension :618px\*300px x3. Image 2 Type: JPEG Image Size: 283500 bytes Class: unit 8 px x33- image 3 Type: JPEG Image Size: 359976 bytes Class: Dimensions: 350px \* 270 unit 8 Dimensions: مع اطوال مختلفة الاقطار SE والسبب باستعمال اقطار مختلفة ل SE هو الوصول الى كل متجاورات عناصر الصورة. اظهرت النتائج التجريبية كيف ان الاقطار المختلفة تؤثر على تحديد الخلايا السرطانية في الصور. استعمل مرشح لتحسين الصور الناتجة من تطبيق تحويل Top-Hat.

### INTRODUCTION

The most common diseases which affect men and women around the world is cancer and it especially a concern in women. According to the statistics this cancer is one of the major causes for the increase in among middle-aged women in both developed and developing countries the etiologies of this cancer are unknown and no single dominant cause has emerged. Still, the way of preventing of breast cancer no known. The treatment of this cancer can be easily if it early detection before it is spread to other parts of the body. Moreover a very important role to reducing the morbidity and mortality rates to the detection of breast cancer [1,2].

Breast imaging modality has been known X-ray mammography due to its simplicity, portability and cost effectiveness and it is the most effective and economical, an important source of radiological information of breast imaging is the presence and distribution of micro

calcifications in the breast, this anatomical information can be obtained with high resolution technology using X-rays, as yet there is no comprehensive imaging modality for all radiological applications and needs, although the ability to computerize and analyze medical images provides a powerful means to assist physicians thus computer programs, processing methods that get the data and information from medical imaging scanners must be carefully used [3].

The language of mathematical morphology is set theory. Such as; morphology offers a unified and powerful approach to numerous images. In image processing, mathematical morphology is a means of identifying and extracting meaning image. Descriptors based on properties of form or shape within the image [4]. Morphological operations apply a structuring element to an input image then creating on output image with the

same size. In a morphological operation, the value of each pixel in the output image is based on a comparison of the corresponding pixel in the input (original) image with its neighbors. By choosing the size and shape of the neighborhood, a morphological operation can be constructed that is sensitive to specific shapes in the input image [5]. Two morphological operations are the dilation and erosion. Mathematical morphology (MM) is a theory devised for the shape analysis of objects and functions. MM operators treat the processed image as the set and are made of two parts: a reference shape called the structuring element (SE) or function that is translated and compared with the original function all over the plane and a mechanism that details how to carry out the comparison [6].

**1- Structuring Elements and Neighborhoods**

A structuring element is a rectangular array of pixels containing the values either 1 or 0. A number of example structuring elements are depicted in Figure (1). Structuring elements have a designated centre pixel. This is located at the true centre pixel when both dimensions are odd (e.g. in 3-3 or 5-5 structuring elements). When either dimension is even, the centre pixel is chosen to be that pixel north, north-west or west (i.e. above and/or to the left) of the geometric centre (thus, a 4-3, 3-4 and a 4-4 structuring element would all have centre pixels at location [2,2]). The centre pixel of the structuring element being placed directly above the pixel under consideration in the image, then the neighborhood of that pixel is determined by those pixels which lie underneath those pixels having value 1 in the structuring element. This is illustrated in Figure (2). In general, structuring elements may consist of ones and zeros so as to define any neighborhoods, but the practicalities of digital image processing mean that they must be padded with zeros in an appropriate fashion to make them rectangular in shape overall. The most art in morphological processing is to choose the structuring element so as to suit the particular application or aim. In Figure (2) there are some examples of morphological structuring elements. The centre pixel of each structuring element is shaded the local neighborhoods defined by a structuring element. This is given by those shaded structuring element would all have centre pixels at location [2, 2] [4].

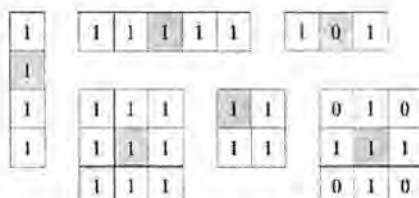


Figure 1: Some Examples of Morphological Structuring Elements; The Centre Pixel of each Structuring Element is Shaded [4]

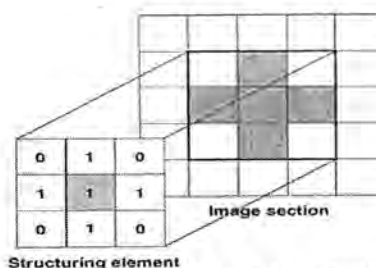


Figure 2: The Local Neighborhood Defined by a Structuring Element [4]

In this paper we can use top-hat transformation to Extract Cancer Cells of Mammographic Images [7]. detected the intensity values of the scale-specific features of the image using multi-scale top-hat transformation are modified for achieving local contrast enhancement [8]. They implemented six efficient digital mammogram enhancement algorithms based on wavelet transformed top-hat filtering. Ritika and Sandeep [9] performed morphological contrast enhancement using the white and black top-hat transformation and they used structuring element of various shapes and sizes [10]. Application and software computer processing algorithms, application and software intelligently, that is why we proposed an application used on math lab software to detect cancer in mammogram breast cancer images.

**2-Erosion and Dilation**

In image processing, mathematical morphology has been used is usually used as a tool to extract image components that are useful in the representation and description of region shape [4]. Erosion and dilation are fundamental operations of morphological processing. Before we discuss the erosion and dilation processing, we will briefly introduce the definitions of them.

**A-Erosion**

To perform erosion of a binary image, the center pixel of the structuring element successively placed on each foreground pixel (value 1). If any of the neighborhood pixels are background pixels (value 0), then the foreground pixel is switched to background. Formally, the erosion of image A by structuring element B is denoted [4]:

$$\text{Erosion} = A \ominus B \dots (1)$$

One of the simplest uses of erosion is to eliminate irrelevant detail (in terms of size) from a binary image [4]. In order to eliminate the white areas as many as possible except the large one, the object, eroded the image with a structuring element of a size somewhat smaller than the objects wished to keep.

**B-Dilation**

To perform dilation of a binary image, successively placed the center pixel of the structuring element on each background pixel. If any of the neighborhood pixels are foreground pixels (value 1), then the background pixel is switched to foreground. Formally, the dilation of image A by structuring element B is denoted [11]:

$$\text{Dilation} = A \oplus B \dots (2)$$

One of the simplest applications of dilation is bridging gaps.

Clearly, the erosion operation can eliminate the irrelevant detail from the binary image, and the dilation operation is good to retrieve the original image [11].

### 3- Morphological Operations

On initial consideration of the morphological operations, it is not easy to see how the opening and closing can be useful or indeed why they differ from one another in their effect on an image. After all, erosion and dilation are logical opposites; and superficial consideration would tempt to conclude that it will make little practical difference and which one is used first? However, their different effects stems from two simple facts .Grey-scale opening and closing are defined in exactly the same way as for binary images and their effect on images is also complementary. Grey-scale opening (erosion followed by dilation) tends to suppress small bright regions in the image whilst leaving the rest of the image relatively unchanged, whereas closing (dilation followed by erosion) tends to suppress small dark regions [12].

#### A-Opening Operation

Opening is the name given to the morphological operation of erosion followed by dilation with the same structuring element. The opening operation of A by structuring element B can be written as [13]:

$$A \circ B = (A \ominus B) \oplus B \dots (3)$$

The general effect of opening is to remove small, isolated objects from the foreground of an image, placing them in the background. It tends to smooth the contour of a binary object and breaks narrow joining regions in an object.

#### B-Closing Operation

Closing is the name given to the morphological operation of dilation followed by erosion with the same structuring element. The closing operation of A by structuring element B as [14]:

$$A \cdot B = (A \oplus B) \ominus B \dots (4)$$

Closing tends to remove small holes in the foreground, changing small regions of background into foreground. It tends to join narrow isthmuses between objects.

### 4- The Top-Hat Transformation

The Top-Hat transformation is a very useful tool to extract features less the structuring element chosen from the processed image. The top-hat transformation is defined as the difference between the image and the image after opening with structuring element B [14]:

$$\text{Top - Hat Trans.} = I - I \ominus B \dots (5)$$

Opening has the general effect of removing small light details in the image whilst leaving darker regions undisturbed. The difference between original and the opened image, thus, tends to lift out the local details of the image independently of the intensity variation of the image as a whole. For this reason, the top-hat transformation is useful for uncovering detail which is rendered invisible by illumination or shading variation over the image as a whole [14].

### Error Metrics

Two of the error metrics used to compare various image compression techniques which are the Peak Signal to Noise Ratio (PSNR) and maximum error. The Max error is a cumulative error between the compressed and the original image, whereas PSNR is a measure of the peak error. The mathematical formula is [13]:

$$\text{MSE} = \frac{1}{MN} \sum_{y=0}^{M-1} \sum_{x=0}^{N-1} [I(x,y) - I'(x,y)]^2 \dots (6)$$

$$\text{PSNR} = 10 \log_{10} \frac{(I-1)^2}{\sqrt{\text{MSE}}} \dots (7)$$

Where:  $I(x, y)$  is the original image,  $I'(x, y)$  is the approximate diversion (which is actually the decompressed image) and  $MN$  are the dimensions of the images.

### The Proposed Approach

In this paper an approach has proposed based on Top-Hat transformation applied on color images. Detecting cancer cells from an image one application of these transforms is in using a structuring element in the opening and closing. The difference then yields an image with the detecting cancer cell .I the white top-hat transform of input image is given by:

$$T_1 = I - (I \circ B) \dots (6)$$

While the bottom-hat transform of input image I is given by:

$$T_2 = (I \cdot B) - I \dots (7)$$

Where "I" means the input image and "B" is the structure element. " $T_1$ " Shows the top-hat transform output and " $T_2$ " shows output bottom-hat transform. Also, " $\circ$ " denotes the opening operation and " $\cdot$ " denotes closing operation.

An important use of top-hat transformation is in detecting cancer cells. In our suggested approach we use top hat transformation using circular structuring element with various diameters values to remove the non-uniform background illumination from an image.

The suggested approach algorithm steps are:

- 1- Take the color image
- 2-Apply the circular structuring element with different diameter values.
- 3-To perform the top hat transformation and display the image.
- 4-Use image adjust to extract cancer cells of the result.

### RESULTS AND DISCUSSION

The proposed method was evaluated by using of the MATLAB software. This work using circular structuring element (SE) with different diameters values using to extraction cancer cells of mammographic images based on Top-Hat transformation means of an open top-hat morphological operation. The proposed algorithm effectiveness was evaluated by comparing the input image with the recovered image. These evaluations depend on PSNR and MR criteria between these two images. The important parameters considered are the circular structuring element with different diameters obtained cancer cell .Other variables shown in the Table1. Figure

(3) illustrates the Top-Hat to increase the local image detail with increase the diameter length of SE. Also we can see from Fig.3 a, and e the output of Top-Hat need to make some post-processing to enhance and detect cancer cells brightness, therefore, we used the adaptive mask called contrast mask (see Figure. 1a and e). The coefficient of this mask is  $\begin{bmatrix} 0.1 & 0.3 \\ 0.1 & 0.3 \end{bmatrix}$ .

Also we applied Top-Hat transform on three different mammography cancer images with properties

1-Image 1 Type: JPEG image size: 556200 bytes class: unit 8 dimension: 618\*300 pixels

2-Image 2 Type: JPEG image size: 283500 bytes class: unit 8 dimension: 350\*270 pixels

3-Image 3 Type: JPEG image size: 359976 bytes class: unit 8 dimension: 424\*283 pixels

Fig 4 showing the results of image 2 and fig 5 showing the results of image 3.

### Conclusions and Future work

In our suggested approach the size of the structuring element are calculated and used to detect the cancer cells from different mammography color images. Calculating the SE size automatically applied with different mammography images to be processed. Further development of the method will demand obtaining more exact criteria PSNR and Max.Error as well as a thorough evaluation of the possible effects of noise. PSNR values proportional with SE length when the SE length increase PSNR values are increased too. Also, the effects of parameters like lengths of SE (when the SE length increase MR values are decreased). Our suggested method need to post processing therefore an adaptive mask to enhance the results after applied top-hat transformation is suggested. Experimental results show that the suggested method is simple and effective, which makes the extraction the cancer cells from different mammography

images. The extraction cancer cell regions from the given image are highlighted in the final output of the image. The proposed system can be extended for some other modality of images like CT and for different parts of human such as brain and this proposed method can be it application in the Medical field and other research areas.

Table 1: circular structuring element with different diameter values for Cancer of Mammographic image.

Circular structuring element of diameter	Image 1		Image 2		Image 3	
	PSNR (dB)	Max Error	PSNR (dB)	Max Error	PSNR (dB)	Max Error
10	12	228	10.9	221	11.9	225
20	12.7	205	11.4	215	12.7	219
30	13.6	172	11.7	215	13.2	203
40	14.7	119	11.8	214	13.6	197
50	15.5	103	12.1	211	14	186

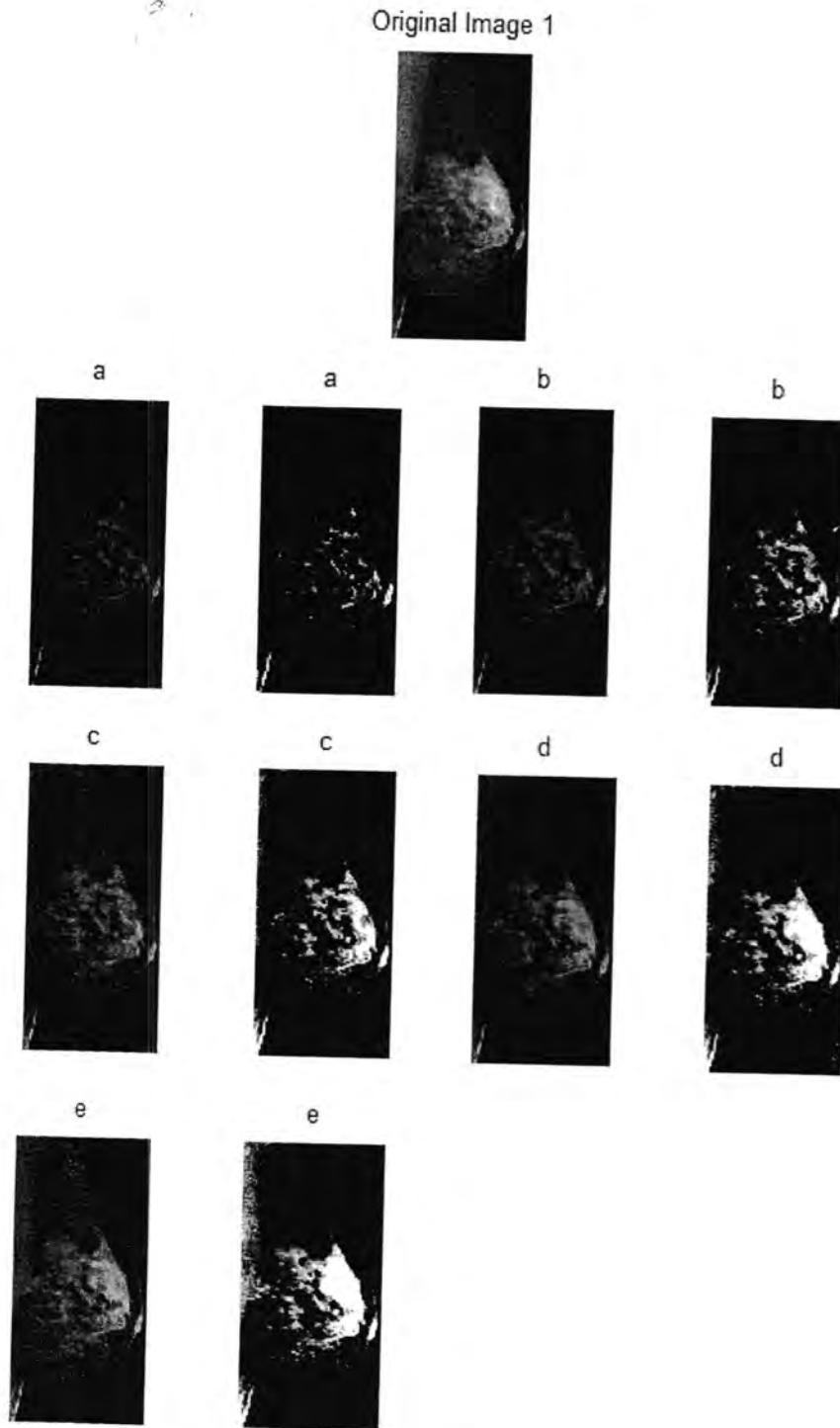


Figure 3: Top-Hat extraction from Left to right: original image (1) ; (a) and (e): Top-Hat with different SE length is 10 and 50 and Top-Hat transformation after detecting cancer cells

Original Image 2

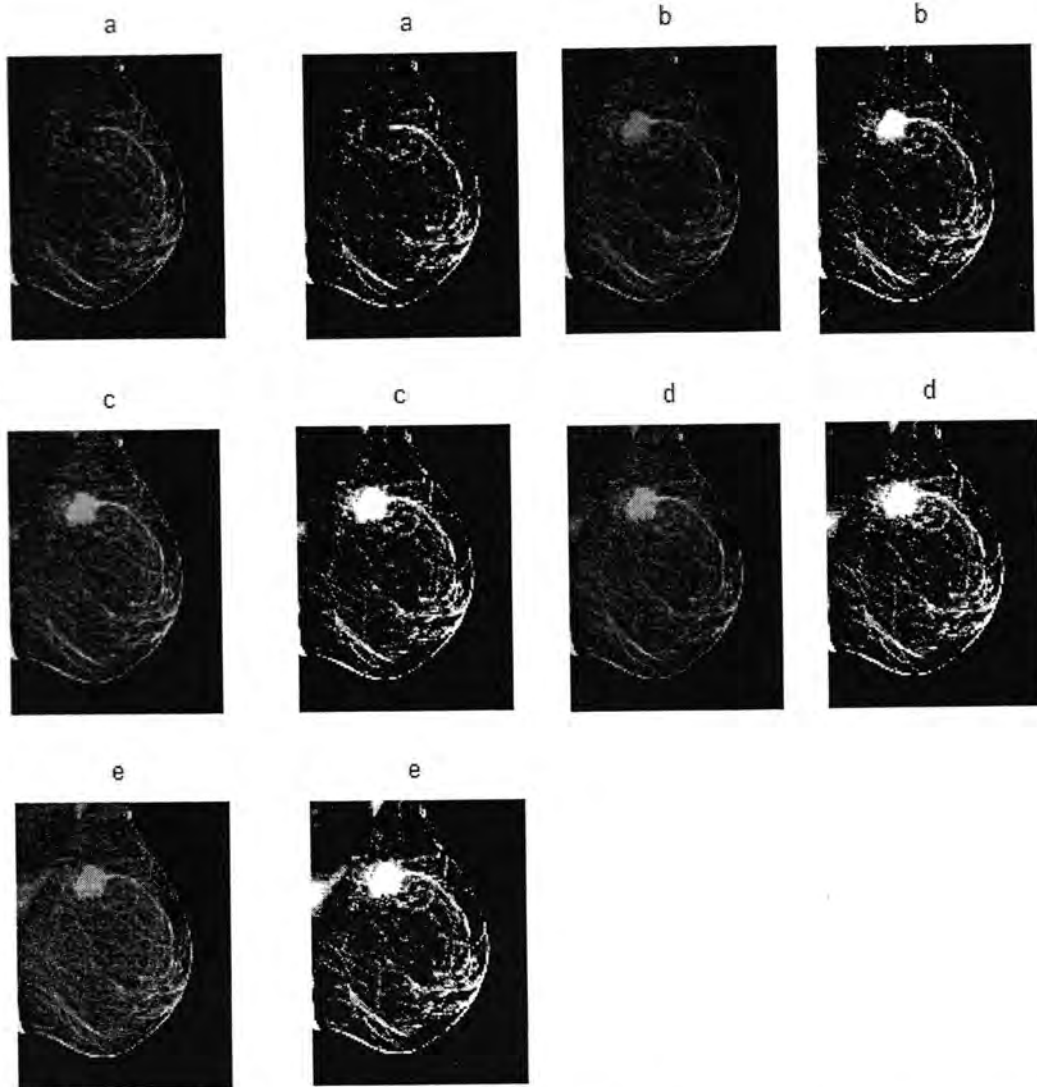


Figure 4: Top-Hat detecting: original image (2); (a) and (e): from Left to right after application of top-hat (circular structuring element of diameter are (10, 20, 30, 40 and 50); right after contrast enhancement

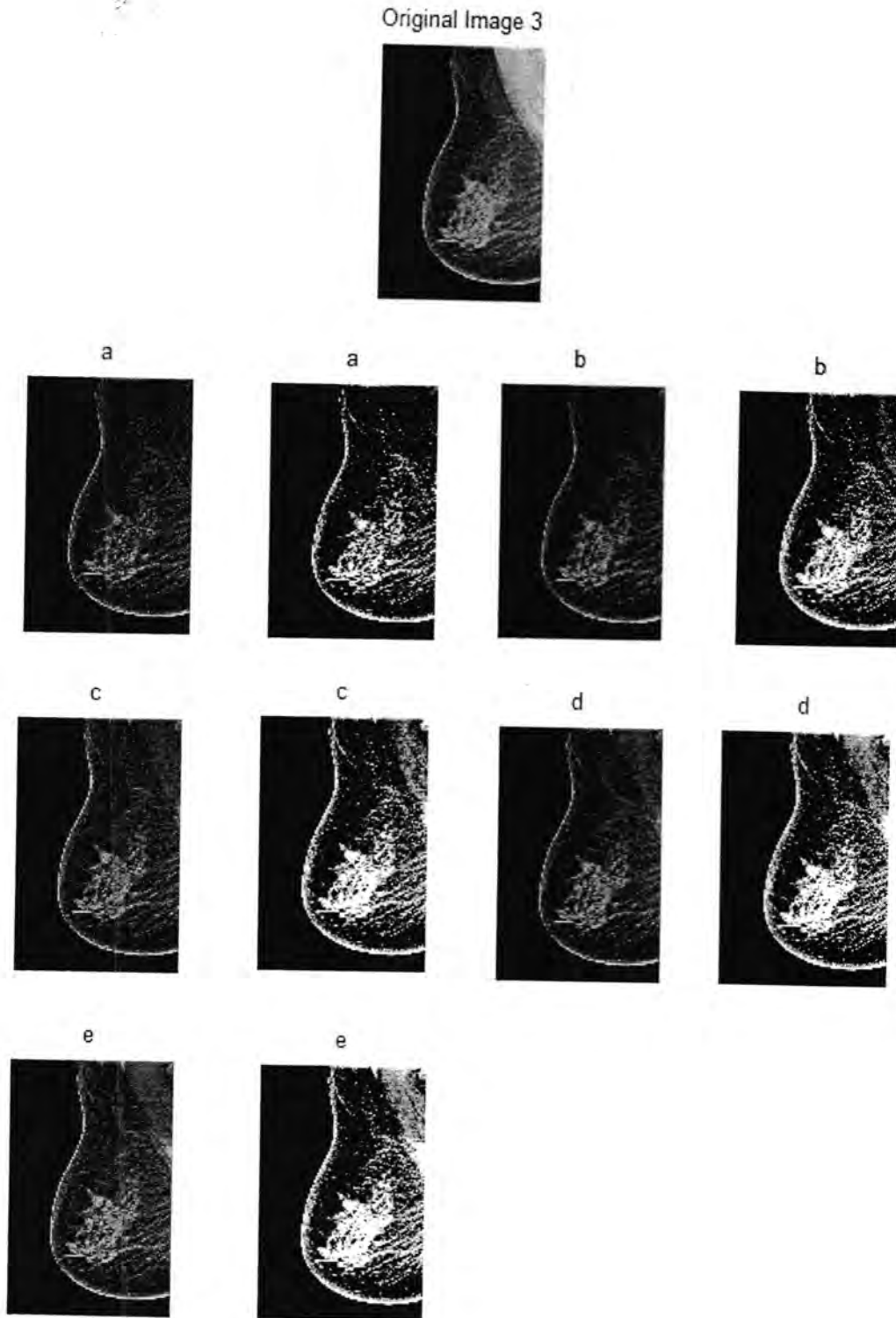


Figure 5: Top-Hat detecting: original image (3), (a) and (e): from Left to right after application of top-hat (circular structuring element of diameter are (10, 20, 30, 40 and 50); right after contrast enhancement

**REFERENCES**

1. Rajesh C. and Bhalchanda.A.S,'Brain Tumor Extraction from MRI images using MATLAB" TJCSCE, ISSN, 2277-9877, 2(2011), 2011.
2. Sam Lister C. February 11, 2009, urine test could speed treatment of prostate cancer, London: The Sunday Times. Retrieved 9 August 2010.
3. Beucher S., "Road Segmentation by Watershed algorithms processing of PROMETHEUS", workshop, Sophia-Antipolice, France, 1990.
4. Gonzalez. R. C., Woods .R. E., "Digital Image Processing", 2nd ed., Prentice Hall, USA, '423-425, 2003.
5. Suman, T Shevani G"Study Implementation of various Morphology Based Image Contrast Enhancement Techniques"Internatonal Journal of Computing &Business Research ISSN (on line):2229-666 2012.
6. Gasteratos A., Andreadis I., "Non-Liner image processing in hardware", pattern Recognition .33.101-1021, 2000.
7. Susant M. and Bhabatos Ch., "A Multi-Scale Morphological Approach to Contrast Enhancement", Singnal processing 80 .685-697, 2000.
8. Rajkumar K. K., et al., "Enhancement of Mammograms Using Top-Hat Filtering and Wavelet Decomposition", Journal of Computer and Mathematical Sciences Vol. 2, (6), 780-898, 2011
9. Ritika and Sandeep K., "Contrast Enhancement Techniques for Images: A Visual Analysis", International Journal of Computer Applications (0975 – 8887) Vol. 64, No.17, 2013.
10. Dhawan, A., Medical image analysis' .IEEE Computer Society Press.2003.
11. Zadorozny .A. and Zhang. H., " Contrast Enhancement using Morphological Scale Space", 804-807, 2009.
12. AlperPahsa, "Morphological Image Processing With Fuzzy Logic", HavacilikVcUzayTeknolojileri Der GisiOcak, CICK2SAY 13(27-34), 2006.
13. Chen T., and Wu Q.H., "A Pseudo Top-Hat Mathematical Morphological Approach to Edge Detection in Dark Regions", Pattern Recognition, 35, 199-210, 2002.
14. Tang J., Peli E., and Acton S.. "Image enhancement using a contrast measure in the compressed domain", IEEE Signal Processing Letters, 10(110):289-292, October 2003.
15. Gasteratos A., Andreadis I., " Non-linear image processing in hardware", Pattern Recognition Vol. 33, pp. 1013-1021, 2000.





## New Watermark Technique Based on $B^+$ Tree and Mathematical Morphology

Hala Bahjet Abdul Wahab

Computer Science Department, University of Technology,

### Article info

Received 28/5/2014

Accepted 30/11/2014

### Key words:

Watermark  
Techniques,  
Mathematical  
Morphology,  
Image Processing,  $B^+$   
Tree Indexing,  
Parametric  
Polynomial  
And Lagrange  
Interpolation.

### ABSTRACT

In this paper, a new gray level image watermarking approach based on  $B^+$  tree, parametric Lagrange polynomial and morphology operations is proposed. First, the new approach utilizes the  $B^+$  tree to obtain the characteristic compression and efficient store with speed retrieval by building efficient indexing  $B^+$  tree as database for many watermark image positions. Second, the new approach encrypts it by a symmetric encryption algorithm based on robust interpolation polynomial depend on time parameter (t) in its processing called parametric Lagrange polynomial (PLP). Third, it is exploiting the abilities of morphology operation to detect the border of host image objects to use in embedding stage based on different value pixels (DVP) method in order to increase the transparency features to embedding stage. Experimental results show using  $B^+$  tree successful to give the facility to use more than watermark if needed with more flexibility.  $B^+$  tree produces high level indexing rate with efficient retrieval and solved the ambiguity problem that some embedding methods suffer. And using the  $B^+$  tree with PLP solve time execution problem that appear with PLP when perform only. The proposed approach is invisible and robust against commonly used gray level image processing methods.

### الخلاصة

قدمنا في هذا البحث، نهج جديد للعلامة المائية ذات المستوى الرمادي استنادا على الهيكل الشجري  $B^+$  و متعدد الحدود لاغرانج و عمليات التشكل. أولا، النهج الجديد يعمل على الاستفادة من الهيكل الشجري  $B^+$  للحصول على ميزات الضغط وكفاءة تخزين مع سرعة الاسترجاع عن طريق بناء فهرسة كفاءة للهيكل الشجري مثل قاعدة بيانات للعديد من مواقع العلامات المائية. ثانيا التشفير بواسطة خوارزمية تشفير متمائل بالاعتماد على قوة متعدد الحدود لاغرانج التي تعتمد على عامل الوقت (t) في معالجتها وتسمى (Parametric Lagrange polynomial). ثالثا، استغلال قدرات عملية التشكل (morphology) للكشف عن الحدود الموجودة في الصورة المضيف لاستعمالها في مرحلة الطمر اعتمادا على قيم مختلفة للوحده اللونية (DVP) من أجل زيادة صفات الشفافية في مرحلة التضمين. أظهرت النتائج التجريبية أن استعمال الهيكل الشجري نجح في الفهرسة على مستوى عالي مع كفاءة الاسترجاع وحل لمشكلة الغموض التي تعاني منها بعض أساليب التضمين. كما ان استخدام الهيكل الشجري مع متعدد الحدود معا نجحت في حل مشكلة الوقت التي كانت تظهر عند تنفيذ متعدد الحدود فقط. النهج المقترح هو غير مرئي وقوي ضد استعمالات طريقة معالجة الصور ذات المستوى الرمادي.

### INTRODUCTION

A watermark is a unique or special image that is embedded on a paper or document that consist text or images. The watermark is designed in a way through which appears only when it is viewed by transmitted light or holding it in a particular angle [1, 2, 3]. Watermarks are used to identify the owner of the image/content and to prevent counterfeiting them. But, this was not possible in digital content. The vast growth of Internet has allowed users to copy the digital content and distribute them without control of ownership. Copy protection system is one of the widely used applications of digital watermarking [4]. It can be used either to prevent unauthorized copies of digital media or tracking the source of any data. Digital watermarking techniques provide high security to digital content by allowing only authorized person(s) to modify or detect the watermark [5]. Some recent watermark techniques [6, 7, 8, 9, 10, 11] prevent others from modifying or detecting the embedded watermark in a

digital content. Watermarks that are embedded on a digital content should be imperceptible both statistically and perceptually. Once the watermark is embedded in a digital content, it is not possible to retrieve the original content by separating the watermark from the content. The quality of an image should not get affected when a watermarking is embedded to it. i.e., when a watermark is embedded in an image, it should not be visible to the naked eye. Each application might have data with different sizes to be embedded as watermark. The perceptual impact and robustness will be directly affected because of various sizes of data. Possibility is always there for a user to know the exact algorithm to detect and render to inactivate a watermark. Therefore, selecting a unique key for watermarking is the only way to secure it. Now, it is impossible for the unauthorized user to know the exact key even if he/she knows the exact algorithm. This increases the strength or reliability of the watermark. Visible

watermarks are similar the paper watermarks, as the watermarks will be visible to the naked eye. Invisible watermarks are imperceptible and cannot be viewed through naked eye. Numbers of techniques are used to implement invisible watermarking. An invisible watermark can be either robust or fragile. The use of a fragile watermark is important when one wants to verify if the protected media was tampered with or not.

**Problem Statement**

Robust watermarking is a technique in which modification to the watermarked content will not affect the watermark [1, 12, 13, and 14].

The B-tree was created by [15]. They are general classes of balanced multi way trees which serve as an indexing mechanism for structured data, and are geared in particular towards large paged files. Two classes of B-tree variants were recognized, B<sup>+</sup>trees and B\*trees, they offer additional properties over the original model. B-tree keeps data sorted and allows searches, sequential access, insertions, and deletions in logarithmic amortized time. The B-tree in which is a generalization of a binary search tree in that more than two paths diverge from a single node [16, 17]. B+ Tree is a variation of B-Trees a structure of nodes linked by pointers and anchored by a special node called the root, and bounded by leaves has a unique path to each leaf, and all paths have equal length stores keys only at leaves, and stores reference values in other, internal, nodes guides key search, via the reference values, from the root to the leaves.

The shape of the curve is basically based upon a set of control points that fundamentally describe its properties and its curvature. The algorithms that are used to generate the curves are primarily based on these control points. Thus if the intruder knows the set of control points it may lead to discover the shape of the curves with a trial and error on the method or algorithms that are originally used to produced the curve[21].

The rest of this paper is organized as follows. Lagrange polynomials are presented in section 2. Mathematical morphology are presented in section 3. B<sup>+</sup> tree are presented in section 4. In section 5 the proposed watermark approach is given. In section 6 the Performance Analysis for the proposed approach is presented. Finally, conclusion and discussion are presented in section 7.

**Objective of Research**

In this paper new approach to generate key watermark by using B+ tree as novel utilization to improvement digital image watermarking algorithms and to get good quality watermarked image for effective watermarking . The proposed approach consist of four preprocessing stage, B+ tree as compression and indexing stage, security stage based on parametric Lagrange polynomial and embedding stage based on methodical morphology.

**Related Work**

Several researches in the field of Digital Watermark were developed. The presents survey include previous related work to the research objective:

1- *Suhad M. Kadhem "Using B+ Tree To Represent Secret Messages For Steganography Purpose"[22].* In this research was suggested approach based on used B+ tree for store the secret messages (that want to be sent) for increased the steganography system efficiency in a manner that prevent redundancy of these messages or even sub messages in order to provide efficient memory usage. Flexibility of the B+ tree gives good result to build many meaningful messages and builds a special dictionary. In this method, there is no ambiguity in retrieving secret message from its code.

2- D.Phani Kumar, G.RoslineNesakumari, S.MaruthuPerumal, "Contrast Based Color Watermarking using Lagrange Polynomials Interpolation in Wavelet Domain" [24]. Robust and blind color based watermarking scheme are proposed based on embeds color watermarks in color images using Lagrange Polynomial Interpolation (LPI) in wavelet domain. Only a tiny quantity of information is required to extract the watermark key. From the watermark key easily can retrieved original color watermark from the watermarked image. The watermark key was generated by using chaotic mapping technique.

3- G.RoslineNesakumari,Dr.V.Vijayakumar, Dr.B.V.Ramana Reddy , "Generation of An Efficient Digital Watermark Key Based on Honey Comb Polynomial Interpolation Approach" [25]. A new mechanism proposed consists of two stages for efficient authentication based on Honey Comb Polynomial Interpolation (HCPI) and Morphological Border Sorted Pixel Value Difference (MBSPVD) scheme. A simple polynomial interpolation technique on new hexagonal structure called Honey Comb structure (HCS) is used for generating the key of the digital watermark.

**Theoretical Background**

**1- Lagrangian polynomials**

Lagrange Interpolation formula is one of the most commonly used interpolation functions. When constructing interpolating polynomials, there is a tradeoff between having a better fit and having a smooth well-behaved fitting function. The more data points that are used in the interpolation, the higher the degree of the resulting polynomial, and therefore the greater oscillation it will exhibit between the data points. Therefore, a high-degree interpolation may be a poor predictor of the function between points, although the accuracy at the data points will be "perfect"[18],[19].The Lagrange interpolating polynomials  $L_{N,K}$  has degree N and is 1

at  $x = x_k$  and 0 at  $x = x_j$ , where  $j \neq k$ .

$$L_{N,K}(x) = \frac{(x-x_0)(x-x_1)...(x-x_{k-1})(x-x_{k+1})...(x-x_N)}{(x_k-x_0)(x_k-x_1)...(x_k-x_{k-1})...(x_k-x_N)} \quad (1)$$

$$= \frac{\prod_{j=0, j \neq k}^N (x-x_j)}{\prod_{j=0, j \neq k}^N (x_k-x_j)}$$

Note that  $\prod_{K=1}^N K = 1.2.3...N$ .

The interpolating polynomial may be written as follows:

$$P_N(x) = \sum_{K=0}^N y_K L_{N,K}(x) = y_0 L_{N,0}(x) + y_1 L_{N,1}(x) + \dots + y_N L_{N,N}(x) \quad (2)$$

It is just a linear combination of the Lagrange interpolation polynomials  $L_{N,K}(x)$  with the  $y_K$  as the coefficients [20].

## 2- Mathematical morphology

Mathematical morphological, which started to develop in late of 1990's stand as a relatively separate part of image analysis. The word morphological commonly denoted a branch of biology that deals with the form and structure of the animal and plants, we use the same word here in context of mathematical morphological as a tool for extracting image component that are useful to represent and description the region shape, such as boundaries. The most basic morphological operations are dilation and erosion. Dilation adds pixels to the boundaries of objects in an image, while erosion removes pixels from object boundaries. In the morphological dilation and erosion operations, the state of any given pixel in the output image is determined by applying a rule to the corresponding pixel and its neighbors in the input image [23].

### A- Dilation

The *dilation* process is performed by laying the structuring element B on the image A and sliding it across the image in a manner similar to convolution but the difference is in the operation that is performed. With a dilation operation, all the 'black' pixels in the original image will be retained, any boundaries will be filled, as in figure 1.

$$A \oplus B$$

- 1- If the origin of the structuring element coincides with a 'white' pixel in the image, there is no change; move to the next pixel.
- 2- If the origin of the structuring element coincides with a 'black' in the image, make black all pixels from the image covered by the structuring element.

### B- Erosion

The *erosion* process is similar to dilation, but we turn pixels to 'white', not 'black'. As in figure 2 slides the structuring element across the image and then follow these steps:

1. If the origin of the structuring element coincides with a 'white' pixel in the image, there is no change; move to the next pixel.
2. If the origin of the structuring element coincides with a 'black' pixel in the image, and at least one of the 'black'

pixels in the structuring element falls over a white pixel in the image, then change the 'black' pixel in the image (corresponding to the position on which the center of the structuring element falls) from 'black' to a 'white'.

$$A \ominus B$$

### C- Border

Border detection is an important function for object identification and is also a critical pre-processing step in image segmentation. Result of the final processed image is obtained by the detection of borders of an image. Mathematical Morphology (MM) is a new mathematical theory which can be used to process and analyze the images. It provides an alternative approach to image processing based on shape concept stemmed from set theory, not on classical mathematical modeling and analysis. In the MM theory, images are treated as sets and morphological transformations which derived from Minkowski addition and subtraction are defined to extract features in images. The structuring element (SE) decides the performance of morphological operation.

$$G(A) = (A \oplus E) - (A \ominus E) \quad (3)$$

Where  $G(A)$  denote the border of the image A. It is defined as the difference set of the dilation and Erosion [23].

### B+ Tree

B+ tree is called an index of database, such that each record will be stored in the database, the reference number (and the key) of that record will be stored in the B+ tree. So when we want to reach a certain record, we need to know its key to get its reference number from the B+ tree. When we get the reference number of that record we can retrieve the required record directly. B+ tree is an arranged and balanced tree (see figure 1), and this is why it is so fast in retrieving the required data. B+-trees distinguish internal and leaf nodes, keeping data only at the leaves, whereas ordinary B-trees would also store keys in the interior. B+ tree insertion, therefore, requires managing the interior node reference values in addition to simply finding a spot for the data, as in the simpler B-tree algorithm [15,16, 17].

B+ tree used as a special dictionary for storing data (with their codes) in a manner that prevent redundancy of these data or even sub data in this dictionary (in order to provide efficient memory usage), with Accordance to the following conditions [22]:

1. Store data in this dictionary (if it is not found) and get its unique code (at send process).
2. Retrieve the unique data when we have its code from this dictionary (at received process).

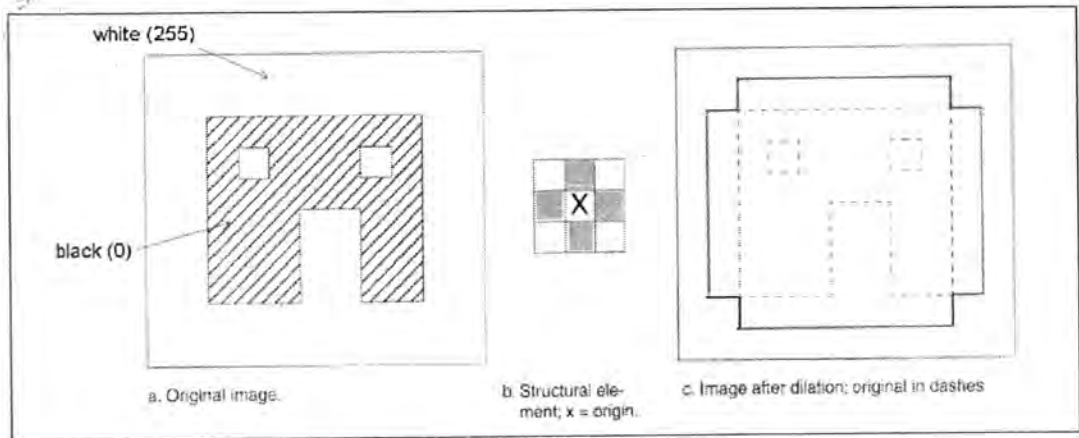


Figure1: Morphological dilation

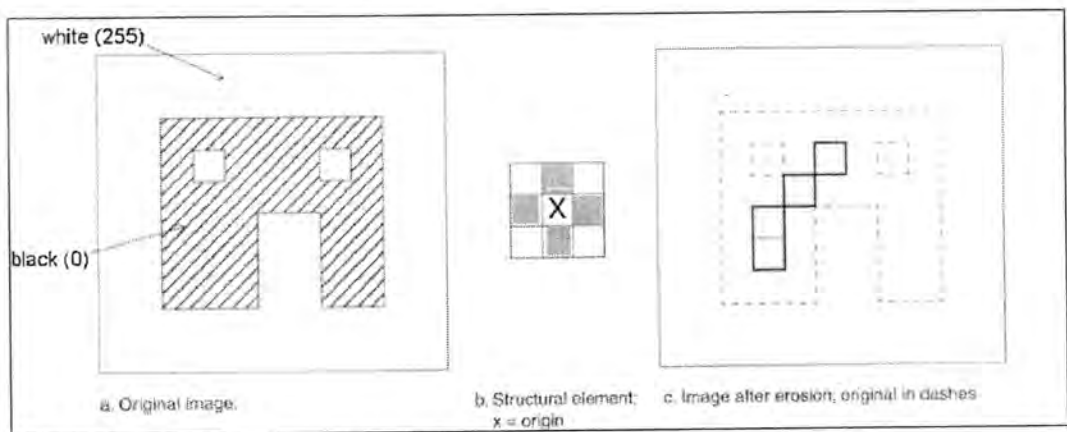


Figure 2: Morphological Erosion.

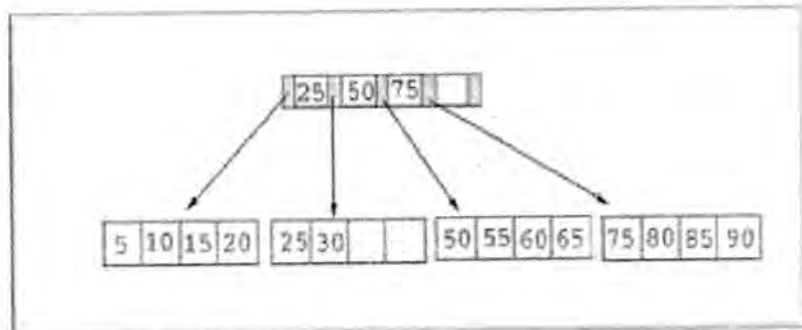


Figure 3: An Example of B<sup>+</sup> Tree.

**The Proposed Approach**

In the following section describe the main stages for the proposed approach at sender side that shown in figure (4). The proposed approach consists of three main stages. The first stage is Digital Watermark Key generation (DWK), based on sensitive pixel values from watermark image and B+ tree indexing method , Second stage is the security phase based on parametric Lagrange polynomial that represent as encryption stage, and third stage is embedded the encrypt DWT in the host image based on morphology operations.

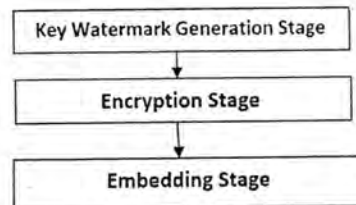


Figure 4: The Main Structure of the Proposed Approach.

### 1-Key Watermark Generation Stage

#### A-Preprocessing Operations

Generate watermark key is produce in this paper by using small as possible information that refer to watermark image that agreed between the authorized parties, I.e. the proposed approach starts by selecting the gray image watermark image(secret image) to generate the watermark key.

The preprocessing operations play main role on gray image to extract the positions (x, y) pixels only that contain the same pixels values for example white or black

that refers to the main feature of the watermark image to represent the watermark key and store it in matrices (i.e.the proposed approach used the gray level image to reduce the B+ tree indexing size). Preprocessing operations perform on the Pixel Positions Vector (PPV) black or white, PPV divided in sub vectors according to the number of rows in order to preparing the compression operation that perform in B+ tree that illustrated in details in next subsection, figure (5) illustrates the preprocessing operations.

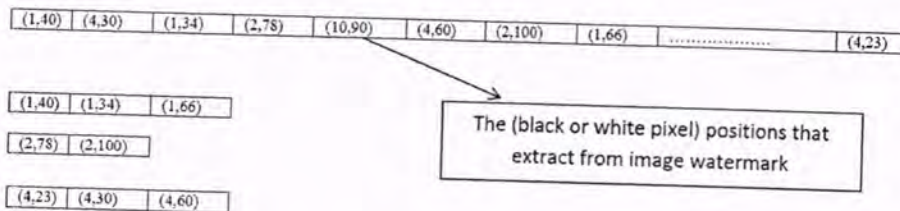


Figure 5: Preprocessing Operations.

#### B-Compress Operation Based on B+ Tree

B+ tree converts the DWK to small code numbers by investigating from the compression feature that available in B+ tree structure (indexing structure), that was operating in a manner that prevents redundancy of these DWK or even sub DWK in order to provide efficient memory usage. This stage represents by storing the one or more DWKs and getting its unique code based on B+ tree indexing, in order to reach unique codes for every DWK. One of the most important parameters, in this stage represented by *code counter (n)*.

This parameter refers to total number of rows of DWKs those stored in dictionary. The method uses one database (dbase) that represents the dictionary of the secret watermark position images and its corresponding codes, and uses two index trees (Bt1, Bt2) that refer to the same database (dbase). Each new secret image (positions) will be converted to a list of words and these words will be stored in dbase in a manner that prevents the redundancy of these positions or even sub positions. Bt1 is used for storing purpose to check if the row of positions or even sub positions is already found in dbase. So Bt1 use the first position of the row as a key, while Bt2 is used for retrieving purpose, so it uses the code of the position (DWK) as a key. In general the DWK is composed of [word1, word2, ..., wordn].

In the following figure (6) shown the B+ tree algorithm to compress DWT to unique cods.

**Algorithm 1: Compressed the Black pixel position values and get the unique code**

**Input:** vectors for black pixel positions value after perform preprocessing operation

**Output:** List of code, Code counters (n).

**Process:**

*Step 1: store the vector for position as matrices  $I(x_i, y_i)$*

*Step 2: For each row do the following { store one image watermark position in B+ tree indexing }*

- 2.1 If (row suppose as a (new row) Then do the following
  1. Put the first position(x,y) of the row as a key in b+ tree (Bt1),
  2. Compute the number of positions in the row
  3. give the row a new unique code
  4. and use this code as a key for b+ tree (Bt2)
- 2.2 If (row has points that already found in dbase ) Then
  - give it a new code
  - store it in Bt2 as a key
- 2.3 If (row has points that already found in dbase except the last point) Then
  - store the point in dbase and the reference of the previous point
  - store at the previous point the new reference with its specific code ,
  - Give it a new code

*Step 3: For each row do the following { store more than one image watermark in B+ tree indexing }*

- 3.1 If (row has some points that are already found in dbase) Then
  - Duplicated the common point between new row and dbase
  - give its specific code for each point
  - Store the point in dbase and the reference of the previous point with its specific code
  - Store at the previous point the new reference with its specific code .
  - Give it a new code.

**Step 4: End**

Figure 6: the B+ tree algorithm to compress DWT to unique cods.

## 2- Encryption Stage.

In this stage, represent a new improvement on watermark key generation technique, based on parametric Lagrange polynomial is use as encrypting function to encrypt DWK instead of traditional Lagrange polynomial to increase the security robust and solve the time execution problem that appear with traditional Lagrange polynomial. Parameterization method use efficient secure parameter (t) that increases the robust and complexity features for key watermark. A parametric Lagrange interpolation suggests the movement of a point through value of time (t), two function (x(t), y(t)). The position of the particle at time (t), increase the security in polynomial generation and for more effort for attacker. Where dealing with Lagrange polynomial from two dimensions (2D) to three dimension (3D) as show in equation below.

$$p_i(t) = y_i \prod_{k=1, k \neq i}^n \frac{x-t_k}{t_i-t_k} \quad (4)$$

Where:

$$P(t) = \sum_{i=1}^n p_i(t) \quad (5)$$

The value of (ti) generate by using random generation to get the value of (t) more random and Difficulty guessing by attacker.

$$t(i) = t(i-1) * a + b \quad (6)$$

Where a and b integer random value and b change by this equation ((b+2) mod i) to get more randomization for (t) value and prevent redundancy. And increased the isolation of the polynomial coordinates. The value of (t) the same at the sender and receiver just they agree about the initial value of (t (1), a, and b) value to generate the complete value of (t) vector.

That very important note any change in the value (a, b, t(1)) due to change the key generated because it dependent on (t) value. These values provide more flexibility features in key generation process to product different efficient keys.

The DWMK unique code that obtain from algorithm-1 use as inputs to parametric Lagrange polynomial function with pi(t).

In the following figure (7) shown the complete algorithm to generate parametric Lagrange interpolation.

**Algorithm -2: Parametric Lagrange Interpolation Method**  
**Input:** control point of curve (xi,yi) where are list of code, t, and i=0 t0 n ( where n is Code counter (n) ),and t(i) than generate by the equation(6)  
**Output:** Digital watermark key (DWMK).

---

**Process:**  
**Step 1:** Let x=1  
**Step2:** while (x<=n) do  
**Step3:** let sum=0  
**Step 4:** For i = 0 to n do  
**Step 5:** Let p = 1  
**Step 6:** For j = 0 to n do  
**Step 7:** if i and j are not equal then let  
 $p = p \frac{x-t_k}{t_i-t_k}$   
**step8:** next j  
**Step 9:** sum=sum + p \*xi  
**Step10:** next I; f(x) =sum  
**Step11:** x=x+1  
**Step 12:** End

Figure 7: Generate Parametric Lagrange Interpolation.

## 3- Embedding Stage

Watermark key is embedded in the sorted pixel locations of morphological border pixels on host image using morphology operations to extract the border that illustrated in section (2). This approach overcomes the weak robustness problem of embedding the watermark. The basic PVD method, determines whether the two consecutive pixels belong to an edge or smooth area by checking out the difference value between two consecutive pixels. If the difference value was large, i.e. the two pixels are located in an edge area; more secret data can be hidden here. On the contrary, if the difference value was small, i.e. the two pixels are located in a smooth area; less secret data can be embedded. Therefore, this scheme produces watermarked images that are more similar to the original images than those produced by LSB substitution schemes, which directly embed secret data into the covering image without considering the differences between adjacent pixels for more detail see [23].

### Algorithm:" Multi-structure elements morphological border detection"

**Step 1:** Construct structure elements  $E_r$  of different directions according to the method presented section (C).

**Step 2:** Use the structure elements got in step 1 respectively to detect the borders  $Gr(D)$  of original image by morphological gradient border detector.

$$Gr(D) = (D \oplus E) - (D \ominus E)$$

**Step 3:** According to every detected border  $Gr(D)$  in step 2, use synthetic weighted method to calculate final detected border by:  $G(D) = \sum_{r=1}^m W_r Gr(D)$

Where:  $G(D)$  is the final detected border of original image,  $m$  is the number of structure elements and  $W_r$  is the weight of different detected border information. It can be calculated by different methods. In this paper, we calculate  $W_r$  by  $w = 1/m$ .

The proposed watermarking approach which is used to embed the watermark key in the host image is summarized in the following figure (8) that shown an example in the sender side.

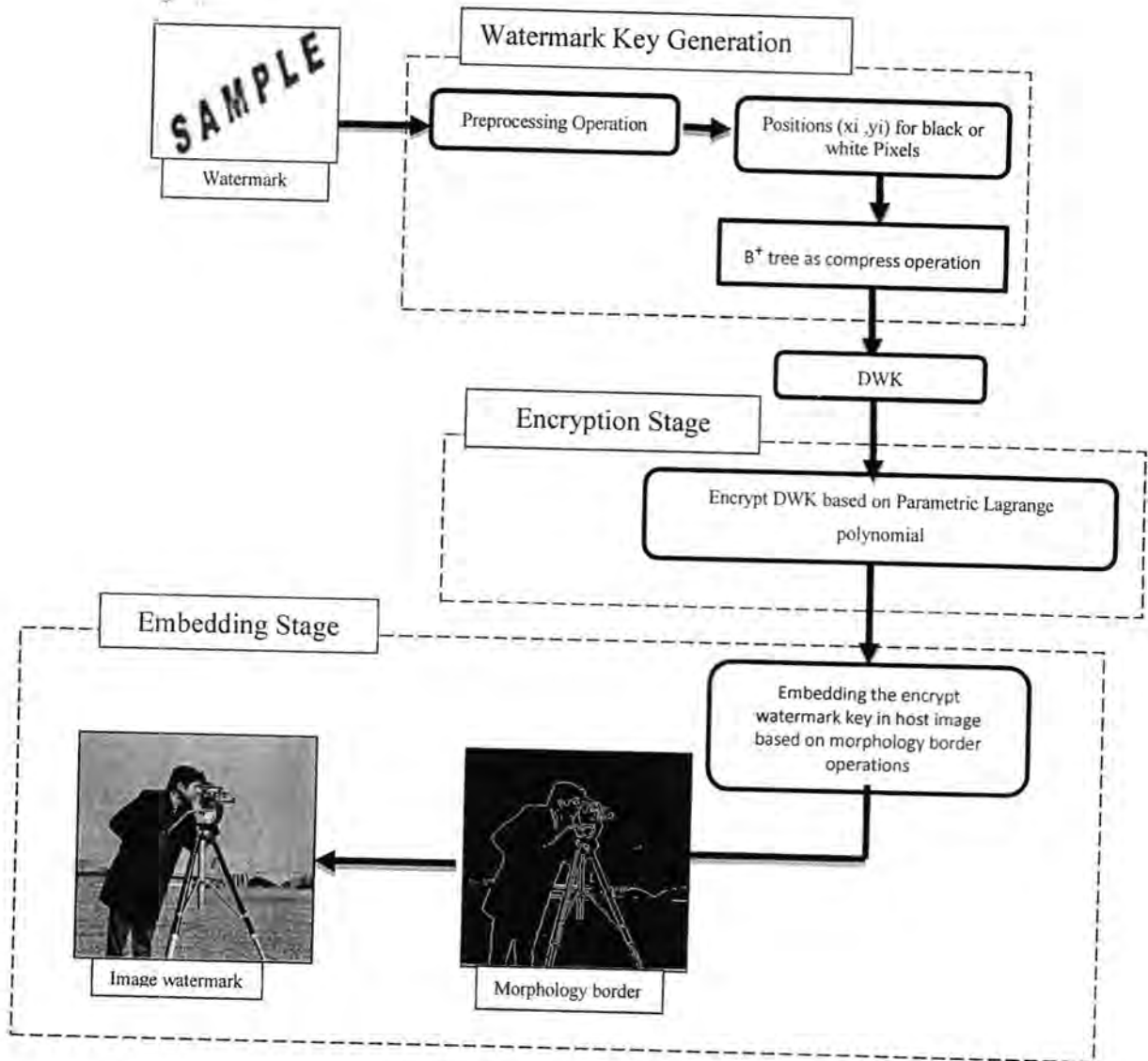


Figure 8: the Proposed Approach in Sender Side.

**Algorithm-3: Retrieve the Unique Position White Pixels from List of Code**  
**Input:** List of code  
**Output:** vector for whit pixel position

**Process:**  
**Step1: For each code in List of code do the following**  
**If**(the code is found in Bt2) **Then** do the following

1. Retrieve the term of the last point of the vector that the code refer to it
2. Search in the list of this term on this code
3. Get the length of the row that have the last point, and the reference of the previous point
4. Follow the reference of the previous point with their specific code, and take its point and concatenate it with next point, then follow the reference of its previous point with their specific code and so on, until we get the row.

**Step 2: End**

Figure 9: The B+ Tree Algorithm to Retrieve the DWK.

### Reconstruct Watermark Process

Extraction procedure is a nature blind extraction which uses only host image as input. Morphology operations started on watermarked image extract the DWK. DWT is decrypt using parametric Lagrange polynomial as symmetric encryption key to obtained on sequence of unique codes, apply B+ tree algorithm to speed retrieve the black pixel position for watermark image and reconstruct the watermark. In the following figure (9) shown the B+ tree algorithm to retrieve the DWK.

#### Example

In the following simple example illustrated the storing with compression features that available in B+ tree to produce compression unique cods (DWT).

- B+ tree store one watermark image positions  
 Image 1 (position vectors) =  
 [(1,4),(1,6),(1,7),(1,8),.....]  
 [(2,3),(2,4),(2,5),(2,10),.....]  
 (1,4) → 00001 word ([ind(1,4),00011,~0,0,1])

00010 word ([ind(1,5),00011,00001,0,0])  
 00011 word ([ind(1,6), 00100, 00001,0,1])  
 00100 word ([ind(1,7), 01000, 00011,0,1])  
 01000 word ([ind(1,8), ~0,00100,4,1]) --- 1

• B+ tree store multi images

Image vector 1= [(1,4), (1,6), (1,7), (1,8), (2,3), (2,4), (2,5), (2,10),.....]  
 Image vector 2= [(1,4), (1,5), (1,6), (2,3), (2,4), (2,5), (2,10), .....]

(1, 4)→  
 00001 word([ind(1,4),00011,~0,0,1])  
 00001 word([ind(1,4), 00010,~0,0,2])  
 00010 word([ind(1,5),00011,00001,0,2])  
 00011 word([ind(1,6), 00100, 00001,0,1])  
 00011 word([ind(1,6), 00100, 00010,3,2])----- 2  
 00100 word([ind(1,7), 01000, 00011,0,1])  
 01000 word([ind(1,8), ~0,00100,4,1])-----1

• Retrieve process from B+ tree to obtain from positions vector If code =1 then

- Code (1) have 4 points, and will connate them from
1. Ref (01000) is pointer to(00100) that have (1,7) with code 1.
  2. Ref (00100) is pointer to two references, Ref(00011) that have (1,6) with code 2 and Ref(00011) that have (1,6) with code 1. B+ tree will match the code and retrieve the specific point with code 1.
  3. Ref(00011) is pointer to (00001) that have two previous references ,Ref(00001) that have (1,4) with code 2 and Ref(00001) that have (1,4) with code. B+tree will match the code and retrieve the specific point with code 1.Code=1,{(1,4),(1,6),(1,7),(1,8)}.
- The entire reconstruct process of the proposed approach is as shown in Figure (10).

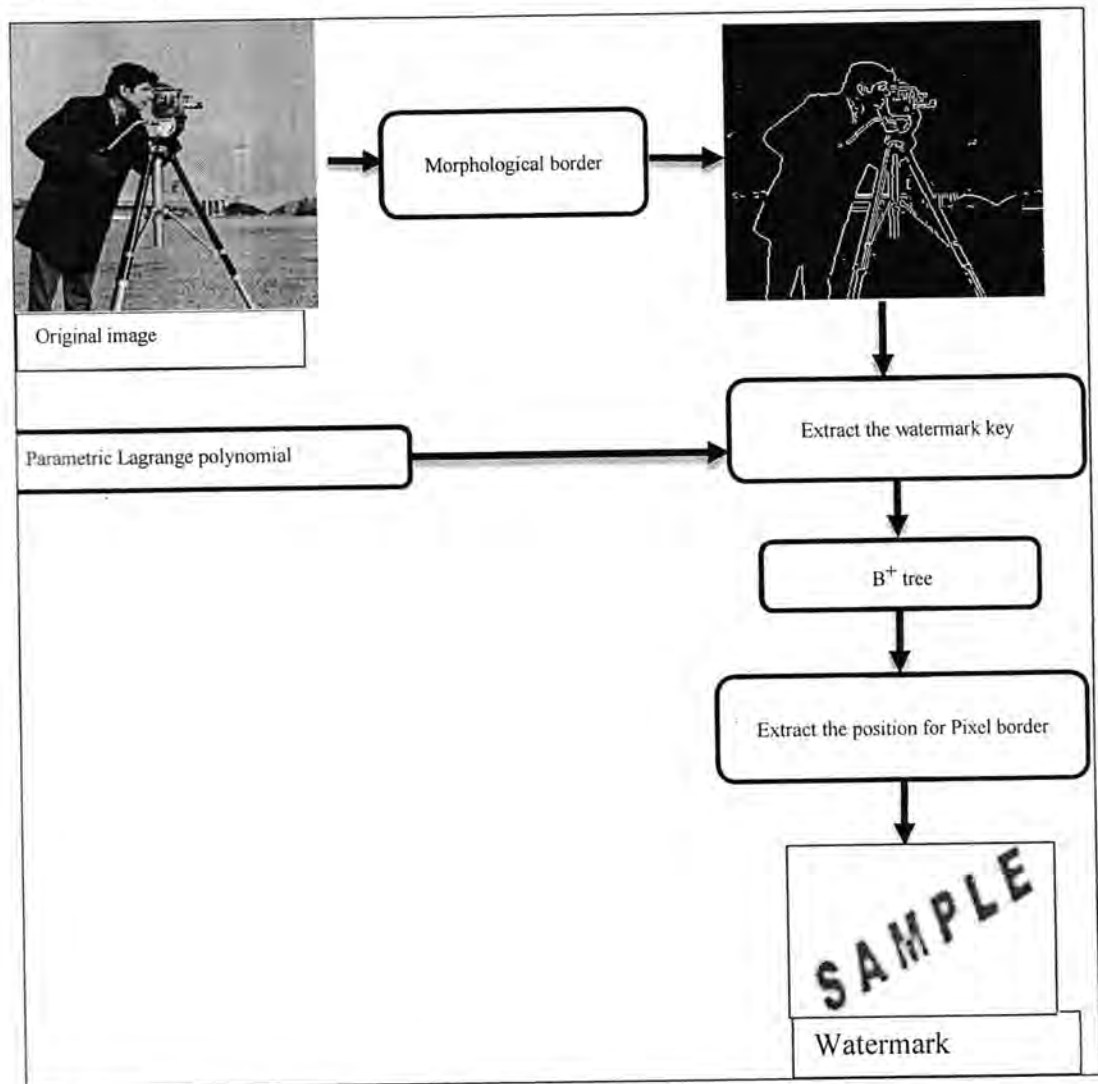


Figure 10: Reconstruct Watermark of the Proposed Approach.



**Results and Discussion**

The proposed approach is experimented on all 4 images Cameraman, Lena, and lines of size 256×256 of Figure (11). The gray watermark considered for the experiments with different of sizes as shown in Figure (12). Figure (13) represents the boundary images based on morphological boundary algorithm given in stage-2. Figure (14) represents the watermarked images using the proposed approach. The watermark key bits are inserted in the boundary pixel locations. Table (1) shows the Mean Square Error Ratio (MSE), Peak Signal-to-Noise Ratio (PSNR) and similarity tests values for all the 4 images. From the Table (1) it is clearly evident that all the images show high MSE, PSNR and similarity values which

indicate high robustness and high quality of image after watermark insertion. Using B+ tree indexing as store and compression stage gave efficient compression data rate from black pixels position of watermark, table(2) shows the indexing ratio to five watermark samples and B+ tree indexing succeed to reach the following features:-

- Efficient time in storing and in retrieving the DWK
- Solved the ambiguity problem that some steganography methods suffer from.
- Providing high capacity for steganography stage.



Figure11: The Host Images.



Figure12: The Morphology Images

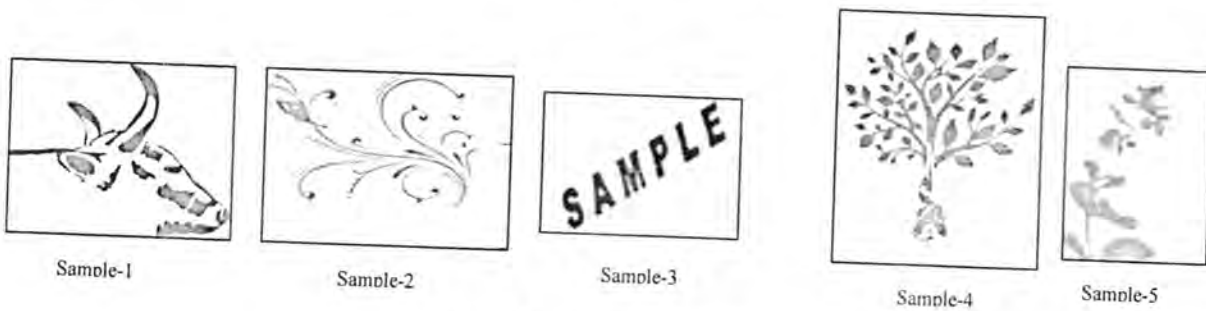


Figure13: Watermark Samples (Logo).



Figure14: Watermark Images.

Table1: Imperceptible Test

Host watermark	Image	MSE	PSNR	similarity
cameraman		144.5	58.14	1
Lena		131.34	47.54	1
Lines		94.40	46.63	0.96
Circles		83.86	45.21	0.98

Table 2: B<sup>+</sup> Tree Indexing Ratio.

watermark samples	size	rows	columns	Indexing ratio
Sample-1	3.35 KB	251	201	88%
Sample-2	2.81 KB	290	208	85%
Sample-3	1.10 KB	112	80	89%
Sample-4	4.08 KB	189	267	87%
Sample-5	991 KB	80	113	90%

Table3: Fidelity Criteria for Gray Logo Comparison between Traditional and Proposed Approach

Logo size	Traditional Lagrange			Parametric Lagrange			The proposed approach		
	MSE	PSNR	SIM	MSE	PSNR	SIM	MSE	PSNR	SIM
32*32	24.82	33.23	0.99	40.20	32.08	0.99	46.72	31.52	0.97
50*50	32.1	32.07	0.98	81.84	29.00	0.98	106.7	29.76	0.98
60*60	18.49	35.46	0.99	12.60	37.12	0.99	46.52	31.54	0.96

Table4: Time Executed Comparison between the Traditional and Proposed Approach.

Logo Size	Traditional method Time	Parametric Lagrange Time	The proposed approach
32*32	3.47m	2.17m	0.02m
50*50	6.46m	3.45m	0.04m
60*60	7.01m	3.14m	0.07m

Table 5-1: Gray Logo with 10% Cropping Attack.

Logo size	Traditional method			Parametric Lagrange			Proposed approach		
	MSE	PSNR	SIM	MSE	PSNR	SIM	MSE	PSNR	SIM
32*32	23.95	34.33	0.99	40.20	32.08	0.99	45.72	31.52	0.99
50*50	320.1	32.07	0.89	81.84	29.00	0.98	108.7	27.76	0.95
60*60	18.49	35.46	0.99	12.60	37.12	0.99	45.52	31.54	0.99

Table 5-2: Gray Logo with 15% Cropping Attack.

Logo size	Traditional method			Parametric Lagrange			Proposed approach		
	MSE	PSNR	SIM	MSE	PSNR	SIM	MSE	PSNR	SIM
32*32	23.95	34.33	0.99	40.20	32.08	0.99	45.72	31.52	0.99
50*50	320.1	32.07	0.89	81.84	29.00	0.98	108.7	27.76	0.95
60*60	18.49	35.46	0.99	12.60	37.12	0.99	45.52	31.54	0.99

Table 5-3: Gray Logo with Salt and Pepper Attack.

Logo size	Traditional method			Parametric Lagrange			Proposed approach		
	MSE	PSNR	SIM	MSE	PSNR	SIM	MSE	PSNR	SIM
32*32	4773	11.34	0.79	1926	15.28	0.89	45.72	31.52	0.99
50*50	320.1	32.07	0.89	81.84	29.00	0.98	108.7	27.76	0.95
60*60	502.6	21.11	0.87	51.64	31.01	0.97	45.52	31.54	0.99

### Security and Analysis

The evaluation the performance for proposed approach based on the security features and comparisons between the proposed approach and traditional method are performed according security robust and time execution. Figure (14) shows the gray logo with different sizes, which use in the test measurements.

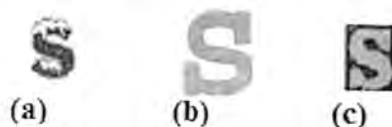


Figure 15: Gray Logo with Size a-(32\*32), b- (60\*60), and c-(50\*50)

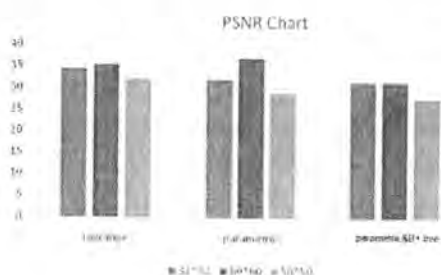


Figure16: PSNR Comparison



a



b



c

Figure 17: a-Watermark Image, b- 10% Cropping Image, c-15% Cropping Image.



A



b

Figure 18: a-Watermark image, b- Image with Salt and Pepper Attack.



Figure19: The result of extract Logo under salt and pepper attack .

1. Table(3)and figure(16) illustrates traditional to generation watermark key by using Lagrange polynomial without parametric form and give acceptable in MSE, PSNR and the similarity between host image and watermark image, but time execution problem is appear as shows in table (4).
2. In table (3&4) show the results of the proposed algorithm based Parametric Lagrange that provide more robust for watermark generation by adding the secret parameter (t) with decrease the time execution .
3. In table (3&4) show the results of the proposed algorithm using B+ tree indexing succeed to solve the execution time problem and make the key generation so faster and at the same time kept the acceptable results of fidelity criteria .
4. In tables (5-1) and (5-2) shown the result of the cropping attack with 10% and 15% ratios from watermark image appear that the proposed algorithms succeed to stand cropping attack, where the results shown in figures(17and 18) that no change from the standard watermark image, therefore show this algorithm not effective with cropping attacker.
5. In table (5-3) and figure(19) the results shown less effect to the noise( salt and paper attack) than Lagrange interpolation, and some result stayed as same result under the noise that show the robustness of algorithm under attacker.

## CONCLUSIONS

This paper was presented a new gray level image watermarking approach that combines between  $B^+$ tree, parametric Lagrange polynomial, morphological operations and watermark techniques in order produce an efficient watermark approach. Through the current research work, the following conclusions are derived:-

- 1- Using  $B^+$ tree in proposed watermark approach provide efficient results to reduce amounts of data that embedding in host image. And  $B^+$  tree succeed to compress with efficient manner to produce few unique cods about 50% at least from the number of black pixel positions.
- 2- Using parametric Lagrange polynomial based on time parameter (t) as secret key that agreement between two parties increase the secrecy and integrity and increase the difficulty in front of intruder with consuming time.
- 3- Combine parametric Lagrange polynomial and  $B^+$ tree succeed to solve time execution problem that appear with traditional Lagrange polynomial.
- 4- The proposed approach robust against noise and cropping attacks with efficient results.
- 5- The quality of an image not affected when a watermarking is embedded to it. i.e., when a watermark is embedded in an image, it not be visible to the naked eye according test results.

## REFERENCES

- 1- Potdar V., Han S., and Chang E., "A Survey of Digital Image Watermarking Techniques", in Proc. of the IEEE International Conference on Industrial Informatics,; 709-716, Perth, Australia 2005.
- 2- Sameh O., Adnane C., and Bassel S., "A Fuzzy Watermarking System Using the Wavelet Technique for Medical Images", International Journal of Research and Reviews in Computing Engineering Vol.1, No.1, March 2011.
- 3- Hanaa A. Abdallah, Mohiy M. Hadhoud, Abdalhameed A. Shaalan and Fathi E.AbdElsamie, "Blind Wavelet-Based Image Watermarking", International Journal of Signal Processing, Image Processing and Pattern Recognition, Vol. 4, No.1, March 2011.
- 4- Sumalatha L., Venkata Krishna V., Vinay Babu A., "Image Content Authentication based on Wavelet Edge Features", International Journal of Computer Applications Vol. 49- No.23: 0975 – 8887, July 2012.
- 5- Dr. Eswara Reddy B., Harini P., MaruthuPerumal S., Dr. VijayaKumar V., "A New Wavelet Based Digital Watermarking Method for Authenticated Mobile Signals", International Journal of Image Processing (IJIP),Vol.5 ,Issue.1 ,2011.
- 6- G.RoslineNesaKumari , B. VijayaKumar , L.Sumalatha , and Dr V.V.Krishna, "Secure and Robust Digital Watermarking on Grey Level Images", International Journal of Advanced Science and Technology Vol. 11, October, 2009.
- 7- B. Vijaya Kumar,M.Radhika Mani, G. Roseline NesaKumari, and Dr. V. Vijaya Kumar, "A New Marginal Color Image Water Marking Method based on Logical Operators ", International Journal of Security and Its Applications Vol. 3, No. 4, October, 2009.
- 8- Vijayakumar B., Dr. Vijayakumar V., Rosline Nesa kumari G. ,"A Significant Root Leaf Wavelet Tree (SRLWT) Image Watermarking Technique Based on Tree Quantization", International Journal of Scientific and Research Publications, Vol.2, Issue 4, ISSN :2250-3153, April 2012.
- 9- Rosline Nesa kumari G., Sumalatha L., Dr. Vijayakumar V. "A Fuzzy Based Chaotic And Logistic Method For Digital Watermarking Systems", International Journal of Scientific & Engineering Researc Publications, Vol.3 , Issue. 6, June 2012.
- 10- Maruthuperumal S., Rosline Nesakumari G., Dr. Vijayakumar V., "Complete Qualified Significant Wavelet Tree Quantization for Image Watermarking", in International Journal of Computer Science and Technology,Vol.3, Issue 2, April-June 2012.
- 11- Maruthuperumal S., Dr. Rosline Nesakumari G., VijayakumarV., "Region Based Even Odd Watermarking Method with Fuzzy Wavelet ", International Journal of computer Engineering & Science(IJCES), Vol. 2 Issue.8 ,August 2012.
- 12- Chu.W, "DCT-Based Image Watermarking Using Sub-sampling", IEEE Trans. Multimedia, 5(1): 34-38, 2003.
- 13- Rosline Nesakumari G., Rajendran S., Dr. Vijayakumar V., "Integrated Normalized Content System for Efficient Watermarking", International Journal of Computer Applications, Vol.53,No.15, Sept, 2012.
- 14- Jiankun Hu , Fengling Han, "A pixel-based scrambling scheme for digital medical images protection", Journal of Network and Computer Applications, Published by Elsevier Ltd.,2009.
- 15- Jan Jannink, "Implementing Deletion in  $B^+$  Trees",Sigmoid Recire,Vol.24,No.1,1995.
- 16- Gotez, Graefe, "B-tree indexes interpolation search, and skew", Chicago Iiinois,USA,2006.
- 17- Anderson,S,"B+Trees",Freed,1998.Http://bannage.cl arku.edu/~achou/cs160/B+Trees/B+Trees.htm.
- 18- Anthony Ralston and Philip rabinowitz,. " First Course in Numerical Analysis", second edition, McGraw-hill Inc, 1978.
- 19- Shan S.,kuo, "Computer Applications of Numerical Methods", Addison wesely publishing company, 1972.
- 20- Goldman Ron, "Lagrange Interpolation and Neville's Algorithm", 2002.
- 21- Firas Husham Al-Mukhtar, "Parallel Generation of Non Linear Curves with Computer Aided Application", PhD. Thesis, Computer & Informatics Information Institute for Postgraduate Studies,2003 .

- 22- Suhad M., "Using  $B^+$  Tree to represent secret Message for steganography purpous", Eng.&Tech. Journal, Vol.28.No.15, 2010
- 23- Chung-Ming Wang a, Nan-I Wu a, Chwei-Shyong Tsai b, Min-Shiang Hwang, "A high quality steganographic method with pixel-value differencing and modulus function", the Journal of Systems and Software, 2007.
- 24- D.Phani Kumar, G.RoslineNesakumari, S.MaruthuPerumal, "Contrast Based Color Watermarking using Lagrange Polynomials Interpolation in Wavelet Domain", International Journal of Engineering and Advanced Technology (IJEAT), 2013.
- 25- G.RoslineNesakumari, Dr.V.Vijayakumar and Dr.B.V.Ramana Reddy, "Generation of An Efficient Digital Watermark Key Based on Honey Comb Polynomial Interpolation Approach", I. J. Computer Network and Information Security, 2013.



## Net Correlation between Surface Temperature and Pressure Anomaly at Sea Level and North Atlantic Oscillation (NAO) of Baghdad City

Ahmed S. Hassan and Iqbal Kh. Khams

The University of Mustansiriyah, College of Science, Department of Atmospheric Science

### Article info

Received 1/9/2013  
Accepted 11/1/2015

### ABSTRACT

The climate system is very sensitive to the changes caused by the temperature of sea surface, which extremely affecting it, and to understand this relationship, the coefficient oscillation of the North Atlantic and its association with climate variables, which include all anomalies of surface minimum and maximum temperatures. So, were calculated this study, used both the National Center (U.S.) for the environment and forecasting (NCEP) to calculate the coefficient of fluctuation of the North Atlantic, and the General Authority form meteorological and seismic monitoring data to calculate the anomaly of minimum and maximum surface temperatures of (January, April, July, October) for the period (1989-2010). The results shows that the climatic changes represented by anomaly surface temperatures and pressure over Baghdad city is associated with the coefficient of fluctuation of the North Atlantic (NAO) coefficient of correlation value equals (0.168 and 0.201), respectively, while the value of the correlation coefficient between the coefficient of fluctuation of the North Atlantic (NAO) and surface pressure anomaly equals (-0.240), so impact of both these climate variables and the coefficient of the North Atlantic oscillation are more in winter than in summer.

### الخلاصة

يعد النظام المناخي حساس جدا للتغيرات التي تحدثها درجات حرارة سطح البحر وهي تؤثر عليه بشكل كبير ولغرض فهم هذه العلاقة حسب معامل التذبذب لشمال الأطلسي وارتباطه مع المتغيرات المناخية التي تشمل كل من شذوذ درجات الحرارة السطحية الصغرى والعظمى، لذا استعمل في هذه الدراسة بيانات كل من المركز الوطني (الأمريكي) للتنبؤات البيئية (NCEP) National Center for Environment Prediction، اذا استعملت في حساب معامل تذبذب شمال الأطلسي، وبيانات الهيئة العامة للأحوال الجوية والرصد الزلزالي لحساب شذوذ درجات الحرارة الصغرى والعظمى السطحية لأشهر (كانون الثاني و نيسان و تموز و تشرين الأول) للمدة (1989-2010). أظهرت النتائج ان التغيرات المناخية والمتمثلة بشذوذ درجات الحرارة السطحية والضغط السطحي الجوي فوق مدينة بغداد ترتبط بمعامل تذبذب شمال الأطلسي (NAO) بمعامل ارتباط قيمته (0.168 و 0.201) على التوالي، في حين كانت قيمة معامل الارتباط بين معامل تذبذب شمال الأطلسي (NAO) وشذوذ الضغط السطحي الجوي (-0.240)، لذا يكون تأثير هذه المتغيرات المناخية مع معامل التذبذب لشمال الأطلسي في فصل الشتاء أكثر منه في فصل الصيف.

### INTRODUCTION

The North Atlantic Oscillation is the most important oscillation of atmospheric variability over the North Atlantic Ocean. It defined as the difference between sea level pressure at two stations representing the centers of actions that occur over Iceland and Azores. In calculating the pressure difference between the two pressure systems, Stykkisholmur data in Iceland evaluated using various other stations to represent the more southerly center of action [1]. NAO plays a major role in weather and climate variations over Eastern North America, the North Atlantic, and the Eurasian continents. The NAO Index is defined using winter season; December through March [2][3]. The Northern oscillation has two phases which are positive and negative; the positive phase represents a stronger than usual subtropical high pressure and a deeper than normal Icelandic Low. Accordingly, the negative phase shows a weak subtropical high and a weak Icelandic Low [4].

In the positive phase, there is a strengthening of the Icelandic low and the Azores high lead to further strengthening slope of pressure over the North Atlantic, and then which causes increased wind power and this increase allows cold air of the North American continent somewhat have built himself and moves South [5]. The positive phase occurs when a very large pressure differences between Iceland and the Azores, and this causes more and deeper cross-Atlantic Winter storms in the Northeast direction. Accordingly, it brings heat from the Atlantic to Northwest Europe dwellers and to the warm wet winters there but get dry and cold winter in the Mediterranean region. North West winds strongly moves on the Labrador Sea causing cooling, dwellers and forming new deep water and dry cold winters in Canada, green wind is not formed. In a sea of green so much cool causing the formation of deep water.

Either the negative phase in winter occurs when there is a small pressure difference between those two regions, and

winter storms occurs least and weakest. These storms track more southern tracks associated with the North Atlantic oscillation conditions for positive phase. Accordingly, brings warm moist air to the Mediterranean [6]. In Western Europe, the positive phase factor causes the warm wet winter storm tracks that carry air to the North and the subtropical high levels will prevail. At the same time, the eastern parts of the United States is likely to face a mild and humid winter. Conversely, in negative phase Eastern North America would be more cool air invasions as well as Western Europe, especially the Mediterranean [7].

## RESULTS AND DISCUSSION

To describe the impact factor of the North Atlantic oscillation on surface air temperature and pressure at sea level in (January, April, July and October) for the period (1989-2010) of Baghdad city the relationship between each was drawn.

The method of contrast of surface temperature and surface air pressure to abnormally temperature according to the following equation has been used in this study.

$$T_{\text{anomaly}} = \sum_{i=1}^n \bar{T} - T_i, \dots, (1)$$

*T<sub>anomaly</sub>*: Surface temperature and atmospheric pressure anomaly

$\bar{T}$ : Average surface temperature and atmospheric pressure anomaly

*T<sub>i</sub>*: Surface temperature and atmospheric pressure.

The anomaly of  $T_{\text{min}}$ ,  $T_{\text{max}}$ , and SLP were calculated within two steps:

1. Find monthly average of climate variable for ( $T_{\text{min}}$ ,  $T_{\text{max}}$ , and SLP) for four-selected months at the same period of study.

2. Calculated anomalies of climatic variables by subtract the monthly average of variables from the monthly values of climatic variables

Figures (1), (2) and (3) describe the behavior of minimum and maximum surface temperatures and anomalies pressure at sea level Baghdad for four months for the period (1989-2010).

For  $T_{\text{min}}$  in January, which represented in figure (1,a) act for the time series for the  $T_{\text{min}}$ , anomalies and NAO. The positive phase (same phase) happen in 2008, and 2010 where the values for  $T_{\text{min}}$  (3.09 and -4.03)°C, and for NAO (0.53 and -1.8), while in the negative phase (reverse phase) found in 1992 where the values of  $T_{\text{min}}$ , and NAO equal (2.75)°C, and (-0.66) respectively.

Figure(1,b) shows the series of time in April between  $T_{\text{min}}$ , anomalies and NAO. It has two phases one of them is positive phase in 1992, 2008, and 2010,  $T_{\text{min}}$ , equals (2.44, -1.76 and -1.45)°C, NAO equals (1.88, -1.31 and -0.93), second phase is negative in 1989, and 1998, and these values are also equal (2 and -0.3)°C, and (0.16 and -0.88), respectively.

In July, figure (1,c) shows the relation between  $T_{\text{min}}$ , anomalies and NAO, it confirms two phase of the Teleconnection, the first phase is positive in 1993, 1997, and 2005 and  $T_{\text{min}}$ , are equal to (0.56, 0.48, 0.69)°C, NAO are equal to (-3.14, 0.37, -0.48), the second phase is negative in 2010 (-2.59)°C, (-0.39), respectively.

In October, figure (1,d) shows the time series between  $T_{\text{min}}$ , and NAO, it confers two phases of the link (positive and negative). Positive phase in 1995, 1998, and 2000 and these values equal (2.85, 2.25 and 2.6)°C, (0.72, 0.2 and 1.51), whereas negative phase in 1993 value equals (1)°C, (-0.26), respectively.

Other climate variable named  $T_{\text{max}}$ , Correlated with NAO. In January the time series of both  $T_{\text{max}}$ , anomalies and NAO were shown in figure (2,a), which have positive phase in 2008, and 2010,  $T_{\text{max}}$ , equals (2.6 and -4.55)°C, and NAO (0.53 and -1.8), but it have negative phase in 1992,  $T_{\text{max}}$ , equals (2.77)°C, and NAO equals (-0.66).

The time series of  $T_{\text{max}}$ , anomalies and NAO in April, shown in figure (2,b) that noted two phases, the first phase is positive in 2002, 2008, and 2009,  $T_{\text{max}}$ , that equals (1.27, -3.11 and 0.85)°C, and NAO equals (1.14, -1.31, -0.36). The second phase is negative in 1991, and 1994, these values equal (1.81 and -3.07)°C, and (0.17 and 1.1), respectively.

In July,  $T_{\text{max}}$ , anomalies and NAO that shown in figure (2,c) has positive phase in 1993, 1995, and 2000, that values equal (0.42, 2.04 and -2.66)°C, and (-3.14, -0.19 and -1), while negative phase in 1989, and 2009 and the  $T_{\text{max}}$ , and NAO equal (-1.07 and 1.75)°C, and (1 and -2.11), respectively.

$T_{\text{max}}$ , anomalies correlates with NAO in October and have positive phase in 1995, and 2000 as shown in figure (2,d), that are equal to (1.12, 2.1)°C, and (0.72, 1.51), respectively. while have negative phase in 2007, and 2010 and their values are equal to (-1.69, -1.76)°C, and (1, -0.5), respectively.

In January, Teleconnection between the SLP anomalies and NAO representation in the figure (3,a), it noted that time series has two phases. One of them positive phase in 1992, 2007, and 2008, and their values are equal to (-12.72, -28.91 and -4.66) hpa and (-0.66, -0.25 and 0.53). Another phase is negative in 1995, and 2010 SLP values equal (-14.03 and 10.22) hpa, NAO are equal (0.57 and -1.8), respectively. SLP anomalies in April correlates with the series of time of NAO in having two phases, figure(3,b), one phase is a positive in 1990, 2002, and 2005, and SLP values equal (-0.91, 11.60 and -9.69) hpa, NAO values equal (2.03, 0.14 and -0.47). Second phase is negative in 1995, and 1998 and these values equal (0.72 and -7.83) hpa, (-1.07 and -0.88), respectively.

In July SLP that shown in figure (3,c), correlates with time series for NAO, in having two phases, a positive phase in 1995 and their values equal (9.85) hpa and (-0.19), and negative phase in 1989, 1992 and 2004 and their values equal (-6.82, -12.49 and -10.78) hpa, (1, 0.19, 1.16), respectively.

The time series in October between SLP anomalies and NAO shown in (3,d) noted two phases, one is positive phase in 1997 and equals (-8.04) hpa, the second phase is negative and appears in 1993, 2000, and 2006 and their values equal (-12.67, -0.78 and 5.57) hpa, and (-0.26, 1.15 and -1.92), respectively.

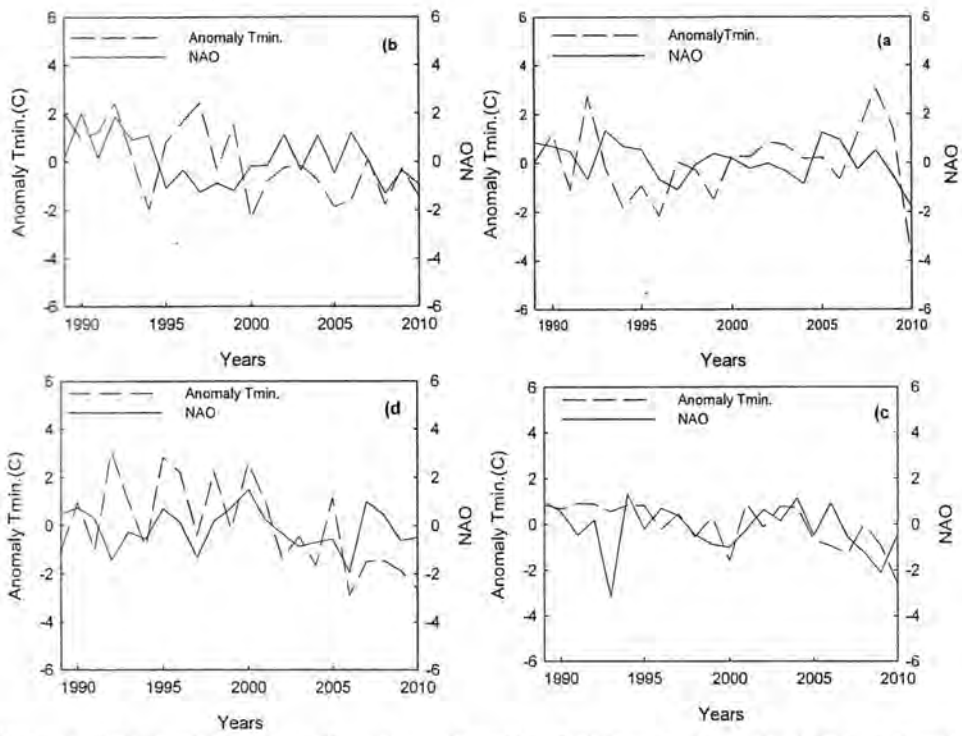


Figure 1 : Relationship between  $T_{min}$ . Anomaly and NAO a) January b) April c) July d) October

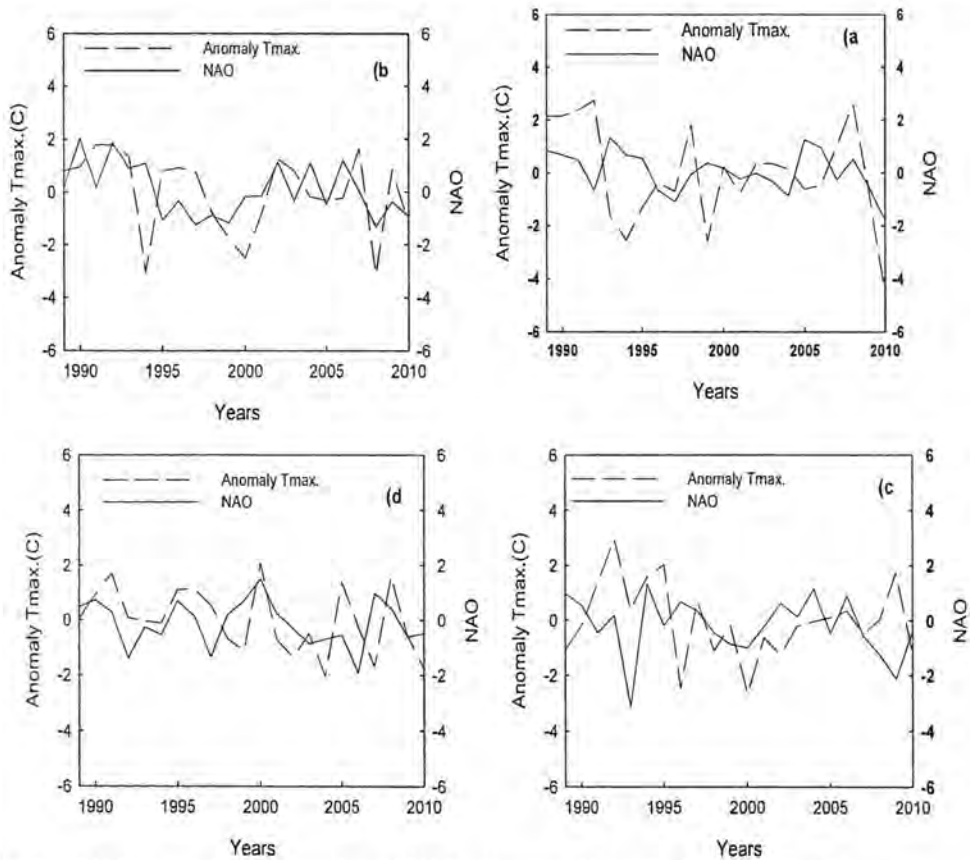


Figure 2 : Relationship between  $T_{max}$ . Anomaly and NAO a)January b) April c) July d) October



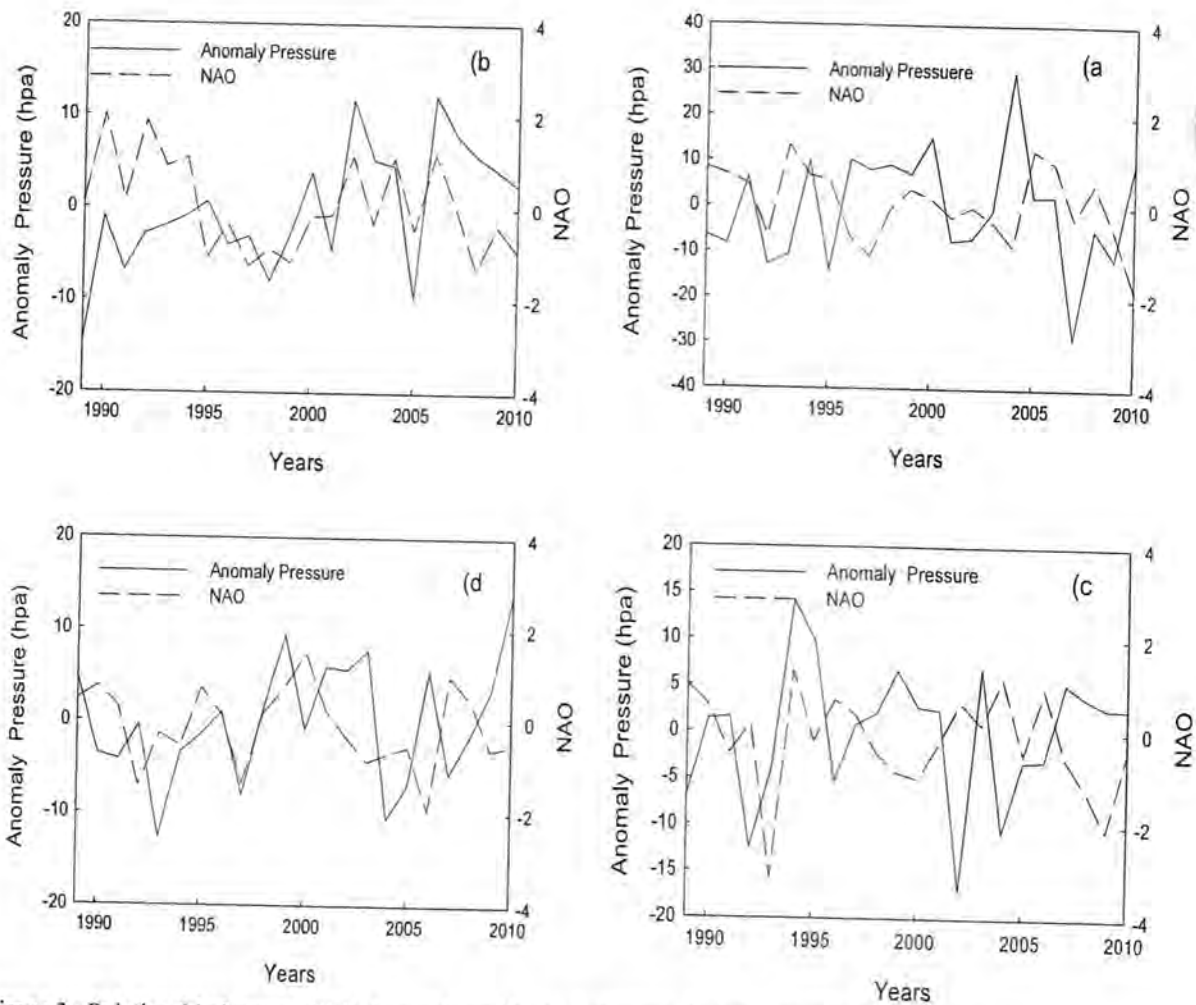


Figure 3 : Relationship between SLP Anomaly and NAO a) January b) April c) July d) October

### CONCLSIONS

Sea surface temperature has a great ability to influence in minimum and maximum surface temperature anomalies and anomaly of sea surface pressure by the North Atlantic oscillation factor .therefore ,it has been found that the value of the correlation coefficient of January between the anomalies of minimum, and maximum surface temperature and surface pressure anomaly with the North Atlantic oscillation factor equals (0.168,0.201and-0.240) respectively, while in April the value of the correlation coefficient between the anomalies of minimum and maximum surface temperature and surface pressure anomaly with the North Atlantic oscillation factor equals (0.039, 0.324 and 0.183), In July the value of the correlation coefficient between the anomalies of minimum and maximum surface temperature and surface pressure anomaly with the North Atlantic oscillation factor equals (0.250, -0.075 and -0.182), while the value of

the correlation coefficient between the anomalies of minimum and maximum surface temperatures and surface pressure anomaly with the North Atlantic oscillation factor equals to (0.319,0.264 and -0.017).

### REFERENCES:

- [1]Howard A.P., and John ,E.O., "The global climate system" ,Cambridge ,New York, Melbourne, Madrid, Cape Town, First published, 2006.
- [2]Yu R., and Zhou T., " Impacts of winter-NAO on March cooling trends over the subtropical Eurasia continent in the recent half century" , Geophysics . Res .Letts. 31,2004.
- [3]Rogers J.C., " North Atlantic storm track variability and it's a ssociation to the North Atlantic Oscillation and Climate variability of Northern Europe ",Journal of climate, 10:1635-1647, 1997.

- [4] Harrell J.W., " Decadal trend in the North Atlantic Oscillation and Precipitation" ,science,269:676-679, 1995.
- [5] Jones P. D., Jonson T. and Wheeler D.," Extension to the North Atlantic Oscillation using early instrumental pressure observations from Gibraltar and south-west Iceland", International Journal of Climatology, 17:1433–1450, 1997.
- [6] <http://www.nc-climate.ncsu.edu/climate/patterns/NAO.html>.
- [7] Latif M., and Barnett T.P.," Causes of decadal climate variability over the North Pacific and North America", Science , 266, :634-637, 1994.



## Seasonal Variations of Atmospheric Radio Noise Field Strength of Sunrise and Sunset during Minimum Solar Cycle Over Baghdad

Fahmi. A. Mohammed

Department of space environment, Center of space and atmosphere sciences, Communications and space directorate, Ministry of science and technology

### Article info

Received 3/9/2014

Accepted 30/11/2014

### ABSTRACT

This paper includes studying the seasonal variations in radio signal strength and its interference, due to atmospheric noise, which is caused by electric discharge in the atmosphere and emitted by thunder-storms at sunrise and sunset during minimum solar cycle, as well as, variations with bandwidth of radio receiver. In general, it is found that interference is stronger in Winter months than in Summer months during sunrise, while it is smaller in Winter months than in Summer months during sunset. It is found that the interference is stronger in Autumn months than in Spring months during sunrise and is stronger in Spring months than in Autumn months during sunset and for any bandwidth used. This investigation also showed that the interference increases with increasing radio receiver bandwidth

### الخلاصة

يهدف هذا البحث الى دراسة التغيرات الفصلية في شدة الاشارة الراديوية وتداخلها، بسبب الضوضاء الجوية والمتكونة عن طريق التفريغ الكهربائي في الجو، والمنبعث بواسطة العواصف الرعدية عند فترتي شروق وغروب الشمس خلال الدورة الشمسية الصغرى بالإضافة الى التغيرات مع عرض حزمة المستلمة الراديوية. بصورة عامة، وجد ان التداخل يكون أكبر في الاشهر الشتوية مما هو عليه في الاشهر الصيفية خلال فترة شروق الشمس في حين يكون اقل في الاشهر الشتوية مما هو عليه في الاشهر الصيفية خلال فترة غروب الشمس. كما وجد ان التداخل يكون أكبر في الاشهر الخريفية مما هو عليه في الاشهر الربيعية خلال فترة شروق الشمس ويكون اكبر في الاشهر الربيعية مما هو عليه في الاشهر الخريفية خلال فترة غروب الشمس ولاي عرض حزمة مستخدمة. وجد ايضا ان التداخل يزداد مع زيادة عرض حزمة المستلمة الراديوية.

### INTRODUCTION

The atmospheric radio noise field strength (in dB referenced to one microvolt per meter), which is dependent on it in this search, and expressed in the following equation:

$$E = F_a + 20 \log f_M + 10 \log b - 95.5 \text{ dB } \mu\text{V/m} \quad (1)$$

Where  $F_a = 10 \log f_a$

$f_a$  is effective antenna noise factor (dimensionless).

$b$  is bandwidth in (Hz).

$f_M$  is the frequency in (MHz).

Is derived, depending on:

1. Noise power spectral density,  $p$

$$p = s A_e = k T_a \quad \text{W}/\text{Hz} \quad (2)$$

Where  $p$  noise power spectral density.

$s$  noise field power spectral density.

$A_e$  effective aperture of the antenna, ( $\text{m}^2$ ).

$k$  Boltzmann's constant =  $1.38 \times 10^{-23}$

Joules/Kelvin.

$T_a$  effective antenna noise temperature in the presence of an external noise field.

2. The available noise power,  $P_R$ , at the antenna output terminals:

$$P_R = p b = s A_e b = k T_a b \quad \text{W} \quad (3)$$

Where  $b$  is bandwidth in Hz (Noise power is proportional to bandwidth).

3. The effective antenna noise factor,  $f_a$ , which is defined as the ratio of noise power available from a loss-free antenna to the noise power generated by a resistor at the reference temperature  $T_o$  (288 K).

$$f_a = \frac{P_R}{k T_o b} = \frac{P}{k T_o} = \frac{s A_{em}}{k T_o} = \frac{T_a}{T_o} \quad (4)$$

Where

$$F_a = 10 \log f_a \quad (5)$$

$P_R$  available noise power from an equivalent loss-free antenna.

$k T_a b$  noise power available in a bandwidth  $b$  from a resistor at temperature ( $T_o$ ).

From (4), we have

$$P_R = f_a k T_o b \quad (6)$$

$$P_R = F_a + 10 \log b - 204 \quad \text{dBW} \quad (7)$$

And

$$P = f_a k T_o \quad (8)$$

$$P = F_a - 204 \quad \text{dBW}/\text{Hz} \quad (9)$$

Where  $10 \log k T_o = -204$ .

$$s = \frac{e_n^2}{120\pi} \quad \text{W}/\text{m}^2/\text{Hz} \quad (10)$$

Then

$$e_n = \sqrt{120\pi s} \quad V/m/\sqrt{H_z} \quad (11)$$

Where  $e_n$  is noise field spectral intensity.

From (4)

$$s = \frac{f_a k T_o}{A_{em}} \quad (12)$$

Substituting (12) into (11) yields:

$$e_n = \sqrt{\frac{120\pi f_a k T_o}{A_{em}}} \quad V/m/\sqrt{H_z} \quad (13)$$

And

$$E_n = 20 \log e_n = F_a + 25.76 - 204 - 10 \log A_{em} \quad (14)$$

Values of  $F_a$  are referenced to a short lossless vertical monopole which has a maximum effective aperture of:

$$A_{em} = 0.0595 \lambda^2 = 0.0595 \left(\frac{300}{f_M}\right)^2 \quad (15)$$

Where  $f_M$  is the frequency in (MHz).

$$\text{Then} \quad 10 \log A_{em} = 37.2 - 20 \log f_M \quad (16)$$

Substituting (16) into (14) gives:

$$E_n = F_a + 20 \log f_M - 95.5 \quad \text{dB } \mu V/m/\sqrt{H_z} \quad (17)$$

Noise field strength,  $e$ , is related to  $e_n$  by:

$$e = e_n \sqrt{b} \quad (18)$$

$$\text{Or} \quad E = 20 \log e = E_n + 10 \log b \quad (19)$$

Substituting (17) into (19) gives the final equation (1) above [1].

For more information about atmospheric radio noise field strength, see the references [2] and [3].

### MATERIALS AND METHODOLOGY

Due to the absence of ionospheric station to measure the critical frequencies of F<sub>2</sub>-layer over Baghdad during 2009, it was derived from International Reference Ionosphere (IRI-2012) model [4], based on the monthly mean predicted sunspot number. The monthly smoothed sunspot number data were taken from Australian radio and space weather services [5]. The global contour maps, which illustrate the predicted distribution of atmospheric radio noise values in the world of frequency of (1MHz) and, also, the variation of mean values of atmospheric noise with the frequency for each season and for every four hours local time, are shown in [6]. The same steps given in [7] were used to calculate the field strength values of atmospheric radio noise.

### RESULTS AND DISCUSSION

The results were listed in the following table:

Table-1 Values of Atmospheric Radio Noise Field Strength at Different Values of Bandwidth during Sunrise and Sunset for Four Seasons Over Baghdad City.

Season	Date	Hour (LT)	Frequency foF2(MHz)	RMS noise field strength (E)in(0.5KHz) bandwidth( $\mu V/m$ )	RMS noise field strength (E)in a (1KHz) band width (dB above $\mu V/m$ )	RMS noise field strength (E) in a (3KHz) band width ( $\mu V/m$ )
Winter	1/1/2009	7	3.22	9.5815	9.7325	9.971
		17	4	9.176	9.327	9.5655
Spring	1/4/2009	6	3.43	9.359	9.51	9.7485
		18	5.8	9.587	9.738	9.9765
Summer	1/7/2009	5	3.3	8.8925	9.0435	9.282
		19	6	9.602	9.753	9.9915
Autumn	1/10/2009	6	4.03	9.579	9.73	9.9685
		18	5.46	9.561	9.712	9.9505

Values of atmospheric radio noise field strength, vary according to seasons variation and during sunrise and sunset, where it is seen from table-1 that, higher value of field strength was (9.5815  $\mu V/m$ ) in Winter at sunrise, while it's lower value, was (8.8925 $\mu V/m$ ) in Summer at sunrise too. As it is seen that higher value was (9.602  $\mu V/m$ ) in Summer at sunset, and lower value was (9.176  $\mu V/m$ ) in Winter at sunset too. It is seen that values of field strength are bigger in Winter than the values in Summer at sunrise, and smaller in Winter than in Summer at sunset. The value of field strength is higher in Winter and Autumn at sunrise than Winter and Autumn at sunset, and the inverse is true for Spring and Summer. The values of field strength vary according to solar activity cycle, where it is seen that, the values are higher in all seasons of 2009(minimum solar cycle) than of it in 1999 (maximum solar cycle) [5]. Finally, the field strength values vary with bandwidth of radio receiver, where it increases from (9.5815  $\mu V/m$ ) when (b is 500 Hz) to (9.7325  $\mu V/m$ ) when (b is 1000 Hz) and to (9.971  $\mu V/m$ ) when (b is 3000 Hz) at sunrise in Winter, while it increases from (9.176  $\mu V/m$ )

when (b is 500 Hz) to (9.327  $\mu V/m$ ) when (b is 1000 Hz) and to (9.5655  $\mu V/m$ ) when (b is 3000 Hz) at sunset in Winter too. The same results are for other seasons and at sunrise and sunset.

### CONCLUSIONS

1. At sunrise, the interference is stronger, during Winter months than Summer months.
2. At sunset, the interference is less, during Winter months than Summer months.
3. At sunrise, the interference is stronger, during Autumn months than Spring months.
4. At sunset, the interference is stronger, during Spring months than Autumn months and for any bandwidth used.
5. The interference increases when the received radio bandwidth increase, and vice versa.
6. The interference is larger during the minimum solar cycle than that during the maximum solar cycle.

## REFERENCES

1. Albert A., Smith J.R., "Radio Frequency: Principles and Applications", The Generation, Propagation, Reception of Signals and Noise, The Institute of Electrical and Electronics Engineers, Inc., New York, USA, 1998.
2. Lossmann E., Meister M.A. and Madar U., "Electronics and Electrical Engineering", No. 6, 112, 2011.
3. Perez R., "Wireless Communications Design Handbook: Aspects of Noise", Interference and Environmental Concerns, Academic Press, USA, 2, 61, 1998.
4. [http://omniweb.gsfc.nasa.gov/vitmo/iri-2012\\_vitmo.html](http://omniweb.gsfc.nasa.gov/vitmo/iri-2012_vitmo.html).
5. <http://www.ips.gov.au/solar/1/6>.
6. ITU, "Radio Noise", ITU-Rep., Geneva, Switzerland; International Telecommunications Union, 2009.
7. فهمي الرحمن محمد فهمي، "حساب شدة المجال للضوضاء الراديوية الجوية للفترتين النهارية والليلية فوق مدينة بغداد"، مجلة علوم المستنصرية، 24(4):73-80، 2013.



## The Index of Ground Water Quality For Selective Area Of Dibdibba Aquifer Southern Iraq Using Gis

Laith Khalil Ibrahim  
Chemistry Department, Collage of Science, Mustansiryah University

### Article info

Received 4/1/2015  
Accepted 23/2/2015

### ABSTRACT

This research aims to apply the Ground Water Quality Index (GWQI) to evaluate the groundwater samples in the selective area of upper part of dibdibba aquifer southern Iraq. The parameters (TDS, Ca, Mg, Na, Cl, HCO<sub>3</sub>, SO<sub>4</sub>, Cd, Pb, Ni, and B) were used to calculate the (GWQI). The analysed values of these parameters were only exceeding the limits of WHO drinking water standard. The results of compared the (GWQI) values in the study area with GWQI water classes type showed that ground water in study area was very polluted and unsuitable for drinking use. The GIS maps show the GWQI values range not only in sample location but for whole study area which useful to choose a less polluted areas for wells drilling.

### الخلاصة

يهدف البحث لاستخدام مؤشر نوعية المياه الجوفية (GWQI) لتقييم نوعية نماذج المياه الجوفية لمنطقة مختارة للجزء العلوي من تكوين الديدبة جنوب العراق. تم اختيار العناصر ( TDS, Ca Mg, Na, Cl, HCO<sub>3</sub>, SO<sub>4</sub>, Cd, Pb, Ni, and B, لغرض حساب المؤشر بحيث ان قيم هذه العناصر قد تجاوزت محدداتها حسب (WHO) لأغراض الشرب. بعد مقارنة نتائج (GWQI) لمنطقة الدراسة مع تصنيف (GWQI) الرئيسي، اتضح ان المياه الجوفية ملوثة جدا وغير صالحة لأغراض الشرب. استخدمت خرائط GIS لتعميم قيم (GWQI) على كل منطقة الدراسة وليس فقط لمواقع النماذج، وبالتالي يعتبر هذا مقيدا لأختيار المناطق الأقل تلوثا لأغراض حفر الآبار.

### INTRODUCTION

Water in all its types is very important for human's life. Surface and ground water are most popular resources for human activities (drinking, domestic uses, industrial, and irrigation). Also, with increasing and development of these activities caused contamination of these water resources more and more. Therefore, a demand for quality evaluation of water resources is very important to ensure safe use. Ground Water Quality Index (GWQI) is an appropriate method for this goal. It's considered as a recent way that most recent studies walk with its lines.

### THE STUDY AREA

The study area lies in the southern of Iraq within Basra governorate including Safwan area. The area also consists of population area and one of most agriculture area. So these activities depend on ground water of upper part of Dibdibba formation in this area. Therefore, the necessity of good water is very important for population and agriculture uses, and that require evaluate ground water and make it suitable for that. Figure (1) shows the location of the samples of surface and ground water within study area.

### AIM OF STUDY

The study aims evaluate the ground water quality in study area for drinking purposes as compared with WHO

standards [1]. That will be done using Ground Water Quality Index (GWQI).



Figure 1: The location of the samples of ground water within study area.

### GEOLOGIC SETTING

The Didibba Formation extends over large area of southern part of Iraq, and its part of alluvial fans deposits of the stable shelf. The age of Dibdibba Formation was Upper Miocene-Pliocene [2]. The formation comprises sand and gravel containing pebbles of igneous rocks (including pink granite) and white quartz, often cemented into a hard grit [3]. The type locality is in the Burjisiya area of the Zubair oil field in south Iraq. The contact of the

formation with the underlying Fatha Formation is conformable in SE Iraq [2].

The formation is often covered by sand sheets or by the alluvial fan sands of Wadi Al Batin [3]. The Dibdibba Formation deposits in study area covered by the Quaternary alluvial fans deposits.

Its sediments are generally known as being changed gradually from marine sediments into river sediments which are crumbs increased (in quantity and the size of granules changed from oldness into moderns, which does not have any index fossils) [4].

### TECTONIC SETTING

According to the tectonic divisions of Iraq, the study area is located within Al-Zubair secondary zone, which is located within the Mesopotamia zone, which belongs to the stable shelf that is characterized by thick sedimentary cover and the disappearance of complex geological structures. Basis on transversal tectonic divisions of Iraq, the study area is located within Basra block. This block is characterized by the presence of many of the subsurface faults, parallel to each other with direction of north east – south west [4].

### HYDROGEOLOGICAL SITUATION

The Dibdibba Formation aquifer in study area contains permeable sandstones (partly pebbly) with beds of mudstone, siltstone, and marl associated with secondary gypsum. It is 30-260 m thick. The sandstones are probably hydraulically connected due to lateral pinch out of the impermeable layers. Available hydrogeological data indicate that the Dibdibba aquifer is complex; stratification affects groundwater movement and chemical composition [3].

Direct rainfall recharge is considered as the a source of recharge in study area The Dibdibba aquifer has high values of permeabilities, direct recharge within rainstorms, accessibility and association with soils suitable for cultivation. The average of infiltration of soil is more than 2 m/day in Safwan area [5].

### DATA COLLECTION AND ANALYSES

The research samples data and its analyses were taken from ministry of water resources. Twenty three samples of ground water (gw 1,....., gw23) were located and taken from study area. The ground water samples were taken from upper part of Dibdibba Aquifer formation for dry sesean.

The data analyses procedure includes the parameters of TDS, and major ions Ca, Mg, Na, Cl, HCO<sub>3</sub>, SO<sub>4</sub>, and NO<sub>3</sub>. Also the trace elements of Cd, Pb, Ni, Fe, Mn, Cu, Zn, and B were analysed.

### GROUNDWATER ASSESSMENT USING (GWQI) FORMULA

This approach consists in producing a set of stochastic simulations, each of which provides a map of the groundwater quality classes. Probabilistic summaries (post-processing) from the set of simulations allow producing maps of different types, so to draw the

boundaries of the contaminated areas and evaluate the uncertainty of such boundaries. Moreover, knowing hydro-geology of an aquifer could make decisions about groundwater monitoring and reclamation easier. Directly simulating groundwater quality index or some parameter related to it is often not enough to produce a realistic numerical model of contamination. Hydro-geology must also be taken into account to characterize the water quality of an aquifer.

There are many common Indexes used different numerical formulas to describe the water quality, like The Water Quality Index Technical Subcommittee was formed by the Water Quality Guidelines Committee of the CCME in 1997 to assess different approaches to index formulation and to develop an index that could be used to simplify water quality reporting in Canada. Also, the National Sanitation Foundation Water Quality Index (NSFWQI), and the British Columbia Water Quality Index are another example [6].

### GROUND WATER QUALITY INDEX (GWQI)

The ground water samples were evaluated using the Ground Water Quality Index which was proposed by [7]. The procedure consists of following steps:

#### 1. Transformation of raw chemical data into rating values (Y) as regards to standards

In order to relate data to global norms, each value of a parameter, P<sub>ij</sub> (field data value of parameter i in cell j), is related to its desired standard value P<sub>id</sub> ([1] drinking water standards considered in present study). Each relative value, X<sub>ij</sub>, can be estimated as:

$$X_{ij} = P_{ij} / P_{id} \quad \dots (1)$$

To express X<sub>ij</sub> as a corresponding index rating value, related to groundwater quality, Y<sub>i</sub> has been assigned to each X<sub>ij</sub> value as follows:

- For good water quality, with X<sub>ij</sub> equal to 0.1, the corresponding index rating value would be around 1;
- For acceptable water quality, with X<sub>ij</sub> equal to 1 (the raw value of the parameter P<sub>i</sub> equal to its standard desired value), the corresponding index rating value would be 5; and
- For unacceptable groundwater quality, with X<sub>ij</sub> equal to or higher than 3.5 (the initial value of the parameter P<sub>i</sub> equal to or higher than 3.5 times its standard desired value), the corresponding index value would be 10.

Operational hydrological experience indicates that Y<sub>1</sub>=1 for X<sub>1</sub>=0.1; Y<sub>2</sub>=5 for X<sub>2</sub>=1; and Y<sub>3</sub>=10 for X<sub>3</sub>=3.5 (usually values of Y<sub>i</sub> lies between 1 and 10).

For any parameter i in any cell j, an adjusted parabolic function of rates Y<sub>ij</sub> = f(X<sub>ij</sub>) can be determined for each cell from 2<sup>nd</sup> order polynomial as in Equation (2):

$$Y_i = -0.712 X_i^2 + 5.228 X_i + 0.484 \quad \dots (2)$$

From this equation the corresponding rating Y<sub>i</sub> can be estimated for any value of X<sub>i</sub>. After this transformation of the field data, the index formula (GWQI) involves only Y values, representing input data for the next step in the development of the indexation formula.

#### 2. The (GWQI) Formula

The proposed GWQI formula is to assess numerically any groundwater quality situation can be stated as a

summation of weights multiplied by respective ratings of various parameters *i* for each cell *j* as follows:

$$IAWQ = C/n \left[ \sum_{i=1}^n (W_i Y_i) \right] \dots (3)$$

Where: *C*=a constant, used to ensure desired range of numbers (in this case, *C*=10); *i*, *n*=number of chemical parameters involved (*i*=1, . . . , *n*).

This value is incorporated in the denominator to average the data; *W<sub>i</sub>*=the relative value of *W<sub>i</sub>/W<sub>max</sub>*, where *W<sub>i</sub>* is a weight for any given parameter and *W<sub>max</sub>* is the maximum possible weight.

Such a weight is a numerical value given to a parameter to characterize its relative anticipated pollutant impact; lower numerical values define lower pollution potential, whilst higher values define heightened pollution potential. A *W<sub>i</sub>* value would be larger if a given parameter were toxic or hazardous to ground water quality. Each parameter *P<sub>i</sub>*, receives a relative weighting (*W<sub>i</sub>*); *Y<sub>i</sub>*=the value of *Y<sub>i</sub>/Y<sub>max</sub>*; where, *Y<sub>i</sub>* is the rating as related to *X<sub>i</sub>* [obtained from Equation (2)], and *Y<sub>max</sub>* is the maximum possible rating for any parameter (*Y<sub>max</sub>*=10).

After viewed the analyses results for groundwater, the parameters shows violated of the WHO standards for drinking water, only chosen to enter to (GWQI) equation. Therefore, the parameters (TDS, Ca<sup>2+</sup>, Mg<sup>2+</sup>, Na<sup>+</sup>, Cl<sup>-</sup>, HCO<sub>3</sub><sup>-</sup>, SO<sub>4</sub><sup>2-</sup>, Ni, Pb, Cd, and B) were chosen to calculate the (GWQI) for groundwater samples (Table 1).

Then, the Weights (*W<sub>i</sub>*) were assigned according to [7] procedure to these parameters based on their Analytical Hierarchy Process (AHP) (influencing) in the human health significance and not in a subjective manner. Table (2) exhibit these Weights.

The group (1) gives maximum weight (5) than other because of the great influence of its parameters on human health more than groups 2, 3, and 4 which give its a less weight (0.38). The extracted weights entered together with other parameters of (GWQI) equation, to calculate the Index of water quality.

Table 1: Percentage and Violation of ground water samples in study area which exceeding the WHO Standards [1]

Parameter	Percentage of samples exceeding the WHO standard	WHO water quality standard
TDS	100	1000
Ca <sup>2+</sup>	100	75
Mg	100	125
Na <sup>+</sup>	100	200
Cl <sup>-</sup>	100	250
HCO <sub>3</sub> <sup>-</sup>	100	200
SO <sub>4</sub> <sup>2-</sup>	100	250
Ni	100	0.02
Pb	100	0.01
Cd	100	0.003
B	82	0.5

Table 2: The (GWQI) parameters Weights (based on [7])

Group	Weights
Group 1 (Ni, Pb, Cd, B)	5
Group 2 (TDS)	1.21
Group 3 (Cl <sup>-</sup> , SO <sub>4</sub> <sup>2-</sup> )	0.65
Group 4 (Ca <sup>2+</sup> , Mg <sup>2+</sup> , Na <sup>+</sup> , HCO <sub>3</sub> <sup>-</sup> )	0.38

**RESULTS AND DISCUSSION**

1. Tables (3) exhibit the (GWQI) values for groundwater samples that were compared with (GWQI) ground water classes' type base on the range of Index values exhibited in Table (4). The value in every cell of Index Value (GWQI) field in Table (4) result from (GWQI) formula of correspond cell values of *Y<sub>i</sub>* field [7].

Table 3: The (GWQI) values for groundwater samples

well	E	N	GWQI
1	47.75	30.19	4.764
2	47.76	30.22	4.398
3	47.79	30.21	4.810
4	47.87	30.23	4.260
5	47.79	30.15	4.608
6	47.81	30.15	4.789
7	47.84	30.12	4.140
8	47.84	30.10	4.377
9	47.79	30.10	4.333
10	47.77	30.08	4.661
11	47.72	30.10	4.824
12	47.75	30.14	3.961
13	47.68	30.16	4.823
14	47.72	30.18	4.025
15	47.81	30.18	4.725
16	47.69	30.15	4.793
17	47.63	30.18	4.056
18	47.60	30.21	4.465
19	47.58	30.16	4.619
20	47.67	30.23	4.199
21	47.75	30.26	4.769
22	47.73	30.28	4.797
23	47.68	30.16	4.615

- 2. The comparison shows that all groundwater samples lie within very polluted class water. So, all samples are not suitable for drinking purposes according to (WHO) standard [1]. Therefore, the ground water in study area need to special treatment operation before any human use.
- 3. Table (3) represents the (GWQI) values just for groundwater samples node location. So, it will need to separate the (GWQI) to cover the whole study area. This method uses the GIS techniques based on interpolates principle which was used by [7]. Therefore, this process was applied for the ground water samples of Dibdbiba aquifer.

Table 4: (GWQI) ground water classes type base on the range of Index values.

<i>Y<sub>i</sub></i>	Index Value (GWQI)	Groundwater Class
1	0.481 (0-0.481)	Very Good
2.5	1.202 (0.481-1.202)	Good
5	2.403 (1.202-2.403)	Permissible
7.5	3.605 (2.403-3.605)	Polluted
10	=>4.806 (3.605-4.806)	Very Polluted

4. Figure (2) shows the (GWQI) GIS map of groundwater in study area. The (GWQI) GIS maps used Arc GIS (V. 10.2) software show the GWQI values range not only in samples location but for whole study area. This will be useful to choose less polluted areas to drill wells in order to give less polluted water which may can treated



subsequent . Figure (3) shows the GIS map of (GWQI) class type based on Table (4). The map shows the very polluted water class.

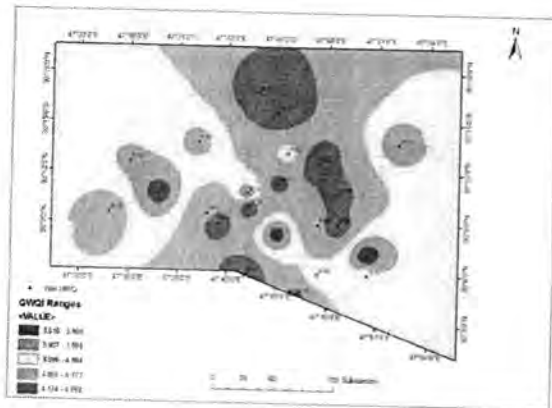


Figure 2: (GWQI) GIS map of groundwater in study area.

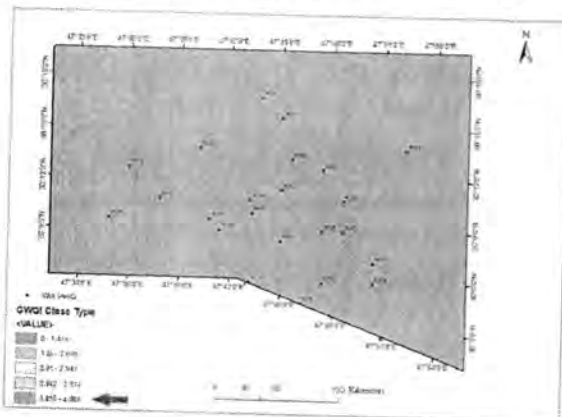


Figure 3: GIS map of (GWQI) class type based on Table (4).

## REFERENCES

1. World Health Organization (WHO). International standard for Drinking water.9th, ed., Geneva, 2007.
2. Bellen, R.C. Van, Dunnington, H.V. and Morton, D. "Lexique Stratigraphique International". Asie Fascicule 10 a. Iraq, Paris, :333, 1959.
3. Jassim, S.Z. and Coff, J.C. "Geology of Iraq". Published by Dolin, Prague and Moravian Museum, Brno, 2006.
4. Buday, T. and Jassim, S. Z. "The regional Geology of Iraq, Vol. 2: Tectonism, Magmatism and Metamorphism". Publication of GEOSURV, Baghdad, 1987.
5. Haddad, R.H. and Hawa, A. j. "Hydrogeology of the Safwan-Zubair area,South of Iraq". Tech. Bull., 132, Sci. Res. Foundations, Iraq, 1979.
6. <http://wqm.igsb.uiowa.edu/wqi/wqi.asp>
7. Hussain, H.M. "Assessment of Ground Water Vulnerability in an Alluvial Interfluvium using GIS", Unpublished Ph.D Thesis, Department of Hydrology, Indian Institute of Technology Roorkee, Roorkee-247 667 (India), 2004.

Vol. 26  
No. 1  
2015

# مجلة علوم المستنصرية

تصدر عن كلية العلوم الجامعة المستنصرية

رئيس التحرير  
أ.د. صاحب كحيط جاسم

مدير التحرير  
أ.م.د. صلاح مهدي الشكري

الكادر الفني

همسة علي احمد  
ميساء نزار مصطفى  
شذى جاسم محمد

[www.mjs-mu.com](http://www.mjs-mu.com)

e-mail: [mustjsci@yahoo.com](mailto:mustjsci@yahoo.com)

Mobile: 07711184399

رقم الايداع في دار الكتب في دار الكتب والوثائق العراقية 278 لسنة 1977

## المحتويات

رقم الصفحة	الموضوع
5-1	دراسة تأثير بعض العزلات الفطرية المعاملة بالنفط الخام على انبات بذور الكرفس اصيل منذر حبه ورامي محمود عيدان و هبة فرحان دلي
11-6	دراسة حول بكتريا <i>Peptostreptococcus anaerobius</i> المعزولة من التهابات قرح الفراش بشرى علي كاظم وياسمين حسن علي
15-12	مقارنة فعالية نبات العرعر الفينيقي وبعض المضادات الحيوية ضد بكتريا <i>pseudomonas aeruginosa</i> و <i>Klebsiella. pneumoniae</i> المعزولة من اصابات الحروق محمد توفيق عبد الحسين و لقاء جميل ابراهيم ونادية كامل بشار
19-16	تأثير حليب جوز الهند ومستخلص أوراق الياس في نمو وحاصل الباقلاء <i>Vicia</i> <i>faba L.</i> وفاق أمجد القيسي و رهن وائل محمود و سناء عبد حمود و زينب عباس الكبيسي
26-20	تقييم تراكيز الغازات $CO$ و $SO_2$ وتأثيرها على الهواء المحيط بمنطقة الجادرية في مدينة بغداد عباس مجيد عناد و عوني ادوار عبد الاحد

## مجلة علوم المستنصرية

مجلة علمية محكمة تصدر عن عمادة كلية العلوم في الجامعة المستنصرية بأختصاصات الكيمياء والفيزياء والرياضيات وعلوم الحياة وعلوم الحاسبات وعلوم الجور. تنشر المجلة البحوث العلمية التي لم يسبق نشرها في مكان آخر بعد إخضاعها للتقويم العلمي من قبل مختصين وباللغتين العربية او الانكليزية وتُصدر المجلة اربعة اعداد سنوياً على الاقل وبكلا اللغتين.

### تعليمات النشر في المجلة

1. يقدم الباحث طلباً تحريراً لنشر البحث في المجلة ويكون مرفقاً بثلاث نسخ من البحث مطبوعة على ورق ابيض قياس (A4, 21.6×27.9 cm) مع ترك حاشية بمسافة انج واحد لكل طرف من اطراف الصفحة ومطبوعة باستعمال برنامج (Microsoft Word, 2007) او (2010) بصيغة (.doc) اضافة الى نسخة الكترونية لأصل البحث مخزنة على قرص (CD).
2. يرفق مع البحث ملخص باللغة الإنجليزية على ان لا تزيد كلمات الملخص عن (150) كلمة.
3. عدد صفحات البحث لا تتجاوز 10 صفحة بضمنها الاشكال والجدول على ان تكون الاحرف بقياس 14 نوع (Time New Roman) وبمسافة مزدوجة بين الاسطر. وينبغي ترتيب اجزاء البحث دون ترقيم وبالخط العريض (Bold) كالآتي: صفحة العنوان، الخلاصة باللغة العربية، الخلاصة باللغة الإنجليزية، مقدمة، المواد وطرائق العمل (الجزء العملي)، النتائج والمناقشة، الاستنتاجات وقائمة المراجع.
4. يطبع عنوان البحث واسماء الباحثين (كاملة) وعناوينهم باللغتين العربية والانكليزية اضافة الى البريد الالكتروني للباحث الرئيس وتطبع على ورقة منفصلة شرط ان لا تكتب اسماء الباحثين وعناوينهم في أي مكان اخر من البحث، وتعاد كتابة عنوان البحث فقط على الصفحة الاولى من البحث.
5. ترقم الجداول والاشكال على التوالي حسب ورودها في المتن، وتزود بعناوين، ويشار إلى كل منها بالتسلسل ذاته في متن البحث.
6. يشار الى المصدر برقم يوضع بين قوسين بمستوى السطر نفسه بعد الجملة مباشرة وتوضع بين قوسين كبيرين مثلاً [1] وفي حالة وجود اكثر من مصدر ويتسلسل فيكتب من الراقم الاول الى الاخير مثلاً [1-4]. تطبع المصادر على ورقة منفصلة، ويستعمل الاسلوب الدولي المتعارف عليه عند ذكر مختصرات اسماء المجلات.
7. يتبع الاسلوب الآتي عند كتابة قائمة المصادر على الصفحة الاخيرة كالآتي: ترقيم المصادر حسب تسلسل ورودها في البحث، يكتب الاسم الاخير (اللقب) للباحث او الباحثين ثم مختصر الاسمين الاولين فعنوان البحث، اسم المجلة، المجلد، العدد، الصفحات الاولى والاخيرة، سنة نشر. وفي حالة كون المصدر كتاباً يكتب بعد اسم المؤلف او المؤلفين عنوان الكتاب، الطبعة، الصفحات، اسم دار النشر، الدولة واخيراً سنة النشر.



## دراسة تأثير بعض العزلات الفطرية المعاملة بالنفط الخام على انبات بذور الكرفس

اصيل منذر حبه و رامي محمود عيدان و هبة فرحان دلي  
الجامعة المستنصرية /كلية العلوم /قسم علوم الحياة

### الخلاصة

اظهرت نتائج دراسة العزلات الفطرية المعزولة من عينات التربة الملوثة بالنفايات البترولية في منطقة القاهرة /بغداد ، تباينا لأنواع الفطريات ونسبة تردها حيث سجل: *Bipolaris hawaiiensis* اعلى نسبة تردد *Fusarium pallidoroeseum* 11.7% و *paecilomyces variotii* 29.4%. وبلغت نسب نمو الفطريات في النفوط الخفيفة (7، 7.5، 4.8، 7.5) سم و النفوط المتوسطة (6، 6.5، 5.5، 7.5) سم ، و اظهرت النتائج تأثير الفطريات على انبات البذور وجود فروقا واضحة في النسب المئوية للإنبات ( قبل وبعد معاملة الفطريات بالنفط الخام ) إذ سجلت % (42.3-59.3) للفطر *Bipolaris hawaiiensis* ، % (30-46.6) للفطر *Emericella nidulans* ، % (36.6-42.6) للفطر *Fusarium pallidoroeseum* و % (28.3-52.3) للفطر *paecilomyces variotii* مقارنة بالسيطرة (100) %، وكان تأثير الفطريات بتثبيط طول الجذير والرويشة قبل المعاملة بالنفط (0 سم) لكل الاجناس . وعلى العكس بلغ معدل اطوال الجذير 1.4، 1.2، 0.5 و 1.4 سم ومعدل اطوال الرويشة 0.8، 0.5، 0.1 و 0.6 سم للفطريات *Bipolaris hawaiiensis*، *Emericella nidulans*، *Fusarium pallidoroeseum* و *paecilomyces variotii* على التوالي بعد معاملتها بالنفط .

### Article info.

تقديم البحث: 2014/11/16  
قبول البحث: 2015/2/23

### ABSTRACT

The study of fungal isolates that collected from petroleum-contaminated soils in different locations in al qahira/ Baghdad showed a variation in the isolated fungi and the percentage of frequency. Where the record: *Bipolaris hawaiiensis* higher frequency% 35.2, *Emericella nidulans* 23.5%, *Fusarium pallidoroeseum* 11.7%, *paecilomyces variotii* 29.4%. And amounted to fungal growth rates in the light oils (7, 7.5, 4.8, 7.5 cm) and medium oils (6, 6.5, 5.5, and 7.5) cm. The results showed the effect of fungi on seed germination Significant differences in the percentages of germination (before and after the fungus that treated by crude oil) as recorded: (42.3-59.3)% *Bipolaris hawaiiensis* , (30-46.6)% *Emericella nidulans* , (36.6-42.6) % *Fusarium pallidoroeseum* ,(28.3-52.3)% *paecilomyces variotii* compared to control (100)% . effect fungus inhibiting of the length of radicle and plumule isolates the oil before treatment (0 cm) for all genus, on the contrary, radicle lengths averaged 1.4, 1.2, 0.5 and 1.4 cm and average lengths plumule 0.8, 0.5, 0.1 and 0.6 cm for fungi *Bipolaris hawaiiensis*, *Emericella nidulans*, *Fusarium pallidoroeseum* and *paecilomyces variotii* respectively after oil treatment .

### المقدمة

وتحويلها إلى مواد ابسط " التحلل البيولوجي (Biodegradation) ، التمكن (Mineralization) ، التحول البيولوجي (Biotransformation) ، المعالجة الحياتية والتراكم الحياتي (Bioremediation and Bioaccumulation) . تتضمن عملية التحلل البيولوجي لمعالجة التلوث الهيدروكربوني في التربة " تكسير المواد عن طريق سلسلة من التفاعلات البايوكيميائية التي تحدث للمواد الهيدروكربونية . وعند إكمال عملية التكسير تدعى بالتسعين حيث إن الناتج هو ماء وغاز CO<sub>2</sub> ومواد غير العضوية (6) . اما المعالجة الحياتية تكمن في تحويل المواد الأكثر سمية إلى اقل سمية واحدى خطوات المعالجة الحياتية هي التراكم الحياتي الذي تعمل فيه الاحياء على تركيز وتراكم المواد في اجسامها، وقد اشارت بحوث كثيرة حول القدرة العالية للأحياء المجهرية في تحليل المواد الهيدروكربونية (7) . منها Pickard وجماعته (8) حيث اوضح قدرة فطريات white rot fungi على هضم polychlorinated biphenyls، وامتلاك الفطر *Coriolopsis gallica* القابلية على أكسدة 10 مركبات هيدروكربونية باستخدام أنزيم Laccase ، في حين اظهرت دراسة أخرى قدرة *Phanerochaete chrysosporium* لتحليل المواد الهيدروكربونية وذلك لامتلاكه أنزيم لكنين lignin (9) اما اشاره Mancera-Lopez وجماعته (10) عن وجود وتشخيص ثلاثة فطريات

التلوث البيئي كارثة لا حدودا إقليمية لها ومع وجود الرياح والتيارات المائية سيأخذ التلوث البيئي مساحات اوسع . وتحديدا المواد الهيدروكربونية PAHs (Polycyclic aromatic hydrocarbons) فهي احدى ملوثات البيئة يابسة كانت ام ماء (1) ، فهي مركبات عضوية، مقاومة للتحلل منها الالفاتية و الاروماتية (2)، تتجمع بكميات ضخمة جدا في بيئتنا من جراء حرق الوقود ، انبعاثات عوادم السيارات ، عمليات استخراج النفط ، وعمليات سرقفة النفط الخام من انابيب النقل والتخريب الارهابي ، بالإضافة إلى المخلفات الصناعية و عمليات معالجة التربة بمخلفات المجاري كمخضبات تراكيها (1-10) ملغم / كغم من (PAHs) (3) . وتوجد (PAHs) طبيعيا كالتربين ، ايزوبرين ، الأتلين ، الناتج من التنفس البكتيري المعروف بغاز المستنقعات (4)، ومن الاستخدام الواسع للمواد الكهربية بالحقبة الزمنية الاخيرة ادى لرفع نسبة التلوث بالغازات المنبعثة ( CO<sub>2</sub> ، والرصاص ) من عوادم المولدات مسببة بذلك زيادة حالات الصداع والضعف العام والغيبوبة والتشنجات وحالات الإجهاض المتكرر ، انخفاض نسبة الكالسيوم مسببة بذلك هشاشة العظام وتآكل عظام الجسم ، التخلف العقلي لدى الأطفال والأمراض السرطانية (5). اما عن دور الاحياء المجهرية كالبكتريا والفطريات في تحلل المواد الهيدروكربونية يمكن بان كل كائن له دور معين ضمن سلسلة عمليات التحلل والتكسير لهذه المواد

وبعد معاملتها بالنفط وبثلاث مكررات من كل فطر ثم حضنت الإطباق، تم بعدها عد البذور النابتة في كل طبق و اعتماداً على عدد البذور النابتة ومعدل طول الرويشة والجذير في اليوم السابع. استخدمت طريقته الطبق الحاوي على وسط PDA خالي من المستعمرة الفطرية. وحاو على عشر بذور معقمة بثلاث مكررات للمقارنة (17). وبعد ذلك تمت دراسة تأثير العزلات الفطرية على انبات بذور نبات الكرفس في اطباق بتري من خلال عدد البذور النامية وطول الجذير والرويشة .

وحسبت النسبة المئوية لتردد العزلات حسب القانون الآتي (17) :  
النسبة المئوية للتردد = (عدد مستعمرات الجنس أو النوع الفطري / ( العدد الكلي لمستعمرات الأجناس أو الأنواع الفطرية) \* 100

#### النتائج والمناقشة

اظهرت نتائج العزل والتشخيص لعينات التربة الملوثة بتبينها من حيث أنواع الفطريات المعزولة والنسبة المئوية لتردها (جدول 2) . وفيما يخص الفطريات المعزولة فقد تم عزل الفطريات التالية *Bipolaris hawaiiensis* ، *Fusarium* ، *Emericella nidulans* ، *paecilomyces variotii* (صورة 1). وقد اظهر الجنس *Bipolaris hawaiiensis* أعلى نسب مئوية للتردد بلغت 35.2 % ، في حين سجل الفطر *Fusarium pallidoroseum* أقل نسبة مئوية للتردد بلغت 11.7% (جدول 2) (شكل 1).

وبلغت نسب نمو الفطريات في النقوظ الخفيفة (7 ، 7.5 ، 4.8 ، 7.5) سم وفي النقوظ المتوسطة كانت (6 ، 6.5 ، 5.5 ، 7.5) سم للفطريات

*Fusarium pallidoroseum* ، *Bipolaris hawaiiensis* ،

*Emericella nidulans* و *Paecilomyces variotii* على التوالي.

(شكل 2) تتواجد الفطريات في جميع البيئات، ويعود سبب انتشارها الواسع

الى قدرتها على النمو في مدى واسع من درجات الحرارة ، pH و امتلاكها

انظمة انزيمية واسعة تمكنها من تحطيم واستغلال مدى واسع من المركبات

المعقدة، بالإضافة الى انتاجها للسموم (18). مما شجع على استخدام

الفطريات كمحطومات حيوية للمركبات الهيدروكربونية في جميع البيئات

(19). اما في ما يخص تأثير الفطريات على انبات البذور فقد اظهرت النتائج

وجود فروقاً واضحة في النسب المئوية لإنبات البذور (قبل وبعد) لتلويثها

بالعزلات الفطرية إذ كانت النسبة على التوالي *Bipolaris hawaiiensis*

% (42.3-59.3) ، *Emericella nidulans* % (30-46.6) ،

*Fusarium pallidoroseum* % (36.6-42.6) و *paecilomyces*

*variotii* % (28.3-52.3)، مقارنة لمعاملة السيطرة % (100) (جدول 3).

اظهرت النتائج بعد التلويث الفطري للبذور قبل معاملتها بالنفط الى قدرة

الفطريات على تثبيط نمو البذور وربما انتاج السموم في أو على البذور مما

يؤدي الى خفض نسبة الانبات [20] ، اما الزيادة الطفيفة في نسبة الانبات

المئوية بعد المعاملة بالنفط ، قد تعود الى فعاليته مركبات النفط المتحللة على

تحفيز وزيادة نشاط الهرمون النباتي الجبرلين Gibberellin ، والجبرلين

مركب يتألف من مجموعه كبيره من Tetracyclic Diterpenoid

Carboxylic acid ، ويحوي على 4-5 حلقات من ent-kaurene . حيث

ان استهلاك النفط من قبل الفطريات الموجودة في الوسط كمصدر وحيد

للكاربون ، ادى الى تحطيمه وتحويله الى مركبات ايسط وغير سامه وهذه

المركبات البسيطة ادت الى زيادة نشاط الهرمون مما ادى الى نمو البذور

على الرغم من تواجد الفطريات المثبطة لنموها شكل (3) . حيث اثبتت

الفطريات القدرة على تحليل النقوظ نتيجة لإنتاجها الانزيمات التي تعمل على

تحطيم وتحليل النفط الخام [20] . اما في ما يخص تأثير الفطريات على

الجذيرات فقد اظهرت وجود انخفاض و تثبيط طول الجذير للبذور قبل

معاملة العزلات الفطرية بالنفط ، مقارنة بطوله عند استخدام بذور المقارنة

المعاملة بالماء المقطر (1.5 سم) فقط (جدول 4)، إذ وصلت نسبة تثبيط الى

(0 سم) لكل الاجناس الفطرية. ويعزى الانخفاض الحاصل بالنمو الى تأثير

نمو الفطريات او انزيماتها او سمومها في منع تخليق واحد او أكثر من

هرمونات النمو (الوكسين والجبرلين والسابتوكينين) ١ و نتيجة لتخليق

انزيمات محطمة لها IAA oxidase كما هو الحاصل في العديد من

النباتات نتيجة الإصابة بالمسببات المرضية ، وعلى العكس حيث تأرجحت

معدل اطوال الجذيرات بعد معاملة الفطريات بالنفط على النحو التالي

*Bipolaris hawaiiensis* (1.4) ، *Emericella nidulans* (1.2) ،

لها القابلية لإزالة الهيدروكربونات وهي *Rhizopus sp* .

*P.funiculosum* ، *A.sydowii* .

يعد نبات الكرفس (*Apium graveolens* (Celery) ، والذي يعود إلى

العائلة الخيمية Umbelliferae ، من الخضروات المهمة طبيياً لاهميته في

علاج مرض فقر الدم، الخناق، النقرس، الارتفاع الزائد لضغط الدم، ارتفاع

الكوليسترول، خافض لحمض اليوريك، ومنشط جنسي كما انه مزيل للسمنة

وينصح به للأشخاص المصابين بالسكر والتهابات المفاصل والروماتيزم

والتهاب الكلى وحماية الكبد من التليف. وفي العديد من الدراسات على

الحيوانات مختبرياً أظهرت بذور الكرفس فعالية ومقدرة عالية على منع

نمو الخلايا السرطانية، ويكون بذلك لها تأثير وقائي قوي ضد احتمالية

الإصابة بسرطان القولون والمستقيم [11].

ونظراً لمشاكل التلوث البيئي التي تعاني منها جميع مدن عراقنا الحبيب ، تم

تسليط الضوء على احد مصادر التلوث ، فقد استهدفت هذه الدراسة الى تقييم

قدرة بعض الفطريات المعزولة من التربة الملوثة بالمخلفات النفطية ودراسة

مدى تأثيرها على نبات الكرفس *Apium graveolens* ، وطول الجذير

و طول الرويشة.

#### المواد وطرائق العمل

لقد تم جمع عينات من التربة الملوثة بالمخلفات النفطية من محطات تجهيز

الوقود والكراجات و محال تصليح السيارات في منطقة القاهرة في بغداد.

كانت هذه التربة متعرضة للتلوث على مدى 15 عاما الماضية. عشرة

عينات من التربة جمعت بصورة عشوائية على بعد 3 و 5 و 10 امتار من

مركز التلوث (النقطة الاكبر لتلوثا)، حملت و نقلت العينات بكيس بلاستيكي

معقم الى المختبر مباشرة بعد تسجيل المعلومات عليها. بعد ذلك تمت عملية

مجانسة الحجم الحبيبي بوساطة منخل ( 2 ملم ) و تم ازالة الحصى.

لأغراض فصل مستعمرات الفطريات الأولية، نقل 1 غرام من التربة

بواسطة ملعقة معقمة الى انابيب اختبار تحتوي 10 مل من الماء المقطر

المعقم (stock) ، اجري بعد ذلك سلسلة من التخفيف وصولاً الى التخفيف

الثالث (10<sup>-3</sup>) ، تم بعد ذلك اضافة 1 مل من كل تخفيف الى وسط Potato

(PDA) Dextrose Agar ، المحضر. اضيف المضاد الحيوي

Chloramphenicol (50 mg L<sup>-1</sup>) الى الوسط بعد التعقيم ليثبط النمو

البكتيري ، بعد ذلك تم حضن العينات في درجة حرارة 28 - 31 م° لمدة 7

ايام بالاعتماد على نسبة نمو الفطريات (12). شخّصت الفطريات النامية

بالاعتماد على المفاتيح التصنيفية (13 و 14) ، للحصول على عزلات فطرية

نقية ، تم اجراء زرع ثانوي (sub culture) للعزلات المعزولة وحضنت

لمده 5 ايام بدرجة حراره 25 م°، في هذه الاثناء تم تحضير الوسط السائى

(water agar) بأذابة 20 غم من agar في 1 لتر من الماء المقطر. يوزع

المحلول الناتج في قناني بمعدل 100 مل لكل قنينة ، تم تعقم القناني الحاوية

على الوسط بجهاز التعقيم ( بدرجة 121 منوي و ضغط 15 باوند / انج 2

لمدة 15 دقيقة ) . من ثم يضاف 20 مل من النفط الخام لكل قنينة (15). اخيراً

يصب المحلول في اطباق بتري و يترك الى ان يتصلب.

لُحقت الاطباق بقرص قطره 0.5 سم من طرف مستعمرة نقيه بعمر 3 ايام

، ثم حضنت العزلات في درجة حرارة الغرفة ( 28 - 31 منوي ) لمدة

عشرين يوماً. لاختبار قدرة الفطريات المعزولة من التربة الملوثة على النمو،

استخدمت عينتين من النفط الخام و المحللتين في المعهد الامريكي

(GEOMARCK RESEARCHES INC.) للحصول على النسبة

المئوية للمكونات العضوية. ان ملخص النتائج الجيوكيميائية تختصر النتائج

للاستفادة من المعلومات النفطية. اخذت العينات النفطية من ابار نفطية في

جنوب العراق وكما موضح معلوماتها في الجدول (1) حيث ان العينتين كانتا

من نوع النقوظ الخفيفة والمتوسطة ذات درجة جودة 36.7 و 27.5 على

التوالي حسب تصنيف معهد البترول الامريكي. يعطي ملخص النتائج

الجيوكيميائية معلومات عن نسب المركبات نوع (saturate) ،

(aromatic) ، النابتروجين، الكبريت، الاوكسجين، والاسفلتئين. وتعتبر كل

هذه المعلومات مهمة في تقييم قدرة الفطريات لتحليل انواع النفط الخام

(16). وضعت البذور في اكياس من النايلون المعقمة والمحكمة الغلق .

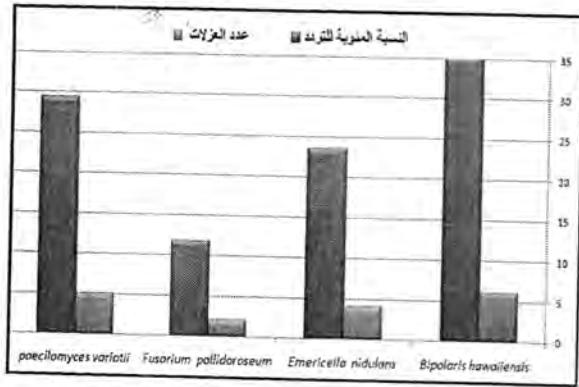
عقمت البذور بمحلول هيبوكلوريت الصوديوم 5% ولمدة 5 دقائق ، بعدها

رشح المحلول المعقم ، ونقلت البذور إلى ماء مقطر معقم للتخلص من تأثير

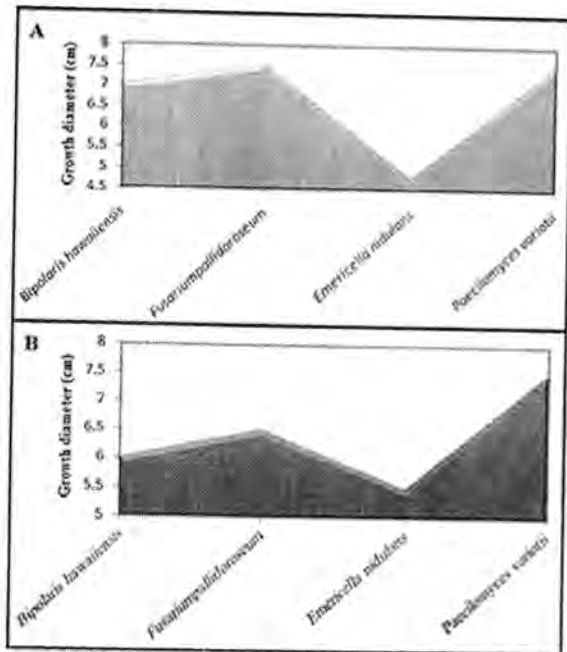
المادة المعقمة ، ثم جففت البذور باستخدام ورق النشاف المعقم ونقلت بوساطة

ملقط معقم وربتت في اطباق بتري بمحيطين متبادلين وواحدة في المركز ،

مع ترك مسافة 2سم بين بذرة وأخرى الحاوية على المستعمرة الفطرية قبل



شكل 1: يوضح النسب المئوية للتردد وعدد العزلات لكل فطر من الفطريات المدروسة.



شكل 2: يوضح نسبة نمو الفطريات المستعملة في الدراسة على عينات النفط الخام من النوع الخفيف (API 36.7)، (B) النوع المتوسط (API 27)

جدول 3: النسبة المئوية للإنبات قبل وبعد معاملة العزلات الفطرية بالنفط الخام

الفطر	بذور نبات الكرفس	
	النسبة المئوية للإنبات قبل المعاملة بالنفط الخام	النسبة المئوية للإنبات بعد المعاملة بالنفط الخام
Bipolaris hawaiiensis	42.3 %	59.3 %
Emericella nidulans	30 %	46.6 %
Fusarium pallidoroseum	36.6 %	42.6 %
paecilomyces variotii	28.3%	52.3%
control	100%	100%

*paecilomyces variotii* (0.5) *Fusarium pallidoroseum* (1.4) سم وان دلت النتيجة على تحفيز هرموني للنبات التي ادت الى نتيجة ايجابية في زيادة معدل اطوال الجذير بوجود النفط (شكل 4) [20]. تم قياس التثبيط بمعدل طول الرويشة للنبات قبل معاملة العزلات نفطياً، مقارنة بطول الطبيعي (1) سم، حيث وصلت نسبة التثبيط الى (0 سم) لكل الاجناس الفطرية (جدول 5). وقد يعود التأثير لنقص السبب في ان السموم الفطرية تثبط واحد او اكثر من هرمونات النمو او تم تخليق انزيمات فطرية محطمة للهرمونات. في حين كانت معدل اطوال الرويشة على النحو التالي بعد المعاملة بالنفط *Bipolaris hawaiiensis* (0.8) *Emericella nidulans* (0.5) *Fusarium pallidoroseum* (0.1) *paecilomyces variotii* (0.6) وتؤكد النتيجة على تحفيز الهرمونات النباتية مثل السيتوكينينات Cytokinins هرمونات منشطة للانقسام الخلوي فهو يعتبر هرمون الشباب في النبات (شكل 5) [20].

التوصيات:

- عمل دراسة كروموسومية و جينية للنباتات بعد تلوينها بالفطريات النامية بالوسط النفطي .
- دراسة تغاير الانزيمات في الفطريات المختلفة.
- دراسة شاملة لأنواع الترب وقابليتها على الاستفادة من الكائنات الحية المجهرية كعوامل مفيدة للإنبات وعمل دراسة جيو-أحيائية لمعرفة فيما اذا كانت الملوثات النفطية تصلح كسماد مغذي للتربة بوجود او عدم وجود الكائنات الحية الدقيقة.

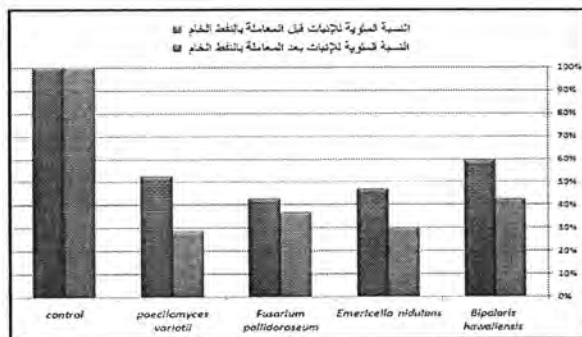
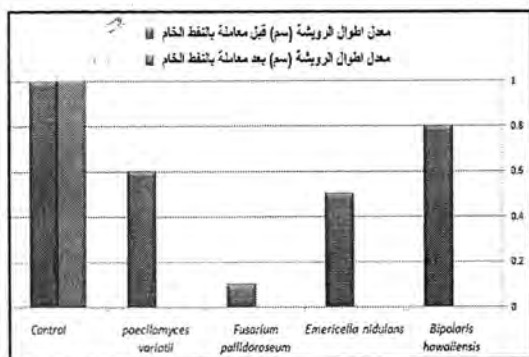
جدول 1: نتائج تحاليل عينات النفط الخام المستخدمة في البحث والتي تمت في مؤسسة الجيومارك الامريكية وتشتمل على نوع النقط، وزنه النوعي، محتواه الكيميائي، ونظائر الكاربون 15 فيه.

Well and formation name	Lu 3, Mishrif Formation	Lu 3, Zubair Formation
Oil Type	Light	Medium
API Gravity	36.7	29
% < C15	50.4	36.1
% S	1.93	1.98
C15+ Saturate	-27.40	-27.68
C15+ Aromatic	-27.05	-27.45
Canonical Variable	-2.38	-2.65
Saturate %	59.2	46.5
Aromatic %	30.6	38.7
NSO %	10.2	11.5
Aspheltene %	0.0	3.3

- NSO = مجموع عناصر النيتروجين والكبريت والاكسجين في العينة المحللة.
- (Lu 3) هو بئر نفطي في حقل الحميس النفطي جنوب العراق، ينتج النفط من تكويني المشرف والزيبر.

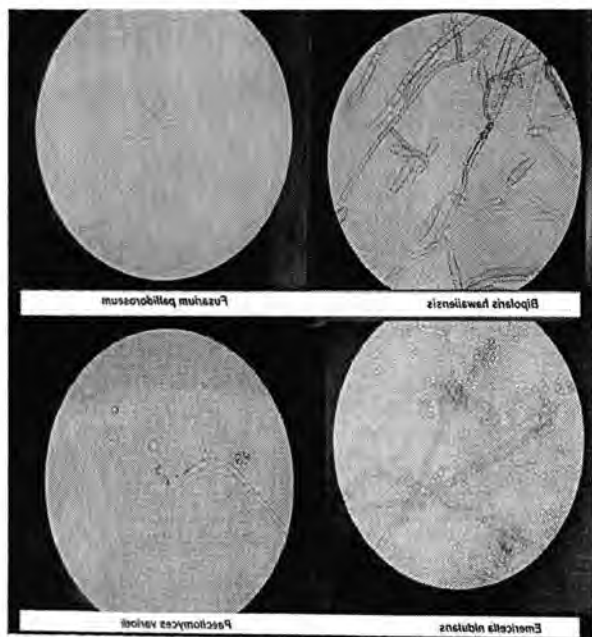
جدول 2: الفطريات المعزولة من التربة الملوثة مع عدد عزلاتها والنسبة المئوية لتردها

الفطر	التربة الملوثة	
	عدد العزلات	النسبة المئوية للتردد
Bipolaris hawaiiensis	6	35.2%
Emericella nidulans	4	23.5%
Fusarium pallidoroseum	2	11.7%
paecilomyces variotii	5	29.4%



شكل 3: يوضح النسبة المئوية للإنبات قبل وبعد اضافة النفط الخام للزلات الفطرية.

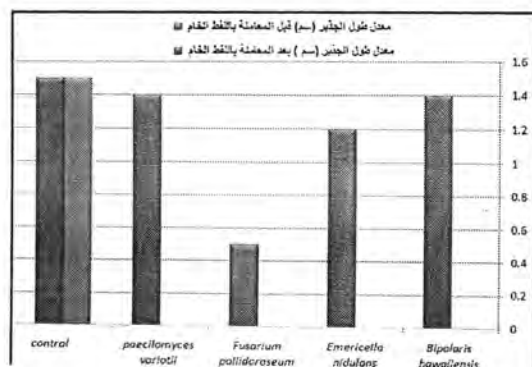
شكل 5: يوضح معدل اطوال الرويشة لنبات الكرفس (سم) قبل وبعد معاملة العزلات الفطرية بالنفط الخام



صورة 1: انواع الفطريات الاربعة التي تم عزلها

جدول 4: طول الجذير قبل وبعد معاملة العزلات الفطرية بالنفط الخام.

الفطر	معدل طول الجذير (سم) قبل معاملة بالنفط الخام	معدل طول الجذير (سم) بعد معاملة بالنفط الخام
Bipolaris hawaiiensis	0	1.4
Emericella nidulans	0	1.2
Fusarium pallidoroseum	0	0.5
paecilomyces variotii	0	1.4
Control	1.5	1.5



شكل 4: يوضح معدل طول الجذير (سم) قبل وبعد معاملة العزلات الفطرية بالنفط الخام.

جدول 5: معدل اطوال الرويشة سم قبل وبعد معاملة العزلات بالنفط الخام.

الفطر	معدل اطوال الرويشة (سم) قبل معاملة بالنفط الخام	معدل اطوال الرويشة (سم) بعد معاملة بالنفط الخام
Bipolaris hawaiiensis	0	0.8
Emericella nidulans	0	0.5
Fusarium pallidoroseum	0	0.1
paecilomyces variotii	0	0.6
Control	1	1

#### المصادر

- [1] Pickard ,M.A.,Roman ,R., Tinoco ,R. and Duhalt ,R.V.1999. Polycyclic aromatic hydrocarbon metabolism by white rot fungi and oxidation by *Coriopsis gallica* UAMH8260 Laccase. AEM 65, no 9 ,3805-3809.
- [2] Awad, Kazem Mahot (1986) Principles of soil chemistry. The Ministry of Higher Education and Scientific Research, the University of Basra.
- [3] Wild, S. R. and Jones ,K.C. 1993 .biological and abiotic losses of polynuclear aromatic hydrocarbons (PAHs) from soils freshly amended with sewage sludge .Environmental. Toxicology .Chem. 12(1) : 5-12.
- [4] Cerniglia,C.E. 1997 .Fungal metabolism of polycyclic aromatic hydrocarbon :past ,present and future application in bioremediation. J Ind Microbial .Biotechnol 19:324-333.
- [5] Khansa, Bioar. (2005) oil and its importance and its risks and challenges .. Netherlands.



- Brace Jovanovich Publishers London. New York. Toronto. Sydney.SanFrancisco.Vol.1.Academic Press.1980.
- [15] Lingappa, Y. and J. L. Lockwood. Superior media for isolation of actinomycetes from soil. *Phytopathology* 50:644. 1960.
- [16] Waples, D.W., and Machihara, T. Biomarkers for Geologist. AAPG Methods in Exploration Series.9:91. 1991.
- [17] M. A. Mia; S. B. Mathur and P. Neergard, Gerlacia oryzae in rice seed. *Trans. Br. Mycol Soc.*, 48:337-8. (1985
- [18] Robert , A.S.,Ellen , S.H., and Connie ,A.N.Introduction to Food Borne Fungi Contamination .2Ed.Drukkerij.J.Van Gestol and Zn.Publishers.1:205.1984.
- [19] Okerentugba, P.O. and Ezeronye, O.U .Petroleum degrading potentials of single and mixed microbial cultures isolated from rivers and refinery effluent in Nigeria. *African Journal of Biotechnology* 2(9): 288 – 292. 2003.
- [20] Ekpo, MA., and Ekpo, EI. Utilization of Bonny light and Bonny medium crude oil by microorganisms isolated from Qua Iboe River Estuary. *Nig.J.Microbiol.*20: 832-839. 2006.
- [6] Alexander ,M.1981 .Biodegradation of chemicals of environmental concern .*Science* 211;132-138
- [7] Leahy .J.G. and Colwell, R.R. 1990 *Microbiol .Rev.*54. 305-315
- [8] Pickard ,M.A.,Roman ,R., Tinoco ,R. and Duhalt ,R.V.1999. Polycyclic aromatic hydrocarbon metabolism by white rot fungi and oxidation by *Corioloropsis gallica* UAMH8260 Laccase.*AEM* 65, no 9 ,3805-3809.
- [9] Benner.B.A. ,et al .(1990).Polycyclic aromatic hydrocarbons emissions from the combustion of crude oil on water.*Environ .Sci .Technol .*24 ;1418-1427.
- [10] Mancera-lopes ,M.E. et al.(2007) .Fungi and bacteria isolated from two highly polluted soils for hydrocarbon degradation .*Acta .Chim. Slov .* 54 ,201-209.
- [11] Benefits of celery seeds .
- [12] Harrigan, W.F., and McCance, M.E. *Laboratory Methods of Food and Dairy Microbiology.*Academic Press, London. P:452.1990.
- [13] Samson, R.A., Hoekstra, E.S. and Frisvad, J.C. *Introduction to Food Borne Fungi.*6<sup>th</sup> edition.American Society Microbiology Inc. 2001.
- [14] Domsch ,K.H., Gams ,W., Anderson ,T-H. *Compendium of Soil Fungi.* A subsidiary of Harcourti



## دراسة حول بكتريا *Peptostreptococcus anaerobius* المعزولة من التهابات قرح الفراش

بشرى علي كاظم وياسمين حسن علي  
جامعة بغداد، كلية التمريض

### الخلاصة

جمعت (60) مسحة من التهابات قرح الفراش من المرضى الراقدين. عزلت بكتريا *Peptostreptococcus anaerobius* بنسبة (34.7%) من هذه الإلتهابات، فضلاً عن عزل جراثيم أخرى هوائية ولا هوائية منها *coli* المعزولة هوائياً ولا هوائياً تبايناً واضحاً في حساسيتها للمضادات الحيوية فكانت المضادات *Metronidazole* و *Ciprofloxacin* و *Augmentin* هي افضل المضادات الحيوية لعلاج قرح الفراش، إذ تراوحت حساسية العزلات لها ما بين (66-100%). أكدت نتائج التحري عن عوامل الضراوة لبكتريا *P. anaerobius* ان العزلات البكتيرية اظهرت نتيجة موجبة لإختبار انتاج الهيمولاسين وانزيمات البيتا لاكتاميز واللايباز والبروتيز وانتاج الغشاء الحيوي وبنسبة (100% و 100% و 64.7% و 70.5% و 100%) على التوالي.

### ABSTRACT

(60) swabs were collected from patients with bed sores infection. The bacterium *Peptostreptococcus anaerobius* was isolated from these infections with (34.7%), as well as, others bacteria where isolated aerobically and anaerobically such as *Escherichia coli*, *Pseudomonas aeruginosa* and *Bacteroides fragilis*. The bacteria which isolated aerobically and anaerobically showed clearing differences in their susceptibility to antibiotics and the antibiotics *Metronidazole*, *Ciprofloxacin*, *Cefoxitine* and *Augmentin* were the best antibiotics to treat the bed sores infection, which their susceptibility to them were between (66.6% -100%). The Screening results for virulence factors of *Peptostreptococcus anaerobius* confirmed that the bacterial isolates showed positive results to haemolysin, betalactamase, lipase, protease and biofilm production with percentage (100%, 100%, 64.7%, 70.5% and 100%) respectively.

### Article info.

تقديم البحث: 2014/9/7  
قبول البحث: 2014/11/30

**Key words:**  
Bed sores and  
*Peptostreptococcus*.

أكار الدم، وتتميز مستعمراتها بكونها مدورة مرتفعة قليلاً عن الوسط وذات لون ابيض لامع أو رصاصي مخضر [15، 16]. نظراً لكون الدراسات والبحوث على هذه البكتريا قليلة جداً وغالبية تلك الدراسات مهيمنة بالبكتريا الهوائية ولتسليط الضوء على هذه البكتريا ارتأينا عزلها من إصابات قرح الفراش ودراسة بعضاً من عوامل ضراوتها.

### المواد وطرق العمل

#### جمع العينات:

جمعت (60) مسحة من إصابات قرح الفراش من المرضى الراقدين في ردهات مستشفى بغداد التعليمي والذين تجاوزت فترة وقودهم ثلاثة أشهر ذلك باستعمال مسحات معقمة للفترة من 2014/3/1 ولغاية 2014/6/11، وضعت هذه المسحات بعد اخذ العينات في انابيب حاوية على الوسط الناقل مرق تقيع المخ والقلب المعقم، ثم نقلت الى المختبر لغرض زرعها.

#### زرع العينات:

##### 1. التحضين الهوائي:

زرعت العينات على الوسطين (أكار الدم وأكار الماكونكي) بطريقة التخطيط وحضنت هوائياً بدرجة 37°م لمدة 24 ساعة لغرض عزل البكتريا الهوائية [17].

##### 2. التحضين اللاهوائي:

زرعت العينات على الوسطين (أكار الدم وأكار الدم المسخن) بطريقة التخطيط وحضنت لاهوائياً باستعمال المرطبان اللاهوائي (*anaerobic jar*) ووضع نظام التحضين اللاهوائي *Gas pak* داخل هذه الحاوية ما يوفر ظروف لاهوائية لعزل البكتريا اللاهوائية، ثم حضنت الإطباق بدرجة 37°م لمدة 24 ساعة [18].

#### تشخيص العزلات:

أخذت جميع العزلات البكتيرية النامية في التحضين الهوائي واللاهوائي ونقبت بطريقة التخطيط الرباعي، ثم زرعت على موائل الأكار المغذي في حالة العزل الهوائي وعلى موائل أكار الدم المسخن في حالة العزل اللاهوائي

### المقدمة

تعد التهابات قرح الفراش من الإصابات المهمة جداً والتي تؤدي الى نسبة عالية من الوفيات نتيجة المضاعفات التي تحدث بتطور القرحة والتي تصيب المرضى الراقدين لفترات طويلة [1، 2]. يعرف قرح الفراش (Pressure Sores و Bed Sores) بأنه القرحة الذي يحدث نتيجة للضغط المسلط على الأنسجة الرخوة، ما يؤدي الى منع سريان الدم لتلك الأنسجة واخيراً فقدانها لوظيفتها الفسيولوجية [3، 4]. يحدث هذا القرحة في مناطق مختلفة من الجسم مثل الظهر والجانبين والبطن وجوانب الرأس ومنطقة الكتف والساق والركبة وظاهر القدمين ومنطقة المقعد لاسيما عند المرضى الذين يستعملون الكرسي المتحرك [5، 6]. ويمر قرح الفراش، بدءاً من حدوث الإصابة الى حين فقدان العضو لوظيفته وحدثت مضاعفات أخرى، بأربع مراحل وتعد المرحلة الثالثة من المراحل المهمة جداً والخطيرة، إذ يكون القرحة عرضة للغزو من الاحياء المجهرية الممرضة المختلفة ومن ثم حدوث مضاعفات وتعقيدات أخرى منها وصول القرحة الى العظم والتهاب السحايا والشلل الجزئي وتجترثم وتسمم الدم وحدثت الوفاة في حالة عدم السيطرة على الإلتهاب في الوقت المناسب [7، 8]. إن التهابات قرح الفراش تسببها العديد من البكتريا الهوائية مثل *Escherichia coli* و *Pseudomonas aeruginosa* و *Staphylococcus aureus* فضلاً عن جراثيم أخرى لاهوائية [9]، وتعد بكتريا *Peptostreptococcus anaerobius* من البكتريا اللاهوائية المسببة لهذه الإلتهابات فضلاً عن إحداثها إصابات أخرى مثل التهاب المسالك البولية والتناسلية والتهاب غشاء سقف الفم ولاسيما لدى الاطفال، إذ عزلها العالم *Lewkowicz* سنة 1901 لأول مرة من هذه الإصابات [10-12]، كما تعد إحدى المسببات المهمة لحصى النقبس *Purperal fever* [13، 14]، وهذه البكتريا تعود الى عائلة *Clostridiaceae*، وتتميز بكونها لاهوائية مجبيرة وحجم خلاياها يتراوح بين 0.3 - 2 مايكرومتر وذات شكل كروي وقد تتواجد أحياناً بشكل أزواج او رباعيات او تجمعات او سلاسل قصيرة مؤلفة من 7 - 8 خلايا وهي موجبة لصبغة كرام ولها القدرة على النمو في الاوساط الصلبة الغنية مثل

### 5. التحري عن إنتاج الغشاء الحيوي Biofilm:

اختبرت قابلية العزلات البكتيرية على إنتاج الغشاء الحيوي Biofilm باستخدام طريقة الأنابيب Tube method وذلك بتلقيح العزلات البكتيرية في أنابيب حاوية على وسط مرق التربتون والصويا Tryptone soya broth، ثم حضنت هذه الأنابيب لاهوائياً لمدة 24 ساعة، وبعد انتهاء فترة التحضين لوحظت تكتلات الغشاء الحيوي ولتوضيح النتيجة أكثر سكب العالق الجرثومي واضيف الى الأنابيب (1مل) من محلول صبغة الكرسنال البنفسجية والمحضر بتركيز 1%، ثم قرنت النتائج وسجلت [27].

### النتائج والمناقشة

أظهرت النتائج في حالة العزل الهوائي أن بكتريا *Proteus mirabilis* هي الممرض المائد، إذ عزلت بنسبة (18.29%) تليها بكتريا *S. aureus* إذ عزلت بنسبة (14.63%) جاءت بعدها البكتريا *P. aeruginosa* و *Streptococcus pyogenes* و *E. coli* و *Proteus vulgaris* و *Enterobacter cloacae* و *Klebsiella pneumoniae* والتي عزلت بنسبة (13.41%) و (12.19%) و (10.97%) و (7.31%) و (6.1%) و (6.1%) على التوالي، فيما تأتي البكتريا (*Staphylococcus epidermidis*) و (*Enterococcus faecalis*) و (*Klebsiella oxytoca*) بالمراتب الأخيرة وبنسبة عزل (4.87%) و (3.7%) و (2.43%). هذه النتائج تشير الى ان التهابات قرح الفراش تسببها جراثيم هوائية مختلفة، تلك الجراثيم استطاعت بما تملكه من خصائص وعوامل إمراضية على غزو أنسجة القرح والتغلغل في داخلها وإحداث التهابات في حالة عدم علاجها وبوقت قياسي تؤدي الى فقدان النسيج وظيفته البيولوجية وحدوث حالة الوفاة وهذا يتفق مع [28] والجدولان (1) و (2) يوضحان هذه النتائج ومن الجدير بالذكر أن بعض العينات أظهرت وجود أكثر من نوع واحد من البكتريا لذا اعطيت العزلات أرقاماً إضافية مما جعل عدد العزلات يرتفع من (60) الى (82).

جدول 1: الاعداد والنسب المئوية للبكتريا المعزولة هوائياً من التهابات قرح الفراش

نوع البكتريا	عدد العزلات	النسبة المئوية
<i>Proteus mirabilis</i>	15	18.29
<i>Staphylococcus aureus</i>	12	14.63
<i>Pseudomonas aeruginosa</i>	11	13.41
<i>Proteus vulgaris</i>	10	12.19
<i>Escherichia coli</i>	9	10.97
<i>Streptococcus pyogenes</i>	6	7.31
<i>Klebsiella pneumoniae</i>	5	6.1
<i>Enterobacter cloacae</i>	5	6.1
<i>Staphylococcus epidermidis</i>	4	4.87
<i>Enterococcus faecalis</i>	3	3.7
<i>Klebsiella oxytoca</i>	2	2.43
العدد الكلي للعزلات	82	100

لغرض حفظها واستعمالها في اجراء الإختبارات اللاحقة، بعدها شخصت هذه العزلات باجراء الفحوصات المجهرية والكيموحيوية والتي اجريت طبقاً لما جاء في [19-21]، ثم سجلت النتائج في جدول.

### فحص الحساسية للمضادات الحيوية:

اجريت على البكتريا المعزولة في هذا البحث إختبارات الحساسية لمجموعة من المضادات الحيوية والمستعملة بشكل واسع لعلاج إصابات قرح الفراش مثل (Ciprofloxacin و Cefoxitin و Cephalothin و Amoxicillin و Augmentin و Amikacin و Kanamycin و Metronidazole و Cloxacillin و Ticarcillin)، إذ استعملت اقراص المضادات المذكورة اعلاه والمحضرة تجارياً وحسب التراكيز الموصى بها من قبل منظمة الصحة العالمية، اجري هذا الفحص على وسط أكار مولر - هنتون في حالة البكتريا الهوائية، بينما على وسط أكار الدم المسخن في حالة البكتريا اللاهوائية وباستعمال المرطبان اللاهوائي، ثم حضنت جميع الاطباق بدرجة 37°م لمدة 18 ساعة ثم قيست اقطار مناطق التثبيط وقورنت مع الجداول القياسية وطبقاً لما جاء في [22]، ثم سجلت النتائج في جدول.

التحري عن عوامل الضراوة لبكتريا *Peptostreptococcus anaerobius*

نتخبنت العزلات البكتيرية والتي شخصت على انها تابعة للنوع *P. anaerobius* للتحري عن بعض عوامل ضرورتها وشملت ما يأتي:

1. التحري عن إنتاج السموم المحللة لكريات الدم الحمر *Haemolysin* اجري هذا الإختبار بتلقيح العزلات البكتيرية على وسط أكار الدم المعقم، إذ لقت هذه الاطباق بطريقة التخطيط الرباعي، ثم حضنت لاهوائياً في المرطبان اللاهوائي وباستعمال نظام التحضين اللاهوائي Gas pak بدرجة 37°م لمدة 24 ساعة، ثم قرنت النتائج وسجلت [22].

### 2. التحري عن إنتاج إنزيم *Betalactamase*:

اجري هذا الإختبار باستعمال طريقة اليود *Iodomethod* القياسية السريعة للتحري عن قابلية العزلات البكتيرية على إنتاج هذا الإنزيم، وكما جاء في [24]، ثم قرنت النتائج وسجلت.

### 3. التحري عن إنتاج إنزيم *Lipase*:

درست قابلية العزلات البكتيرية على إنتاج هذا الإنزيم، إذ زرعت هذه العزلات على وسط أكار صفار البيض (egg yolk agar) بشكل خطوط متوازية، حضنت الاطباق بعدها لاهوائياً بدرجة 37°م لمدة 24 ساعة، ثم قرنت النتائج وسجلت [25].

### 4. التحري عن إنتاج إنزيم *Protease*:

اجري التحري عن إنتاج هذا الإنزيم بتلقيح العزلات البكتيرية على وسط أكار حليب الفرز المعقم *Skimmed milk agar* بشكل خطوط متوازية، ثم حضنت الاطباق لاهوائياً بدرجة 37°م لمدة 18-24 ساعة وقرنت النتائج وسجلت [26].

جدول 2: نتائج الفحوصات المجهرية والكيموحيوية للبكتريا المعزولة هوائياً

الفحوصات	<i>Enterobacter cloacae</i>	<i>Streptococcus pyogenes</i>	<i>Enterococcus faecalis</i>	<i>Klebsiella oxytoca</i>	<i>Klebsiella pneumoniae</i>	<i>Proteus mirabilis</i>	<i>Proteus vulgaris</i>	<i>Staphylococcus epidermidis</i>	<i>Staphylococcus aureus</i>	<i>Pseudomonas aeruginosa</i>	<i>Escherichia coli</i>
شكل الخداج	عصوية	كروية	كروية	عصوية	عصوية	عصوية	عصوية	كروية	كروية	عصوية	كروية
تمت المجهر	+	+	+	+	+	+	+	+	+	+	+
تأطها مع صبغة كرام	+	+	+	+	+	+	+	+	+	+	+
التكثيف	+	+	+	+	+	+	+	+	+	+	+
التوريط	+	+	+	+	+	+	+	+	+	+	+
الحركة	-	-	-	-	-	-	-	-	-	-	-
إنتاج الأنتون	-	-	-	-	-	-	-	-	-	-	-
التثبيط الأحمر	+	+	+	+	+	+	+	+	+	+	+
فوكس	+	+	+	+	+	+	+	+	+	+	+
بروس كور	+	+	+	+	+	+	+	+	+	+	+
استهلاك السرات	+	+	+	+	+	+	+	+	+	+	+
تغير الكوكوز	+	+	+	+	+	+	+	+	+	+	+
تغير الكالكوز	+	+	+	+	+	+	+	+	+	+	+
تغير الكالكوز	+	+	+	+	+	+	+	+	+	+	+
تغير الكالكوز	+	+	+	+	+	+	+	+	+	+	+
تغير الكالكوز	+	+	+	+	+	+	+	+	+	+	+
تغير الكالكوز	+	+	+	+	+	+	+	+	+	+	+
تغير الكالكوز	+	+	+	+	+	+	+	+	+	+	+

النتيجة السالبة / - ، النتيجة الموجبة / +

طرائق التعقيم المستعملة في العراق عن تلك المستعملة في الدول الاجنبية، فضلاً عن اختلاف ضراوة البكترياتبعاً لموقع عزلها ومكان إجراء الدراسة، والجدولان (3) و(4) يوضحان تلك النتائج وعن الجدير بالذكر ان (11) عينة لم يظهر فيها نمو في العزل اللاهوائي لهذا حسبت نسبة العزل على ضوء (49) عينة موجبة ظهر فيها نمو جرثومي.

جدول 3: الاعداد والنسب المئوية للبكتريا اللاهوائية المعزولة من التهابات قرح الفراش

نوع البكتريا	عدد العزلات	النسبة المئوية للعزل
<i>Peptostreptococcus anaerobius</i>	17	34.7
<i>Bacteroides fragilis</i>	12	24.48
<i>Clostridium butyricum</i>	10	20.4
<i>Bacteroides urealyticum</i>	5	10.2
<i>Fusobacterium ssp</i>	3	6.12
<i>Propionabacterium freudenreichii</i>	2	4.1
العدد الكلي للعزلات	49	100

في حالة العزل اللاهوائي بينت الدراسة عزل مجموعة من البكتريا اللاهوائية، إذ تصدرت بكتريا *P.anaerobius* المرتبة الاولى اذ عزلت بنسبة (34.7%) جاءت بعدها بكتريا *B.fragilis* والتي عزلت بنسبة (24.48%)، في حين تأتي البكتريا *B.urealyticum* و *C.butyricum* بنسبة 20.4% و 10.2% و *Fusobacterium ssp* بنسب عزل مختلفة (6.12%) و 4.1% على التوالي، في حين عزلت بكتريا *P.freudenreichii* بنسبة (4.1%) وهي أقل نسبة عزل حصل عليها في هذه الدراسة وتشير هذه النتائج الى أن قرح الفراش من الإصابات التي تكون مسبباتها جراثيم لاهوائية لكون هذه البكتريا تتركز إصاباتهما في الجزء العميق من القرع بعيداً عن تعرضها للاوكسجين الجوي ولهذا نجد أن غالبية القرع في المرحلة الثالثة والرابعة والتي يقترب فيها الإلتهاب من العظم تسببها جراثيم لاهوائية ذات فوعة عالية لإحداث الإصابة وهذه النتائج تتفق مع [29] ولاتتفق مع [30] الذي عزل بكتريا *P.anaerobius* بنسبة (16%) من قرح الفراش، وقد يعود هذا الى اختلاف الموقع الجغرافي الذي أجريت فيه الدراسة والى طبيعة

جدول 4: نتائج الفحوصات المجهريه والكيموحيوية للبكتريا المعزولة لاهوائياً

المحوصات	<i>Propionebacterium freudenreichii</i>	<i>Clostridium butyricum</i>	<i>Fusobacterium ssp.</i>	<i>Bacteroides urealyticum</i>	<i>Bacteroides fragilis</i>	<i>Peptostreptococcus anaerobius</i>
شكل الخلايا تحت المجهر	عصوية ذات أشكال مختلفة	عصوية غير منتظمة لوجود السموات الداخلية	عصوية غير منتظمة مع وجود أشكال خيطية	عصوية منتظمة مع وجود خلايا غير منتظمة	عصوية	خلايا مفردة قروية مع وجود أزواج
تفاعلها مع صبغة تروم الحركية	+	+	-	-	-	+
نتائج السموات	-	+	-	-	-	-
التفتيز	+	-	-	-	-	-
تخمير الجلوكوز	+ / حامض / غاز	+	+ / حامض فقط	-	-	+ / حامض غاز
تخمير اللاكتوز	+ / حامض / غاز	+	+ / حامض فقط	-	-	+ / حامض غاز
تخمير السكروز	+ / حامض / غاز	+	+ / حامض فقط	-	-	+ / حامض غاز
نتائج الامون	-	+	-	-	-	+
البوريز	-	-	-	+	-	-

النتيجة السالبة / - و النتيجة الموجبة / +

جدول 5: نتائج اختبار الحساسية للمضادات الحيوية للبكتريا المعزولة هوائياً

نوع البكتريا	Cf *(5)	Ce *(30)	Cl *(30)	AM *(30)	AMC *(30)	AK *(30)	K *(30)	MET *(10)	CX *(1)	TIC *(75)
<i>E.coli</i>	(100)9	(100)9	(33.3)3	(22.2)2	(88.8)8	(66.6)6	(55.5)5	(77.7)7	(0)0	(0)0
<i>E.cloacae</i>	(100)5	(100)5	(100)5	(60)3	(80)4	(60)3	(60)3	(100)5	(40)2	(40)2
<i>E.faecalis</i>	(66.6)2	(66.6)2	(66.6)2	(33.3)1	(66.6)2	(33.3)1	(66.6)2	(100)3	(66.6)2	(0)0
<i>K.oxytoca</i>	(100)2	(100)2	(100)2	(50)1	(100)2	(0)0	(0)0	(100)2	(50)1	(0)0
<i>K.pneumoniae</i>	(100)5	(80)4	(80)4	(40)2	(100)5	(60)3	(60)3	(100)5	(80)4	(80)4
<i>P.aeruginosa</i>	(72.7)8	(63.6)7	(54.5)6	(54.5)6	(100)11	(54.5)6	(36.3)4	(100)11	(18.1)2	(18.1)2
<i>P.mirabilis</i>	(100)15	(80)12	(80)12	(33.3)5	(93.3)14	(66.6)10	(33.3)5	(86.6)13	(13.3)2	(13.3)2
<i>P.vulgaris</i>	(80)8	(70)7	(50)5	(30)3	(90)9	(50)5	(50)5	(80)8	(20)2	(10)1
<i>S.aureus</i>	(75)9	(66.6)8	(66.6)8	(16.6)2	(100)12	(25)3	(41.6)5	(66.6)8	(0)0	(8.3)1
<i>S.epidermidis</i>	(100)4	(100)4	(50)2	(50)2	(100)4	(25)1	(25)1	(100)4	(50)2	(0)0
<i>S.pyogenes</i>	(100)6	(100)6	(100)6	(33.3)2	(100)6	(66.6)4	(66.6)4	(100)6	(83.3)5	(83.3)5

\* تركيز المضاد مقاساً بالميكروغرام لكل قرص.

Metronidazole / MET, Amoxicillin / Am, Kanamycin / K, Cephaloxin/ Cl , Ticarcillin/ TIC, Amikacin / AK, Cefoxitine / Ce , Cloxacillin / CX , Augmentin / AMC, Ciprofloxacin / CF

جدول 6: نتائج اختبار الحساسية للمضادات الحيوية للبكتريا المعزولة لاهوائياً

نوع البكتريا	Cf *(5)	Ce *(30)	Cl *(30)	AM *(30)	AMC *(30)	AK *(30)	K *(30)	MET *(30)	CX *(1)	TIC *(75)
<i>B.fragilis</i>	(100)12	(91.6)11	(75)9	(58.3)7	(75)9	(41.6)5	(58.3)7	(100)12	(41.6)5	(0)0
<i>B.urealyticum</i>	(100)5	(100)5	(100)5	(60)3	(80)4	(60)3	(60)3	(100)5	(60)3	(80)4
<i>C.butyricum</i>	(80)8	(80)8	(70)7	(90)9	(90)9	(90)9	(50)5	(90)9	(80)8	(80)8
<i>Fusobacterium ssp.</i>	(100)3	(100)3	(100)3	(66.6)2	(66.6)2	(33.3)1	(66.6)2	(100)3	(66.6)2	(66.6)2
<i>P.anaerobius</i>	(100)17	(100)17	(100)17	(17.6)3	(58.8)10	(29.4)5	(29.4)5	(100)17	(0)0	(0)0
<i>P.freudenreichii</i>	(100)2	(100)2	(100)2	(100)2	(100)2	(50)1	(50)1	(100)2	(100)2	(100)2

\* تركيز المضاد مقاساً بالميكروغرام لكل قرص.

Metronidazole / MET, Amoxicillin / Am, Kanamycin / K, Cephaloxin/ Cl , Ticarcillin/ TIC, Amikacin / AK, Cefoxitine / Ce , Cloxacillin / CX , Augmentin / AMC, Ciprofloxacin / CF

أن بكتريا *P. anaerobius* تمتلك من عوامل الضراوة بما يمكنها من إحداث التهابات قرح الفراش إذ كانت الممرض السائد من بين البكتريا اللاهوائية المعزولة في هذه الدراسة.

جدول 7: نتائج التحري عن عوامل الضراوة لبكتريا *P. anaerobius*

اسم الإختبار	النتيجة الموجبة	العزلات الموجبة (عدد %)
1- إنتاج Haemolysin	ظهور مناطق شفافة من التحليل الكامل لكريات الدم الحمر حول المستعمرات	17 (100%)
2- إنتاج إنزيم Betalactamase	تحول لون المحلول من الأزرق الى الأبيض خلال دقيقة من رج الانابيب	17 (100%)
3- إنتاج إنزيم Lipase	ظهور مناطق رافقة حول المستعمرات	11 (64.7%)
4- إنتاج إنزيم Protease	ظهور مناطق رافقة حول المستعمرات	12 (70.5%)
5- إنتاج Biofilm	ظهور تكتلات من النمو الجرثومي على جدران الانابيب	17 (100%)



شكل 1: مستعمرات *P. anaerobius* القلبيّة على وسط اكار الدم



شكل 2: النتيجة الموجبة لاختبار الهيموليسين

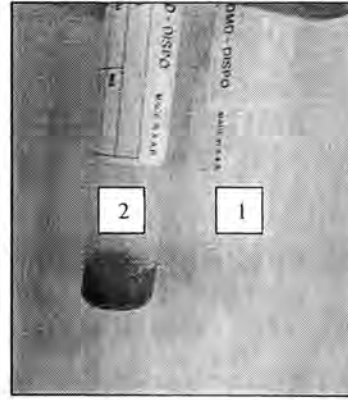
أما فيما يخص إختبار الحساسية للمضادات الحيوية، ففي حالة البكتريا المعزولة هوائياً نلاحظ أن غالبية العزلات أظهرت حساسية للمضادات Cefoxitine و Ciprofloxacin وبنسبة تراوحت بين (63.6% - 100%) وهذه نسبة جيدة تشير الى أن هذين المضادين يمكن استعمالهما في علاج التهابات قرح الفراش وهذه النتيجة تتفق مع [31]، كما نلاحظ أن المضادات Augmentin و Metronidazole كانا مناسبين لعلاج قرح الفراش، إذ أظهرت غالبية العزلات حساسيتها لهما وبنسبة تراوحت بين (66.6% - 100%)، فيما نلاحظ أن غالبية العزلات البكتيرية أبدت حساسيتها للمضاد Amikacin وبنسبة تراوحت (25% - 66.6%) وهذه النتائج اتفقت مع [32]، أما المضادات Amoxicillin و Cephalixin و Kanamycin و Cloxacillin و Ticarcillin فقد أظهرت غالبية البكترياحساسية ضعيفة الى متوسطة لها وحسب ماجاء في الجدول رقم (5) ما يشير أن تلك المضادات نتيجة للاستعمال الخاطئ والعشوائي لها قد زادت من مقاومة البكتريا المسببة لالتهابات القرح لها نتيجة لإمتلاك تلك البكتريا القدرة على إنتاج إنزيمات تؤدي الى تحطيم التركيب الفعال للمضاد الحيوي أو تغيير في نفاذية الغشاء البلازمي بالنسبة للمضاد الحيوي ما يشير الى ضرورة إجراء إختبار الحساسية للمضادات الحيوية قبل الشروع بإعطاء العلاج للمريض الأمر الذي يزيد نسبة نجاح خطة العلاج وشفاء القرح وهذه النتائج تتفق مع [33، 34]، وفيما يتعلق بنتائج إختبار الحساسية للمضادات الحيوية بالنسبة للجراثيم المعزولة لاهوائياً فقد أظهرت غالبية العزلات البكتيرية حساسيتها للمضادات Ciprofloxacin و Cefoxitine و Cephalothin وبنسبة تراوحت بين (70% - 100%) تليها المضادات Amoxicillin و Augmentin و Amikacin وبنسبة تراوحت بين (17.6% - 100%)، إذ أظهرت العزلات تبايناً في حساسيتها لتلك المضادات، فيما نلاحظ أن المضاد Metronidazole يعد من الأدوية المناسبة جداً لعلاج التهابات قرح الفراش المتسببة عن جراثيم لاهوائية، إذ أبدت غالبية العزلات حساسية له وبنسبة عالية تراوحت بين (90% - 100%)، فيما نجد أن العزلات التابعة لبكتريا *P. anaerobius* و *B. fragilis* أظهرت مقاومة بنسبة 100% لمضاد Ticarcillin والجدول رقم (6) يوضح ذلك ما يعطي إشارة واضحة الى ان تلك البكتريا لها القدرة على مقاومة مضادات البيتا لاكتام لإمتلاكها عوامل ضراوة فضلاً عن قدرتها على تحطيم المركب الفعال في تركيب تلك المضادات وجميع هذه النتائج قد اتفقت مع [35، 36].

#### التحري عن عوامل الضراوة لبكتريا *P. anaerobius*:

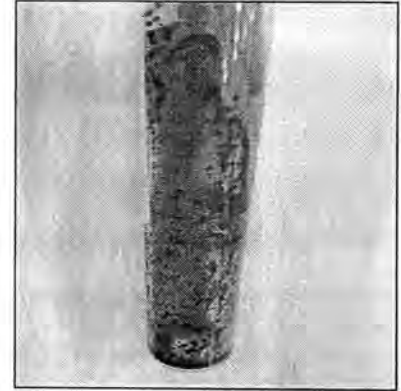
تحريفاً في هذه الدراسة عن إمتلاك بكتريا *P. anaerobius* بعضاً من عوامل الضراوة، إذ أختبرت عزلات هذه البكتريا حول قابليتها على إنتاج السموم المحللة لكريات الدم الحمر Haemolysin فكانت منتجة له بنسبة (100%) وهذه النتيجة تتفق مع [37]، إذ يعد عامل ضراوة مهم جداً للبكتريا إذ يحلل كريات الدم الحمر وبالتالي يساعد على الإنتشار وإحداث الإصابة مسبباً نخر وتحطم للانسجة كما بينت النتائج قدرة هذه البكتريا على إنتاج إنزيم Betalactamase بنسبة (100%)، إذ يعد هذا الإنزيم مهماً جداً في ضراوة البكتريا ومقاومتها لمضادات البيتا لاكتام، إذ يعمل هذا الإنزيم على تحطيم حلقة البيتا لاكتام في نواة البنسلينات والسيفالوسبورينات وكسراً صرة الأمايد ما يجعل البكتريا أكثر مقاومة لهذه المضادات علماً أن تشفير هذه الإنزيمات قد يكون كروموسومياً أو بلازميدياً وهذه النتيجة تتفق مع [8] الذي اشار الى أن (90%) من عزلات بكتريا *P. anaerobius* منتجة لهذا الإنزيم. كما أظهرت النتائج أن هذه البكتريا لها القدرة على إنتاج إنزيمات محللة للانسجة بتأثيرها على المكونات الدهنية والبروتينية الموجودة في الانسجة ما يزيد من قابليتها على غزو النسيج وإحداث قرح الفراش العميق وبالمرحلة الرابعة، إذ أكدت النتائج ان 11 (64.7%) من عزلات *P. anaerobius* لها قابلية إنتاج إنزيم اللايباز وأن 12 (70.5%) منتجة لإنزيم البروتياز و هما إنزيمان مهمان جداً في غزو النسيج وإحداث الإصابة، كما تساهم هذه الإنزيمات في حماية البكتريا من دفاعات الجسم مثل الكلوبولينات المناعية عن طريق تحليلها [38]، كما بينت النتائج قدرة بكتريا *P. anaerobius* على إنتاج الغشاء الحيوي Biofilm والذي يعد من عوامل الضراوة التي تساعد البكتريا على غزو النسيج وتحطيمه والإفلات من عمليات البلعمة ومن تأثير المضادات الحيوية والمطهرات لاسيما الموضعية منها، إذ كانت العزلات 17 (100%) منتجة لهذا الغشاء وهذه النتيجة تتفق مع [39] والجدول (7) والاشكال من (1-6) توضح هذه النتائج، مما تقدم يتبين

المصادر

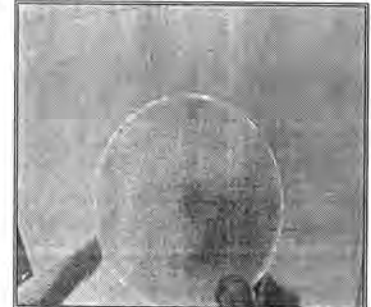
1. Lozano R., "Global and regional mortality from 235 causes of death for 20 age groups in 1990 and 2010 : asystematic analysis for the Global Burden Disease", Lancet, 380(9859): 2095-2128, 2012.
2. Vanderwee K. P.; Clark M.; Dealey C.; Gunningberg L. and Defloor T., "Pressure ulcer prevalence in Europe", J. Eval. Clinic. Practic., 13(2):227-235, 2007.
3. Ubaishat A.; Anthony D. I. and Saleh M., "Pressure ulcers in Jordan ; Apoint Prevalence Study", J. Tissu. Viab., 19(4):132 - 136, 2010.
4. Montroy R. E. and Eltorai I., "Complications of Pressure sore Neglect, Demos", Medical Puplishing Neglect . D. Medical Puplishing, INC, 22(3):15-31, 2003.
5. Thomas D. R.; Diebold M.R. and Eggemeyr L.M., "Acontyolled, Randomized and Comparative, Study of aradiant heat Bandage on the healing of 3-4 Pressure Ulcers", J.Am. Med. Dir. Assoc., 6(1):46-55, 2005.
6. Bain D.S. and Ferguson P.M., "Remote Monitoring of Sitting behavior of People with Spinal Cold injury", J. Rehabil. Res. Dev., 39(4):513-520, 2002.
7. Raahave D.; Friis M. A.; Thiis K. J. and Rasmussen L. B., "The infective dose of aerobic and anaerobic bacteria in postoperative wound sepsis", J. Arch. Surg., 121:924-929, 2002.
8. Aldridage K. E. and Armstronge K.C., "Anaerobes in polymicrobial surgical infections:incidence, pathogenecity and antimicrobial resisstance", Eur. J. Surg., 2(4):573-580, 2003.
9. Ryan K. J. and Ray C. G., "Systematic, Medical Miorbiology", 4th. ed. Mc Graw Hill, 2004.
10. Hibaki S.; Tagawa K. T.; Kagoura M.; Morohashi M. and Yamagishi T., "Characterization of *Peptostreptococcus* species in skin infections", J. Int. Med. Res. 28(3):143-147, 2000.
11. Melvin L. S., "Studies on the anaerobic Streptococci, certain biochemical and immunological properities of anaerobic Streptococci", J. Bacteriol., 39(5) :559-570, 2000.
12. Arak H.; Kuriyama T.; Nakagawa K. and Karassaea T., "The microbial synergy of *Peptostreptococcus* and *Prevotella intermedia* in a urine abscess model", Oral. Microbiol. Immunol., 19(3):177-181, 2004 .
13. White E., "Source of purperal infections with anaerobic Streptococci", J. Obstet. Gynaecol. Brit. Empire., 40(21):630-632, 2003.
14. Colebrook L. and Hard R., "Anaerobic Streptococci associated with purperal fever", J. Obstet. Gynaecol. Brit. Empire., 25(1):609-629, 2002.



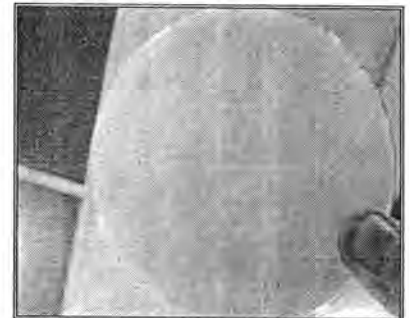
شكل 3: اختبار البيثالاكتاميز ، 1: النتيجة الموجبة ، 2: اختبار السيطرة



شكل 4: النتيجة الموجبة لاختبار انتاج Biofilm



شكل 5: النتيجة الموجبة لاختبار اللايبيز



شكل 6: النتيجة الموجبة لاختبار البروتينيز

30. Hambræus A.; Bengtsson S. and Gurell L., "Anaerobic Bacteria Causing Wound infections after Surgery in a modern operating Suite", Clin. Bacterio. Epidemio. Finding. J. Hyg. Cam., 83(1):41-56, 2000.
31. American Family Physician (Rep.), "Pressure Ulcers:Prevention, Evaluation and Management", 7<sup>th</sup>. Rep. P.(210-225), 2012.
32. Niezgoda J. A. and Mendez E. S., "The effective managements of Pressure Ulcers", Adv. Skin Wound Care., 19(1):3-15, 2006.
33. Guy H., "Preventing Pressure Ulcers Choosing amatress", J. Prof. Nurs., 20(4):43-46, 2004.
34. Baker P. G. and Haig G., "Metronidazole in the treatment of chronic pressure sores and wounds", J. Microbiol. 225(1):569-573, 2001.
35. Brook I., "Treatment of anaerobic infection", Expert. Rev. Ant. Infect. Ther., 5(54):991-1006, 2007.
36. Kaley Z. M.; Zebad G. M. and Tang A. T., "Susceptibility of Anaerobic Bacteria to Betalactam antibiotic and Betalactamase Production", J. Med. Microbiol. Ther., 5(7):301-311, 2006.
37. Osek J., "Detection of enteroaggregative *E. coli* heat stable enterotoxin gene and its relationship with fimbrial and enterotoxin markers in *E. coli* isolated from pigs with diarrhoea", Vet. Microbio., 91(1):65-72, 2003.
38. Omran R., "The virulence factors of *P.aeruginosa* isolated from eye infections", J. Kav. Microbiol., 3:143-155, 2005.
39. Matt M. and Abdul N., "Next Science Wound Gel Technology, A novel agent that inhibit Biofilm developed by Gram Positive and Gram negative Wound pathogenesis", J. Antimicrob. Agent. Chem. Therap., 58(6):3060-3072, 2014.
15. Montejo M.; Ruiz G.; Amutio E. and Hernandez J. L., "Prosthetic valve endocarditis caused by *Peptostreptococcus anaerobius*", Clin. Infect. Dis. 20(1):1431-1436, 2000.
16. Vander K. A. J. and Bakker D. J., "Soft Tissue Infections Including Clostridial Myonecrosis:Diagnosis and Treatment in Hand book of Hyperbaric Medicine. Springer Verlag, K. G., Berlin, Germany, 2000.
17. Murray E.; Anderson D. and Abba, I., "Manual of Clinical Microbiology ", 8<sup>th</sup> ed. Washington DC:ASMPress, 2003.
18. Helen E. M.; Morello J. A. and Paul A. G., "Laboratory Manual and work book in Microbiology. Application To patient care", 8 th ed. The McGraw Hill Company, P. 224, 2006.
19. Chernecky C.C. and Berger B. J., "Laboratory Tests and Diagnostic Procedure", 5th. ed. St. Liuis:Saunders, 2008.
20. Fischbach F. T. and Dunning M. B., "Manual of Laboratory and Diagnostic Tests", 8th. ed. Philadelphia:Lippincott Williams and wilkins, 2009.
21. Pagana K. D. and Pagana T. J., "Mosby's Manual of Diagnostic and Laboratory tests", 4th. ed. St. louis:Mosby Elseerie, 2010.
22. NCCLS., "Performance Standards for Antimicrobial Susceptibility Testirg 40th informational Supplement, M100-S14", Wayne, PA, 2004.
23. Hamando M.M. and Farg D. N., "The effect of aqueous and alcoholic extracts of *Punica granata* . *L. pericarp* on hemolysin production of several bacterial species", J. Science., 1(7):309-316, 2010.
24. Chanal C.; Bonnt R.; Champs C. D.; Sirot D.; Labia R. and Sirot J., "Prevalence of beta-lactamase among 1.072 clinical strains of *Proteus mirabilis*:a 2 year Survey in A French Hospital", Ant. Micro. Agent. Chemo. Therap., 44(7):1930-1935, 2000.
25. Isenberg H. D., "Essential Procedures for Clinical Microbiology", 2nd ed. Washingtone,DC:ASMPress, 2004.
26. Forbes B. A.; Sabm D. E. and Weissfeld A. S., "Baily and Scott's Diagrostic Microbiology", 11th ed. St. Louis:Mosby, 2002.
27. Percival S. L.; Walker H. T. and Hunter P.R., "Microbiological Aspects of Biofilms and Drinking water", Baca Raton, Fl:CRCpress, 2000.
28. Edwards D. J. and Elvans D. G., "Colonization Factor Antigens of Human Pathogenes", Curr. Top. Microbiol. Immunol. 151(2):129-133, 2007.
29. Greif R.; Akca O.; Horn E. P.; Kurz A. and Sessler D. I., "Supplemented perioperative oxygen to reduce the incidence of surgical wound infections", N. Engl. J. Med. 342(11):161-167, 2002.



## مقارنة فعالية نبات العرعر الفينيقي وبعض المضادات الحيوية ضد بكتريا *Klebsiella pneumoniae* و *Pseudomonas aeruginosa* المعزولة من إصابات الحروق

محمد توفيق عبد الحسين و لقاء جميل ابراهيم و نادية كامل بشار  
قسم علوم الحياة / كلية العلوم - الجامعة المستنصرية

### الخلاصة

اجريت هذه الدراسة لغرض المقارنة بين تأثير مستخلص *Juniperus phoenicea* وبعض المضادات الحيوية على عزلات سريرية لبكتريا *Pseudomonas aeruginosa* و *Klebsiella pneumoniae* ولهذا جمعت 40 مسحة من إصابات الحروق من مستشفى الحروق في مدينة الطب و مستشفى الإمام علي (ع) في بغداد للعدة من 2012 / 11 / 20 ولغاية 2012 / 12 / 20 شخصت 9 منها على انها *Pseudomonas aeruginosa* و 15 على انها *Klebsiella pneumoniae* وكانت منها (5) سالبة للزرع البكتيري أظهرت النتائج ان نسبة الإصابة لدى الإناث اعلى من الرجال كانت لدى الإناث 66.6% بينما كان نصيب الذكور 33.4%، كما ظهر ان الفئة العمرية (20-29) سنة أكثر عرضة للإصابة بالحروق. كما بينت النتائج ان لعزلات بكتريا *Pseudomonas aeruginosa* مقاومة عالية لمضاد Cefazidime حيث كانت نسبة المقاومة له 93%، في حين أظهر مضاد Imipenem فعالية ضد بكتريا *Pseudomonas aeruginosa* حيث كانت نسبة المقاومة له 20%. اما عزلات *Klebsiella pneumoniae* أظهر المضاد Imipenem فعالية عالية ضد هذه البكتريا حيث كانت نسبة المقاومة له 18% على عكس مضاد Cefepime حيث أظهر نسبة مقاومة 100% مقارنة بتعالية مستخلص نبات العرعر الفينيقي *Juniperus phoenicea* حيث أظهرت الدراسة بان البكتريا كانت حساسة الى مستخلص نبات العرعر الفينيقي واقل تركيز مؤثر على هذه البكتريا بين (100-400)mg/ml.

### Article info.

تقديم البحث: 2014/12/15

قبول البحث: 2015/2/23

### ABSTRACT

The aim of this study for compared between effect of *Juniperus phoenicea* and some of antibiotic on isolates to *P. aeruginosa* and *K. pneumoniae* and for this were collected (40) smear with burn infection from burn hospital in medical city and Alemam-Ali hospital in Baghdad during the period between November 2012 to December 2012. (15) isolates were diagnosed as *P. aeruginosa*, (11) isolates were *K. pneumoniae* and (5) swabs have no grow. The results showed that percentage of infection in female was 66.6% more than the male 33.4% and the range of age (20-29) year more than the other range years to exposure to burn infection. The results showed that *P. aeruginosa* was sensitive to imipenem with resistant was 20%, while bacteria showed resistant to cefazidime the percentage of resistant was 93%. also *K. pneumoniae* isolates were sensitive to imipenem with the percent of resistance 18%, while the percent resistant to cefepime was 100%. The results showed that *P. aeruginosa* was sensitive to *Juniperus phoenicea* and less of concentration effect on these bacteria between (100-400)mg/dl.

### المقدمة

البكتريا موضعية و سطحية و سرعان ما تنتشر الى الانسجة العميقة بسرعة و تسبب تسمماً sepsis وبالتالي تسبب نسبة وفيات كبيرة (3). يعد إنتاج أنزيم ال  $\beta$ -Lactamase من أكثر المقاومات شيوعاً التي تستخدمها هذه البكتريا تجاه المضادات الحيوية ( $\beta$ -Lactams) يقوم هذا الأنزيم بتحليل هذه المضادات. ونظر لهذا المقاومة التي تبديها الاحياء المجهرية للمضادات اصبح التوجه نحو النباتات الطبيعية كبراً لكونها تحتوي في كل او في جزء من اجزائها على مواد فعالة مؤثرة (4). وقد تناولنا نبات العرعر في دراستنا لانه يعد من النباتات الطبية المهمة فهو يحتوي على زيت طيار و انثولين و مواد سكرية و راتنجية و صمغية و شمعية طعمها مر و يحتوي على مركبات كثيرة تصل إلى 80 مركباً أهمها باينين، بايونيك أميد، كامفين، سدرال، سيدرين، و سيسكوتربين، قلويدات و جلوكوزيدات قلبية و احماض عضوية بالإضافة إلى املاح من اهمها الكالسيوم، وكل جزء منه يستخدم في معالجة الامراض المختلفة فأوراقه و حباته لها استخدامات طبية كثيرة في طب الأعشاب، لأنها مطهرة و مدرة للبول و منبهة و طاردة للريح، و متنوع حب العرعر يساعد في حالات الانتفاخ و عسر الهضم و يستخدم مغلي الفروع لمعالجة الروماتزم المفصلي و العضلي.

الحروق هي الإصابات الحرارية للانسجة و التي تؤدي إلى تخثر و تتخر و أنسجة الجسم التي تتعرض لمسببات الحروق . يعاني الآلاف من البالغين و الأطفال سنوياً من إصابات الحروق و تعد الحروق المتسببة عن التماس بالنار هي السبب المسبب الحادي عشر من مسببات الوفيات لدى الأطفال (1). الأنواع البكتيرية التي تصيب الحروق هي البكتريا الموجبة لملون كرام و على وجه الخصوص *Staphylococcus methicillin-resistant aureus* (MRSA) و البكتريا السالبة لملون كرام و على بكتريا *Pseudomonas* و *Klebsiella sp.* و تأتي أهمية هذه الممرضات من ابدانها مقاومة متزايدة للعديد من المضادات الحيوية (2). تظهر ال *Pseudomonas aeruginosa* إحدى الممرضات المتواجدة في بيئات المستشفيات حيث تسبب عدوى الإصابات المكتسبة من المستشفيات Nosocomial infection و التي تحدث التهابات خطيرة تؤدي بحياة مريض الحروق الشديدة، تسود هذه البكتريا ضمن مجموعة البكتريا السالبة لملون كرام و يعزى خطر هذه البكتريا الى امتلاكها العديد من اليات المقاومة للعديد من المضادات الحيوية و تكسب المقاومة لبقية المضادات الحيوية بشكل سريع جداً، و سيادة بكتريا *P. aeruginosa* في جروح الحروق يأتي من قابلية هذه البكتريا على التواجد في البيئات الرطبة و الدافئة، كما أن العدوى بهذه البكتريا خطيرة جداً و صعوبة في معالجتها، تبدأ الإصابة بهذه



**تحضير المستخلص المائي الحار لنبات العرعر**  
اتبعت الطريقة التي ذكرها (11) وتضمنت اخذ 25 غم من المسحوق النباتي واضيف له 250 مل من الماء المغلي ووضع في حاضنة هزازة في درجة حرارة 28 ولمدة 30 دقيقة بعدها رشح المزيج باستعمال شاش طبلي ثم وزع الراشح في انابيب الطرد المركزي وبسرعة 3000 دورة /دقيقة لمدة 10 دقائق من ثم جمع الراشح ووضع في اطباق ذات مساحة سطحية كبيرة وجفف الماء في الفرن oven الى ان يتبخر كلياً من بعدها تم الحصول على مسحوق المستخلص المائي الحار وضعت العينة في انبوبة زجاجية محكمة الغلق ومعممة لحين الاستعمال.

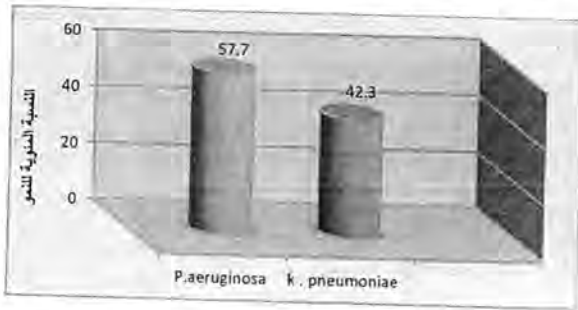
#### اختبار فعالية المستخلص النباتي

اعتمدت طريقة الحفر Agar-welldiffusion اذا استخدم وسط Muller-hintonagar ونشر العالق البكتيري باستخدام قطيلات قطنية معقمة وتركت الاطباق لمدة 15 دقيقة بعد ذلك عملت تقويب بالوسط الزراعي باستخدام ثاقب الفلين المعقم قطرهم 5ملم، اضيف الى كل حفرة 0.05 مل من المستخلص بالتركيز (400,350,300,250,200,150,100,0) ملغم/مل، والذي عمق من خلال امراهه على ورق ترشيح (Millipore filter) بسماية 0.4 مايكروميتر، تم تحضير التراكيز باستخدام القانون التالي CIVI=C2V2، حضنت الاطباق في درجة حرارة 37 لمدة 24 ساعة، اجريت التجربة بثلاث مكررات، تم قياس منطقة التثبيط حول كل حفرة بالمليلتر (12).

#### النتائج والمناقشة

##### عزل وتشخيص البكتيريا

تم جمع (40) مسحة لمرضى مصابين بالحروق من مستشفى مدينة الطب و مستشفى الإمام علي(ع) في مدينة بغداد جميع المرضى الخاضعين للدراسة كانت حروقهم تتباين بين الدرجة الثانية والثالثة المسحات المأخوذة زرع على الأوساط التالية (وسط أكار الدم، وسط أكار المغذي ووسط ماکونكي) حيث كانت (5) عينات منها sterile وباقي العينات اظهرت نمواً بكتيرياً على (وسط أكار الدم ووسط أكار المغذي) لكن (26) مسحة من المجموع (35) مسحة فقط التي نمت على وسط أكار الماکونكي وهذا يدل على أن (9) عزلات التي لم تنمو على هذا الوسط كانت بكتيريا موجبة لملون كرام لأحتواء الوسط الأخير على مثبطات تمنع نمو البكتيريا الموجبة. كانت منها (15) عزلة تعود لبكتيريا *P.aeruginosa* ووجدت بكتيريا *P.aeruginosa* بنسبة 57.7% (11) عزلة تعود لبكتيريا *K.pneumoniae* وكانت بنسبة 42.3% كما في الشكل (1).



شكل 1. النسبة المئوية للعزلات البكتيرية قيد الدراسة

هذه النتيجة تتفق مع نتائج دراسة سابقة والتي اظهرت بكتيريا *P.aeruginosa* بنسبة 30% تليها بكتيريا *Staphylococcus aureus* بنسبة 28%، *Klebseilla pneumonia* بنسبة 16%، *Proteus* بنسبة 14%، *Escherichia coli* وأخيراً *Staphylococcus epidermidis* بنسبة 6% (13).  
نسبة الإصابة عند الإناث الى الذكور كانت 1:2 (16) حالة حرق كانت لدى الإناث 66.6% بينما كان نصيب الذكور 33.4% اي عشرة ذكور كما في الشكل (2)

وتدخل جبات العرعر في صناعة الكثير من الأدوية، لعلاج الديدان الشريطية وعلاج البطن والشرج والربو ويستخدم مغلي خشب العرعر لعلاج الأمراض الجلدية المزمنة. (5).

#### طرائق العمل

##### جمع العينات

تم جمع 40 مسحة من مرضى الحروق من مستشفى الحروق في مدينة الطب و مستشفى الإمام علي(ع) في بغداد للمدة من 11 / 11 / 2012 ولغاية 20 / 12 / 2012 كانت منها (5) سالبة للزرع البكتيري و9 عينات كانت تحتوي على بكتيريا G+ve و(30) عزلة كانت منها (15) عزلة شخصت كونها تعود لبكتيريا *P.aeruginosa* و(11) عزلة تعود لبكتيريا *K.pneumoniae*.

اخذت عينات نبات العرعر الفينيقي الجافة من الاسواق المحلية وتم طحنها طحناً ناعماً واستخدمت في الدراسة.

##### العزل والتشخيص

تم زرع المسحات على وسط أكار الدم، أكار الماکونكي، والاکار المغذي استناداً الى نتائج العزل الأولي المعتمد على الصفات المظهرية للمستعمرات التي تضمنت حجم وشكل ولون وقوام المستعمرات شخصت البكتيريا السالبة لملون غرام من خلال نموها على وسط أكار الماکونكي لملاحظة ان كانت مخمرة أو غير مخمرة لسكر اللاكتوز شخصت المستعمرات الغير مخمرة لسكر اللاكتوز التي كانت شاحبة اللون والعائدة لعائلة ال *Pseudomonas aeruginosa* من خلال انتاجها البيوسيانين Pyocyanin ملاحظتها على وسط الأكار المغذي وحضن بدرجة 37 م لمدة (18-24) ساعة وكذلك من خلال اختبار الأوكسيديز حيث اتبعت طريقة (6) وذلك بغمر ورقة ترشيح في محلول الأوكسيديز الجاهز ونقلت اليه المستعمرات المطلوب اختبارها بواسطة أعواد خشبية معقمة فكان ظهور الللون البنفسجي خلال (10-60) ثانية دليلاً على النتيجة الموجبة للتفاعل وكذلك من اختبار النمو بدرجة حرارة 42 م حيث أن العزلات الموجبة لأختبار الأوكسيديز تم تخطيطها على الأكار المغذي Nutrient agar وحضن بدرجة 42م تم مراقبة النمو وملاحظة قابلية البكتيريا على النمو في هذه الدرجة لان بكتيريا ال *Pseudomonas aeruginosa* تنمو جيداً بدرجة 42م وهذه صفة تشخيصية تميزها عن بقية أنواع ال *Pseudomonas* (7) أما المستعمرات المخمرة لسكر اللاكتوز ظهرت باللون الوردی مستعمرات مخاطية ولعامة حيث اجريت عليها الأختبارات التالية:

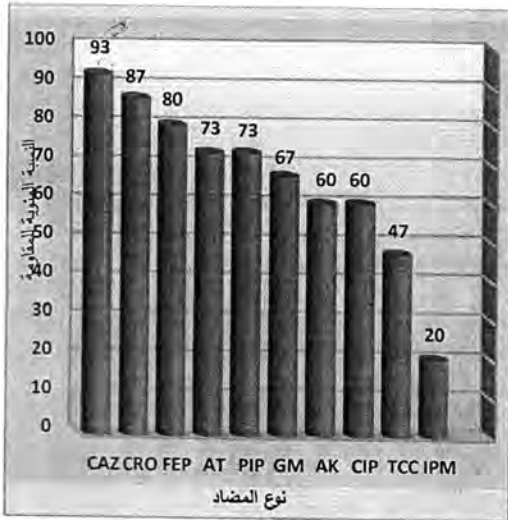
##### أختبار اللزوجة

تم اجراء الأختبار ولذلك بتخطيط وسط اكار الماکونكي أو وسط الأكار المغذي بالعزلة المراد اختبارها تحضن بدرجة 37C/24 hrs درجة مئوية بعد ذلك تلمس المستعمرة المطلوبة بالوب ثم يرفع بصورة عمودية على سطح الطبق الخاصة بالمخاطية لهذه البكتيريا تظهر بشكل خيوط من النمو String like growth - مستعمرات ال *K.pneumonia* خيوط النمو ترتفع لمسافة أكبر او تساوي 5 ملم. (8).

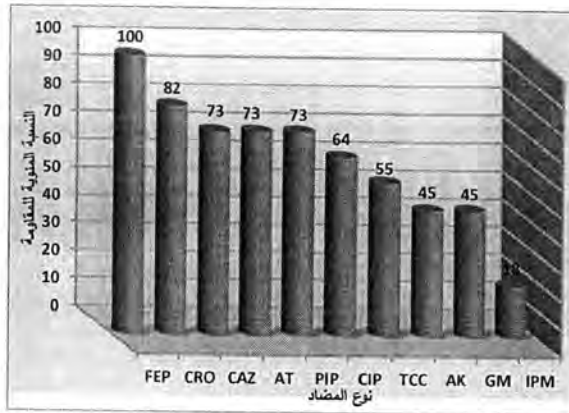
بعد التشخيص الأولي لجميع العزلات البكتيرية أكد تشخيصها باستخدام نظام Api - 20 E من الشركة المصنعة (BioMarieux) الفرنسية حسب ما ورد في (9) وهو نظام الاختبارات الكيموحيوية لتشخيص أنواع البكتيريا ويشمل 20 فحصاً.

##### فحص حساسية البكتيريا للمضادات الحيوية

اختبرت حساسية عزلات بكتيريا *P.aeruginosa* و *K.pneumoniae* ضد 10 أنواع من المضادات الحيوية هي (Ceftriaxone (CRO 30µg) (IPM10) (CAZ 30µg) Cefazidime (30µg) ImipenemCefepime (FEP 30µg) Amikacin (AK 30µg) (µg) Ciprofloxacin (CIP 5µg) Gentamicin (GM 10 µg) (Tcc) Aztreonem (AT30µg) Piperacillin (PIP100µg) (75µg) Ticarcillin لمجهزة من شركة Bioanulys (Turkey) بطريقة الاقراص على وسط مولر هنتون الصلب ( Mueller-Hinton agar )، وتم تحديد المقاومة والحساسية اعتماداً على الاقطار القياسية حسب CLSI (10).



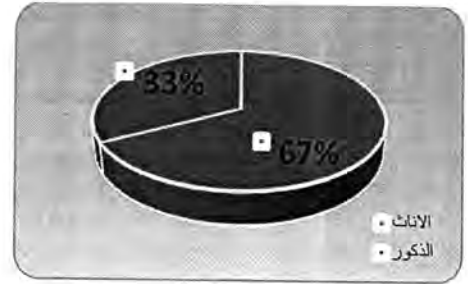
شكل 3: النسب المئوية لعزلات بكتريا *P. aeruginosa* المقاومة للمضادات الحيوية



شكل 4: النسب المئوية لعزلات بكتريا *K. pneumoniae* المقاومة للمضادات الحيوية

كانت نسبة المقاومة أيضاً لمضاد Imipenem هو المضاد الحيوي الفعال لهذه البكتريا حيث كانت نسبة المقاومة له 18% وبلغت نسبة المقاومة للـ Gentamycin هي 45% بينما كانت نسبة المقاومة للـ Amikacin هي 45% أما نسبة المقاومة للـ Ticarcillin هي 55% وكانت نسبة المقاومة للـ Ciprofloxacin هي 64% بينما أعطت المضادات التالية Piperacillin و Aztreonem و Cefazidime نسبة المقاومة 73% وكذلك أعطت مضاد Ceftriaxone نسبة المقاومة هي 82% وأخيراً حقق مضاد Cefepime أعلى نسبة المقاومة قد بلغت 100%. إن مقاومة بكتريا الـ *K. pneumoniae* للـ سيفالوسبورينات الواسعة الطيف ناجم عن إنتاجها لأنزيمات الببتالاكتاميز الواسعة الطيف (17) و (18).

الفعالية التثبيطية للمستخلص المائي الحار لنبات العرعر الفينقي بينت نتائج الدراسة الموضحة في الشكل (5) أن للمستخلص فعالية تثبيطية متباينة اتجاه العزلات المعزولة من الجروح والحروق ، فقد بين (19) في دراسته ان الفعالية المايكروبية لنبات العرعر تعود بالدرجة الاساس الى مركب Alpha-pinene المعروف بتأثيره على البكتريا ، اظهرت النتائج ان المستخلص المائي لم يؤثر على عزلتين حتى في التركيز 400 mg/ml وهذا يتفق مع ما وجدته (20) في دراسة لانواع مختلفة من نبات العرعر حيث يظهر ان المستخلص المائي لم يعطي فعالية تجاه أي عزلة مختبرة اما المستخلص الكحولي فقد اعطى فعالية متباينة اتجاه 57 عزلة من البكتريا وان مستخلص نبات العرعر يكون اكثر فعالية على الفطريات عنه في



شكل 2: النسب المئوية لاصابات الذكور والاناث

و هذه النتيجة مقارنة لتلك التي أظهرتها دراسة محلية اجريت في جامعة الموصل شملت الدراسة تسعين مريض مصاب بجروح الحروق 63 منهم اناث اي (70%) بينما كان عدد الذكور 27 مريض (30%) (14). كما اكدت دراسة اخرى ان تكرار الحروق لدى الاناث (64,2%) بينما تكراره في الذكور (35,8%) (15). تراوحت اعمار المرضى التي شملتهم الدراسة بين الثلاث سنوات والأربعين سنة

جدول 1: الفئات العمرية للبيئة قيد الدراسة

الفئات العمرية (بالسنوات)	العدد	النسبة المئوية (%)
1-9 سنة	8	20%
9-19 سنة	12	30%
20-29 سنة	16	40%
30-40 سنة	4	10%

أظهرت الدراسة ان اعلى الفئات العمرية التي كانت عرضة لأصابات الحروق هي بعمر الشباب 40% تلتها الأشخاص بعمر المراهقين بنسبة 30% الأصابات عند هاتين الفئتين قد تكون اما اصابات مهنية أو جراء الانتحار المتعمد في حين ان سبب ارتفاع نسبة حوادث الحروق لدى الاناث جراء الأهمال والأستعمال الخاطيء لمصادر الطاقة الحرارية أو نتيجة الحرق المتعمدة وجاءت مرحلة الطفولة بالمرتبة الثالثة بنسبة 20% جميع الحالات كانت نتيجة سكب سوائل حارة السلق بالماء الحار أو سكب أباريق الشاي كما في الجدول (1) .

#### فحص الحساسية للمضادات الحيوية

تم إجراء فحص الحساسية الدوائية لعشرة من المضادات الحيوية و اعتمدت على قياس قطر منطقة التثبيط ومقارنة ذلك مع ما ورد في (10) أبدت العزلات المدروسة استجابة مختلفة للانواع للمضادات الحيوية المستعملة. أظهرت النتائج ان المضاد الحيوي Imipenem هو المضاد الأكثر فعالية ضد بكتريا الـ *P.aeruginosa* حيث كانت نسبة المقاومة %20 ونسبة المقاومة للـ Ticarcillin هي 47%، بينما كانت نسبة المقاومة للـ Ciprofloxacin 60% وكذلك نسبة مقاومة للـ Amikacin كانت 60% أما بالنسبة لمضاد Gentamicin أعطت نسبة مقاومة هي 67% وبينما أعطت المضادين Piperacillin و Aztreonem نسبة مقاومة 73% لكل منهما و بلغت نسبة المقاومة للـ Cefepime هي 80% وكذلك نسبة المقاومة للـ Cefazidime هي 87% وأخيراً أعطت Ceftriaxone أعلى نسبة مقاومة حيث بلغت 93%. وكما موضح في الشكل (3)

اتفقت النتائج مع نتائج دراسة سابقة حيث كانت مقاومة عزلات بكتريا الـ *P.aeruginosa* للـ gentamicin كانت 69,4% حيث أظهرت 34 عزلة من مجموع 49 عزلة كانت مقاومة للجنتاميسين وللـ cefepime والـ ciprofloxacin كانت 61,2% اي 30 عزلة كانت مقاومة للـ ceftazidime هي 38,8% اي تسعة عشر عزلة كانت مقاومة و 42,9% للـ Aztreonam و 42,9% للـ meropenem (16)

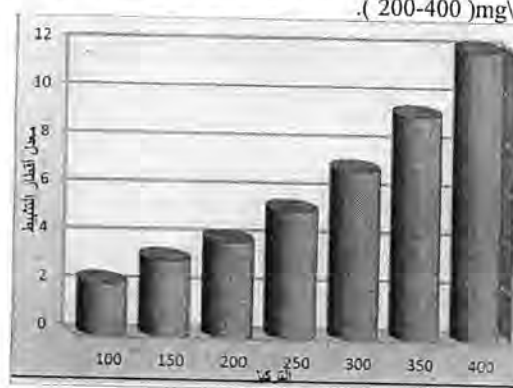
مقاومة بكتريا *P.aeruginosa* للـ Ceftriaxone و Cefepime. Cefazidime يعزى الى انتاجها للأنزيم extended-spectrum B-lactamases (ESBLs) ولوحظ وجود الجين المسؤول عن انتاج هذا الأنزيم في العزلات المقاومة اما بالنسبة لبكتريا الـ *Klebsiella pneumoniae* كما موضح في الشكل (4)

8. Ivring ,P.W., AlaAldeen , P.D. and Bowswell, T . (2006) Medical Microbiology . Taylor & Francis e-Library . New York .P .37.
9. Atlas, R.M.; Brown, A.E. and Parks, L.C. (1995). Laboratory manual of experimtal microbiology. 1<sup>st</sup> ed. Mosby, st. Louis, U.S.A.
10. CLSI( Clinical and laboratory standards Instute) (2009) .standards for antimicrobial .susceptibility Testing,19<sup>th</sup> supplement .CLSI document M 100-S19.29(3) CLSI , Wayne ,Pennsylvania ,USA.
11. El-fattal ,A.A.and El-Kattan.M.H(1997) Effect of plant extract on mycelial growth of some cultivated mushrooms Egypt.S.Microbial 32(1):41-48.
12. Mharma , A.andD.S.Hassawi (2006). The genetic relationship and antimicrobial activity of plantago species against pathogenic bacteria , world Journal of Agriculral sciences , 2 (3) : 311- 318.q.
13. Dilnawaz S ., S. Zaidi DI, A. H., Khurram S., Munima S., Baqir S. N., M.R. Shaikh and M. Harriss S., (2004). (Incidence and resistance pattern of bacteria associated with burn wound sepsis) Pakistan Journal of Pharmacology Vol.21, No.2, July, pp.39-47.
14. Haitham M. Al-Habib, Asmaa Z. Al-Gerir, Ansam M. Hamdoon.(2011) Profile of *Pseudomonas aeruginosa* in burn infection and their antibiogram study(Ann. Coll. Med. Mosul; 37 (1 & 2): 57-65.
15. Fakhredin, T. Ardeshir S. Z., Behnam, B., Jafar, R., and Seyed, H. (2010) ( A survey of suicide by burning ) ActaMedicaIranica, Vol. 48, No. 4 (266- 272).
16. Kuo, C.-H ., S.-J. Du, H.-C. Cheng, A.C.Y. Fei, H.-W. Wei, S.-K. Chang.(2010) Molecular mechanisms of ceftazidime resistance in *Pseudomonas aeruginosa* isolates from canine and human infections . VeterinarniMedicina, 55, (4): 172–182.
17. Arlet G , M. Rouveau, I. Casin, P.J.M. Bouvet, P.H Lagrange and A. Phillippon.(2002) Molecular epidemiology of *Klebsiella pneumonia* strains that produce SHV-4 B-lactamase and which were isolated in 14 french hospitals. J.Clin.Microbiol., 32: 2553-2558.
18. Buehlmann M, Fankhauser H, Laffer R, Bregenzer T, Widmer AF.(2010) The inguinal skin: An important site of colonization with extended-spectrum beta-lactamase-producing Enterobacteriaceae. Infect Control HospEpidemiol;31:427-8.
19. Bourkhiss, M.,M, Hnanch, Mouhssins and A. chaouch (2007). Composition chimique, 03:232-242.
20. Karamman, I.; Sahin, F.; Gulluce, M. Sengul, M. and Adiguzel, A.(2003). Antibacterial activity of aqueous and methanol extracts of *juniperus oxycedrus* L. Journal of Ethnopharmacolog. Apr 85(2-3):231-235.
21. Stassiv, Verykokidou E, Loukis A, Harvala C, Philianos S(1996). Theantimicrobial activity of the essential olis of four *Juniperus* species growing wild in 15reece. Flav. Fragr. J. 11:71-74.
22. Derwich, E., Z. Benziane and A. Boukir, (2010). Chemical Composition Of *J. phoenicea* and evolution of its antibacterial activity. *Int J.Agric, Bio*, 12:199-204.

البكتريا فأدى الى تثبيط نمو الهايغان في فطر *phaseolinem acrpheimina* بنسبة 98.2%.

بينما اثر على عزلتين في التركيز 400mg / ml فقط وباقطار تثبيط ( 7.6 ، 5.8 )ملم وعلى عزلتين في التركيز ( 350, 400 ) وباقطار تثبيط ( 9.5 ، 7.7 ) ملم للاولى و ( 10 ، 7.2 ) ملم للثانية وقد تكون فعالية النبات المنخفضة راجعة لقلته وجود مادة Alpha - terpinol وهذا ما بينه (21) في دراسة التي تقول ان فعالية العرعر من نوع *J. oxycedrus* تعود لوجود مركب terpinol.

بينما العرعر الفينيقي لا يحتوي على هذا المركب لكن له فعالية ضد مايكروبية وهناك عزلة واحدة فقط اثر عليها المستخلص ابتداءا من التركيز 300 . mg / ml وباقطار تثبيط ( 9.2 ، 8 ، 6.7 ) ملم واخرى من التركيز 250 . mg / ml وباقطار تثبيط ( 9.4 ، 7.6 ، 7 ، 5.3 )ملم ، اما بقية العزلات فكانت حساسة للمستخلص بجميع التركيزات (100-400) mg/ml وباقطار تثبيط تتراوح بين 3.8ملم في تركيز 100 الى 22.4ملم في تركيز 400 وكما مبين بالشكل (5) وهذا ما ينطبق مع دراسة اجراها (22) ضد مجموعة من البكتريا المسالبة والموجبة لصيغة كرام من ضمنها *p.aeruginosa* حيث كانت البكتريا حساسة للمستخلص وكان اقل تركيز له تأثير على البكتريا بين (200-400) mg/ml .



شكل 5: تأثير التركيز في معدل أقطار التثبيط لنبات *J.phoenicea* على عزلة *P.aeruginosa*

#### المصادر

1. Harrison, J & Steel, D. October (2006). Burns and Scalds. National Injury Surveillance Unit.
2. van'tVeen A, van der Zee A, Nelson J, Speelberg B, Kluytmans JAJW, Buiting AGM.(2005) Outbreak of infection with a multiresistant *Klebsiella pneumoniae* strain associated with contaminated roll boards in operating rooms. J ClinMicrobiol;43:4961-7.
3. Brook, G.F.; Butel, J.S. & Mores , S.A. (2004). *Klebsiella* in: Jawetz, Menick & Adelberg's Medical Microbiology. 23<sup>rd</sup> ed.McGraw-Hill Companies . Appleton & Lang, New York.
4. د. عنبر محمود احمد ، النباتات الطبيعية والعصرية ، قسم البساتين - كلية الزراعة ، جامعة سوهاج . 2007 [1-30]
5. مهتد عبد الستار ، علي حسين سليم ، فرح رسول جعفر ، التأثير التكتري الفعال لمستخلص ثمار العرعر *J.phoenicea* في اثاث الجرذان البالغة [2001-10-voli].
6. Baron ,E . J and Finnegold , S. M .(1990) Bailey & Scott ( Diagnostic Microbiology .C.V. Mosbey Company St.Louis ,Baltimore ,Philadelphia , Toronto.
7. Jawetz, Melnick & Mdelbergs, (2004): Medical Microbiology (23<sup>rd</sup>)ed. McGraw-Hill companies, Apleton & Lange:250-54.



## تأثير حليب جوز الهند ومستخلص أوراق الياس في نمو وحاصل الباقلاء *Vicia faba L.*

وفاق أمجد القيسي و رهن وائل محمود و سناء عبد حمود و زينب عباس الكبيسي  
قسم علوم الحياة، كلية التربية للعلوم الصرفة/ ابن الهيثم، جامعة بغداد

### الخلاصة

أجريت تجربة حقلية لموسم النمو 2012-2013 بهدف دراسة تأثير حليب جوز الهند *Cocos nucifera* بالتركيزين 50 و 100 جزء من المليون، ومستخلص أوراق الياس *Myrtus communis* بالتركيزين 10 و 20% في نمو حاصل نبات الباقلاء *Vicia faba*، أظهرت النتائج زيادة معنوية في ارتفاع النبات وعدد الأوراق وعدد الأوراق وقطر الساق وعدد العقد والوزن الجاف للنبات والمساحة السطحية للأوراق وسرعة نمو المحصول ونسبة مساحة الأوراق والنمو المطلق والمحتوى الكلي للكلوروفيل وعدد القنات ووزن البذرة ووزن وطول القرنة والنسبة المئوية للبروتين في البذور في جميع المعاملات مقارنة مع نباتات السيطرة.

### ABSTRACT

The field experiment was conducted during the growth season of (2012-2013). The experiment aimed to study the effect of coconut *Cocos nucifera* milk in two concentration 50, 100 ppm and the extract of *Myrtus communis* leaves with two concentration 10, 20% on growth and yield of *Vicia faba*.

The result showed that increased significantly in plant height, leaves number, branches number, stem diameter, nudes number, dry weight, surface area, crop growth ratio, LAI, absolute growth, chlorophyll content, pods number, seed weight, weight and length of pod and percentage of protein in seeds in all treatment compared with control plants.

### Article info.

تقديم البحث: 2014/11/19  
قبول البحث: 2015/2/23

الزراعة بتاريخ 2012/10/22 وأجريت عملية الرش الورقي عند وصول النبات لعمر 4-5 أوراق بتاريخ 2012/12/2 بالمعاملات التالية:

1- تركت النباتات بدون أية معاملة (معاملة السيطرة).  
2- رش النباتات بحليب أو سائل جوز الهند بالتركيزين 50 و 100 جزء من المليون وتم تحضيره بأخذ 300 مل من حليب جوز الهند ثم غلي في حمام مائي لمدة 10 دقائق لغرض ترسيب البروتين ثم رش خلال ورق الترشيع No.4 ثم أخذ منه 100 مل وأكمل الحجم إلى لتر بالماء المقطر ثم حضر منه 50 و 100 جزء من المليون [1].

3- تم تحضير المستخلص المائي لأوراق نبات الياس الجافة بالتركيزين 10% و 20%.

تم أخذ العينات بمعدل ثلاثة نباتات لكل وحدة تجريبية وبفترتين أو حستين الأولى D<sub>1</sub> بتاريخ 2012/12/23 والثانية D<sub>2</sub> بتاريخ 2013/1/13 لأجراء القياسات المطلوبة.

دراسة الصفات التالية في الفترة أو الحشة الأولى D<sub>1</sub>:

1- ارتفاع النبات: تم قياس النبات من قاعدته إلى آخر عقدة قيه بواسطة المسطرة.

2- عدد الأوراق لكل نبات.

3- عدد الأفرع لكل نبات.

4- قطر الساق (مم): تم قياسه بواسطة آلة القدمة Vernier caliper.

5- عدد العقد في الساق الرئيس للنبات.

6- الوزن الجاف للنبات (غم): تم تجفيف النباتات باستعمال فرن درجة حرارته 80°م لمدة يومين وأخذ الوزن بعد ثباته.

7- المساحة السطحية للأوراق سم<sup>2</sup> وحسبت استناداً إلى طريقة الأقراص [12] حيث أخذ عدد معين من الأقراص وتم تجفيفها وأخذت الأوراق الجافة لتلك الأقراص ثم حسبت المساحة السطحية للأوراق حسب المعادلة التالية:

المساحة السطحية للأوراق = الوزن الجاف للأوراق / مساحة الأقراص المعطومة المساحة

الوزن الجاف للأقراص

تم دراسة الصفات التالية في الفترة أو الحشة الثانية D<sub>2</sub>:

1- ارتفاع النبات (سم).

2- عدد الأوراق لكل نبات.

3- عدد الأفرع لكل نبات.

4- الوزن الجاف للنبات (غم).

### المقدمة

يعد محصول الباقلاء *Vicia faba L.* نباتاً حلوباً شتوياً ينتمي إلى عائلة Fabaceae [1]، للباقلات استعمالات عديدة حيث يزرع كمحصول أخضر لاستهلاك قرنته أو كمحصول حقل للحاصل على بذوره الجافة لتغذية الإنسان أو كمحصول علف أخضر كما في أوروبا [2]، تحتوي بذور الباقلاء على نسبة عالية من البروتين تتراوح بين (26-38)% وللباقلات كثيرها من المحاصيل البقولية القدرة على تثبيت النتروجين الجوي عن طريق العقد الجذرية مما يزيد من خصوبة التربة [3].

ان نبات جوز الهند *Cocos nucifera* يعود إلى عائلة Palmae [1]. ان سائل أو حليب جوز الهند يحتوي مكونات غذائية مهمة جداً مثل البروتينات والدهون وأحماض عديدة Caprotique و Linolique و Nicolinique و Lactique فضلاً عن العناصر الغذائية كالبيوتاسيوم والحديد والكالسيوم والفسفور [4، 5]، وقد وجد ان هناك مواد موجودة في جوز الهند تحفز انقسام وتميز الخلايا وقد أطلق عليها السايوتوكاتين وهو هرمون نباتي يعمل على تنظيم نمو النبات [6]. يعد السايوتوكاتين من منظمات النمو المهمة في النبات حيث يحث الانقسام الخيطي ويزيد من لدونة الجدار الخلوي مما يساعد في اتساع الخلايا ويحفز حركة المغذيات ويقلل من السيادة القمية ويساعد في بناء البروتين [7].

يعود نبات الياس أو الاسم *Myrtus communis* إلى العائلة Myrtaceae [1]، تحتوي أوراقه على السكريات والزيوت الطيارة والثابتة وحامض الستريك وحامض المالك، والتانينات، وفيتامين C ومركبات أخرى فعالة Myrtol، Resin، Myrtenol والفلافونيات [4، 5، 8، 9، 10].

تهدف الدراسة لمعرفة تأثير سائل أو حليب جوز الهند بتركيز 50 و 100 جزء من المليون ومستخلص أوراق نبات الياس الجافة بالتركيزين 10 و 20% في بعض الصفات المورفولوجية والفلسجية لنبات الباقلاء.

### المواد وطرائق العمل

نفذت التجربة في حقل تجارب قسم علوم الحياة في الحديقة النباتية في كلية التربية للعلوم الصرفة (أبن الهيثم) جامعة بغداد خلال موسم النمو 2012-2013 وباستخدام تصميم القطاعات العشوائية RCBD وبثلاث مكررات وكانت مساحة اللوح الواحد 1.08 م وعقد الوحدات التجريبية 15 وحدة. وتم الحصول على بذور الباقلاء الصنف المحلي من الأسواق المحلية وتمت

تشير نتائج الجدول نفسه الى وجود زيادة معنوية في قطر الساق لنبات البقلاء فقد ازداد بمقدار 140.69% و 159.03% لمعاملتي حليب جوز الهند وازداد بمقدار 20.46% و 44.57% لمعاملتي مستخلص أوراق الياس على التتابع مقارنة بنباتات السيطرة.

تبين نتائج جدول (2) الى وجود فروق معنوية في عدد العقد في الساق الرئيس وازداد بنسبة مقدارها 76.12% و 30.68% لمعاملتي حليب جوز الهند وازداد بنسبة مقدارها 42.21% و 26.87% لمعاملتي مستخلص أوراق الياس على التتابع مقارنة بنباتات السيطرة. وقد ازداد الوزن الجاف لنبات البقلاء بصورة معنوية عند الحشة أو الفترة الأولى  $D_1$  بنسبة مقدارها 138.41% و 141.46% لمعاملتي حليب جوز الهند 50 و 100 جزء من المليون وازداد بنسبة 24.39% و 62.24% لمعاملتي مستخلص أوراق الياس 10 و 20% على التتابع مقارنة بنباتات السيطرة، أما عند دراسة المساحة السطحية للأوراق في الجدول نفسه فقد ازدادت بنسبة 3.65%، 4.40%، و 30.50% و 10.00% بصورة معنوية للمعاملات كافة بالنسبة لحليب جوز الهند أو مستخلص أوراق الياس على التتابع مقارنة بنباتات السيطرة.

جدول 1: تأثير حليب جوز الهند ومستخلص أوراق الياس في ارتفاع النبات وعند الأوراق وقطر الساق لنبات البقلاء عند الحشة أو الفترة الأولى  $D_1$

المعاملات	ارتفاع النبات (سم)	عدد الأوراق	عدد الافرع	قطر الساق (مم)
السيطرة	29.67	8.27	1.00	0.83
حليب جوز الهند ppm 50	42.33	10.32	2.00	2.00
حليب جوز الهند ppm 100	46.76	11.33	3.50	2.15
مستخلص أوراق الياس 10%	38.33	12.33	2.50	1.00
مستخلص أوراق الياس 20%	32.87	10.00	2.00	1.20
LSD عند مستوى 0.05	2.22	1.48	0.18	0.04

جدول 2: تأثير سائل أو حليب جوز الهند ومستخلص أوراق الياس في عدد العقد والوزن الجاف للنبات والمساحة السطحية لأوراق نبات البقلاء عند الحشة أو الفترة الأولى  $D_1$

المعاملات	عدد العقد	الوزن الجاف للنبات (غم)	المساحة السطحية للأوراق
السيطرة	8.67	1.64	104.66
حليب جوز الهند ppm 50	9.33	3.91	108.49
حليب جوز الهند ppm 100	11.33	3.96	104.27
مستخلص أوراق الياس 10%	12.33	2.04	136.59
مستخلص أوراق الياس 20%	11.00	2.71	115.13
LSD عند مستوى 0.05	1.48	0.07	0.01

اما نتائج جدول (3) فقد أشارت الى وجود فرق معنوي بين المعاملات فقد ازداد ارتفاع النبات وعدد الأوراق وعدد الافرع والوزن الجاف للنبات عند الحشة أو الفترة الثانية  $D_2$  لمعاملتي حليب جوز الهند ومستخلص أوراق الياس مقارنة بنباتات السيطرة.

اما عند دراسة نتائج الجدول (4) فقد ازدادت سرعة نمو المحصول لنبات البقلاء بصورة معنوية لجميع معاملات مقارنة بنباتات السيطرة وبنسبة مقدارها 100% و 200% لمعاملتي حليب جوز الهند و 250% لمعاملتي مستخلص أوراق الياس. اما عند دراسة نسبة مساحة الأوراق فقد ازدادت بصورة معنوية بنسبة 10.10% و 150.01% لمعاملتي حليب جوز الهند وبنسبة مقدارها 102.92% و 164.84% لمعاملتي مستخلص أوراق الياس على التتابع مقارنة بنباتات السيطرة. يتبين من نتائج الجدول نفسه وجود فروق معنوية في المحتوى الكلوروفيلي للأوراق فقد ازدادت بنسبة 45.12% و 54.03% لمعاملتي حليب جوز الهند وبنسبة مقدارها 44.13% و 18.00% لمعاملتي مستخلص أوراق الياس على التتابع مقارنة بنباتات السيطرة.

مسرعة نمو المحصول غم/سم<sup>2</sup>/يوم (GGR) Group Growth Rate تم حسابه حسب المعادلة التالية [13]:

$$GGR = \frac{W_2 - W_1}{T_2 - T_1} \times \frac{1}{A}$$

حيث ان

$W_1$  = الوزن الجاف للنبات عند الفترة الأولى  $D_1$ .

$W_2$  = الوزن الجاف للنبات عند الفترة الثانية  $D_2$ .

$T_1$  = عمر النبات عند أخذ الوزن عند الفترة الأولى  $D_1$ .

$T_2$  = عمر النبات عند أخذ الوزن عند الفترة الثانية  $D_2$ .

A = المساحة التي يشغلها النبات الواحد

6-نسبة مساحة الأوراق سم<sup>2</sup> لكل غم (LAR) Leaf Area Relative: أخذت القراءات لثلاثة نباتات مختارة بصورة عشوائية وللفترة الثانية  $D_2$  وتم حسابها حسب المعادلة [14]:

$$LAR \text{ سم}^2/\text{غم} = \frac{\text{مساحة أوراق النبات}}{\text{الوزن الجاف للنبات}}$$

7-محتوى الكلوروفيل الكلي للورقة Spad:

تم حساب المحتوى الكلوروفيلي للأوراق بجهاز (Chlorophyll meter) موديل Spad المجهز من شركة Minolta اليابانية المحدودة. أخذ معدل قراءات لثلاث أوراق لثلاثة نباتات اختيرت عشوائياً من وسط النبات في كل معاملة في الفترة الثانية  $D_2$  وذلك بوضع اعراض جزء من الورقة تحت ذراع الجهاز والضغط عليه حيث تظهر القراءة على شاشة الجهاز. 8-معدل النمو المطلق غم/يوم (CGR) Crop Growth Rate: تم قياسه حسب المعادلة التالية [14]:

$$CGR = \frac{W_2 - W_1}{T_2 - T_1}$$

حيث ان

$W_1$  = الوزن الجاف للجزء الخضري عند الفترة الأولى  $D_1$ .

$W_2$  = الوزن الجاف للجزء الخضري عند الفترة الثانية  $D_2$ .

$T_1$  = عمر النبات عند الفترة الأولى  $D_1$ .

$T_2$  = عمر النبات عند الفترة الثانية  $D_2$ .

9-عدد الأيام للتزهير: تم حساب عدد الأيام منذ رش النباتات بالمعاملات المختلفة حتى بدء التزهير.

تم أخذ القياسات التالية عند حصاد النباتات بتاريخ 2013/4/7 وهي:

1-ارتفاع النبات (سم).

2-عدد القترات لكل نبات.

3-عدد البذور لكل قرنة.

4-وزن البذرة (غم).

5-وزن القش (غم).

6-وزن القرنة (غم).

7-طول القرنة (سم).

8-دليل الحصاد = وزن البذور  $\times 100$

الحاصل البايولوجي

9-تقدير نسبة البروتين في البذور: تم قياس النتروجين باستخدام جهاز مايكروكالدال Microkjeldhal بعد هضم وزن معلوم من البذور ثم حسبت نسبة البروتين وفق المعادلة التالية:

نسبة البروتين في البذور = نسبة النتروجين  $\times 6.25$  [15، 16].

تم تحليل النتائج احصائياً حسب البرنامج الاحصائي [17] وتم مقارنة المتوسط بأقل فرق معنوي LSD عند مستوى احتمال 0.05.

### النتائج والمناقشة

تشير نتائج جدول (1) الى وجود فروق معنوية في صفة ارتفاع النبات فقد ازداد بنسبة 42.66% و 57.60% لمعاملتي حليب جوز الهند وازداد بنسبة 29.18% و 10.78% لمستخلص أوراق الياس، وقد ازداد عدد الأوراق بنسبة مقدارها 24.78% و 37.00% و 49.09% و 20.91% على التتابع مقارنة بنباتات السيطرة. اما بالنسبة لعدد الافرع فقد ازدادت بصورة معنوية بنسبة مقدارها 100% و 200% لمعاملتي حليب جوز الهند بالتركيزين 50 و 100 جزء من المليون على التتابع ولمعاملتي مستخلص أوراق الياس بنسبة مقدارها 250% و 200% للتركيزين 10 و 20% على التتابع مقارنة بنباتات السيطرة.

تشير نتائج جدول (6) الى ازدياد وزن القش بصورة معنوية في معاملي حليب جوز الهند وبنسبة مقدارها 42.21% للتركيز 50 جزء من المليون وبنسبة مقدارها 84.42% للتركيز 100 جزء من المليون وبنسبة مقدارها 26.64% للتركيز 10% من مستخلص أوراق اليباس وبنسبة 30.44% للتركيز 20% من مستخلص أوراق اليباس مقارنة بنباتات السيطرة، اما وزن القرنة فقد ازاد بصورة معنوية في المعاملات المختلفة وبنسبة 89.06% و40.62% لمعاملي حليب جوز الهند و42.18% و34.37% لمعاملي مستخلص أوراق اليباس على التتابع مقارنة بنباتات السيطرة، اما بالنسبة لصفة طول القرنة فقد ازادت بنسبة 78.67% و53.59% و71.48% و417.89% للمعاملات المختلفة على التتابع مقارنة بنباتات السيطرة، تبين نتائج الجدول نفسه وجود فروق معنوية في دليل الحصاد في معاملي حليب جوز الهند ولمعاملي مستخلص أوراق اليباس مقارنة بنباتات السيطرة، اما عند دراسة نسبة البروتين في البذور فقد ازادت بنسبة مقدارها 61.65% و72.38% لمعاملي حليب جوز الهند وبنسبة زيادة مقدارها 17.14% و41.05% لمعاملي مستخلص أوراق اليباس مقارنة بنباتات السيطرة.

ان سائل أو حليب جوز الهند يحتوي على منظم النمو السايوتوكاينين والذي يعمل على زيادة انقسام الخلايا واتساعها واستطالة الأجزاء العلوية للبادرات النامية وتساعد في نمو المجموع الخضري والحفاظ على حيوية الأوراق النباتية وعدم شيخوختها ويمنع تهديم الكلوروفيل [6، 18]، ان السايوتوكاينين يعمل على تنظيم بناء البروتين من خلال زيادة بناء mRNA وربطه مع tRNA مؤثراً في زيادة نمو النبات فضلاً على تشجيعه في زيادة نمو البراعم الجانبية من خلال تثبيط السيادة القمية ويصبح النبات أكثر تفرعاً ويؤدي هذا الى زيادة الوزن الجاف للنبات [19] وأنه يعمل على زيادة بناء البروتين وقلة هدمه ويساعده الاوكسين الداخلي في النبات حيث يعمل على

جدول 6: تأثير حليب جوز الهند ومستخلص أوراق اليباس في وزن القش ووزن القرنة وطول القرنة ودليل الحصاد والنسبة المئوية للبروتين في البذور لنبات الباقلاء عند الحصاد.

المعاملات	وزن القش	وزن القرنة (غم)	طول القرنة	دليل الحصاد %	النسبة المئوية للبروتين
السيطرة	2.89	0.64	9.33	50.67	12.13
حليب جوز الهند ppm 50	4.11	1.21	16.67	74.21	19.61
حليب جوز الهند ppm 100	5.33	0.90	14.33	53.93	20.91
مستخلص أوراق اليباس 10%	3.66	0.91	16.00	70.88	12.21
مستخلص أوراق اليباس 20%	3.79	0.86	11.00	76.25	17.11
LSD عند مستوى 0.05	0.13	0.01	1.81	2.51	0.12

انتقاله الى الافرع الجانبية بعد بناءه في الجذور [20]، يساهم السايوتوكاينين في كسر حالة السكون للبراعم الجانبية وتزداد الفروع الجانبية وتعمل أيضاً على دفع نمو النبات في المرحلة الخضرية الى مرحلة النمو الزهري وتساهم أيضاً في تكوين البذور داخل الثمار وتزيد من سرعة العقد وتكبير نضج الثمار خاصة عندما تعمل مع هرمون الجبرلين الداخلي [21، 22]، كما يظهر من نتائج الدراسة ان حليب جوز الهند يعمل على زيادة جميع الصفات الخضرية والفلسجية ومكونات الحاصل لنبات الباقلاء وقد عمل السايوتوكاينين عند رشه مع البوتاسيوم في زيادة عدد التفرعات ونسبة البروتين ونسبة الكاربوهيدرات ومعدل النمو المطلق لنبات العنبد [23].

ان حليب جوز الهند وبالتركيز 100000 مايكروليتر/ لتر عمل على زيادة ارتفاع وقطر الساق وعدد الافرع الثانوية ووزن الساق والوزن الجاف للأوراق والمجموع الخضري ووزن المجموع الجذري في نبات الحبة السوداء [24]. لقد ازاد ارتفاع النبات وعدد الافرع الثانوية والوزن الجاف لنبات الحبة السوداء عند رشه بالسايوتوكاينين [25].

اما بالنسبة للمستخلص المائي لأوراق نبات اليباس أو الاس فقد ازادت معنوياً اغلب الصفات الخضرية والفلسجية لنبات الباقلاء وقد يعزو هذا الى ان المستخلص يحتوي على مغذيات ضرورية للنبات وهي تشمل على جوامض عضوية مثل الستريك والماليك التي تدخل في دورة كريبس وهذه الدورة مهمة جداً لحياة النبات فهي تجهزه بكل متطلبات النمو من احماض امينية واحماض نووية والكاربوهيدرات والبروتينات والدهون والكلوروفيل وغيرها [8]، كما يحتوي المستخلص على فيتامين C ويسمى بحامض الاسكوربيك Ascorbic acid وهو من مضادات الاكسدة Antioxidant

جدول 3: تأثير حليب جوز الهند ومستخلص أوراق اليباس في ارتفاع النبات وعدد الأوراق وعدد الافرع والوزن الجاف لنبات الباقلاء عند الحشة أو القرنة الأولى D.

المعاملات	ارتفاع النبات (سم)	عدد الاوراق	عدد الافرع	الوزن الجاف للنبات (غم)
السيطرة	35.17	10.00	1.75	3.15
حليب جوز الهند ppm 50	48.33	12.50	2.67	4.01
حليب جوز الهند ppm 100	51.33	14.00	3.75	5.15
مستخلص أوراق اليباس 10%	49.81	13.67	3.00	3.92
مستخلص أوراق اليباس 20%	40.00	12.50	3.50	3.18
LSD عند مستوى 0.05	2.44	1.67	0.14	0.08

جدول 4: تأثير حليب جوز الهند ومستخلص أوراق اليباس في سرعة نمو المحصول ونسبة مساحة الأوراق ومحتوى الأوراق من الكلوروفيل والنمو المطلق وعدد الأيام للتزهير لنبات الباقلاء عند الحشة أو القرنة الأولى D.

المعاملات	سرعة نمو المحصول	نسبة مساحة الأوراق	محتوى الأوراق من الكلوروفيل	معدل النمو المطلق	عدد الأيام للتزهير
السيطرة	0.010	25.33	32.20	101.22	22.00
حليب جوز الهند ppm 50	0.020	27.89	46.73	221.38	17.00
حليب جوز الهند ppm 100	0.030	63.33	49.60	238.33	22.00
مستخلص أوراق اليباس 10%	0.030	51.40	46.43	132.67	17.00
مستخلص أوراق اليباس 20%	0.035	67.08	38.00	107.33	19.00
LSD عند مستوى 0.05	0.01	2.50	2.54	4.62	2.44

اما معدل النمو المطلق فقد ازاد معنوياً في المعاملات المختلفة بنسب مقدارها 118.71% و135.45% و31.07% و6.03% على التتابع لمعاملي حليب جوز الهند ومستخلص أوراق اليباس مقارنة بنباتات السيطرة. اما بالنسبة لعدد الأيام اللازمة للتزهير من بداية رش النباتات بالمعاملات المختلفة فقد انخفض عدد الأيام في معاملة حليب جوز الهند 50 جزء من المليون ومعاملي مستخلص أوراق اليباس 10 و20% بصورة معنوية مقارنة بنباتات السيطرة. اما نتائج جدول (5) فهي تشير الى بعض الصفات الفسيولوجية لنبات الباقلاء عند الحصاد فقد ازاد ارتفاع النبات لجميع المعاملات بصورة معنوية مقارنة بنباتات السيطرة، اما عدد القرنتات فقد ازاد بصورة معنوية وبنسبة مقدارها 42.85% و14.28% لمعاملي حليب جوز الهند وبنسب مقدارها 35.71% و28.57% لمعاملي مستخلص أوراق اليباس مقارنة بنباتات السيطرة. بالنسبة لصفة عدد البذور لكل قرنة فلم توجد فروق معنوية بين المعاملات المختلفة اما بالنسبة لوزن البذرة فقد ازاد بصورة معنوية لمعاملي حليب جوز الهند بنسبة مقدارها 131.57% و310.52% ولمعاملي مستخلص أوراق اليباس بنسبة مقدارها 78.94% و157.89% مقارنة بمعاملات السيطرة.

جدول 5: تأثير حليب جوز الهند ومستخلص أوراق اليباس في ارتفاع النبات وعدد القرنتات وعدد البذور لكل قرنة ووزن البذرة لنبات الباقلاء عند الحصاد.

المعاملات	ارتفاع النبات (سم)	عدد القرنتات	عدد البذور لكل قرنة	وزن البذرة (غم)
السيطرة	55.00	3.50	2.75	0.38
حليب جوز الهند ppm 50	83.00	5.00	3.00	0.88
حليب جوز الهند ppm 100	91.00	4.00	3.60	1.56
مستخلص أوراق اليباس 10%	70.33	4.75	3.00	0.68
مستخلص أوراق اليباس 20%	63.00	4.50	2.76	0.98
LSD عند مستوى 0.05	4.20	0.16	NS	0.01

20. عطية، حاتم جبار وجدوع، خضير عباس. منظمات النمو النباتي، النظرية والتطبيق. دار الكتب للنشر، جامعة بغداد، وزارة التعليم العالي والبحث العلمي: 201-51 (1999).
21. ابو زيد، الشحات نصر. الهرمونات النباتية والتطبيقات الزراعية. دار العربية للنشر والتوزيع، القاهرة، الطبعة الثانية: 209-215 (2000).
22. Jain, V. K. Fundamentals of plant physiology 13<sup>th</sup> ed. S. Chand of company LTD Rsm Nagar, New Delhi: 410-418 pp (2001).
23. القرزا، أمل غانم محمود. تأثير الرش بالبوتاسيوم والسايوتوكاين في بعض مؤشرات النمو لنبات العدس (*Lens culinaris Medic*). مجلة ابن الهيثم للعلوم الصرفة والتطبيقية العدد 2 (25): 135-144 (2012).
24. عطية، حاتم جبار؛ سعد الدين، شروق محمد كاظم و ابراهيم، بشير عبد الله. تأثير منظمات النمو النباتية في بعض الصفات الخضريّة للحبة السوداء. مجلة العلوم الزراعية العراقية، 41(2): 80-81 (2010).
25. الحلبي، حسن عصام صالح. تأثير السايوتوكاين والسماذ المركب NPK في النمو والمركبات الفعالة لنبات الحبة السوداء *Nigella sativa L.* رسالة ماجستير، كلية التربية/ ابن الهيثم، جامعة بغداد (2012).
26. Scientist from university of Exeter and Shimance University in Japan. Cis Essential for Plant Growth Science Daily (Sep. 27) (2007)
- agent الذي يساعد النبات في تحمله الأوزون والاشعة السينية [26] كما ان المستخلص يحتوي على مركبات فعالة مثل Myrtend، الثاينيات و Resine فضلاً عن الفلافونيات والسكريات والراتنجات والتي تساهم في زيادة تحسين الخصائص الفسلجية ودعم نمو النبات [4، 5].
- ننتج مما سبق ان كل من حليب جوز الهند والمستخلص المائي لأوراق الياس الجافة قد ساهما في تحسين الصفات الطواهر المورفولوجية والفسلجية لنبات البقلاء.
- المصادر
1. الكاتب، يوسف منصور. تصنيف النباتات البذرية. جامعة بغداد، وزارة التعليم العالي والبحث العلمي، جمهورية العراق: ص 333، ص 436 (1988).
  2. شفيق، صلاح الدين عبد الرزاق والذبابي، عبد الحميد. انتاج محاصيل الحقل. دار الفكر العربي، كلية الزراعة. مشتهر، جامعة بنها، جمهورية مصر العربية (2008).
  3. شلقم، مفتاح وشوبليه، عباس حسن. الحبوب والبقول الغذائية مطبعة دار الكتب الوطنية، بنغازي، جامعة سيها، ليبيا (2011).
  4. طلاس، مصطفى. المعجم الطبي النباتي. دار طلاس للدراسات والترجمة والنشر، الطبعة الثالثة، دمشق، سوريا: ص 703 (2008).
  5. قنيس، أكرم جميل. مستشار الإنسان في الغذاء والدواء. دار البشائر للطباعة والنشر والتوزيع، دمشق، سوريا: ص 133 (2007).
  6. دفلن، روبرت م وويذام، فرانسيس هد. مترجم. وزارة التعليم العالي والبحث العلمي، الطبعة الرابعة: ص 830 (1991).
  - 7-Verma, S. K. and Verma, M. A Text Book of Plant Physiology, Biochemistry and Biotechnology 10<sup>th</sup> ed., S. Chand and Company LTD. Ram Nagar, New Delhi, India: 112-336 (2010).
  8. شوفالبييه، اندرو. الطب البديل، التداوي بالأعشاب والنباتات الطبية، ترجمة عمر الايوبي، بيروت، لبنان: ص 69 (2010).
  9. قبيسي، حسان. معجم الاعشاب والنباتات الطبية. دار الكتب العلمية، بيروت، لبنان. ص 69 (2004).
  10. محمود، مهتد جميل ومجيد، سامي هاتم. النباتات والأعشاب العراقية بين الطب الشعبي والبحث العلمي، قسم العقاقير وتقييم الادوية، الطبعة الاولى/ بغداد العراق: ص 71 (1998).
  11. علمان، محمد عباس. اساسيات زراعة الخلايا والانسجة النباتية. وزارة التعليم العالي والبحث العلمي، جامعة بغداد: 416 ص (1988).
  12. Ab El-Zahaba, A. A.; Ashor, A. M. and Al-Hateedy, K.H. Comparative analysis of growth development and yield of five field bean cultivators *Vicia faba L.* Zeidachrift fur Ackeround Pflanzebu, 149 (1): 1-13 (1980).
  13. الخواجة، عبد الستار عبد القادر حسن. دروس عملية في مقرر فسيولوجيا محاصيل الحقل. كلية الزراعة، جامعة الزقازيق، جمهورية مصر العربية (1995).
  14. كاردينير، فرانكين ب؛ بيرس، اربرينت وآل ميشيل، رومل. فسيولوجيا نباتات المحاصيل (مترجم). جامعة بغداد، وزارة التعليم العالي والبحث العلمي، جمهورية العراق (1999).
  15. Vopyan, V. G.. Agricultural chemistry english eransaltion, mirpublishers 1<sup>st</sup> ed. (1984).
  16. دلالي، باسل كامل والحكيم، صادق حسن. تحليل الاغذية. دار الكتب للطباعة والنشر، جامعة الموصل، جمهورية العراق (1987).
  17. SAS. Statistical users guide for personal computers, release 7.o. SAS. Inst. Inc. Cry, New York (2004).
  18. مور، توماس. الهرمونات النباتية، فسلجتها وكيميائها الحيوية. وزارة التعليم العالي والبحث العلمي جامعة الموصل، جمهورية العراق: 228-232 (1982).
  19. ياسين، يسام طه. اساسيات فسيولوجيا النبات، كلية العلوم، جامعة قطر: ص 178-509 (2001).



## تقييم تراكيز الغازات CO و SO<sub>2</sub> وتأثيرها على الهواء المحيط بمنطقة الجادرية في مدينة بغداد

عباس مجيد عناد وعوني ادوار عبد الاحد  
قسم علوم الجو، كلية العلوم، الجامعة المستنصرية

### الخلاصة

حللت في هذا العمل بيانات الملوثات الغازية في الهواء الجوي اول اوكسيد الكربون وثاني اوكسيد الكبريت في منطقة الجادرية جنوب بغداد وعليه فقد استعملت البيانات المقدمة من شعبة تلوث الهواء التابعة لدائرة حماية وتحسين البيئة (الدائرة الفنية) في وزارة البيئة- بغداد ولل سنوات 2010 و 2011 و 2012 اضافة الى تأثير بعض العوامل الجوية على كميات هذه الملوثات. لقد اظهرت نتائج الدراسة في محطة الجادرية ان تراكيز الغازات اول اوكسيد الكربون وثاني اوكسيد الكبريت بوسطها معدلات ساعية على التوالي اذ بلغت (1.24 و 0.005 جزء من المليون). اظهرت النتائج ايضاً سلوكاً واضحاً لتأثير العوامل الجوية على هذه الملوثات خلال اشهر ونفصول سنوات الدراسة، فقد اشارت النتائج الى ان معدلات تركيز اول اوكسيد الكربون تصل الى قيم عالية نسبياً خلال فصل الشتاء وان القيم الشهرية والفصلية لغاز ثاني اوكسيد الكبريت تكون عالية خلال فصل الصيف ووجد ان تراكيز الملوثات تتناسب طردياً مع درجة الحرارة وعكسياً مع سرعة الرياح .

### ABSTRACT

In this study, data of gaseous pollutants in the atmosphere namely CO and SO<sub>2</sub> at AL-jadiriya region, southern Baghdad are analyzed. Data was taken from the air pollution and environmental improvement Division (technical department) of ministry of environment/Baghdad for years 2010, 2011 and 2012. Some meteorological factors was employed to study their effect on these gases. Results show that at ALjadiriya station the concentration of CO and SO<sub>2</sub> reaches the order of 0.005 and 1.24 ppm respectively as a high values. Results Also showed that meteorological factors have a obvious effect on these gases, which indicate that CO has high values on winter while SO<sub>2</sub> was high at summer and it was found that the concentration of pollutants are directly correlate with temperature and inversely with wind speed.

### Article info.

تقديم البحث: 2014/9/2  
قبول البحث: 2015/1/11

### المقدمة

تعد قضية تلوث الهواء من القضايا التي اصبحت تزعج الانسان في جميع المجتمعات لا سيما وان الهواء يعتبر ضرورياً للانسان شأنه شأن الماء ، بل هو اكثر اهمية وضرورة. ولم يعد الهواء بذلك النقاء والصفاء الذي خلقه الله عليه ، بل امتدت اليه يد البشر عابثة، فاختل التوازن واهتز هذا النظام الدقيق ، وتلوث الهواء الذي تنتفسمه وكان الانسان هو السبب، فكانت المعامل والمصانع ووسائل النقل ومحطات توليد الطاقة والاستخدامات المنزلية ، هذه المصادر تبث يومياً ملايين الاطنان من الملوثات المختلفة الى الهواء دون وجود ضوابط او عوائق واصبح الغلاف الجوي سديفاً او مكب نفايات غازية . والانسان هو الذي يتنفس هذا الهواء الملوث فهو الذي صنع المشكلة ، وهو الذي يتحمل مسؤوليتها والذي تلقى اثارها سلباً على صحته.

### الجانب النظري

#### الهدف من البحث

يهدف هذا البحث الى تحليل القياسات لبعض الملوثات الجوية في محطة الجادرية، ودراسة تراكيز غاز اول اوكسيد الكربون وغاز ثاني اوكسيد الكبريت في الهواء المحيط بالمواقع خلال الاعوام (2010 و 2011 و 2012)، كما يهدف البحث الى دراسة تأثيرات العوامل الجوية على سلوك الملوثات الجوية اعلاه.

#### دراسات السابقة

1- الربيعي (1998):- درس تلوث الهواء الناتج من مصرفي الدورة، حيث اجرى قيا ماته التحليلية على موقعين قريبين خارج المصفي لمدة 7 ايام لكل من الموقعين لملوثات غازات (CO , SO<sub>2</sub> , NO<sub>2</sub>)، ثم وضع برنامجاً حاسوبياً بلغة Quick Basic يتضمن معادلات كاوس التي تعتمد على استقرارية الجو للتوقع بالتلوث الناتج من المصفي الى 34 نقطة حول

المصفي لتحديد التراكيز الأرضية لهذه الملوثات على مسافات مختلفة لمعرفة صحة المعادلات مع التراكيز الأرضية المحسوبة فعلياً في الموقعين المحددين، وقد اظهرت الدراسة نتائج مقنعة.

2- الساعدي (1999) :- اجرى دراسة تلوث الهواء في مدينة بغداد بغاز (CO) وبعض العناصر السامة مثل النحاس والرصاص، وقد وجد ان للعناصر الجوية (درجة الحرارة، سرعة الرياح، كمية الامطار) علاقة بتراكيز هذه الملوثات في الهواء

3- التكريتي (1999) :- قامت بدراسة تطبيقية عن التلوث الناتج من محطات كهرباء الدورة وبغداد من خلال قياس تراكيز الملوثات الغازية المنبعثة من المحطتين وحساب كميات الغازات (HC, CO, SO<sub>2</sub>, NO<sub>2</sub>) المنبعثة من مداخن المحطتين، كما استخدمت نموذج كاوس لتقدير انتشار تلك الملوثات الغازية مع المسافات، وكذلك المتغيرات المناخية المرافقة لها.

#### مناخ العراق

ان اهم ما يميز مناخ العراق هو التطرف الكبير في درجات الحرارة بين الليل والنهار وبين الشتاء والصيف وهذا التفاوت الكبير هو الذي يعبر عنه بالتطرف المناخي الذي يعتبر صفة عامة للمناخات القارية. من الصفات المميزة الاخرى لمناخ العراق ، الجفاف، الذي يسببه قلة تساقط الامطار واقتصاد سقوطها على فصل الشتاء بشكل رئيس واطراف فصلي الخريف والربيع بدرجة اقل، ومما يزيد الجفاف ارتفاع قيمة التبخر بسبب الكمية العالية للإشعاع الشمسي الساقط على السطح في اواخر فصل الخريف وبدايات فصل الشتاء يكون مناخ العراق مشابهاً لمناخ البحر الابيض المتوسط [1].

تتألف طبقات الغلاف الجوي من:

1- خليط من الغازات التي يطلق عليها الهواء الجاف Dry air.



- 2- تطور الموصلات والمركبات التي تعمل بواسطة المحركات (فيها يحرق الوقود.  
3- تطور صناعي أدى إلى إستعمال مكثف ومتزايد لمصادر الطاقة مثل الوقود والفحم والنفط والغاز الطبيعي، (في الصناعة يحرق الوقود لإنتاج طاقة) [3]

#### اساسيات الغازات الملوثة للهواء

يتطرق هذا البحث الى التعرف على انواع الملوثات الموجودة في الهواء من غازات ومخاطرها البيئية ومعرفة المصادر الرئيسة التي تسبب حدوث التلوث في الهواء وتأثيراتها البيئية والصحية وتحديد العوامل التي تساعد على انتشارها.

#### احادي اوكسيد الكربون

ان غاز CO عديم اللون والطعم والرائحة ويتكون نتيجة الاكسدة غير الكاملة للوقود، خصوصاً في محركات السيارات. على الرغم من ان نسبة هذا الغاز تقل كثيراً عن نسبة ثاني اوكسيد الكربون الا انه يتصف بسميته الشديدة، ويعد من اخطر الغازات على صحة الانسان، فهو يكون مع الدم مركباً صلباً يقلل من كفاءة الدم في نقل الاوكسجين، عندما تزيد كميته قليلاً فقد يتسبب في انسداد الاوعية الدموية محدثاً الوفاة. كذلك يتدخل هذا الغاز في عمل بعض الانزيمات ويقلل من كفاءتها. يتراوح تأثير هذا الغاز على صحة الانسان تبعاً لتركيزه، اذ يؤدي الى الصداع والشعور بالغثاس والاعياء وصعوبة التنفس وارتخاء العضلات وقصور في الشريان التاجي، وقد يصل الامر الى الغيبوبة او الموت. ان الملوثات الناتجة مباشرة عن عملية الحرق تدعى ملوثات أولية، ولكن هنالك أيضاً ملوثات ثانوية تنتج عن التفاعل الكيماوي بين الملوثات الأولية ومواد أخرى موجودة في الجو بوجود او من دون اشعة الشمس [5].

#### ثاني أكسيد الكبريت SO<sub>2</sub>:

ان ثاني أكسيد الكبريت هو غاز عديم اللون ذو طعم ورائحة شديدين يؤديان إلى الشعور بالاختناق، وذائبية الغاز في الماء مرتفعة وتؤدي إلى إنتاج حامض الكبريتوز.

#### مصادر ثاني اوكسيد الكبريت في الهواء يمكن تلخيصها كالآتي:

- عمليات أكسدة H<sub>2</sub>S في الجو.
- ب - انطلاق غاز SO<sub>2</sub> إلى الهواء من البراكين.
- ج - انطلاق SO<sub>2</sub> إلى الجو من احتراق الوقود وبشكل خاص الذي يحتوي على مركبات الكبريت مثل الوقود المستعمل في محطات القوة وفي عمليات تكرير النفط [9]. المصدر الأساس لـ SO<sub>2</sub> هو الطبيعة بينما تشكل كمية SO<sub>2</sub> المنطلقة من عمليات حرق الوقود فقط نسبة 20% في الجو.
- د- SO<sub>2</sub> بتركيز منخفضة يؤدي إلى مضايقات في عملية التنفس وإلى مضايقات في الرؤية وأوجاع في الرأس، في تركيز مرتفعة يؤدي إلى أضرار حادة جداً في جهاز التنفس، اذ يذوب SO<sub>2</sub> جيداً في الماء ما يسرع ذوبان هذا الملوث في الأنسجة الملوثة للجهاز التنفسي مثل أنسجة الفم والأنف والحلق بالإضافة إلى العينين.
- هـ- SO<sub>2</sub> يلحق ضرراً للنباتات والمحاصيل الزراعية.
- و - SO<sub>2</sub> يتأكسد بالجو إلى ثالث اوكسيد الكبريت SO<sub>3</sub>.

#### المصادر الرئيسية

محطات توليد الطاقة:

يمكن التمييز بين ثلاثة أنواع من محطات الطاقة حسب مصدر الطاقة الذي يشغل هذه المحطات:

- محطات تعمل بالفحم الحجري.
  - محطات تعمل بحرق الكاز.
  - محطات تعمل بالطاقة النووية.
- بعد احتراق الوقود بأنواعه (البزيرين والكازولين والفحم والغاز والكبريت) في محطات الطاقة الكهربائية المسبب الرئيس لتلوث الهواء في المدن. وتشير بعض الدراسات ان احتراق الوقود لتوليد الطاقة الكهربائية ينتج عنه (0,2) جزء بالمليون من اول اوكسيد الكربون (CO) و(16,3) جزء بالمليون من اكاسيد الكبريت و(0,1) جزء بالمليون من الهيدروكربونات و(5,5) جزء بالمليون من الكاسيد النتروجين [6].

- 2- العوالق الجوية من المواد الصلبة والسائلة والتي يطلق عليها احيانا بالهباء الجو.  
3- الماء بحالاته الفيزيائية الثلاث.  
ان جميع المواد موجودة بشكل طبيعي في الغلاف الجوي ويتركز واطنة وتعد مواد غير ضارة في اغلب الاحيان [2].  
جدول 1- التركيب النموذجي للهواء النقي الجاف قرب سطح البحر [3].

المكونات	المسبة الكيميائية	التركيز	
		% النسبة المئوية الحجمية	(ppm)
النيتروجين	N <sub>2</sub>	78.09	780900
الأكسجين	O <sub>2</sub>	20.94	209400
الأرجون	Ar	0.93	9300
ثاني اوكسيد الكربون	CO <sub>2</sub>	0.0318	318
النيون	Ne	0.0018	18
الهيليوم	He	0.00052	5.2
الميثان	CH <sub>4</sub>	0.00013	1.3
الكريبتون	Kr	0.0001	1
الهيدروجين	H	0.00005	0.5
اوكسيد النترون	N <sub>2</sub> O	0.000025	0.25
احادي اوكسيد الكربون	CO	0.00001	0.1
الأوزون	O <sub>3</sub>	0.000002	0.2
امونيا	NH <sub>3</sub>	0.000001	0.01
ثاني اوكسيد النتروجين	NO <sub>2</sub>	0.0000001	0.001
ثاني اوكسيد الكبريت	SO <sub>2</sub>	0.00000002	0.0002

تعد بعض المكونات المدرجة اعلاه مواد ملوثة في الهواء عندما يتجاوز تركيزها القيمة الطبيعية (Background value) لانها تسبب تأثيرات عكسية على البيئة.

#### تلوث الهواء

هو دخول مواد غير متواجدة في تركيب الهواء النقي، أو ارتفاع تركيز مواد موجودة في الهواء فوق التركيز المميز لها في الهواء النقي، على اثر ذلك (في كلا الحالتين) تقل جودة الهواء مما يلحق ضرراً في البيئة والكائنات الحية فيها [4].

#### مصادر تلوث الهواء:

يمكن تقسيم مصادر تلوث الهواء إلى مصادر طبيعية وأخرى اصطناعية تنتج عن فعالية الإنسان، وتقسّم لمصادر ثابتة ( المصانع ومباني السكن ومحطات توليد الطاقة) ومصادر متحركة (المركبات).

#### المصادر الطبيعية للتلوث الهوائي:

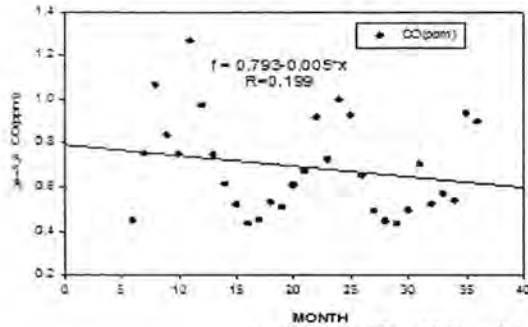
- 1- أكاسيد النيتروجين (NOx) تركيزها في الهواء النقي يساوي 0.52 أجزاء من المليون، تنتج هذه الأكاسيد نتيجة لأشعة الشمس وعمليات البرق اذ ينفكك الرابط بين جزيئات النتروجين وتتفاعل ذرات النتروجين الناتجة مع الأكاسيد لإنتاج تلك الأكاسيد [4].
- 2- الأوزون O<sub>3</sub> ينتج أيضاً بسبب أشعة الشمس وعمليات البرق.
- 3- أول أكسيد الكربون CO ينتج بسبب أكسدة الميثان CH<sub>4</sub> وينتج من مصادر أخرى.
- 4- غبار ومركبات كبريت التي تنطلق من البراكين.
- 5- عمليات التحليل اللاهوائية للمواد العضوية تؤدي إلى انطلاق الغازات CH<sub>4</sub>, NH<sub>3</sub>, H<sub>2</sub>S إلى الهواء.
- 6- العواصف الرملية التي تحمل معها حبيبات غبار إلى الهواء.
- 7- حبيبات اللقاح التي تنطلق من الأزهار.
- 8- أملاح مصدرها قطرات مائية حملت إلى الهواء من مياه البحر.

#### المصادر الاصطناعية للتلوث الهوائي الناتجة عن فعالية الإنسان:

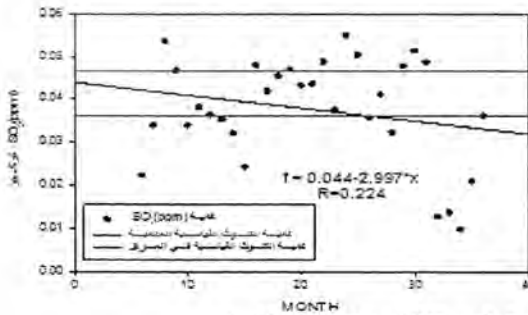
على اثر الثورة الصناعية التي حدثت في القرن التاسع عشر بدأت عملية تطور تكنولوجي سريع أدت إلى تغيرات جذرية في حياة الإنسان. يمكن تمييز ثلاث عمليات رئيسة أدت إلى زيادة كبيرة في كميات الملوثات التي تنطلق إلى الأتموسفير والتي تؤدي إلى تلويث الهواء:

- 1- تطور مراكز مدن ومدن كبيرة مع تزايد انتقال الإنسان من القرية إلى المدينة.

والصيف تكون اكبر من كمية التلوث القياسية العالمية والمبالغة 0.05 (جزء من المليون) اما بقية قيم التلوث العالية للاشهر الباقية فتكون محصورة بين كمية التلوث القياسية العالمية وكمية التلوث القياسية في العراق والمبالغة 0.04 (جزء من المليون). وهذا ينسجم مع ماتوصل اليه الباحث [11]، الذي وجد ان تركيز الملوث غاز ثاني اوكسيد الكبريت يزداد تركيزه من سنة الى اخرى من سنوات الدراسة ويبقى عموما اكثر من المحددات الوطنية والعالمية خلال اشهر ابر (2010) كانون الاول والثاني (2011) وحزيران (2012).

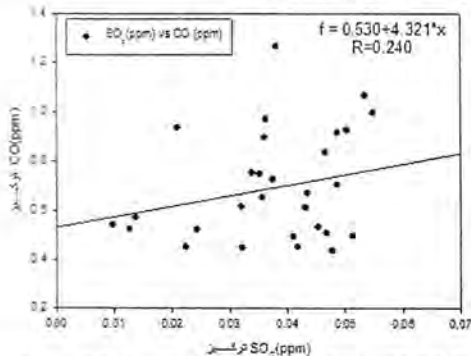


شكل 1: الرسم الانتشاري لاول اوكسيد الكربون



شكل 2: الرسم الانتشاري ثاني اوكسيد الكبريت

تراكيز اول اوكسيد الكربون وثاني اوكسيد الكبريت في محطة الجادرية. ان التغير الشهري لتراكيز اول اوكسيد الكربون ، اوكسيد ثاني اوكسيد الكبريت والمدسوبة بوصفها معدلات شهرية موضحة في الشكل (3) اذا رسمت العلاقة بين تراكيز الملوثين على المحور الصادي توضع تراكيز الملوث اول اوكسيد الكربون وتدرج تراكيز الملوث غاز ثاني اوكسيد الكبريت على المحور السيني. واذا ما اخذ احسن خط مستقيم يمر بنقاط الشكل يشير الى زيادة مستمرة خلال السنوات 2010 و2011 و2012 في قيم التلوث. وكانت قيمة  $R=0.3$  التي تمثل معامل ارتباط النقاط مع الخط المستقيم وهذا يدل على تباعد بين النقاط والخط المستقيم. يلاحظ من الرسم ان قيم تراكيز الملوث اول اوكسيد الكربون تزداد بزيادة قيم تراكيز الملوث ثاني اوكسيد الكبريت بنفس الوقت ما يمكن ان نستنتج منه ان مصدر التلوث يحتمل ان يكون واحد.



شكل 3: العلاقة بين تركيز اول اوكسيد الكربون وثاني اوكسيد الكبريت للسنوات 2010, 2011, 2012

### التأثيرات المناخية والبيئية لتلوث الهواء

تؤثر درجة الحرارة وسرعة الرياح وكميات الامطار الساقطة على كثافة الشوائب الموجود في الغلاف الجوي وبالتالي في احداث تأثيرات مناخية وبيئية في جو الارض. ان زيادة نسبة الشوائب في الغلاف الجوي يزيد من كمية الاشعة فوق البنفسجية التي تصل الارض وهذا يسبب حدوث تغيرات في المعدلات الطبيعية لدرجات الحرارة والرطوبة النسبية خلال فصول السنة مع حدوث زيادة في كمية الاشعاعات الواصلة الى الارض. ان هذه التغيرات تؤدي بالتالي الى بعض الظواهر الجوية مثل ظاهرة الاحتباس الحراري وتذبذب الاوزون [7].

### 1-3 موقع الدراسة وتجميع البيانات

اعتمدت الدراسة بصورة رئيسة على البيانات المقدمة من شعبة تلوث الهواء التابعة الى دائرة حماية وتحسين البيئة (الدائرة الفنية) في وزارة البيئة / بغداد. اجريت القياسات في الاعوام 2010 و2011 و2012 بوصفها بيانات ساعية واستعمل لغرض هذا البحث محطة اختبارت في جانب الكرخ هي محطة الجادرية (سكنية- سياحية). وتضمنت القياسات ما يأتي:

- تراكيز غاز اول اوكسيد الكربون CO - ج - المعدل اليومي لسرعة الرياح
- تراكيز غاز ثاني اوكسيد الكبريت SO<sub>2</sub> - د - المعدل اليومي لدرجة الحرارة



خريطة توضح موقع المحطة الانتشارية في مركز مدينة بغداد

### النتائج والمناقشة

#### محطة الجادرية: تقع محطة الجادرية جنوب بغداد

#### التغيرات الشهرية لمعدلات تراكيز اول اوكسيد الكربون

بما ان تركيز كميات اول اوكسيد الكربون متميزة بقيمتها على الغازات الملوثة الاخرى يظهر التغير الشهري بوصفها معدلات تراكيزها والمدسوبة لمدة ثلاثة اعوام متتالية 2010 و2011 و2012 والموضحة في الشكل (1)، اذ يلاحظ تناقص مستمر خلال السنوات 2010 و2011 و2012 في قيم التلوث. علما ان قيمة معامل ارتباط النقاط مع الخط المستقيم المرسوم كانت  $R=0.2$  وهناك توافقية في كل سنة ولمدى ثلاث سنوات متتالية من خلال الشكل الموجي periodisty ويلاحظ من الرسم اعلى قيمة لتراكيز الملوث اول اوكسيد الكربون تكون في فصل الخريف شهر تشرين الثاني 2010 اذ بلغت القيمة 1.3 (جزء من المليون) اما اقل قيمة لتراكيز هذا الملوث فكانت في شهر نيسان 2012 اذ بلغت القيمة 0.4 (جزء من المليون) وتبقى تراكيز هذا الملوث اقل من كمية التلوث القياسية في العراق والمبالغة 10 (جزء من المليون).

#### التغيرات الشهرية لمعدلات تركيز ثاني اوكسيد الكبريت في محطة الجادرية

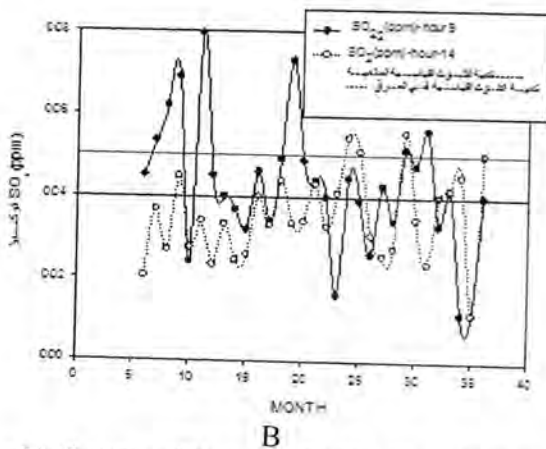
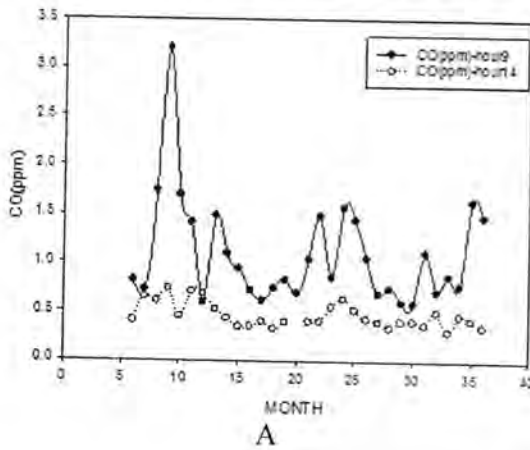
يوضح الشكل (2) التغيرات الشهرية لمعدل تراكيز ثاني اوكسيد الكبريت مع اشهر السنة وثلاثة اعوام متتالية 2010 و2011 و2012. اذ يلاحظ تناقص مستمر خلال السنوات 2010 و2011 و2012 في قيم التلوث. كانت قيمة معامل ارتباط النقاط مع الخط المستقيم  $R=0.2$  وهذا يدل على تباعد بين النقاط والخط المستقيم. يلاحظ من الرسم ان اعلى قيمة لتراكيز الملوث تكون في شهر كانون الثاني 2012 اذ بلغت 0.055 (جزء من المليون) اما اقل تركيز للملوث خلال الثلاثة اعوام في شهر تشرين الاول 2012 اذ بلغ 0.01 (جزء من المليون) ويلاحظ ان قيم التلوث العالية في فصلي الشتاء

قيم التلوث للساعة 2 ظهرا (14 محلي) تتحصر بين (0.0-8.0 جزء من المليون) يلاحظ في شهر كانون الثاني 2010 قيم التركيز للملوث اول اوكسيد الكربون تتناقص الى اقل قيمة لها خلال السنة وتكون اقل من قيمة التلوث في الساعة الثانية ظهرا (14 محلي). وبجميع الاحوال فان تراكيز الملوث اول اوكسيد الكربون تبقى اقل من كمية التلوث القياسية في العراق.

**تغير تراكيز ثاني اوكسيد الكبريت خلال ساعات الصباح وبعد الظهيرة في محطة الجادرية.**

يوضح الشكل 4(b) التغير الشهري لتراكيز الملوث غاز ثاني اوكسيد الكبريت والمحسوبة بوصفها معدلات شهرية على المحور الصادي والتغير الشهري لاشهر السنة ولمدة ثلاثة اعوام متتابعة 2010 و2011 و2012 على المحور السيني، يلاحظ من الشكل ان الزيادة في تراكيز الملوث في الساعة 9 صباحا يكون اكبر بكثير من قيمتها الشهرية في ساعة الظهيرة (14 محلي) وان اعلى قيمة تصلها هذه التراكيز تكون في شهر كانون الاول لسنة 2010 الساعة 9 صباحا وبلغت اكثر من 0.08 (جزء من المليون) واقل قيمة لتراكيز التلوث بهذا الغاز تكون في شهر

تشرين الثاني 2012 في الساعة 2 ظهرا (14 محلي) اذ بلغت 0.01 (جزء من المليون) وتبقى تراكيز الملوث في الساعة التاسعة صباحا في اشهر الصيف اعلى من كمية التلوث القياسية العالمية البالغة 0.05 (جزء من المليون) وتكون في الخريف والشتاء اعلى من كمية التلوث القياسية في العراق اما تراكيز الملوث في الساعة 2 ظهرا (14 محلي) تبقى في اغلب اشهر السنة اقل من كمية التلوث القياسية في العراق ماعدا بعض اشهر الصيف والشتاء تكون القيمة اعلى من كميات التلوث القياسية ويلاحظ ان هناك توافقية في كل سنة من خلال الشكل الموجي Periodicity

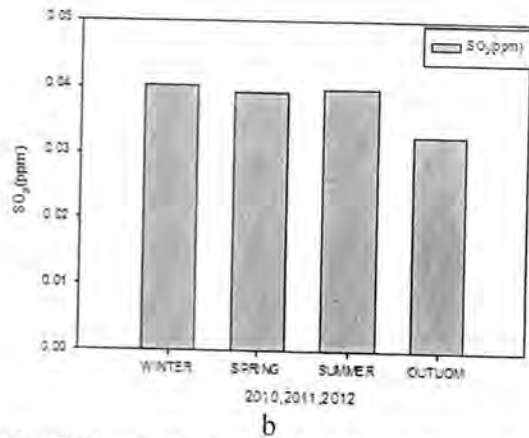
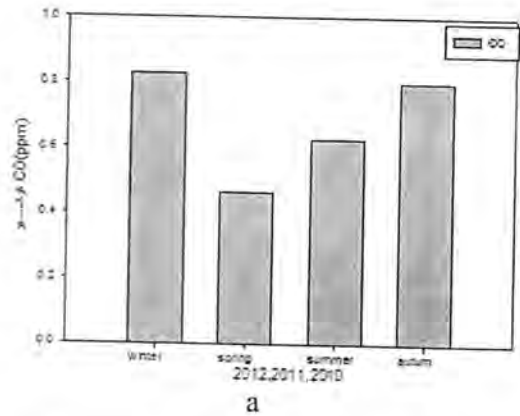


شكل 5: (a) الرسم الانتشاري لأول اوكسيد الكربون و (b) الرسم الانتشاري لثاني اوكسيد الكبريت

التغيرات الفصلية لتراكيز الملوثات الجوية اول اوكسيد الكربون وثاني اوكسيد الكبريت في محطة الجادرية:

يوضح الشكل (4) المعدلات الفصلية لتراكيز الملوثات الجوية اول اوكسيد الكربون وثاني اوكسيد الكبريت ولمدة ثلاثة اعوام متتابعة 2010 و2011 و2012 فاذا ما مارسمت التغيرات الفصلية لثلاث سنوات على المحور السيني والتغير في تركيز الملوث اول اوكسيد الكربون على المحور الصادي، والموضح في شكل 4(a) ويلاحظ ان اعلى تركيز للملوث يكون في فصل الشتاء اذ تكون قيمة 0.8 (جزء من المليون) واقل قيمة للملوث اول اوكسيد الكربون تكون في فصل الصيف اذ تبلغ قيمة (جزء من المليون) 0.41.

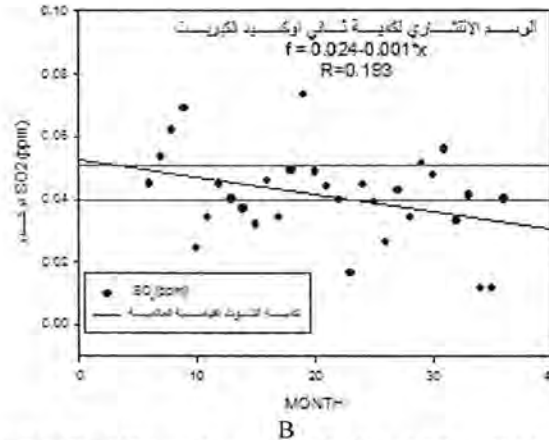
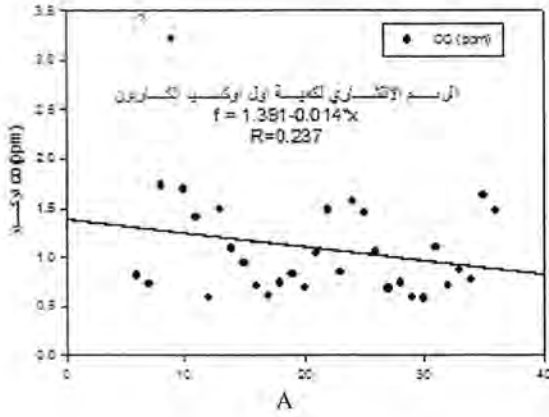
اما الرسم الموضح في الشكل 4(b) ويمثل التغيرات الفصلية لثلاث سنوات متتابعة 2010 و2011 و2012 على المحور السيني وتراكيز الملوث ثاني اوكسيد الكبريت على المحور الصادي اذ يلاحظ ان تراكيز الملوث تزداد في فصل الشتاء اذ بلغت 0.04 (جزء من المليون) اما اقل قيمة لتراكيز الملوث تكون في فصل الخريف اذ بلغت 0.03 (جزء من المليون)



شكل 4: المعدلات الفصلية لتراكيز الملوثات (a) اول اوكسيد الكربون (b) ثاني اوكسيد الكبريت

**تغير تراكيز اول اوكسيد الكربون خلال ساعات الصباح وبعد الظهيرة في محطة الجادرية:**

التغير الشهري لمعدلات تراكيز اول اوكسيد الكربون خلال ساعات الصباح (9 محلي) ووقت الظهيرة (14 محلي) والمحسوبة بوصفها معدلات شهرية والموضحة في الشكل 4(a) مقارنة للقيم في اوقات الصباح مع الظهيرة، اذا ما رسمت تراكيز اول اوكسيد الكربون. لوحظ ان الزيادة في تراكيز الملوث في الساعة التاسعة صباحا يكون اكبر بكثير من قيمتها الشهرية في ساعة الظهيرة (14 محلي). الزيادة في تركيز الملوث في ساعات الصباح الاولى يقابلة انخفاض وبنسبة اقل في ساعات الظهيرة، من الملاحظ ان اعلى قيمة لتراكيز هذا الملوث تكون في الساعة التاسعة صباحا من شهر ايلول 2010 كما يلاحظ ان قيم التلوث لغاز اول اوكسيد الكربون لساعة التاسعة صباحا تتحصر بين (0.5-3.3 جزء من المليون) في حين



شكل 6: (a) الرسم الانتشاري لأول أكسيد الكربون و (b) الرسم الانتشاري لثاني أكسيد الكبريت

#### تأثير العوامل الجوية على ملوثات الهواء في محطة الجادرية:

تأثير تغير درجة الحرارة على كمية غاز أول أكسيد الكربون: التغير الشهري لتركيز أول أكسيد الكربون والمحسوبة بوسطها معدلات شهرية مع التغير بدرجات الحرارة ولمدى ثلاث سنوات متتابعة والموضحة في الشكل 7 (a) فإذا ما رسم خط مستقيم يمر بنقاط الشكل الذي يشير الى تناقص مستمر خلال السنوات 2010 و 2011 و 2012 في قيم التلوث كانت قيمة  $R=0.2$  والتي تمثل معامل ارتباط النقاط مع الخط المستقيم، وهذا يدل على تباعد بين النقاط والخط المستقيم. يلاحظ من الرسم ان قيم تركيز الملوث أول أكسيد الكربون تقل بزيادة درجات الحرارة وان اعلى قيمة لتركيز الملوث عند  $25^{\circ}\text{C}$  اذ بلغت 1.25 (جزء من المليون) و اقل قيمة عند درجة حرارة  $35^{\circ}\text{C}$  اذ بلغت 0.4 (جزء من المليون).

تأثير تغير سرعة الرياح على كمية انتشار غاز أول أكسيد الكربون في محطة الجادرية:

التغير الشهري لمعدلات تركيز الملوث أول أكسيد الكربون مع تغير سرعة الرياح ولمدة ثلاثة اعوام متتابعة 2010 و 2011 و 2012 والمبينة في الشكل 7 (b). النقاط منتشرة فإذا اخذ خط مستقيم يمر بنقاط الشكل والذي يوشر الى تناقص مستمر خلال السنوات 2010 و 2011 و 2012 في قيم التلوث كانت قيمة معامل ارتباط النقاط والخط المستقيم  $R=-0.2$  وهذا يدل على تباعد بين النقاط والخط المستقيم. يلاحظ من الرسم ان قيم تركيز أول أكسيد الكربون تناقص بزيادة سرعة الرياح وان اعلى قيمة لتركيز الملوث عند سرعة رياح 1.55 (م/ثا) بلغت 1.25 (جزء من المليون) وان اقل قيمة لتركيز الملوث كانت عند سرعة رياح 2 (م/ثا) بلغت 0.4 (جزء من المليون)

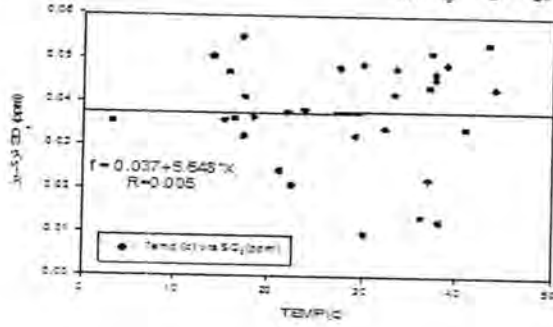
#### المعدلات الشهرية لتركيز أول أكسيد الكربون لمحطة الجادرية التاسعة صباحا في محطة الجادرية.

المعدلات الشهرية لتركيز أول أكسيد الكربون لثلاث سنوات 2010 و 2011 و 2012 والموضحة في الشكل 6(a) فإذا ما رسم احسن خط مستقيم يمر بين النقاط والذي يعتمد على مدى انتشار هذه النقاط عن الخط المستقيم فهذا الخط يشير الى تناقص مستمر اثناء السنوات 2010 و 2011 و 2012 في قيم التلوث. ان النقاط منتشرة وهناك توافقية في كل سنة من السنوات الثلاث من خلال الشكل الموجي Periodicity. علما ان قيمة معامل ارتباط النقاط مع الخط المستقيم المرسوم كانت  $R=0.2$  كما يلاحظ من الشكل ان اعلى قيم تركيز للملوث في الساعة التاسعة صباحا (محلي) في شهر ايلول لسنة 2010 اذ تبلغ 3.3 (جزء من المليون) اما اقل قيمة تركيز للملوث في الساعة التاسعة صباحا (محلي) في شهر ايار لسنة 2011 ومن التوافقية في شكل منحني التراكيز خلال السنوات اعلى قيم التراكيز تكون في فصل الشتاء و اقل قيم لتركيز الملوث أول أكسيد الكربون تكون في فصل الصيف وبجميع الاحوال تبقى قيم تراكيز التلوث بهذا الملوث و لثلاثة سنوات متتابعة اقل من كمية التلوث القياسية في العراق والبالغة 10 (جزء من المليون).

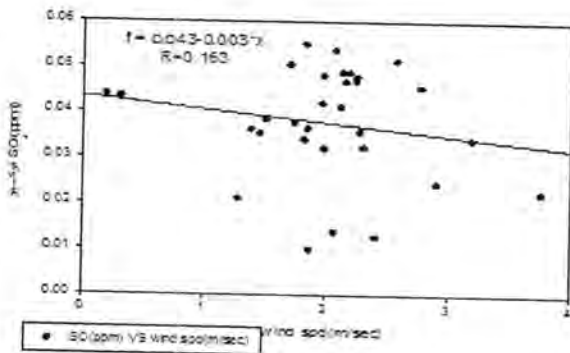
#### المعدلات الشهرية لتركيز ثاني أكسيد الكبريت لمحطة الجادرية عند التاسعة صباحا في محطة الجادرية:

اذا ما رسمت تركيز الملوث ثاني أكسيد الكبريت على المحور الصادي والتغير الشهري لاشهر السنة ولثلاث سنوات 2010 و 2011 و 2012 متتابعة في الشكل 6(b) وإذا ما رسم احسن خط مستقيم يمر بنقاط الشكل والذي يشير الى تناقص مستمر خلال السنوات 2010 و 2011 و 2012 في قيم التلوث. ان نقاط قيم التراكيز منتشرة وهناك توافقية في كل سنة ولثلاث سنوات متتابعة من خلال الشكل الموجي Periodicity كما وجد من معادلة الخط المستقيم قيمة  $R=0.02$  والتي تمثل معامل ارتباط النقاط مع الخط المستقيم يلاحظ من الشكل ان اعلى قيم التلوث في الساعة التاسعة صباحا تكون في اشهر الصيف و اقل قيم تركيز الملوث تكون في فصل الشتاء كما يلاحظ ان القيم العليا لتركيز الملوث تكون اعلى من كمية التلوث القياسية العالمية والبالغة 0.05 (جزء من المليون) واعلى قيمة لتلوث بهذا الغاز تؤشر في شهر اب 2011 وتبلغ 0.077 (جزء من المليون) و اقل قيمة للتلوث بهذا الغاز تؤشر في شهر تشرين الثاني وكانون الاول لسنة 2012 وبمقدار 0.019 (جزء من المليون)، كما يلاحظ ان اغلب قيم التلوث بهذا الغاز في فصل الشتاء وتقع بين كمية التلوث القياسية العالمية و كمية التلوث القياسية في العراق.

الكبريت تنحصر بين 0-06 (جزء من المليون) وهذا يتنجم مع ما توصل اليه [9] الذي يشير الى ان هناك تناسباً عكسياً بين سرعة الرياح وتركيز ثاني اوكسيد الكبريت اذ يبدو ان السرعة العالية للرياح تؤدي الى تخفيف تركيز الملوث في الجو.



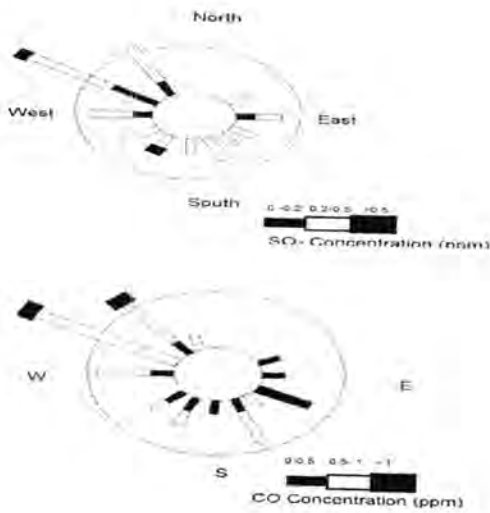
A



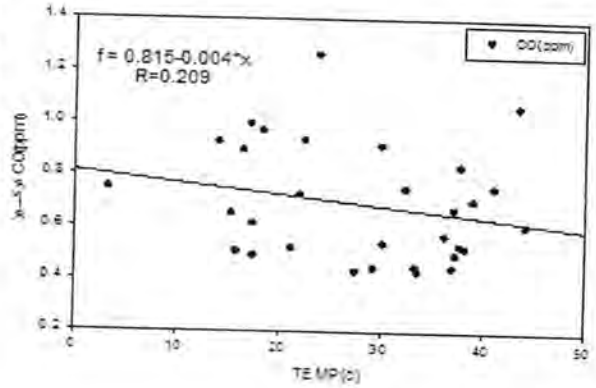
B

شكل 8: (a) الرسم الانتشاري لكمية ثاني اوكسيد الكبريت مع درجات الحرارة و (b) الرسم الانتشاري لكمية ثاني اوكسيد الكبريت مع تغير سرعة الرياح

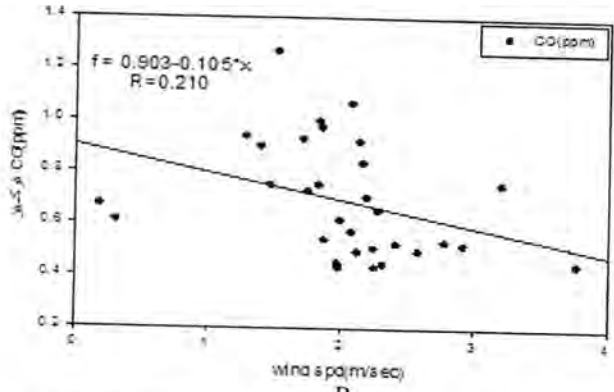
تأثير اتجاه الرياح على تراكيز اول اوكسيد الكاربون وثاني اوكسيد الكبريت في محطة الجادرية  
 يلاحظ من الشكل 9 : ان الاتجاه السائد للرياح في منطقة الجادرية هو الشمالي الغربي كما يلاحظ تأثير واضح للاتجاه الرياح على تراكيز الملوثات.



شكل 9: يمثل ورده الملوثات لغاز اول اوكسيد الكاربون وثاني اوكسيد الكبريت لمحطة الجادرية لثلاث سنوات متتالية 2010, 2011, 2012



A



B

شكل 7: (a) الرسم الانتشاري لاول اوكسيد الكاربون مع درجات الحرارة و (b) الرسم الانتشاري لاول اوكسيد الكاربون مع سرعة الرياح

تأثير تغير درجات الحرارة على تركيز ثاني اوكسيد الكبريت في محطة الجادرية .

اذا مارسم التغير الشهري لتركيز ثاني اوكسيد الكبريت والمحسوبة بوصفها معدلات شهرية على المحور الصادي وقيم درجات الحرارة لمدة ثلاث سنوات متتالية 2010 و 2011 و 2012 كما موضحة في الشكل 8 (a) يلاحظ تناقص مستمر عند امرار افضل خط مستقيم بين النقاط المنتشرة لسنوات 2010 و 2011 و 2012 في قيم التلوث وكانت قيمة معامل ارتباط النقاط مع الخط المستقيم  $R=0.01$  وهذا يدل على تباعد بين النقاط والخط المستقيم. يلاحظ من الرسم ان قيم تراكيز الملوث ثاني اوكسيد الكبريت تزداد بزيادة درجات الحرارة واعلى قيمة لتركيز الملوث تكون عند درجة حرارة 16<sup>o</sup>م اذ بلغت 0.055 (جزء من المليون)، واقل قيمة لتركيز الملوث تكون عند درجة حرارة 30<sup>o</sup>م اذ بلغت 0.01 (جزء من المليون)، وهذا يتنجم مع ما توصل اليه [9] الذي وجد ان درجة الحرارة ليس لها تأثير في ياي مباشر على تركيز الملوثات الجوية عدا ما قد يتعلق بتحولاتها الكيميائية ولكن لها تأثيرات غير مباشرة من خلال ارتباطها مع الظواهر الجوية الاخرى.

تأثير تغير سرعة الرياح على كمية الملوث ثاني اوكسيد الكبريت لمحطة الجادرية:

اذا مارسمت قيم تراكيز ثاني اوكسيد الكبريت بوحدات ppm على المحور الصادي والدرجت قيم سرعة الهواء على المحور السيني بوحدات m/Sec ولثلاث سنوات متتالية 2010 و 2011 و 2012 والموضحة في الشكل 8 (b) ورسم احسن خط مستقيم يمر بنقاط الشكل يوضح تناقصاً مستمراً خلال السنوات 2010 و 2011 و 2012 في قيم التلوث. كانت قيمة  $R=0.2$  التي تمثل ارتباط النقاط مع الخط المستقيم وهذا يدل على تباعد بين النقاط والخط المستقيم كما لوحظ من الرسم ان تراكيز الملوث تقل مع زيادة سرعة الرياح اذ بلغت اعلى قيمة لتركيز الملوث عند سرعة الرياح 2 (م/ثا) 0.055 (جزء من المليون)، اما اقل قيمة لتركيز الملوث عند سرعة الرياح 1.9 (م/ثا) وبلغت 0.01 (جزء من المليون) يلاحظ من الرسم ان سرعة الرياح تنحصر بين 0-4 (م/ثا) اما قيمة تراكيز الملوث ثاني اوكسيد

7. Hales S, Salmond C, Town GI, Kjellstrom T., "Woodward A Daily mortality relation to weather and air pollution in Christchurch, New Zealand. *Australia and New Zealand Journal of Public Health*, 2000.
8. الاسدي كاظم عبد الوهاب، " تكرار منخفض الهند الموسمي فوق العراق واثرة في تحديد اتجاهات الرياح السطحية"، مجلة الجمعية الجغرافية، العدد (37)، 198، 1988 [9].
9. داود عواطف رديف " تأثير الظروف الجوية على بعض العوالق الجوية في بغداد رسالة ماجستير ، الجامعة المستنصرية ، كلية العلوم ، 1988.
10. طارش عروبة جميل : "نمذجة تأثيرات بعض العوامل الانوائية على الملوثات الجوية " رسالة ماجستير - كلية العلوم - الجامعة المستنصرية، 2001.
11. قياس و دراسة تراكيز بعض الملوثات الهوائية في مدينة بغداد 2009 جاسم ، محمد هاشم

جدول 1: معامل الارتباط للمعادلات الخطية للمعدلات الشهرية المساعية لمحطة الجادرية

المعادلة	R	الملوث
$y=0.793-0.005*X$	0.199	Co
$y=0.44-2.997*X$	0.224	So <sub>2</sub>
$y=0.530+40321*X$	0.240	Co vrs So <sub>2</sub>

جدول 2: معامل الارتباط للمعادلات الخطية للمعدلات الشهرية المساعية للمساعية للتاسعة صباحا

المعادلة	R	الملوث
$y=1.391-0.014*X$	0.237	Co
$y=0.024-0.001*X$	0.193	So <sub>2</sub>
$y=0.785+70213*X$	0.210	Co vrs So <sub>2</sub>

جدول 3: معامل الارتباط للمعادلات الخطية للمعدلات الشهرية للعوامل الانوائية

المعادلة	R	الملوث
$y=0.815-0.004*X$	0.209	Co vrs Temp
$y=0.903-0.105*X$	0.210	Co vrs Ws
$y=0.037+5.648*X$	0.005	So <sub>2</sub> vrs Temp
$y=0.043-0.003*X$	0.163	So <sub>2</sub> vrs Ws

### الاستنتاجات

- من بيانات محطة الجادرية نستنتج
- 1- زيادة درجة الحرارة تقلل من التلوث، فالارتفاع الشديد لدرجة حرارة سطح الأرض في ساعات النهار وما يرافقه من تسخين للهواء الجوي القريب من سطح الأرض يؤدي الى حدوث حركات هوائية صاعدة نشطة تعمل على نشر الملوثات شاقوليا على اكبر مدى ممكن. اما في الليل نتيجة برودة سطح الأرض والهواء القريب منه واذما تتقدم التيارات الهوائية العمودية الصاعدة ما يؤدي الى سيطرة حركة الهبوط الهوائية والركود الجوي متولدا عن ذلك تركز الملوثات الجوية قرب سطح الأرض ويكون انتشارها الشاقولي في هذه الحالة محددا ما يرفع من كثافة الملوثات قرب سطح الأرض.
  - 2- زيادة سرعة الرياح تقلل من التلوث، تلعب سرعة الرياح دوراً كبيراً ومهماً في التأثير على انتشار الملوثات باتجاه هبوب الرياح من مكان الى آخر، كما تعمل سرعة الرياح على تقليل تركيز الملوثات بصورة مباشرة بمجرد انطلاقها من المصدر ان زيادة سرعة الرياح تؤدي الى زيادة المسافات بين الجزيئات الملونة وبالتالي التركيز اي ان التركيز يتناسب عكسياً مع السرعة لان الحركة السريعة تعمل على تشتت الملوثات وبالتالي فان الانتشار داخل كتلة الهواء سيقبل من تركيز الملوثات كما ان لسرعة الرياح تأثير اضافي وهو السيطرة على الخلط الاضطرابي [10].
  - 3- لاتجاه الرياح تأثير واضح على تراكيز التلوث.
  - 4- تبدو منطقة الجادرية ملوثة بغاز ثاني اوكسيد الكبريت وغير ملوثة بغاز اول اوكسيد الكربون .

### المصادر

1. حديد ، احمد سعيد و فاضل باقر الحسني و حازم توفيق العاني ، "المناخ المحلي " ، مديرية دار الكتب للطباعة والنشر ، جامعة الموصل ، 1982.
2. Mc Cormdc, B.M, "Introduction to the Scientific study of atmospheric pollution calif", U.S.A. 2, 100, 1971
3. **Waldcott G.L**, "Health Effects of Environmental Pollution", Mos by Com. U.S.A, 1978
4. ليونارد ج. ن، "جولة عبر العلوم"، ترجمة السيد المغربي، الدار المصرية للتأليف والترجمة، مطابع سجل العرب - القاهرة، 1995.
5. WMO, " Air Chemistry and air pollution meteorology", WMO NO , 364, world meteorology, Geneva, 1985.
6. **Reimann C., and Caritat P**, "Chemical Elements in the Environment." Belin, Germany, 1998.